

Defining Non-Contrast CT Markers of the Ischaemic Penumbra in Acute Stroke

Dr Marim Elgasaer MBCHB

Matriculation Number: 0914533

Submitted in fulfilment of the requirements for the Degree of Master of
Science MSc (Med Sci) (R)

Department of clinical Neurosciences

School of Medicine
College of Medical Veterinary and Life Sciences

University Of Glasgow

October\2012

Abstract

Background and purpose: Isodense swelling is a known early ischaemic change, and it is most likely to represent penumbra tissue on acute non-contrast computed tomography (NCCT) scan. However, in general, its detection by observers showed very poor interobserver agreement, which has been attributed to a lack of defining criteria that differentiate it from hypodensity. The aim of this study is to assess the reliability of detecting isodense swelling within the first six hours post stroke onset.

Methods: A three-stage study was designed to test the effect of defining criteria and training on the reliability of detection of isodense swelling on acute NCCT. NCCT and perfusion computed tomography (PCT) scans of patients with acute stroke of less than six hours' duration were reviewed retrospectively. A web-based tool was used to present NCCT scans to readers of different backgrounds (expert and trainee stroke neurologists and neuroradiologists), who evaluated the scans independently by the Alberta Stroke Program Early CT Score (ASPECTS). In the pre-training stage, nine readers assessed 19 repeated scans (a total of 40 scans) obtained at different slice thicknesses (0.9 mm and 5 mm) and both with and without clinical information. In the consensus stage, definitions for isodense swelling and hypodensity were extracted from simultaneous analysis of NCCT and PCT scans used in the pre-training stage, and potential definitions were circulated to participants for agreement. In the post-training stage, 11 readers assessed 32 scans (5 mm slice thickness) with clinical data after training using the consensus definitions and reviewing examples. Cerebral blood volume (CBV), cerebral blood flow (CBF) and mean transient time (MTT) in each ASPECTS region on all PCT scans were calculated and compared across the three NCCT appearances (normal, hypodense or isodense swelling, and the fate of each ASPECTS region was determined on follow-up NCCT scans.

Results: Training increased detection of isodense swelling from 29.4% to 46.8%; significantly ($P = 0.0001$) improved interobserver agreement from very

poor ($k = 0.09$) to fair ($k = 0.30$); and ameliorated the predictive power of isodense swelling for penumbra as classified by ASPECTS regions of interest (ROIs) from [sensitivity 9% (confidence interval (CI): 1.9%-24.3%); likelihood ratios positive and negative, 2.5 (CI: 0.6-10) and 0.95 (CI: 0.84-1.06), respectively] to [sensitivity 41% (CI: 30.3%-52.8%); likelihood ratios positive and negative, 5.5 (CI: 3.3-11) and 0.64 (CI: 0.53-0.77), respectively]. Detection of hypodensity did not change significantly with training. Exclusion of outliers improved interobserver agreement for isodense swelling to moderate ($k = 0.50$). Experience, speciality and clinical information had no significant effect on agreement; however, 5 mm slices increased interobserver agreement on hypodensity significantly ($k = 0.34$ to $k = 0.46$, $P = 0.01$). Intraobserver agreement on both hypodensity and isodense swelling was almost perfect. Hypodensity had low sensitivity for core (41.6% (CI: 33% - 50.7%)) but good likelihood ratios positive and negative (13.7 (CI: 7.5-24.8) and 0.6 (CI: 0.50-0.70), respectively). Both isodense swelling and hypodensity were highly specific (93.8% and 96.9% for penumbra and core, respectively). CBV was increased significantly in isodense swollen areas compared with hypodense areas ($P < 0.05$). Only 38.3% of isodense swollen ROIs ended in infarction and absence of recanalisation increased odds of infarction four-fold, whereas 90% of hypodense ROIs infarcted with odds of infarction 11 times greater than those of ROIs with isodense swelling.

Conclusion: Penumbra tissue in acute stroke patients appears on NCCT as isodense swollen areas that are distinguishable from hypodense regions' appearance. The detection of penumbra tissue can be improved significantly by training. Isodense swelling most frequently returns normal, particularly in evident recanalisation, and its prognostic value might differ from that of hypodensity.

Table of contents

Abstract	2
Table of contents	4
List of Tables.....	9
List of Figures.....	14
Acknowledgement.....	19
Author’s Declaration.....	19
List of abbreviations	20
Aims of chapters I and II;	25
Chapter I: Introduction.....	26
1.1 Definition and epidemiology of stroke.....	27
1.2 Types of stroke.	27
1- Ischemic strokes.....	27
2- Haemorrhagic strokes	27
1.3 Risk factors	28
1.4 Pathophysiology of stroke.....	29
1.5 Ischaemic strokes	30
1.6 Cerebral blood flow	31
1.7 Infarction core and the concept of ischemic penumbra	33
1.8 Viability thresholds.....	35
1.9 Pathogenesis of cerebral ischaemic injury.....	36
1.10 Development of ischaemic oedema.....	39
1.10.1 Cytotoxic oedema.....	39
1.10.2 Ionic oedema	40
1.10.3 Vasogenic oedema	40
1.11 Progression and fate of ischemic injury.....	41
1.12 Thrombolysis	42
Chapter II: Literature Review	46
2.1 Neuroimaging in acute stroke.	47
2.2 Computed tomography (CT) scans.....	49
2.2.1 Unenhanced CT and early stroke.	50
2.2.1.1 Role of NCCT in diagnosis of ischaemic infarction and exclusion of intra-cerebral haemorrhage.	51
2.2.1.2 Early ischaemic changes (EICs) on NCCT.....	52

2.2.1.3 Terminology and definition of EICs on NCCT.	54
2.2.1.4 Systematic measurements of EICs on NCCT.	60
2.2.1.5 Significance of EICs on NCCT.	63
2.2.1.6 Detection of EICs on NCCT.	64
2.2.1.7 Agreement in assessing EICs on NCCT.	65
2.2.1.8 Analysis of agreement variables.	73
A- Speciality and experience of readers.	74
B- Patient characteristics.	75
C- Scan quality.	75
D- Statistics of agreement.	76
D- Early signs being assessed.	78
2.2.1.9 Detection of Penumbra on NCCT.	78
2.2.1.10 Hyperdense middle cerebral artery sign (HMCA).	80
2.2.2 Perfusion Computed Tomography (PCT) in acute stroke.	83
2.2.2.1 PCT technique.	83
2.2.2.2 Reliability of PCT and its prediction of clinical outcome.	88
2.2.2.3 Comparison of PCT with PMR.	92
2.2.2.4 Multimodal evaluation of acute stroke	93
2.2.3 Computed Tomography Angiography (CTA) in acute stroke	94
2.3 Magnetic resonance imaging (MRI) in early stroke.	96
2.4 Other functional imaging techniques are used for evaluation of acute ischaemia	99
2.4.1 Positron Emission Tomography (PET).	99
2.4.2 Single-photon emission computed tomography (SPECT).	99
2.4.3 Xenon-enhanced computed tomography scan (Xe-CT).	100
Chapter III : Methodology	101
3.1 Study design	102
3.2 Patients.	102
3.3 Readers	104
3.4 CT Scans	104
3.5 Reading the scans	105
3.6. Presentation of scans to readers.	108
3.7 Stage I of the study (First Set of Scans)	109
3.7.1 Study Variables	110
A- Slice thickness	111

B- Clinical information	111
C- Readers' experience and speciality.	113
D- Affected side and normality of scan	113
E- Intra-observer agreement.....	113
3.7.2. First set questionnaire	115
3.8 Consensus stage (consensus set of scans).	115
3.8.1 Appearances of EICs	116
3.8.2 Definition of isodense swelling and hypodensity	121
3.8.3 Consensus between readers	123
3.9 Second stage of the study (second set of scans)	124
3.9.1. Second set questionnaire	124
3.10. Analysis of perfusion parameters for all scans.....	125
3.10.1 Perfusion CT scans	126
3.10.2 Measurement of perfusion parameters.....	127
3.11. Cerebral angiography	129
3.12. Follow-up NCCT scan	129
3.13. Statistical analysis	131
3.13.1 Collection of data.....	131
3.13.2 Agreement	132
3.13.3 Tissue compartments and fate	134
3.13.4 Statistical significance testing.....	134
3.13.5 Study graphs	135
3.14 Ethical considerations	135
Chapter IV (Results): Agreement.	136
4.1 Epidemiology data.....	137
1- Patients' Data.	137
2- ASPECTS Areas Data.	137
3- Hemispheric Involvement of the Scans.	139
4.2 Intraobserver Agreement	139
4.3 Effect of Scan's Factors on Interobserver Agreement	140
4.4 Effect of Training on Interobserver Agreement	145
4.4.1 Trained Group Versus Untrained Group	145
A-Comparison of Interobserver Agreement on EICs Between Trained and Untrained Groups of Readers	145
B- Does the effect of training differ among individual readers ?.....	148

C- Comparison of Interobserver Agreement of Trained and Untrained Groups After Exclusion outliers.	152
4.4.2 Pre- and Post-Training Groups of Readers (same readers).....	157
A- Comparison of Pre- and Post-Training Interobserver Agreement on EICs for the Whole Group.	157
B- Comparison of Pre- and Post-Training Interobserver Agreement on EICs for Each Reader.	159
4.5 Effect of Speciality and Experience on Interobserver Agreement	162
4.5.1 Readers' Speciality.....	162
4.5.2 Readers' Experience.	163
1- Interobserver Agreement Comparison Between Experts and Trainees.	163
2- Interobserver Agreement Comparison Between Trained and Untrained readers in relation to experience.....	164
4.6 Overall Interobserver Agreement on Each Area of ASPECTS.	166
4.7 Hyperdense Vessel Sign (HVS)	168
Chapter V (Results): Tissue fate.....	169
5.1 Consensus results	170
5.1.2 Notes from comparison of acute NCCT and PCT in consensus analysis*	170
5.1.2 Conclusions from comparison process	174
5.2 Fate of tissue categories	177
5.2.1 Fate of Tissue Compartments as Categorised by Readers.....	177
5.2.2 Fate of Tissue Compartments as Categorised by Perfusion Parameters	180
5.3 Relation of NCCT Appearances with Perfusion Categories	182
5.4 Prediction of Tissue Perfusion and Fate by NCCT Appearances	184
1- Isodense Swelling.....	184
2- Hypodensity	185
3-Prediction of Perfusion Categories by NCCT Appearances as Categorised by at Least Four Readers.....	186
4- Comparison of Prediction Between Trained and Untrained Groups.	187
5.5 Comparison of Perfusion Parameters Across the Three NCCT Appearances.	188
Chapter VI: Discussion.....	191

6.1 Discussion.	192
6.2 Limitations of the study	203
6.3 Conclusions	204
Appendix.....	206
Reference List	271

List of Tables

Chapter II

Table 2- 1: Terminology of EICs.....	56
Table 2- 2: Studies of EICs reliability.	67

Chapter III

Table 3. 1: Inclusion and exclusion criteria for both; MASIS and POSH studies.	103
Table 3. 2; First set questionnaire.	114
Table 3. 3; Second set questionnaire.	125
Table 3. 4: Landis and Koch’s scale for agreement level.	133

Chapter IV

Table 4. 1 Patients’ data.....	137
Table 4. 2: frequency and proportion of EICs as categorised by readers on all scans and in each set. And frequency and proportion of ASPECTS areas as categorised by patients on NCCT.	137
Table 4. 3: frequency and proportion of ASPECTS areas as categorised by perfusion CT. These are for the whole set and for each set.....	138
Table 4. 4: frequency and proportion of ASPECTS areas fate on follow up NCCT [* this is the percentage from totally infarcted areas and not from all areas].	138
Table 4. 5: statistics of involved scans and hemispheres [K; kappa].	139
Table 4. 6. Intraobserver agreement for individual readers using trichotomised ASPECTS.	139

Table 4. 7: Cohen’s kappa for intraobserver agreement on regions of ASPECTS template using tables of counts.	139
Table 4. 8 Overall interobserver agreement among the nine readers on each category of EICs by using trichotomous ASPECTS.	140
Table 4. 9: Comparison of average pairwise kappa (APK) of each group of variables across the three ASPECTS categories. [significance level is at $P < 0.05$]. [CVD clinical data]	140
Table 4. 10. Overall interobserver agreement on each category of ASPECTS. for trained versus untrained readers as measured by free marginal kappa (FMK), fixed marginal (Fleiss’s Kappa) (XMK) and intraclass coefficient (ICC)....	145
Table 4. 11: The difference of average pairwise kappa of each category of ASPECTS for trained and untrained groups of readers [* Confidence interval, ** standard deviation].....	146
Table 4. 12: Comparison of average pairwise kappa (APK) for each reader in the trained and untrained groups across the three studied categories[* t.test].	148
Table 4. 13: Comparison of average pairwise kappa (APK) for each reader in the trained and untrained groups across the three studied categories [* t.test].	153
Table 4. 14: Comparison of average kappa before and after training across the three ASPECTS categories.....	157
Table 4. 15: ANOVA analysis of each reader response before and after training with reference to average pairwise kappa of each ASPECTS category.....	159
Table 4. 16: Comparison of average kappa pre- and post- training after exclusion of reader B. [* Wilcoxon test].....	159
Table 4. 17: Comparison of average pairwise kappa of neuroradiologists and stroke neurologists (* Kruskal-Wallis test).	162
Table 4. 18: Comparison of average pairwise kappa of neuroradiologists and stroke neurologists before and after training for each ASPECTS category (* Kruskal-Wallis test, ** one-way ANOVA).	162
Table 4. 19: Comparison of average pairwise kappa of untrained experts and trainees (* MWT Mann-Whitney test).....	163
Table 4. 20: Comparison of average pairwise kappa between trained experts and trainees (MWT Mann-Whitney test).....	163
Table 4. 21: Comparison of average kappa of trained experts with that of untrained experts across the three categories of ASPECTS.	164
Table 4. 22: Comparison of average kappa of trained with that of untrained trainees across the three categories of ASPECTS [* values are the average rank by Kruskal-Wallis].	164

Table 4. 23: Overall agreement on isodense swelling for each ASPECTS region among all readers in the trained and untrained groups [free marginal kappa (FMK) and Fleiss's kappa (XMK)]. 166

Table 4. 24: Fleiss's kappa (XMK) and percentage of positive responses for presence of hyperdense vessel sign and its categorisation and in relation to thick and thin slices scans. 168

Chapter V

Table 5. 1: Chi-square test for classification of NCCT appearances fate in relation to recanalisation. 178

Table 5. 2: The odds of developing infarction in isodense swollen areas with confidence interval and p values. 178

Table 5. 3: Chi-square test for classification of tissue compartments according to fate and recanalisation. 180

Table 5. 4: The odds of developing infarction in isodense swollen areas with confidence interval and p values. 181

Table 5. 5: Chi-square test for relation of NCCT appearances with perfusion categorised areas. 183

Table 5. 6: Predictive statistics of isodense swelling to penumbra, core and infarction..... 184

Table 5. 7: Predictive statistics of hypodensity to core, penumbra and infarction..... 185

Table 5. 8: Predictive statistics of hypodensity and isodense swelling in case of agreement by at least four readers. 186

Table 5. 9: Predictive statistics of isodense swelling and hypodensity for the scans of trained group and scans of untrained group. 187

Table 5. 10: Comparison of averages of mean transient time MTT, cerebral blood volume CBV and cerebral blood flow CBF across the three NCCT appearances. 188

Appendix

Table 1: First set invitation e-mails. 207

Table 2: Consensus invitation e-mail. 208

Table 3: Second set invitation..... 208

Table 4: Table of readers' responses to hypodensity in scans of second set. .. 245

Table 5: Table of responses to isodense swelling in scans of second set 246

Table 6: Total ASPECTS scores for Second set' scans.	247
Table 7; ASPECTS scores for hypodensity. Second set	248
Table 8; ASPECTS scores for isodense swelling. Second set.....	249
Table 9; table of readers' responses to hypodensity of scans of first set	250
Table 10; table of readers' responses to isodense swelling of scans of first set	251
Table 11; ASPECTS scores for both changes. first set.....	252
Table 12; ASPECTS scores for isodense swelling. First set	253
Table 13; ASPECTS scores for hypodensity. First set.....	254
Table 14; Perfusion parameters for each NCCT appearance.	255
Table 15: Pairwise kappa for each ASPECTS category when scans are blinded and non-blinded.	259
Table 16: Pairwise kappa for each set of scans in relation to amount of clinical data across the three categories of ASPECTS.....	260
Table 17: Pairwise kappa for scans with thick slices and scans with thin slices across the three categories of ASPECTS.	261
Table 18: Comparison of average pairwise kappa (APK) of each group of variables across the three ASPECTS' categories. [significance level is at P < 0.05]. [C\ D clinical data, SD; standard deviation, CI; confidence interval]	262
Table 19: Pairwise kappa for each category of ASPECTS for trained and untrained groups of readers.	263
Table 20: Pairwise kappa of each untrained reader on total ASPECTS with overall average [APK].	264
Table 21: Pairwise kappa of each trained reader on total ASPECTS with overall average [APK].	264
Table 22: Pairwise kappa of each untrained reader on hypodensity with overall average.	264
Table 23: Pairwise kappa of trained readers on hypodensity with overall average.	265
Table 24: Pairwise kappa untrained readers on isodense swelling with overall average.	265
Table 25: Pairwise kappa of trained readers on isodense swelling with overall average(APK).	266

Table 26: Pairwise kappa of untrained readers after exclusion of outliers on total ASPECTS with overall average.	266
Table 27: Pairwise kappa of trained readers after exclusion of outliers on total ASPECTS with overall average.	266
Table 28: Pairwise kappa of untrained readers after exclusion of outliers on hypodensity with overall average.	267
Table 29: Pairwise kappa of trained readers after exclusion of outliers on hypodensity with overall average.	267
Table 30: Pairwise kappa of untrained readers after exclusion of outliers on isodense swelling with overall average.	267
Table 31: Pairwise kappa of trained readers after exclusion of outliers on isodense swelling with overall average.	267
Table 32: Pairwise kappa of same readers before and after training for each ASPECTS category.	268
Table 33: Pairwise kappa of each reader before and after training for each ASPECTS category. (1) pre training (2) post training.	268
Table 34: Pairwise kappa in each ASPECTS category for neuroradiologists and stroke physicians.	268
Table 35: Pairwise kappa of stroke neurologists for each ASPECTS category before and after training.	269
Table 36: Comparison of average pairwise kappa between different specialities before and after training.	269
Table 37: Pairwise kappa of trained and untrained expert readers for each ASPECTS category.	269
Table 38: Pairwise kappa of trained and untrained trainee readers for each ASPECTS category.	270

List of Figures

Chapter I

- Figure 1. 1** The mechanism of cerebrovascular occlusion by thromboembolism [Reconstructed from Google images for atherosclerosis] 30
- Figure 1. 2:** Different types and sizes of ischemic infarctions with their haemodynamic patterns (modified from Zulch(13) and Brainin(5)). 31
- Figure 1. 3;** A diagram showing the ischemic penumbra. 34
- Figure 1. 4:** A schematic drawing shows the responses to the fall of CPP. Initially, CBF is maintained by vasodilatation. When CBF drops, OEF increases to maintain CMRO₂. [modified from M S Markus(23) and(24)] 36
- Figure 1. 5:** Mechanisms of ischaemic brain injury [Modified from Pusinelli (25)]. 38

Chapter II

- Figure 2. 1.** Appearance of acute intracerebral haemorrhage by NCCT. The 3 slices are from 3 patients post-thrombolysis; A-small area of ICH. B- ICH with ventricular extension. C- Massive ICH. 52
- Figure 2. 2** Early ischaemic changes from three different patients presented within 6 hours from stroke onset. A- Isodense swelling B- Hypodensity C- Hyperdense vessel sign. 53
- Figure 2. 3:** Early signs of acute stroke as seen within the first 4 hours. A; Loss of insular ribbon B- Obscuration of lentiform nucleus C- Cortical sulcal effacement. 56
- Figure 2. 4:** Examples of hypodensity (yellow arrows). 58
- Figure 2. 5:** Examples of brain swelling in early acute stroke. A- Focal swelling with hypodensity (Both were within the first 4 hours post stroke onset). B- Focal swelling without hypodensity (isodense swelling) Right: at 4 hours post stroke. Left: at 2 hours post stroke. 60

- Figure 2. 6:** Examples of hyperdense vessel sign in NCCT and tissue fate on follow up (>24 hours) scans. A-MCA “Dot” sign (arrow); seen after 154 minutes after stroke onset in a 41-years-old woman. Patient received rtPA with recanalisation and disappearance of HVS and good outcome after 3 months. B-HICA sign as seen in a 76-years-old woman who presented after 137 minutes from onset with severe stroke and had poor outcome. Follow up scan showed infarction of the whole left hemisphere. C-HMCA sign as seen in a 76-years-old woman after 164 minutes from stroke onset. There was no recanalisation and patient had poor outcome. 82
- Figure 2. 7:** PCT perfusion parameters from patient with acute stroke with left side perfusion defect at 5 hours from symptoms onset showing CBV\CBF or MTT mismatch [ASPECTS areas are plotted on the maps]. 84
- Figure 2. 8:** Time attenuation curve plotted from perfusion data of normal brain tissue [modified from Tomandle et al.]. 85
- Figure 2. 9:** Perfusion maps with baseline NCCT and 33-hours follow-up scans showing EICs in a 65 years-old patient with acute stroke. Scanning was done within 3 hours of symptoms onset and accomplished in 17 minutes and rtPA was infused and recanalisation approved. Visually, MTT delineates a total ischaemic area of >2\3 of right hemisphere [M1-M3] areas with different levels of CBV\CBF ratio. Areas with severe reduction of both CBV and CBF and areas with a slightly decreased CBF and normal CBV ended in infarction while areas with normal CBF and normal or increased CBV recovered. 91

Chapter III

- Figure 3. 1:** Study design. 102
- Figure 3. 2:** Recollection of CT scan slices in one image maximum 6 slices and minimum 3 slices. 105
- Figure 3. 3:** Scans on Survey Monkey. 106
- Figure 3. 4:** Responses of readers to one survey (one scan). 107
- Figure 3. 5:** Schematic drawing of repetition process with scans coding [C\D Clinical Data]. 109
- Figure 3. 6:** Same scan with thick slices(A) and thin slices(B). In both situations, the ganglionic and supraganglionic levels of ASPECTS template are only shown. 112
- Figure 3. 7:** Core appearance analysis. Upper: from left to right; Penumbrogram, ROI, Acute NCCT, Histogram thresholds. Lower; Right: densitometry readings with averages of HU units in each ROI. Left: Histogram. 118

- Figure 3. 8:** Penumbra appearance analysis. Upper: from left to right penumbra gram, ROIs, NCCT, Histogram thresholds. Lower; Left; Histogram Right; densitometry readings. 119
- Figure 3. 9:** Appearance of areas with mixed penumbra and core tissues. Red arrows indicate on NCCT and green arrows indicate penumbra areas. 120
- Figure 3. 10:** Scan with mixture tissue. Samples from affected areas show low HU for core areas and similar HU values for penumbra and normal tissue. Green arrows show areas of penumbra (isodense), Red arrows show areas of core (hypodensity). 121
- Figure 3. 11;** Perfusion maps with ASPECTS regions. 128
- Figure 3. 12:** Correlation of ASPECTS area's categories with their fate on follow up NCCT scan. In this example parts of lentiform nucleus and insula ended in infarction..... 130

Chapter IV

- Figure 4. 1:**Linear distribution of pairwise kappa in relation to clinical data for each category of ASPECTS. 142
- Figure 4. 2:** Linear distribution of pairwise kappa in relation to amount of clinical data for each category of ASPECTS. 143
- Figure 4. 3:** Linear distribution of pairwise kappa in relation to slice thickness for each category of ASPECTS. 144
- Figure 4. 4:** Linear distribution of pairwise kappa in each group of readers for each ASPECTS category. 147
- Figure 4. 5:** Plot distribution of pairwise kappa on both changes of each reader in trained and untrained group. 150
- Figure 4. 6:** Plot distribution of pairwise kappa on hypodensity of each reader in trained and untrained group..... 150
- Figure 4. 7:** Plot distribution of pairwise kappa on isodense swelling of each reader in trained and untrained group. 151
- Figure 4. 8:** Linear distribution of APK of each trained and untrained reader on each studied category of EICs. 152
- Figure 4. 9:** Plotting of pairwise kappa of each reader in trained and untrained groups after exclusion of outliers for the three categories of EICs. 155
- Figure 4. 10:** Linear distribution of average pairwise kappa of each reader in the trained and untrained groups for the three categories of EICs after exclusion of outliers..... 156
- Figure 4. 11:** Linear distribution of pairwise kappa before and after training for each category of ASPECTS. 158

Figure 4. 12: Distribution of pre- and post-training pairwise kappa of each reader for the three EICs categories.	160
Figure 4. 13: Linear distribution of average pairwise kappa of pre and post trained readers after exclusion of reader B across the three EICs categories.	161
Figure 4. 14: Linear distribution of overall Fleiss's kappa (XMK) values on isodense swelling for each ASPECTS area in untrained (first set) group and trained (second set) group.	166
Figure 4. 15: Linear distribution of overall Fleiss's kappa values on hypodensity for each ASPECTS area in untrained (first set) group and trained (second set) group.	167
Figure 4. 16: Number of responses on each HVS category on thick and thin slices scans.	168

Chapter V

Figure 5. 1: Scans with mixed penumbra and core tissue. Green arrows: penumbra [isodense swelling] red arrows [hypodensity].	171
Figure 5. 2: Obscuration of lentiform nucleus[black arrows].	172
Figure 5. 3: Example of loss of insular ribbon sign A; With evident core by PCT. B; With evident Penumbra by PCT.	174
Figure 5. 4: The proportion and frequency of each NCCT appearance category in relation to fate and recanalisation [I.F. swelling, isodense swelling; REC, recanalisation].	177
Figure 5. 5: Distribution of proportion and absolute numbers of areas fate for penumbra, core and normally appeared tissue [I.F.swelling: isodense swelling, REC: recanalisation].	180
Figure 5. 6: Proportion and frequency of each perfusion categorised areas in relation to NCCT appearances [I.F.Swelling, isodense swelling].	182
Figure 5. 7: Box and whisker plots of CBV values with minimum and maximum values for the three NCCT categories: hypodensity, isodense swelling and normal tissue.	189
Figure 5. 8: Box and whisker plots of MTT values with minimum and maximum values for the three NCCT categories: hypodensity, isodense swelling and normal tissue.	190
Figure 5. 9: Box and whisker plots of CBF values with minimum and maximum values for the three NCCT categories: hypodensity, isodense swelling and normal tissue.	190

Appendix

Figure 1; ASPECTS template [Supraganglionic level image is loaded from the official web site for description of ASPECTS(227)]	209
Figure 2: Example of a scan from first set loaded to Survey Monkey.	210
Figure 3: Example of a scan from second set loaded to Survey Monkey.	211
Figure 4: a to e, are the slides of consensus power point sheet presented to readers.	212
Figure(s) 5: First set scans.	217
Figure (s) 6; Second Set Scans.	228
Figure 7: Scans analysis for consensus. Red dots; hypodensity. Green dots; isodense swelling.	256
Figure 8: Scans of consensus. Red dots; hypodensity. green dots; isodense swelling.....	256
Figure 9: Consensus analysis. Red arrow heads; hypodensity. Green arrows head; Isodense swelling.	257
Figure 10: Consensus analysis; red dots; hypodensity. green dots; isodense swelling.....	258

Acknowledgement

I would like to express my gratitude and thanks to following people for their generosity and participation in reading the scans;

Keith Muir

Ferghal McVerry

Celestine Santosh

Fuzia Nazir

Tracey Baird

Krishna Dani

Jonathan Foley

Evelyne Teasdal

Fiona Moreton

Nial MacDoughall

Hani Benammer

Kenneth Mitchell

Rafid Al-Sam

Xuya Huang

Dheeraj Kalladka

I wish to thank my supervisor *Professor Keith Muir* for his valuable advice, research ideas and guidance during this period of research. I'm also grateful to my colleague *Dr Ferghal McVerry* who provided me with the information on use of MiStar software in analysing the scans. I appreciate also the tips provided by *Dr Krishna Dani* on analysing MRI scans.

Finally, special thanks go to my Mum for all of her support and encouragement.

Author's Declaration

All of the work contained within this thesis was undertaken by me during my time as a research student at University of Glasgow Department of Neurology. All statistical analyses were performed and written solely by me. This thesis in its entirety is my own original work.

List of abbreviations

A	B
ACA	BASIS
Anterior Cerebral Artery	Boston Acute Stroke Imaging Scale
ACCESS	BBB
The Acute Cerebral CT Evaluation of Stroke Study	Blood Brain Barrier
AIF	C
Arterial Input Function	CBF
ANOVA	Cerebral Blood Flow
Analysis Of Variance	CBV
APK	Cerebral Blood Volume
Average Pairwise Kappa	C\ D
ASPECTS	Clinical Data
Alberta Stroke Program Early CT Score	CDGW
ATLANTIS	Complete Loss Of Differentiation Between Grey-White Matters
Alteplase Thrombolysis For Acute Non-Interventional Therapy In Ischemic Stroke	CI
AUC	Confidence Intervals
Area Under Curve	CSE
	Cortical Sulcal Effacement
	CSF
	Cerebrospinal Fluid.

CT

Computed Tomography.

CTA

Computed Tomography
Angiography.

CTA-SI

Computed Tomography Angiography
Source Image.**D**

DBG

The Disappearing Basal Ganglia Sign

DEDAS

The Dose Escalation of
Desmoteplase in Acute Stroke

DEFUSE

The Diffusion Weighted Imaging
Evaluation for Understanding Stroke
Evolution

DIAS

The Desmoteplase in Acute
Ischemic

Stroke Study

DICOM

Modern Digital Imaging and
Communications in Medicine

DSA

Digital Substraction Angiography

DU

Doplar Ultrasonography

DW-I MRI

Diffusion-Weighted Magnetic
Resonance Imaging**E**

ECASS

European Cooperative Acute Stroke
Studies

EEG

Electroencephalogram.

EICs

Early ischaemic changes

EPITHET

Echo planar Imaging Thrombolytic
Evaluation Trial**F**

FMK

Free Marginal Kappa

G

Gr-Wt

Grey- White Matter Interface.	Isodense Swelling
H	IST-3
HMCA	International Stroke Trial
Hyperdense Middle Cerebral Artery.	ITAIS
HU	The Imaging-based Thrombolysis Trial in Acute Ischemic Stroke
Hounsfield Units	K
HICA	K
Hyperdense Internal Carotid Artery	Kappa Coefficient
HVS	L
Hyperdense Vessel Sign	LIR
Hypo	Loss Of Insular Ribbon
Hypodensity	LR
I	Likelihood Ratio
ICA	M
Internal Carotid Artery	MASIS
ICE	Multicentre Acute Stroke Imaging Study
Idealize-Close-Estimate	MCA
ICH	Middle Cerebral Artery.
Intra-Cerebral Haemorrhage.	MCAT
I.F.Swelling	Middle Cerebral Artery Territory.
Isodense Swelling	MOSAIC
IS-SW	

Multimodal Stroke Assessment Using Ct	Obscuration of lentiform nucleus.
MRA	OEF
Magnetic Resonance Angiography	Oxygen Extraction Fraction
MRI	<i>P</i>
Magnetic Resonance Imaging	PABAK
mRS	Prevalence And\Or Bias Adjusted Kappa
Pre-Morbid Modified Rankin Scale	PCA
MTT	Posterior Cerebral Artery
Mean Transient Time	PCT
<i>N</i>	Perfusion Computed Tomography.
NCCT	PDGW
Non-Contrast Computed Tomography.	Partial Loss Of Differentiation Of Grey-White Matter Interface
NIHSS	PET
National Institutes Of Health Stroke Scale	Positron Emission Tomography
NINDS	PMR
The National Institute Of Neurological Disorders And Stroke	Perfusion Magnetic Resonance
NPV	POA
Negative Predictive Value	Percentage Of Overall Agreements
<i>O</i>	POSH
OLN	Post Stroke Hyperglycaemia
	PROACT

Prolyse in Acute Cerebral Thromboembolism	SITS-ISTR
PPV	Safe Implementation Of Treatments In Stroke-International Stroke Treatment Registry
Positive Predictive Value	
PW-I MRI	SITS-MOST
Perfusion-Weighted Magnetic Resonance Imaging	Safe Implementation of Treatments in Stroke in Stroke-Monitoring Study
R	
REC	SPECT
Recanalisation	Single-Photon Emission Computed Tomography
ROC	T
<i>Receiver Operating Characteristic</i>	TTP
ROI	Time to peak
Region Of Interest	V
r-proUK,	VOF
Recombinant Prourokinase	Venous Output Functions
rtPA	X
Recombinant Tissue Plasminogen Activator	Xe-CT
S	Xenon Computed Tomography
SAH	XMK
Subarachnoid Haemorrhage	Fixed Marginal Kappa [Fliess's Kappa]

Aims of chapters I and II;

- 1- Introducing general idea on stroke as a disease.
- 2- Discussion of pathophysiology of brain ischaemia and evolution of the concept of penumbra(the salvageable tissue).
- 3- Giving general idea on thrombolytic therapy.
- 4- Approaching the early signs of acute ischaemia on non-contrast computed tomography scan (NCCT), their terminology, importance, detection and measurement.
- 5- Reviewing the previous studies on observer agreement on early signs of ischaemia in NCCT and comparison of the ways were used to report the final results.
- 6- Shedding light on the multimodal approach of acute ischaemic stroke.
- 7- Contrasting the role of CT in approaching patients with acute stroke with the role of other imaging techniques, particularly, magnetic resonance imaging MRI.

Chapter I: Introduction

1.1 Definition and epidemiology of stroke.

Stroke is defined by The World Health Organization as a rapidly developing focal (or global) brain dysfunction of vascular origin lasting more than 24 hours, thus including ischemic stroke, subarachnoid haemorrhage, intracerebral haemorrhage and cerebral venous thrombosis(1). It is the fourth most common cause of adult disability, the second highest cause of death worldwide(2) and the third highest cause of death in western world(3). Most studies of stroke epidemiology originate from the developed world, although over two thirds of strokes are thought to occur in developing countries(4). Ischemic stroke is by far the most common type of stroke, constituting around 80% of all strokes, of which 60% are attributable to large-artery ischemia[ischaemia of main arteries and their branches and non-small vessel disease ischaemia] (1). According to Framingham's study, the frequency of different types of acute cerebrovascular disease were 60% caused by atherothrombotic brain infarction, 25.1% by cerebral emboli, 5.4% by subarachnoid haemorrhage, 8.3% by intracerebral haemorrhage and 1.2% by undefined disease(5).

1.2 Types of stroke.

1- Ischemic strokes

These constitute the majority of strokes. Thrombosis and embolism of cerebral arteries are the predominant cause. Less common causes include: severe hypotension, which is responsible for "hypotensive stroke"; vasospasm, which follows subarachnoid haemorrhage; arthritis, such as in giant cell arthritis; and chronic subacute infections, such as tuberculosis.

2- Haemorrhagic strokes

These are closely related to hypertension as a classical aetiology but can rarely be caused by other pathologies, such as small vessel malformations. Intracerebral bleeding can occur anywhere in the brain, but mainly in deep penetrating vessels.

1.3 Risk factors

There are a number of factors which predispose a particular person to developing stroke. These include(6);

A) General risk factors: these include age, gender, race, familial clustering, cigarette smoking, drug and alcohol abuse, being overweight and inactivity.

B) Specific risk factors

1- Hypertension; this is the most common precursor of cerebral infarction with increased risk with high systolic and diastolic values, although even alone an elevated systolic pressure is highly predictive of stroke.

2- Heart disease; this is the second most powerful risk factor after hypertension. Cardiac arrhythmia can cause embolic stroke. Atrial fibrillation is a well-known cause.

3- Previous stroke; this increases the risk of recurrent strokes many times.

4- Transient ischemic attacks; these are defined as a neurological deficit similar to that caused by stroke, but which resolves completely within 24 hours of onset. They are caused predominantly by small emboli. Intracerebral bleeding might also be a cause occasionally. Whether it is associated with focal or non-focal symptoms, it carries a high risk of development into stroke(7).

5- Carotid artery disease; atherosclerosis leads to stenosis and subsequent reduction of cerebral blood flow, which increases the risk of ischemic injury. Atheromatous plaques also work as a source of emboli.

6- Hypercholesteremia.

7- Diabetes Mellitus.

1.4 Pathophysiology of stroke.

Disruption of blood supply to brain tissue is the substrate of cerebrovascular diseases (figure 1-1). Changes in the vessel wall may trigger blockage of blood flow in this vessel. Two major mechanisms can lead to obstruction of cerebral blood vessels and cessation of blood supply. The first is *thromboembolism*, which is by far the most predominant cause of stroke. The most common sources of emboli are the heart and large arteries. Atrial fibrillation is considered the highest risk condition among other cardiac arrhythmias associated with developing of stroke. *Heamodynamic failure* is the second mechanism which may cause flow disruption and is very uncommon. For example, it may lead to severe systemic hypotension or low cardiac output. The blood vessel occlusion might be complete or partial (stenosis), however, intracranial disease is rare so stenosis is not often seen. These changes may also weaken the vascular wall causing blood to break through it into brain parenchyma, resulting in compression, displacement and damage.

Atherosclerosis is a notable cause of cerebrovascular diseases, although acute or chronic vascular diseases of inflammatory origin might be engaged in some instances, such as collagen disorders and chronic infection(5). It is thought that chronic fibroproliferative disease supplied by lipids (4) endothelial cells, leucocytes and intimal smooth muscle cells play the major role in the evolution of this disease. Endothelial cell dysfunction leads to aggregation of lipids inside smooth muscle cells and recruits leucocytes to form fatty streaks. The response-to-injury hypothesis gives an explanation of the progression of such precursor lesions to clear atherosclerosis, postulating that an injury that induces fibroinflammatory repair process ends in formation of atheromatous plaque(8). After plaque rupture or erosion, the clotting cascade is activated leading to progressive thrombosis with subsequent obstruction of blood supply and source of emboli.

Cerebral small-vessel disease is another cause of narrowing vascular lumen and failure of cerebral autoregulation. It is responsible for lacunar infarcts and intracerebral large and microbleeds(9). Hypertension and aging are well-known

risk factors. It is caused by subendothelial accumulation of pathological substances which lead to structural alterations rendering the vessel wall fragile. When these vessels do not progress to rupture, segmental vessel occlusion develops(10).

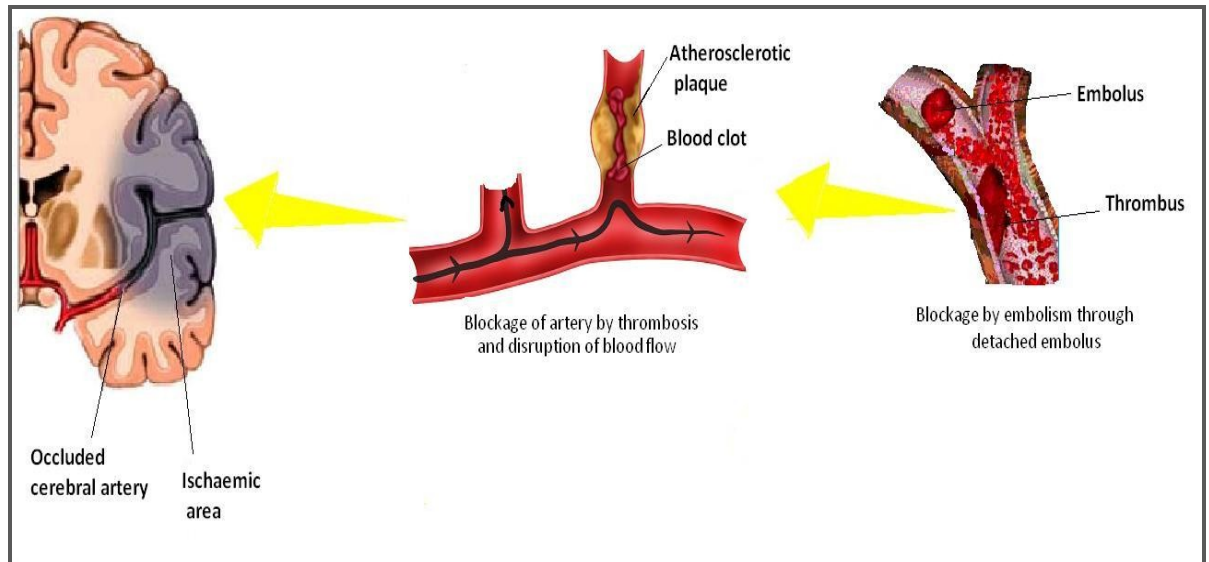


Figure 1. 1 The mechanism of cerebrovascular occlusion by thromboembolism [Reconstructed from Google images for atherosclerosis]

1.5 Ischaemic strokes

Transient or permanent reduction in cerebral blood flow to an area of major brain artery beyond a critical duration of time results in ischemic infarction of brain tissue(11). The development of infarction, its distribution and size depend on the particular patient situation, site and mechanism of occlusion and adequacy of collateral circulation. Infarct sizes can vary from a few millimetres to the whole of a hemisphere(12). Territorial infarcts occur when a major cerebral artery is occluded. When the main stem is blocked and the general haemodynamic situation is poor, it results in total territorial infarct (**figure1-2a**). However, if there is some partial supply from neighbouring anastomoses, the supply area located adjacent to the main stem will infarct (**figure1-2b**), but if the main stem is stenosed and still supplying the periphery then the infarct

area will be shifted to the centre of territory (**figure1-2c**). Sometimes, infarcts may evolve in a watershed area between large territories when arteries are stenosed causing Cerebrovascular insufficiency (**figure1-2d**) (13).

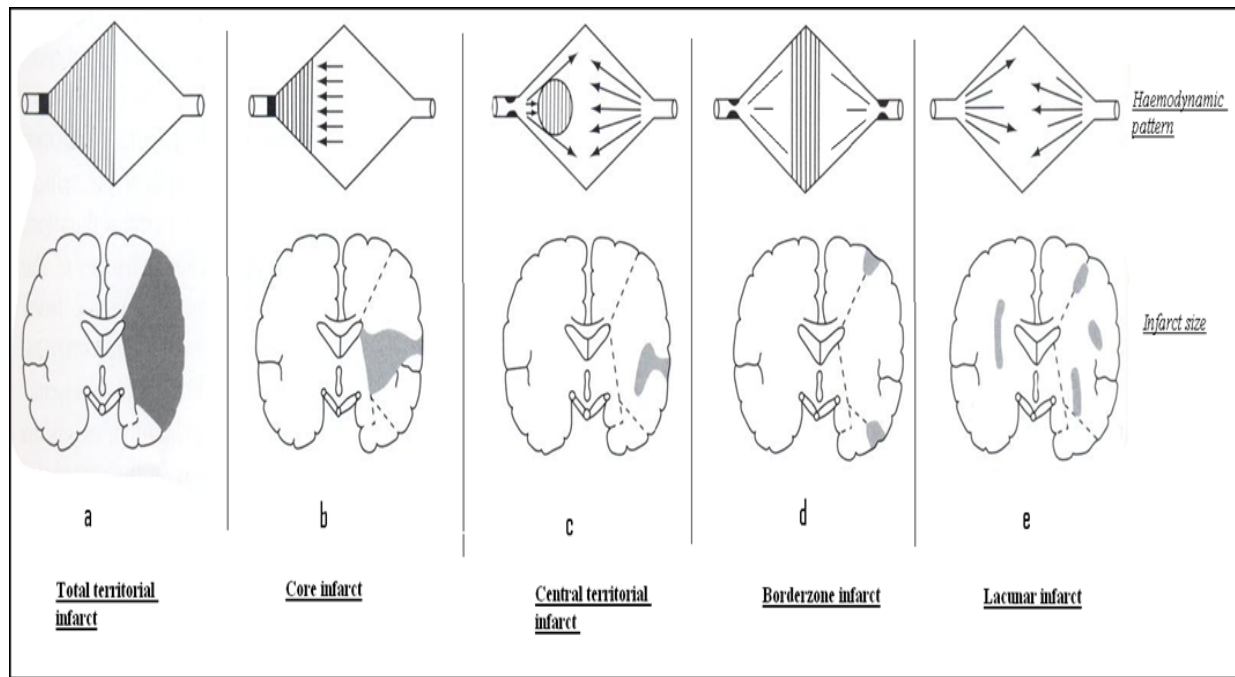


Figure 1. 2: Different types and sizes of ischemic infarctions with their haemodynamic patterns (modified from Zulch(13) and Brainin(5)).

Lacunar infarcts (microinfarcts) are essentially caused by small-vessel disease, and, rarely, by microembolization. They mostly occur in deep-perforating artery territory.(5).

1.6 Cerebral blood flow

Under normal conditions, cerebral blood flow is kept at a relatively constant rate of 50ml/100g/min. It declines gradually with reductions in cerebral perfusion pressure. The cerebrovascular bed is under the control of a number of factors which act to secure energy supply and guarantee the rapid adjustment of local cerebral blood flow (CBF) to the active brain areas. These could be

myogenic, metabolic or neurogenic factors. The flow is largely independent of perfusion pressure alterations over a wide range of pressure, extending in normotensive people from 60mmHg to 130mmHg(14). Vascular resistance is the key to maintaining constant CBF by changing the calibre of principle cerebral resistance vessels (autoregulation). The same change occurs with raised intracranial pressure in the case of fixed arterial blood pressure. However, the pressure-flow regulation cannot maintain CBF beyond its upper and lower limits, but these may be reset in some chronic conditions. For instance, in long-standing hypertension the CBF is kept the same at higher perfusion pressure values which can reach up to 150mmHg, while the lower limit is shifted upward to levels of 80mmHg (12). Cerebral blood vessels are innervated by both, sympathetic and parasympathetic fibres and their effect on CBF regulation is quite small.

In the normal brain, CBF is strictly joined to the physiological conditions of brain regions (metabolic regulation). Thus, increased neuronal activity in a particular brain area entitles it to enhanced cerebral flow. The flow-metabolism coupling mechanism is not fully understood, but release of vasodilators from activated neurons, including nitric oxide, adenosine, potassium and hydrogen, may have a role in this process.

Arterial blood gases are another modulator of CBF. Variations in CO_2 have a profound effect on CBF. Arterial hypercapnia causes cerebral vasodilatation and increases CBF. In contrast, arterial hypocapnia causes vasoconstriction and decreases CBF. CO_2 reactivity is mediated by changes in H^+ concentrations in cerebrospinal fluid surrounding arterioles. With constant pCO_2 , alterations in blood pH have little effect on extracellular pH and CBF. On the other hand, changes in arterial pO_2 are associated with minor changes in CBF, which rises when pO_2 decreases to 50mmHg, and doubles at 30mmHg. Below this threshold, the increase in CBF that accompanies hypoxia is probably because of increased extracellular PH.

1.7 Infarction core and the concept of ischemic penumbra

Cerebrovascular insufficiency is associated with reduced perfusion pressure, which induces local homeostatic mechanisms to preserve normal neuronal function and oxygen uptake. Auto-regulation of CBF compensates for the early drop of perfusion pressure, and, with further drops, CBF begins to fall and this is compensated by increased oxygen extraction. Areas of reduced CBF, which are fully compensated by increased oxygen extraction, are known as oligaemic flow zones. However, with more drop in perfusion pressure, the compensatory mechanisms become exhausted and tissue hypoxia develops. The affected tissue will suffer different levels of ischaemia ranging from moderate to severe with tissue necrosis and infarction (core) according to the level of ischaemic CBF. In this context, the impairment of energy production influences the energy consuming processes in a consecutive manner: first by impairment of the functional activity of the brain, i.e. electrical activity resulting in neurological symptoms; then, at more severe degree of hypoxia, suppression of the metabolic activity is needed to preserve its structural integrity. The blood flow rates of the two different thresholds of hypoxia for preservation of functional and structural integrity are established. When the blood flow range is between “electrical” and “membrane” failure, the neurons become functionally silent but remain structurally intact for a time. During focal ischemia, this flow range correlates with a coronal region embedded between the necrotic infarct core and the normal brain **figure (1-3)**. This has been termed the “penumbra”. This name is a descriptive term in analogy to the partly illuminated zone around the complete shadow of the moon in full solar eclipse. Ischemic penumbra is a dynamic process because tissue tolerance to ischemic damage is dependent on residual blood flow and duration of blood flow disturbance (15).

The concept of penumbra in focal cerebral ischemia was first presented by Astrup in 1981, who defined it as regions of brain tissue where reduced blood flow is sufficient to cause hypoxia severe enough to halt physiological function, but not so complete as to cause irreversible failure of energy metabolism and cellular necrosis (16). Since that time, the concept of penumbra has become

increasingly important with the expansion of the treatment of acute ischemic stroke. However, there is no universal definition of the ischemic penumbra, and the operational definition depends on the way that the penumbra is evaluated (17).

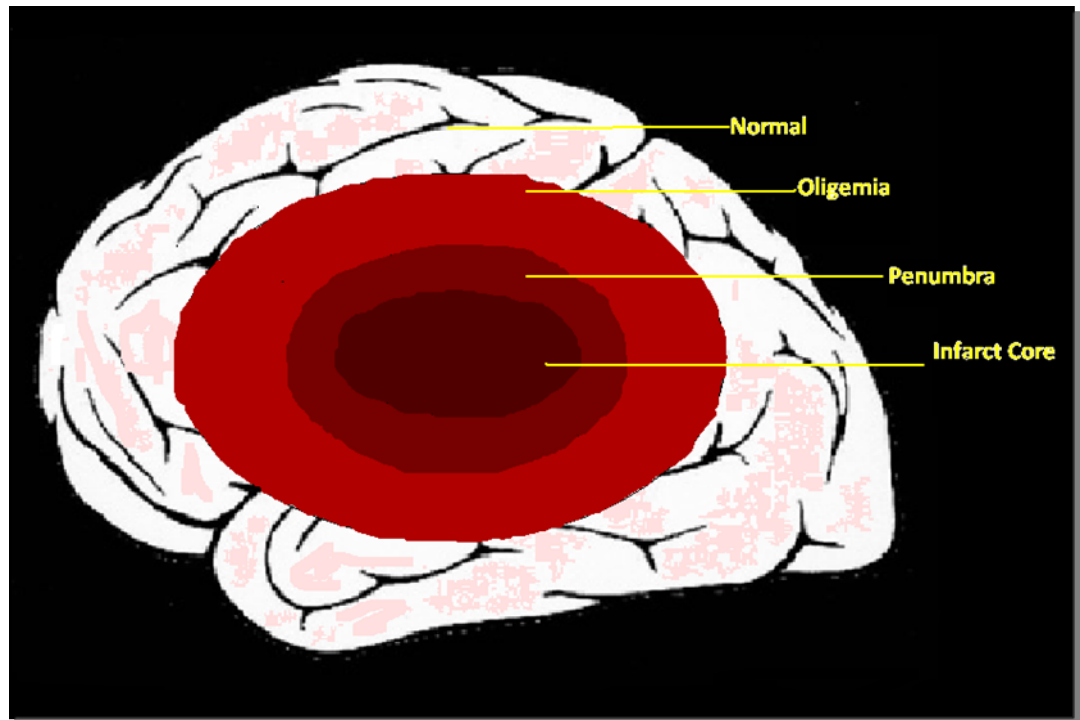


Figure 1. 3; A diagram showing the ischemic penumbra.

Classically, it relied on the electrophysiological and hemodynamic parameters, but more recently the concept has been widened to include metabolic, cellular and therapeutic parameters of ischemic penumbra(18). A broader definition by Hossmann has assumed that the penumbra is an ischemic tissue with limited blood supply and preserved metabolism (19). However, Ginsberg and Pulsinelli assumed that this metabolism could undergo intermittent compromise (20). A more relevant definition in relationship to therapeutic intervention was suggested by Hakim, who prescribed the penumbra as “fundamentally reversible” ischemic tissue(21). This definition gave the penumbra a considerable clinical impact because it identifies the penumbra as a region of

potential reversibility which can be reactivated after arterial occlusion by increasing CBF (19). However, the penumbra is a dynamic and a transient area which develops over time. It is obvious that CBF reductions that characterize potential reversibility early after occlusion likely define irreversibility at later times. Moreover, several factors might affect the evolution of penumbra on an individual patient basis. Aside from the time since onset, these include residual blood flow, temperature, metabolic parameters (such as glucose) and the anatomical resolution of the technique applied. Therefore, the penumbra is unique for each individual patient. In this case, the time window for acute stroke treatment will differ according to each individual pathophysiological state (22).

1.8 Viability thresholds

Complete cessation of cerebral circulation causes loss of function at various flow thresholds. These were determined in different animal species with different reported flow values, but, when compared, a distinct rank order of susceptibilities can be established(19). In human beings, a flattening of EEG occurs directly after the hemispheric flow falls below 0.16-0.17ml/g/min, as evidenced by measurements of cerebral blood flow and EEG during clamping of one carotid artery in an endarterectomy (16). The evoked somatosensory potential is suppressed at local flows between 0.15and 0.23 ml/g/min. However, individual neurons vary in their functional threshold rates between 0.06 to 0.22ml/g/min, which signifies selective vulnerability even within small cortical sectors. The functional threshold is determined when reversible paresis appears at the flow value of 0.23ml/g/min and irreversible paralysis occurs between 0.17 and 0.18ml/g/min (19).

Unlike electrophysiological function, which deteriorates immediately, histological damage needs more time to develop. Whereas neuronal function ceases immediately if the flow drops below the threshold, the development of irreversible morphological damage depends mainly on duration of ischemia. It

starts at low flow values below 0.10ml/g/min after short duration of ischemia with a loss of cell function.

Simultaneous recordings of cortical neuronal metabolism, local blood flow and cerebral perfusion pressure during and after ischemia of different degrees yield a curve which shows the worst possible pattern of residual blood flow and ischemia still permitting neuronal recovery **figure1-4** (12).

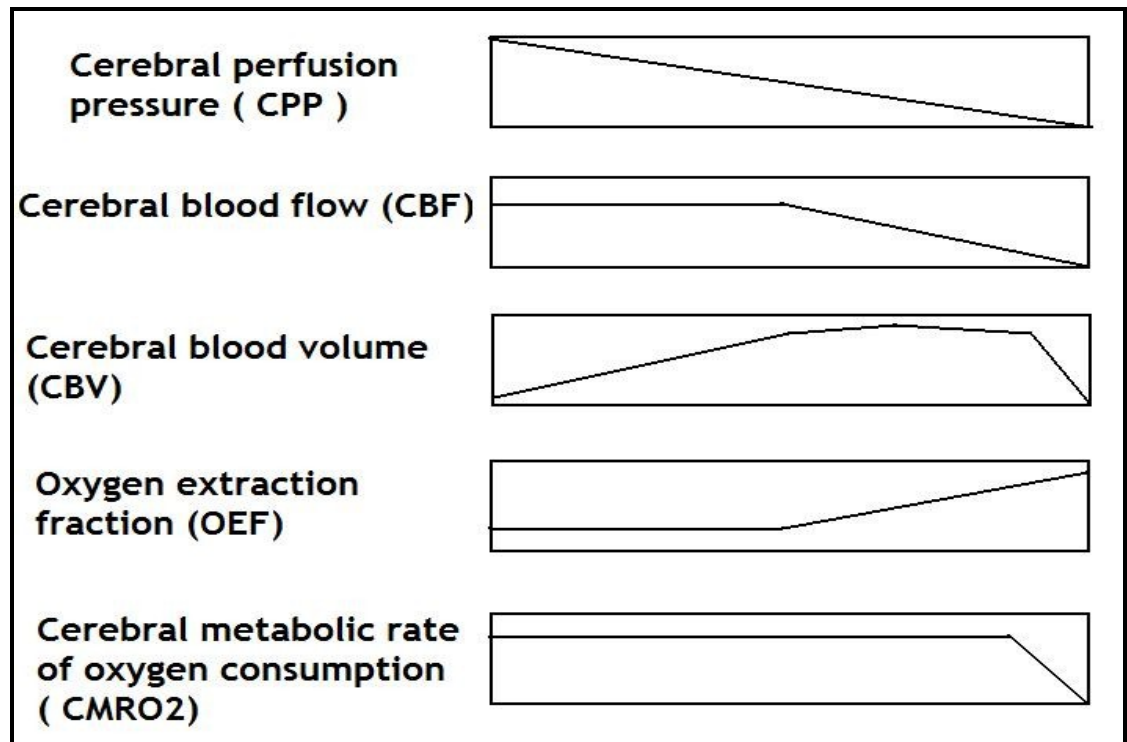


Figure 1. 4: A schematic drawing shows the responses to the fall of CPP. Initially, CBF is maintained by vasodilatation. When CBF drops, OEF increases to maintain CMRO₂. [modified from M S Markus(23) and(24)]

1.9 Pathogenesis of cerebral ischaemic injury.

The brain tissue energy requirements are very high and depend mainly on oxidative phosphorylation for energy production, with glucose as its sole substrate. Therefore, sufficient delivery of substrates, particularly oxygen and glucose, must be constantly maintained. 87% of total energy consumed is

required by signalling, mainly action potential propagation and postsynaptic ion flux (5). Ischaemia triggers a complex chain of reactions which ends in neuronal death and consequent loss of neurological function (**figure 1-5**). Failure of high-energy metabolism due to depletion of high-energy phosphate with overwhelming cellular electrolyte disturbance is the early mechanism responsible for evolving cerebral ischemic injury. Within minutes of ischemia, anaerobic glycolysis leads to the accumulation of acidic metabolites with resultant intra and extracellular acidosis. This facilitates the release of free radicals, thus contributing to cell damage(25). The decreased pH and disappearance of substrate causes an inhibition of mitochondrial activity which augments the decline of high energy compounds (ATP). ATP depletion is associated with ionic-pump failure which results in massive release of intracellular K^+ to extracellular space and marked increase of intracellular Na^+ . This induces persistent anoxic depolarisation which allows Ca^{2+} influx. Subsequently, many neurotransmitters are released at toxic levels, including amino acids, especially glutamate, exacerbating energy demand and disturbance of ion homeostasis. Ca^{2+} overload activates many injurious mechanisms which cause cell membrane degradation, the formation of free radicals and the release of cytochromes (released as a result of mitochondrial damage and most likely to initiate apoptosis). Additionally, it leads to the production of free fatty acids which end in the formation of irritant tissue substances including prostaglandins and thromboxanes, which can induce a strong inflammatory response and cause platelet aggregation, clotting, vasospasm and oedema(26).

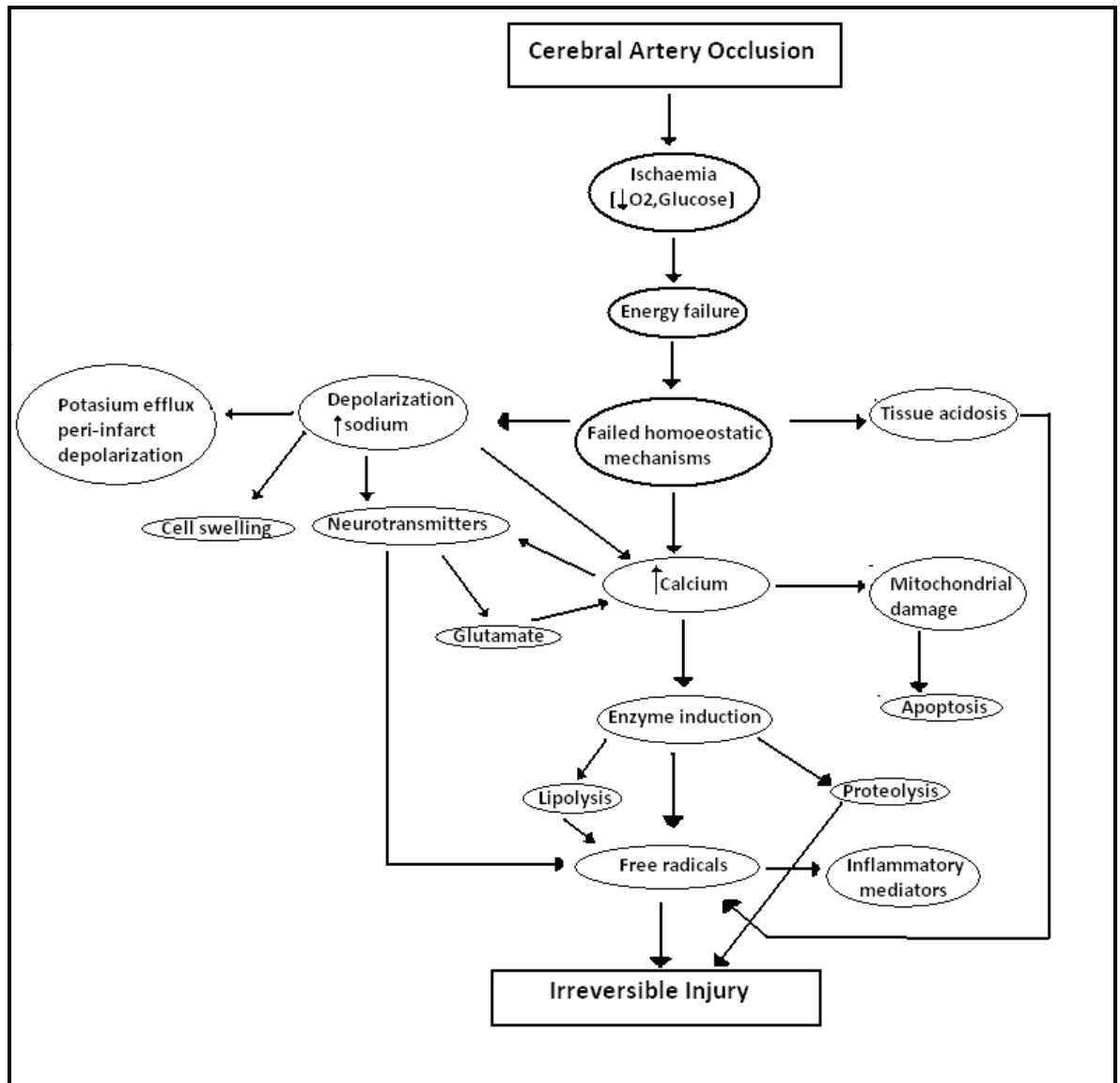


Figure 1. 5: Mechanisms of ischaemic brain injury [Modified from Pusinelli (25)].

The amount of cellular damage is greater with increased glucose concentration, which is most likely due to its effect on lowering the tissue pH. All of these derangements depend on the degree and duration of ischaemia; in severe ischaemia (core region) they are propagated to necrotic cell death, while in moderate ischaemia (penumbra), energy is used to preserve cell viability at the expense of electrophysiological activity, and with a prolonged duration of ischaemia, either necrotic or apoptotic cell death may occur depending on the severity of the initial injury (11;25-27).

1.10 Development of ischaemic oedema

Cerebral oedema is defined as an absolute increase of brain tissue water content. Oedema is damaging because it leads to swelling which aggravates ischaemic injury. Swelling indicates an increased volume of brain tissue because of the shift of water from one space to another. It accounts for the earliest markers of pathological changes associated with acute ischaemic stroke seen on imaging techniques(11). It appears as an area of low attenuation on non-contrast computed tomography scan (CT) due to the excess water content of tissue. In addition, signs of mass effect, including sulcal effacement and ventricular distortion, can be seen on magnetic resonance, and it appears earlier as a white region on T2-weighted images(28). However, very early oedema does not lead to tissue swelling because no new constituent is added to the intravascular space. Ischaemic brain oedema can be divided into three distinctive types: cytotoxic oedema, ionic oedema and vasogenic oedema(29;30); the last two of which require blood flow to cause swelling(5).

1.10.1 Cytotoxic oedema

This is the first to develop after the onset of ischaemia. Osmotically active solutes, mainly Na^+ , accumulate intracellularly, resulting in osmotic expansion of the cell. Failure of ATPase-dependent ion transport across cell membrane is accompanied by a Na^+ influx, which drives chloride ions to enter the cell. The net influx of Na^+ increases intracellular osmolarity, which generates an osmotic gradient that causes water movement from the extracellular into the intracellular space, causing cytotoxic cell swelling. Affected cells depolarize and become deformed. At this early stage, water is not replenished in the extracellular space and total brain volume remains unchanged, although cell size is increased. In brain imaging, this fluid shift is evident as a decreased apparent diffusion coefficient (ADC) of water, which is reflected in increased signal intensity on diffusion-weighted magnetic resonance imaging(31). Eventually, plasma membranes of swollen cells rupture and undergo oncotic or necrotic cell

death. Cytotoxic oedema builds up a new gradient for sodium, chloride and water across the capillary of the blood-brain barrier between the intravascular and extracellular spaces, which creates a transcapillary driving force for the movement of water along with presence of appropriate capillary permeability. Thus, cytotoxic oedema supplies the driving force for the formation of ionic and vasogenic oedema and, eventually, brain swelling (11;29-32).

1.10.2 Ionic oedema

This heralds endothelial dysfunction. Capillary endothelial cell permeability is increased due to an increase in expression of transport proteins induced by ischemia and with the generated force in extracellular space (osmotic gradient), solute and water move from vascular compartment into interstitium of brain tissue, thus replacing them in the extracellular space that was consumed by the formation of cytotoxic oedema(29). The formation of ionic oedema occurs with the normal exclusion of macromolecules, because the blood-brain barrier remains intact. It precedes vasogenic oedema by 6 hours or more(30). Selective flux of Na^+ across the blood-brain barrier can be attributed to two mechanisms, primary and secondary active transport. Secondary active transport mechanisms are determined by pre-existing electrochemical gradients. At this stage of oedema, hydrostatic pressure gradients are irrelevant in formation of oedema,

Essentially, this is all due to intact capillary tight junctions, unlike osmotic pressure which is the main determinant of the driving force. The net tissue water content is increased and consequently brain volume also increases (29;30;33).

1.10.3 Vasogenic oedema

This is initiated when the blood-brain barrier disintegrates and serum proteins start to seep from the blood into the brain. This disturbance further amplifies accumulation of water in interstitium due to increases in its content of osmotically active molecules, including sodium and macromolecules. Capillaries function like fenestrated capillaries when the integrity of the blood-brain barrier

is lost and both hydrostatic and osmotic pressure gradients augment oedema formation. Several molecular mechanisms might be blamed on the permeability of changes during vasogenic oedema (29;33). The latter two types of oedema may reverse the narrowing of extracellular space caused by cytotoxic oedema and the progression of ischemia; it is rapidly enlarged causing marked increase in tissue pressure, which may in turn affect the surrounding tissue resulting in a reduction in regional CBF. The increased total water content of tissue is reflected by increased signal intensity on T2-weighted MRI (33). However, early hypodensity before mass effect on computed tomography scans may be used to distinguish ionic from vasogenic oedema(30).

1.11 Progression and fate of ischemic injury

Progression of ischaemic injury can be differentiated into three phases: the *acute phase* occurs within a few minutes after the onset of ischemia resulting in terminal depolarization of cell membranes and the establishment of an infarct core. Then comes the *sub acute phase*, in which the infarct core expands by means of peri-infarct spreading depression and molecular cell injury until it recruits the entire surrounding penumbra after 4-6 hours. Finally is *the delayed phase*, which may persist for several days or weeks. During this phase, secondary phenomena such as vasogenic oedema, inflammation and possibly programmed cell death may further advance progression of the injury(5).

Recovery of the synaptic transmission and its connection with the severity and duration of ischemia is especially applicable to clinical management. Neuronal vulnerability varies significantly, but most neurons tolerate durations of ischemia of 1-2 hours, at flows only above 15 ml/100g/min, which indicates that a useful recovery of function after hours of ischaemia is only possible from flows in the penumbral range. Irreversible tissue damage can be caused by severe ischaemia below the penumbral range more rapidly than effective treatment can be performed. Within the penumbra, therapeutic intervention may lead to recovery and prevent infarction. As with functional recovery, the severity and duration of ischemia are important determinants of the development of infarction; therefore, failure to recover is correlated with the presence of

structural damage. The penumbra may persist for several hours, maintaining the tissue structure and giving the potential for function recovery(12).

1.12 Thrombolysis

To establish effective therapies for treatment of acute ischaemic stroke, there needs to be easily recognised targets. Logically, the target should be ischaemic tissue, as it is capable of responding to appropriate and timely treatment, meaning it is potentially salvageable and not irreversibly injured tissue which has no potential to recover function. This salvageable tissue is consistent with the ischaemic penumbra. Thus, distinguishing the penumbra from irreversible infarct core and determination of its existence and extent would benefit strategies of stroke therapy(34). Two approaches can be followed to direct treatment toward its primary purpose: a *vascular approach*, such as early reperfusion to limit ischaemia; and a *cellular approach*, such as interference with a pathochemical cascade to prevent further neuronal damage. However, since perfusion disturbance is the fundamental cause of progressive cellular death and infarction, fast and effective restoration of blood supply to flows above the critical threshold is crucial to secure ischaemic tissue(35). Because thromboembolism is responsible for the majority of strokes, thrombolytic therapy was suggested to lyse clots and reopen occluded cerebral arteries. Clinical gains of thrombolysis are related to reperfusion of tissue and limitation of stroke growth. A number of thrombolytic agents were used in clinical trials, including recombinant prourokinase (r-proUK), streptokinase and recombinant tissue plasminogen activator (rtPA) (alteplase)(36). However, rtPA is the only commonly-used thrombolytic agent and its efficacy, safety and feasibility in treatment of acute ischaemic stroke have been widely studied. It can improve neurological and functional outcomes when administered within the first 4.5 hours of symptom onset. While it is a highly effective treatment, it faces the challenge of a narrow therapeutic window and the possibility of developing a brain haemorrhage (37-39).

rtPA was first approved as treatment for acute ischaemic stroke by the US Food and Drug Administration in 1996 (40;41). This was based on results of a randomised controlled trial (NINDS) published in 1995 which found that administration of intra-venous t-PA within the first 3 hours of onset of stroke symptoms in selected patients, according to particular inclusion criteria, improves the clinical outcome at three months(42). Other trials were also conducted to prove the efficacy of thrombolysis in the treatment of acute stroke, the most important was by European Cooperative Acute Stroke Studies (ECASS I), which differed in that the dose of rtPA was higher than that used in NINDS, the time window was expanded to 6 hours instead of 3 (with median time to treatment of 4 hours), and the inclusion of a high proportion of patients with extensive pre-treatment computed tomography (CT) changes of ischaemia.

These factors were the drawbacks of ECASS I which led to a higher mortality rate after one month and significantly increased the incidence rate of intracranial haemorrhage in rtPA-treated patients over placebo-treated patients (43). However, the target population analysis (per-protocol) showed significant differences in favour of the alteplase group. In ECASS II the dose of rtPA was reduced and imaging selection criteria for the trial were more carefully defined, with inclusion of training for physicians to recognize the early ischaemic changes on CT. The results supported the efficacy of rtPA in treating acute ischaemic stroke within 3 hours, and probably within 6 hours, of the onset of symptoms, though only when re-analysed with a different primary end-point(44). The Alteplase Thrombolysis for Acute Non-interventional Therapy in Ischemic Stroke (ATLANTIS) study found no benefit in using rtPA beyond the first 3 hours of onset, but there was increased risk of symptomatic intracerebral haemorrhage(45). However, it added more evidence of its efficacy in the treatment of acute ischaemic stroke when it was given within the first 3 hours(46). The SITS-MOST (Safe Implementation of Treatments in Stroke in Stroke-Monitoring Study) prospective registry further suggested its efficacy and safety in routine clinical use(47). Later, ECASS III proved its efficacy when administered within 3 to 4.5 hours after the onset of stroke with the same incidence rate of haemorrhage reported in previous trials(48;49), although with a less severely-affected clinical population. These results were also confirmed by the SITS-ISTR (Safe Implementation of Treatments in Stroke - International

Stroke Treatment Registry)(50). More recently, the third international trial (IST-III); The Benefits And Harms of Intravenous Thrombolysis with rtPA Within 6 Hours of Acute Stroke Onset, approved the efficacy of thrombolysis in improving the outcome when introduced within the first 6 hours of acute stroke(51). The Echo Planar Imaging Thrombolytic Evaluation Trial (EPITHET) showed that alteplase had an insignificant effect on infarct growth, but a significant effect on reperfusion, and so supported the use of reperfusion as a surrogate for outcome in future proof-of-concept stroke trials. However, when baseline lesions of less than 5ml were excluded there was significantly lower growth of infarct in the alteplase group than in the placebo group(52).

However, the use of rtPA is limited and although most neurologists recommend its use as emergency treatment for acute stroke, many clinicians in emergency departments, in the USA in particular, have concerns about its safety(53). The narrow therapeutic window, the increased possibility of developing brain haemorrhage, and the strict inclusion criteria are the main barriers that make accessible and practical use of thrombolysis difficult. The majority of stroke patients do not meet the inclusion criteria for therapy because of delays in obtaining the treatment(54). These can result from factors related to the patient or the treating staff. Failure to recognize stroke symptoms and seek appropriate medical advice by patients or their families, consideration of stroke as a non-urgent event by emergency staff, delays in neuro-imaging and inefficiency of emergency stroke care were the main reported barriers(54;55). Studies and clinical trials to improve the efficacy of thrombolysis and widen the therapeutic window beyond 4.5 hours have been done. In the Diffusion Weighted Imaging Evaluation for Understanding Stroke Evolution (DEFUSE) study, MR imaging was used and the MRI characteristics that were most likely to significantly benefit from thrombolysis between 3 and 6 hours of onset were employed(54;56). EPITHET also used MRI to assess the infarct growth and reperfusion in patients who had a mismatch between DWI and PWI lesions(52). The Imaging-based Thrombolysis Trial in Acute Ischemic Stroke III (ITAIS III) is an ongoing study recruiting patients into thrombolysis by using CT scan(57). Desmoteplase is a thrombolytic agent which has a longer half-life and higher fibrin specificity than alteplase. It has shown promise when used up to 9 hours from stroke onset with the use of MR imaging as a baseline for treating

patients(57;58). Although the DIAS II trial showed no benefits of desmoteplase between 3-9 hours after stroke onset, the DIASIII/IV trials are currently recruiting patients with more careful selection criteria (59).

Chapter II: Literature Review

The main issue of this review is to shed light on the early signs of acute ischaemia which could be recognised by current imaging modalities, particularly computed tomography (CT) scans. The key words used to search for the appropriate literature were acute, ischaemic, stroke, penumbra, early, changes, signs, hypodensity, x-ray hypoattenuation, focal swelling, inter-rater agreement, computed tomography, scan, MR imaging, CT perfusion and angiography, diagnosis and hyperdense vessel.

The tools for this search were the library data base by connecting to OVID, Pub med and Web of knowledge. Generally, I looked for literature published between 1990 and March 2012. Sometimes, older papers were included because of their relevance and reference to them in the more recent papers. There were around 300 papers reviewed, including clinical trials, observational studies, clinical and systematic reviews and editorial comments by authors. Of these, only the most relevant ones to the aim of this study were included. These were mainly papers which studied early ischaemic changes (EICs) on CT scan, specifically; the reliability of detection of these changes in early stroke and in particular those which aimed to approach the observer agreement on EICs comprehensively.. Also, papers which involved specific study of penumbra tissue in acute CT were included in this review. Other relevant papers were those which studied acute stroke CT techniques and compared it with MRI. However, papers which studied observer reliability using MRI or which used MRI alone in studying acute stroke were irrelevant to this review and also, papers which involved non-human subjects were excluded.

Selected papers were then reviewed according to their relevance to the aim of the study. All papers which studied the observer reliability in detection of EICs were fully reviewed and compared with each other while other literature were either scanned in full or reviewed only by their abstracts.

2.1 Neuroimaging in acute stroke.

Advances in imaging techniques have revolutionised the overall approach to acute stroke management and put neuroimaging forward as its cornerstone (60;61). Previously, it was thought that the brain's plasticity to recover from any

acquired injuries was limited and its ability to withstand oxygen deprivation only lasted a few minutes. Thus, a stroke was considered a hopeless disease which left patients with major disability or in extensive rehabilitation programmes and shortened their life span. Therefore, there was no need for imaging to provide detailed information about parenchyma and blood vessels in the early acute stages of a stroke, but mainly to exclude other differential diagnoses, particularly haemorrhagic stroke, and to follow up the patient. This nihilism around stroke management has changed since the introduction of thrombolytic therapy which converted acute ischaemic strokes into a treatable disease (62;63). A different range of imaging techniques has evolved that gives detailed information about the size, location and nature of an ischaemic lesion, the status of cerebral perfusion and the status of intra and extra cranial vasculature (64). Both functional and structural imaging have played a central role in deepening our understanding of strokes and documenting the differences in subjects' response potential to therapy in relation to individual pathophysiological and hemodynamic states (22). Primarily, imaging in the acute phase of a stroke may be used to diagnose the stroke, rule out other diagnoses, define the site of arterial occlusion, determine the origin of the stroke by evaluating cervical arteries, assess the level of hypoperfusion, evaluate the viability and reversibility of brain lesions, detect early stroke complications such as cerebral herniation or haemorrhagic transformation and provide information about the possible clinical outcome. In routine clinical practice, the precise mapping of potentially salvageable ischaemic tissue is another goal of imaging. However, some of the constraints on the imaging approach include that it should be performed as fast as possible, availability, expense, duration and the ease of data acquisition, processing and interpretation and risks to the patient, such as exposure to contrast and radiation (65). Thus, familiarity with neuroimaging techniques and knowledge of what they tell us about pathophysiology is an essential requirement for all stroke professionals (63). The ideal neuroimaging method in acute strokes should be widely available, inexpensive and provide rapid non-invasive, multimodal information about tissue viability, perfusion and cerebral vasculature. Although no single imaging modality currently meets these criteria, a combination of more than one technique gives clinicians the critical information required to guide treatment decisions (65). However, the ongoing advances and multiplicity of imaging techniques have increased the complexity

of decision making in clinical practice. They are recommended to manage acute strokes on both a clinical and a pathophysiological basis (66).

Recently, newer neuroimaging techniques have allowed evaluation of the haemodynamics of ischaemia and assessment of important pathophysiological variables. Although no single technique can fully investigate acute strokes, a multimodal approach with more than one imaging mode is suggested. The major structural neuroimaging tools are computed tomography (CT) and magnetic resonance imaging (MRI). Positron emission tomography (PET), xenon computed tomography (Xe-CT) and single-photon emission computed tomography (SPECT), diffusion and perfusion MRI and CT perfusion (CTP) are the touchstone of functional neuroimaging. In this review, I will focus on the CT scan's role in acute strokes with some overview on MR imaging and other imaging techniques.

2.2 Computed tomography (CT) scans.

The acute stroke approach has been a giant leap since the introduction of CT scans in the 1970's. The CT scan is considered the most widely used diagnostic technique for evaluation of patients with acute ischaemic stroke and it is highly recommended as the initial modality of choice for stroke investigation (67). This is because it is widely available, accessible, fast, and patient tolerable, i.e. critically ill, uncooperative and restless patients can be imaged. In addition, most thrombolysis trials were CT based (61;68;69). Basically, it is used to rule out non-vascular pathologies such as tumours and exclude haemorrhage with high sensitivity (70). Apart from this, early ischaemic changes can be detected by non-contrast CT scan in around 75% of patients with middle cerebral artery (MCA) stroke (71). These include hypodensity, focal swelling and the hyperdense vessel sign. Subsequently, there has been a growing interest in using CT scan to identify early ischaemic changes, particularly with the advent of alteplase thrombolysis. This has been involved in approaching strokes in the very early phase with the facilities to obtain more accurate, quicker and more comprehensive information about evolving ischaemic injury. Thus, besides the unenhanced CT scan as a structural imaging approach, there are the perfusion CT scan as a functional neuroimaging technique and CT angiography as an

imaging tool for intra and extra-cranial vasculature. All modern CT scanners are now using a helical CT scanning facility which shortens the scan time and allows coverage of the entire head, and with the advent of multi-slice helical CT scanners there has been an increase in the speed and amount of data collection. All of the mentioned modalities of the diagnostic CT scan are used in the initial investigation of early strokes. However, conventional CT contrast enhancement is not recommended in acute strokes and rarely helpful in subacute stroke stages either. Although concerns about extravasations of contrast and worsening of the stroke have arisen, there is as yet no supporting evidence of this (66;72).

2.2.1 Unenhanced CT and early stroke.

Plain CT or non-contrast CT (NCCT) remains the backbone of emergency neuroimaging in acute strokes, mainly to exclude brain haemorrhages and other non-vascular pathologies which are important in determining the further management of the patient. NCCT is typically performed in an emergency department using a multidetector helical scanner. In general, imaging parameters are adjusted to improve overall image quality and reduce the radiation dose, noise and artefacts. These include speed, pitch, rotation time, table speed, slice thickness, image spacing and field of view parameters. Physically, CT scans measure the X-ray beam attenuation through the region of interest using Hounsfield Units to express attenuation values. Hounsfield Units are a linear scale in which water has a value of zero. Thus, any tissue denser than water (high HU values) appears lighter than water on NCCT whereas low-density tissues appear darker than water. Typically, grey matter has attenuation values of 30-35HU and white matter 20-25HU, and hence grey matter appears lighter than white matter on the NCCT. Ischaemic tissue on the NCCT appears with reduced radiolucency or hypoattenuated, due to the increased tissue content of water and decreased blood volume. The HU attenuation is directly proportional to the tissue content of the water; every 1% increase in tissue water content is associated with a 2.5HU drop in attenuation of the NCCT image (73). It can be difficult to see such small changes in HU on NCCT, and hence the subtlety of early ischaemic changes. This is in particular within the first 3 hours of time window for thrombolysis, when these changes might not be seen at all.

The rate of decline of tissue density depends upon the severity and duration of ischaemia. Therefore, the clarity of hypodensity on NCCT may help estimate the time interval since stroke onset. Early ischaemic changes on the NCCT represent different underlying pathological processes. Tissue hypodensity is associated with severe reduction of cerebral blood flow and volume compatible with infarct core and its extent can predict final infarction (74), while areas with isodense swelling are associated with increased cerebral blood volume and moderate hypoperfusion reflecting salvageable tissue (61;65;75). Thus, early ischaemic changes include elements of both core and penumbra [as illustrated in the previous chapter, Section 1.7)

2.2.1.1 Role of NCCT in diagnosis of ischaemic infarction and exclusion of intra-cerebral haemorrhage.

Identification of the signs of ischaemia on the NCCT is important for making a decision concerning thrombolysis. Early signs of acute ischaemic stroke on the NCCT, within the first 6 hours, are typically subtle and sometimes cannot be seen (**Figure 2-2**). Over the first few days, they become more obvious and well-demarcated (68;76-78). Although the clinical evaluation represents the main diagnostic tool of strokes in patients presenting with acute neurological deficit it cannot confirm ischaemia and exclude haemorrhage.

Distinguishing ischaemia from cerebral haemorrhage on bedside examination is difficult due to the lack of feasible differentiating clinical features (79-82). Therefore, imaging the patient using NCCT or MRI, to exclude haemorrhage is required. Acute haemorrhages are large enough to be seen on NCCT (83). They appear with increased density due to clotted blood (**Figure 2-1**). Much of the literature assumes that NCCT has high sensitivity for detection of ICH, and describes it as the diagnostic imaging technique of choice for exclusion of ICH in the hyperacute stage of strokes (68;70;82;84-86). However, there were no studies which evaluated the sensitivity of the NCCT for this detection (86;87). On the other hand, many authors argued that MRI is as sensitive as NCCT in the detection of acute haemorrhage and superior to NCCT for the detection of

chronic haemorrhages and it might substitute NCCT as the first line imaging in acute strokes to avoid use of two imaging techniques and save time and minimise costs (88-95). But the wide availability and easy access to NCCT, in addition to its limited contraindications, have made it preferred to MRI for exclusion of haemorrhage in most guidelines for acute stroke management (80;85;96-100).

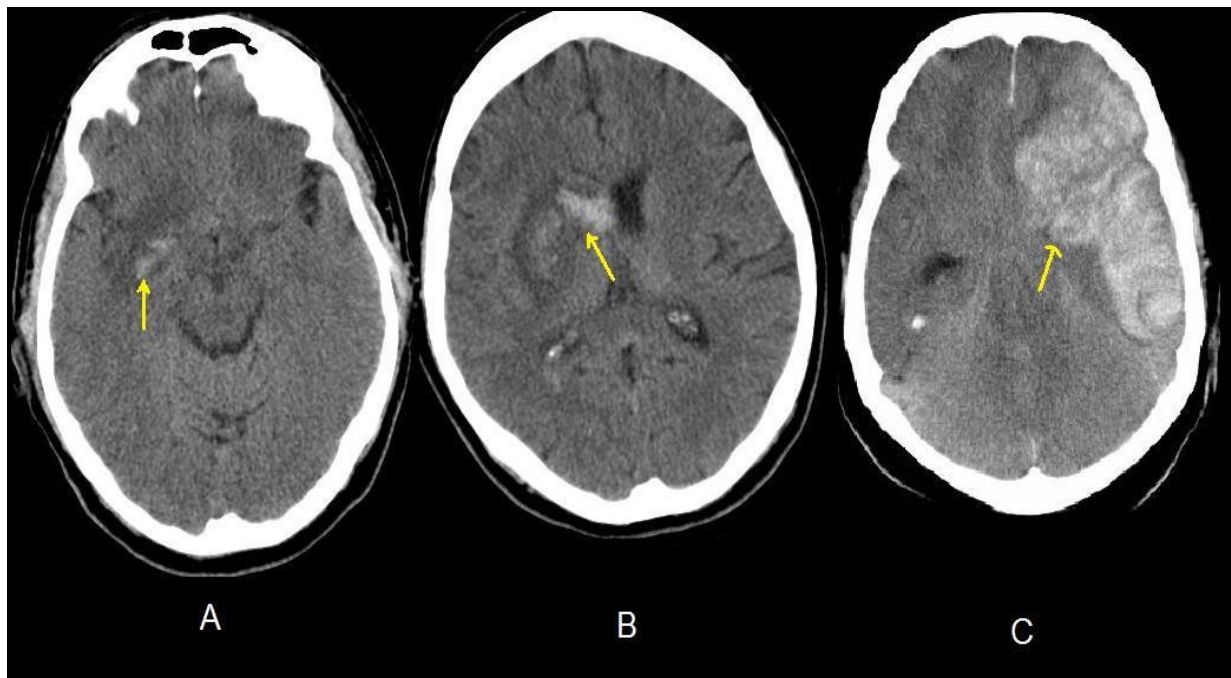


Figure 2. 1. Appearance of acute intracerebral haemorrhage by NCCT. The 3 slices are from 3 patients post-thrombolysis; A-small area of ICH. B- ICH with ventricular extension. C- Massive ICH.

2.2.1.2 Early ischaemic changes (EICs) on NCCT.

The classic early ischaemic changes of acute stroke NCCT are manifested in three major ways: 1- decreased parenchymal density [Parenchymal hypoattenuation or hypodensity]; 2- tissue swelling without change in X-ray attenuation [isodense or isolated focal swelling], and 3- hyperattenuation of an occluded artery MCAT(101) (**Figure 2-2**). These changes are mainly described in

relation to ischaemia in the territory of the MCA. In this review, the EICs will refer only to parenchymal changes and HMCA will not be included. Apart from hyperdense vessel sign, parenchymal hypoattenuation seems to be the most frequently studied and reported early ischaemic change while focal swelling is less commonly seen and under-evaluated (102). In fact, the ways of reading these changes on the NCCT vary greatly among literature reports, with overlapping definitions and poor distinction between hypodensity and swelling (68).

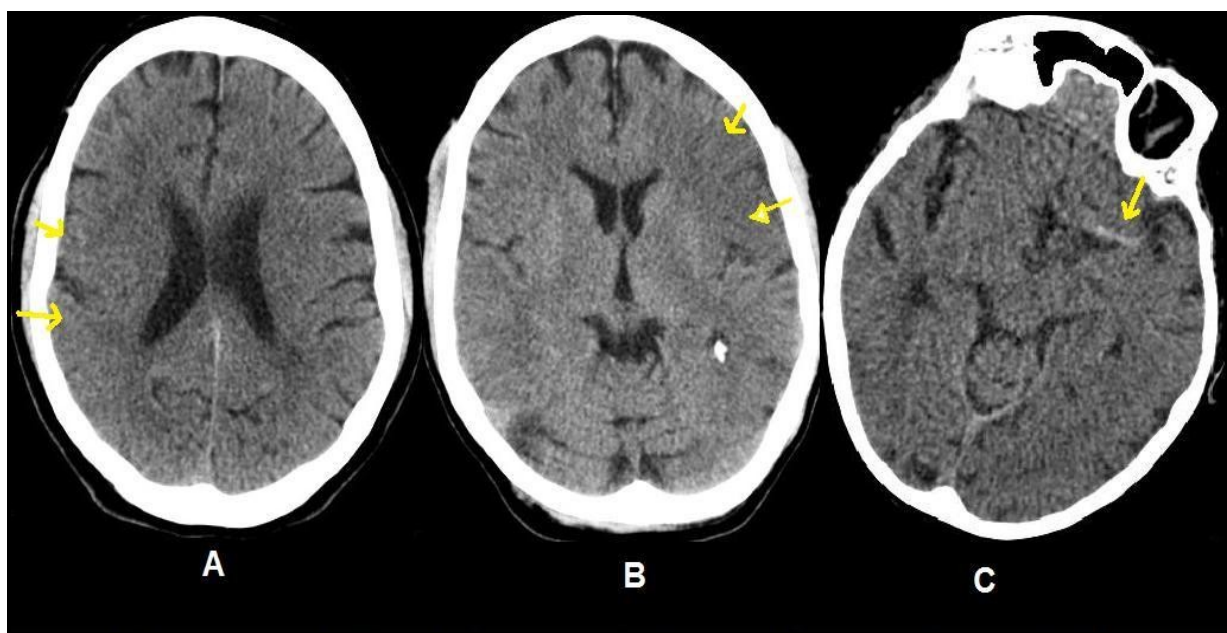


Figure 2. 2 Early ischaemic changes from three different patients presented within 6 hours from stroke onset. A- Isodense swelling B- Hypodensity C- Hyperdense vessel sign.

Authors universally identify two types of abnormalities on NCCT in early stroke: increased radiolucency of brain structures (hypoattenuation) and swelling, but how these two changes can be distinguished from each other is not clearly defined. In **Table 2-1** is a list of terms which have been used for EICs in the literature, with the definitions of some of them when documented by authors. Generally, these are descriptive terms for the morphological and/or anatomical brain changes associated with early stroke.

2.2.1.3 Terminology and definition of EICs on NCCT.

These signs are mainly described in MCA territory hence the anatomical references were mainly restricted to insula and basal ganglia. Loss of insular ribbon, obscuration of lentiform nucleus and cortical sulcal effacement were the most commonly used names for signs of early ischaemia on the NCCT in the literature(103) (**Figure 2-3**). Truwit et al. defined loss of insular ribbon as loss of definition of grey-white matter interface at lateral margins of the insula and stated that it is a reflection of oedema due to infarction (104). The same definition was given by Koga et al. and Wardlaw et al. (105;106). Some authors gave the same definition for obliteration of Sylvian fissure, as in Wardlaw and Mielke's review, which includes an element of swelling. Despite insular changes being able to appear as narrowing or obliteration of Sylvian fissure, which is an indication of swelling, there was not enough clarification whether that always meant hypodensity or could also reflect isolated focal swelling (authors reported it as loss of insular ribbon only) (60;106;107). However, Scott et al. were more precise in defining the insular change by describing it as hypoattenuation of insular ribbon (108). Conversely, the obscuration of lentiform nucleus sign was frankly defined as decreased radiolucency of lentiform nucleus resulting in loss of its precise delineation (105;109). Also, disappearing basal ganglia sign has been attributed to decreased density (106;110).

Loss of insular ribbon; loss of definition of grey-white matter interface in the lateral margins of insula (104;106;111;112).

Obscuration of lentiform nucleus; obscured outline or partial disappearance of the lentiform nucleus (109;111;112).

Cortical Sulcal effacement; decreased contrast, loss of precise delineation of the grey-white interface in the margins of the cortical sulci, corresponding to localised mass effect (106;111-113)

Hemispheric sulcal effacement (72)

Focal hypoattenuation; increased radiolucency of brain structures relative to other parts of the same structure or to contralateral counterparts (106)

Obscuration of Sylvian fissure (106)

The disappearing basal ganglia sign; a loss of the normal delineation of the basal ganglia (110)

Blurring of the clarity of the internal capsule (114)

Parenchymal hypodensity; increased radiolucency of cerebral tissue relative to other parts of the same structure or to its contralateral counterpart (115)

Cerebral oedema; circumscribed effacement of cortical sulci, compression of ventricles, and shift of midline structures (109;115-117)

Loss of grey and white matter differentiation in the basal ganglia; decreased contrast, loss of precise delineation of the grey-white interface of the basal ganglia (106)

Loss of cortical sulci or narrowing of Sylvian fissure (60)

Compression of ventricular system and basal cisterns (60)

Loss of grey-white matter differentiation in cortical gyri, basal ganglia, or insula (60)

Lentiform nucleus hypodensity (72)

Local compression of lateral ventricle (72)

Focal brain swelling; circumscribed effacement of cortical sulci, compression of ventricles and/or shift of midline structures (94)

Focal brain tissue swelling (118)

Isolated focal swelling (102;107)

Focal brain swelling; any focal narrowing of the cerebrospinal fluid space (e.g. effacement of cortical sulci or ventricular compression) (119).

CT sign of brain swelling without concomitant parenchymal hypoattenuation; obvious asymmetric sulcal effacement was observed in more than one section and when there was no concomitant cortical hypoattenuation, including loss of grey-white matter distinction (120)

Isodense brain swelling (72;75)

Hypodense and swollen brain region, isodense and swollen brain region, hypodense brain region (75)

Severe/mild tissue swelling [mass effect]; mild; effacement of the ipsilateral cortical sulci or slight effacement of the lateral ventricle, and severe; complete effacement of the lateral ventricle or midline shift (121)

Severe/mild hypoattenuation; mild; grey matter reduced to that of normal white matter attenuation; severe; grey or white matter attenuation less than normal white matter (121)

Mass effect (122)

Early infarction (68)

Hyperdense middle cerebral artery sign; a part of the MCA that was denser than other parts of the vessel or of its counterpart and denser than any visualised vessel of similar size, as shown by unenhanced CT in which density could not be attributed to calcification (94)

Dot sign; the hyperdensity of an arterial structure (seen as a dot) in the Sylvian fissure relative to the contralateral side or to other vessels within the Sylvian fissure (123)

Table 2- 1: Terminology of EICs.

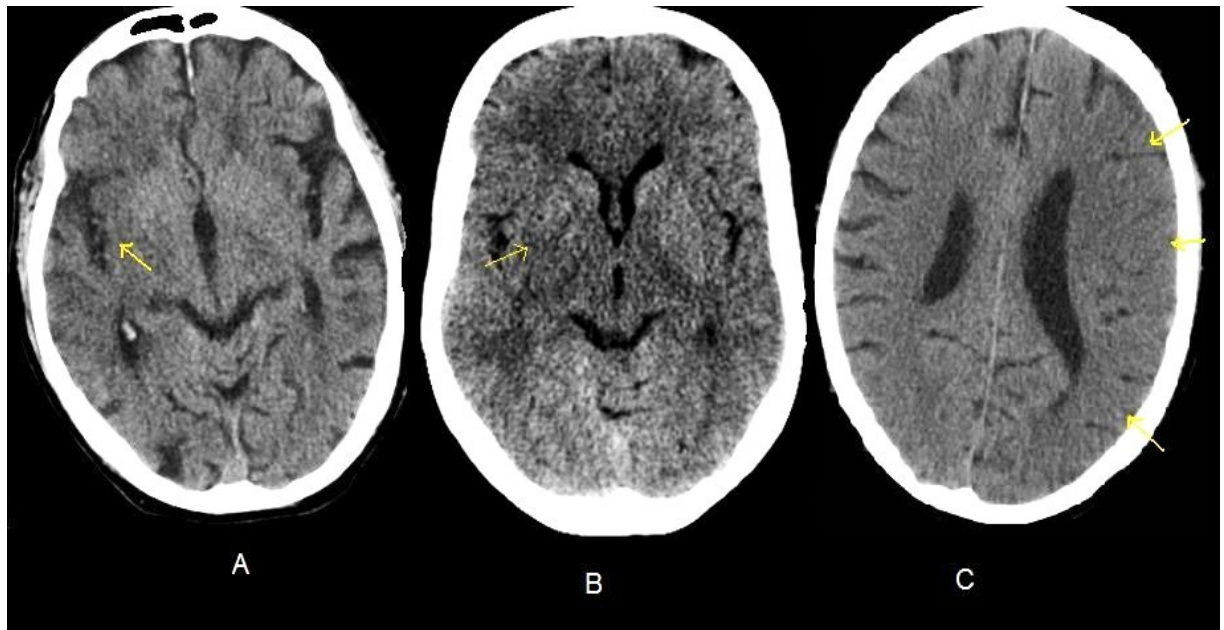


Figure 2. 3: Early signs of acute stroke as seen within the first 4 hours. A; Loss of insular ribbon B- Obscuration of lentiform nucleus C- Cortical sulcal effacement.

All the other terms which have been used to describe ischaemic change in this area also indicated decreased density. For instance, blurring of internal capsule (114), lentiform nucleus hypodensity (72) and loss of grey-white matter differentiation in basal ganglia (60;106). The restriction of use of hypo attenuation in definition of these signs comes from the fact that it is difficult to assess focal swelling in subcortical areas (107). In contrast, authors used the hemispheric sulcal effacement sign to refer to both swelling and hypodensity. Wardlaw and Mielke defined the sulcal effacement sign as a reduction of contrast density with decreased definition of grey-white matter interface at margins of sulci with local mass effect features (106). The same definition had been given by Koga et al. (105). Earlier, Beauchamp et al. considered the sulcal effacement sign to be a morphological change which occurs due to accumulation of intracellular fluid causing swelling and loss of gyral infoldings and regarded it as distinct from attenuation changes which affect the grey-white matter interface, which were considered to follow later (114). On the other hand, Von Kummer et al. stated that sulcal effacement, like local compression of ventricles and midline shift, is a manifestation of focal brain swelling and not hypodensity, which is merely increased radiolucency (94;119).

Hypodensity or parenchymal hypoattenuation was defined more clearly than swelling in most of the literature. In studies of EICs, authors used a general definition for parenchymal hypoattenuation which is decreased radiolucency of brain tissue relative to other parts of the brain. This can be seen in insula, basal ganglia and/or cortical areas and manifests as a loss of grey-white matter differentiation (60;73;74;115;117;119;124) (**Figure 2-4**). Wardlaw and Mielke in their review used the previous signs for EICs beside focal hypoattenuation to refer to hypodensity affecting cortical areas (106). However, Grotta et al. were more specific in describing hypoattenuation. They stated that slight hypoattenuation might manifest as the loss of distinction between grey-white matter, while tissue hypodensity might manifest as marked hypoattenuation in which either the grey or white matter appears darker than normal (122).

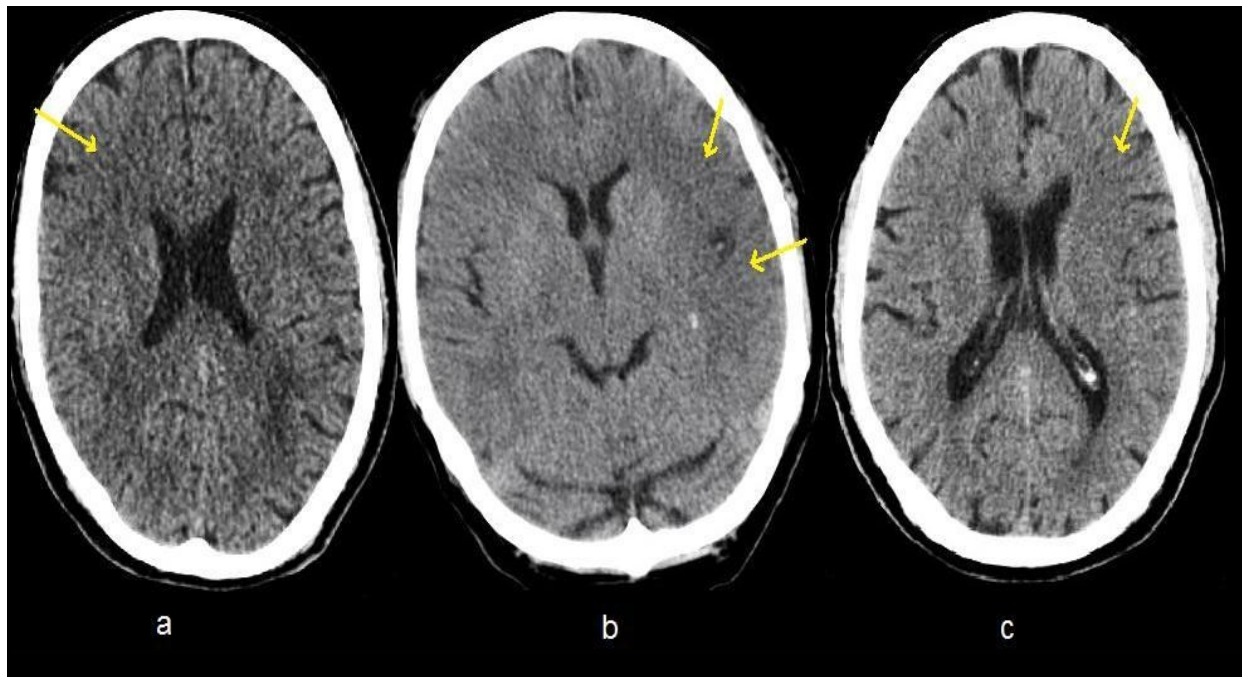


Figure 2. 4: Examples of hypodensity (yellow arrows).

In a similar way, Wardlaw et al. defined mild hypoattenuation as grey matter reduced to the patient's normal white matter attenuation, and severe hypoattenuation as grey and white matter attenuation less than the patient's white matter attenuation (101). This was not the case when swelling was defined in most publications. Von Kummer et al. defined focal brain swelling as circumscribed effacement of sulci, compression of ventricles (narrowing of cerebrospinal fluid spaces) and/or midline shift, but in their analysis of the results they mentioned seeing three patterns of focal swelling on the NCCT: swelling without hypoattenuation, swelling with small hypoattenuation and swelling with large hypoattenuation (**Figure 2-5**) (94;119). Other authors used the term cerebral oedema to refer to swelling and defined it as circumscribed effacement of cortical sulci, compression of ventricles, and shift of midline structures (115-117). Scott used cortical effacement to refer to swelling and defined it as subtle mass effect with sulcal effacement (108). Conversely, Grotta and his colleagues defined oedema as a brain tissue density less than that of white matter but higher than that of CSF, while mass effect was effacement of sulci and basal cisterns and compression of ventricles or Sylvian fissure (122). However, the previous definitions of swelling did not illustrate its importance and difference from hypodensity in regard to the pathophysiological background.

Basically, hypodensity is a reflection of ionic oedema on the NCCT and, originally, oedema results in tissue swelling which can also manifest as tissue shift, compression or effacement of CSF spaces. Subsequently, hypodensity and swelling should signify the same pathology according to the pathophysiological point of view. In an editorial comment by Von Kummer, he mentioned that brain tissue swelling is not closely associated with ischaemic tissue damage and it does not make sense to mix it with hypoattenuation and studying it on CT as one mixture (125). Na and his colleagues explained that CT signs of brain swelling without concomitant hypoattenuation might not represent severe ischaemic injury and they defined it as asymmetric sulcal effacement without presence of hypoattenuation including loss of grey-white matter distinction (120). The same definition for isolated focal swelling was given by Hirano and Parsons (102;126). In the study of the identification of penumbra on the NCCT by Muir and his colleagues, they mentioned two types of swelling, isodense and hypodense swelling. They categorised brain tissue into normal, isodense swollen, hypodense swollen and hypodense (75). In ACCESS study, Wardlaw distinguished brain tissue swelling by the absence of concomitant hypoattenuation change and used quantitative terms to differentiate two types of swelling: mild swelling to refer to sulcal effacement or slight effacement of ventricles and severe swelling to refer to the presence of complete ventricular effacement or midline shift (101).

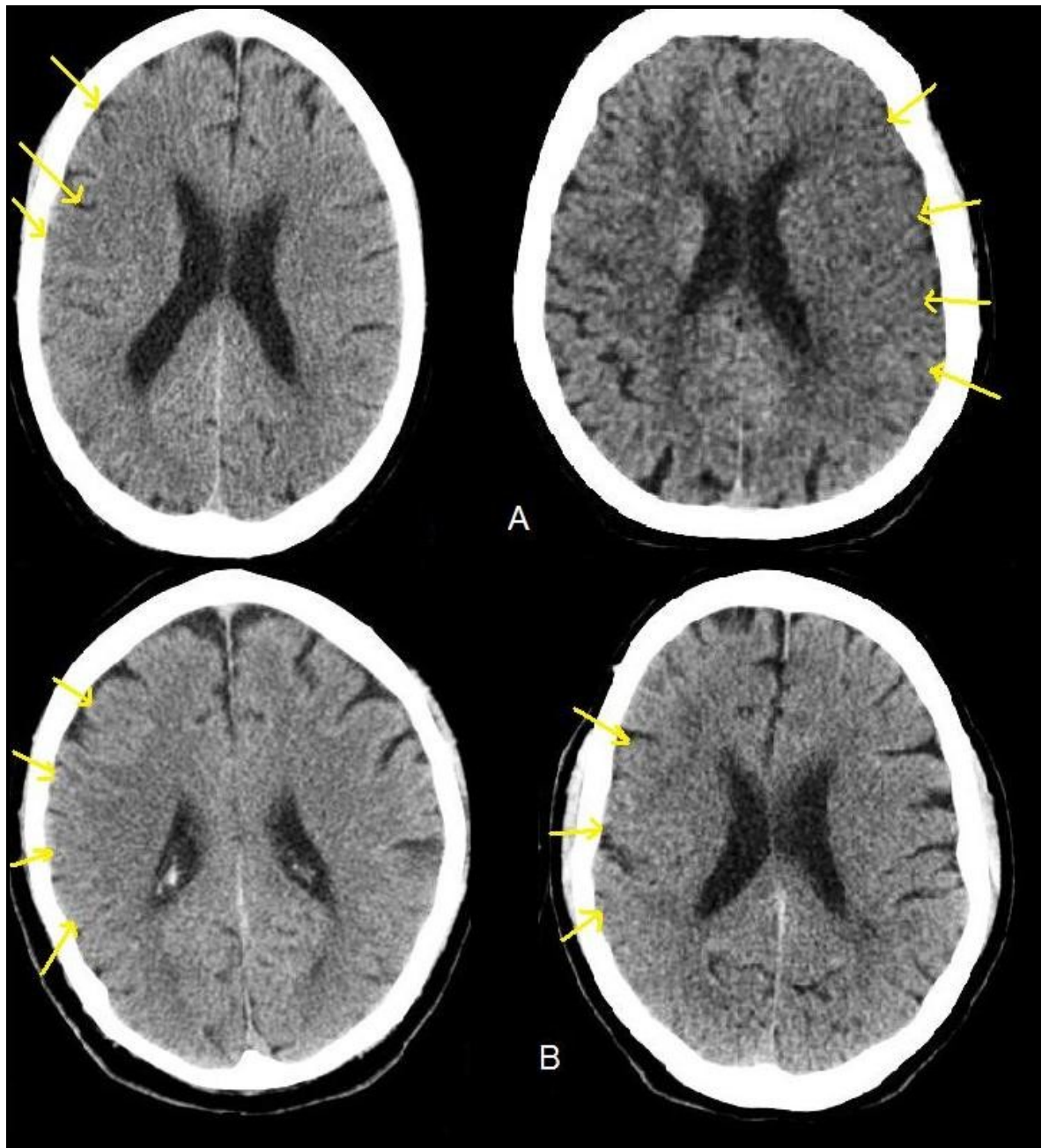


Figure 2. 5: Examples of brain swelling in early acute stroke. A- Focal swelling with hypodensity (Both were within the first 4 hours post stroke onset). B- Focal swelling without hypodensity (isodense swelling) Right: at 4 hours post stroke. Left: at 2 hours post stroke.

2.2.1.4 Systematic measurements of EICs on NCCT.

Since EICs are subtle and difficult to recognise and their significance in predicting ischemic outcome was unclear, methods of systematic evaluation of NCCT for EICs to improve observer recognition, interpretation and agreement and estimate their volume with a standardised approach have been developed. The European Cooperative Acute Stroke Study (ECASS) suggested that

involvement of $>1/3$ of middle cerebral artery territory (MCAT) on early NCCT was associated with increased risk of parenchymal haemorrhage. Despite this, there were no guidelines on how to perform this estimate (43). The Idealise-Close-Estimate (ICE) method was developed by the South-western Ontario Stroke Team to standardise the one third rule for measuring EICs in a systematic approach (127;128). It needs the observer to mentally estimate the affected area ratio to the whole MCAT. This is performed in the following steps: the observer idealises in their mind the area represented by the MCAT. The shape of the area is trapezoidal. Then, the observer looks for areas of asymmetry between the hemispheres which are typically represented in acute stroke by EICs. The observer then closes a geometric figure around the area or areas judged to be abnormal. In step three, the observer estimates the ratio of the geometric figure in step two to the trapezoid in step one.

In their study of the detection of EICs in $>1/3$ of MCAT, Kalafut and colleagues designed a worksheet to make interpretation consistent and to optimise the performance of readers, by incorporating Alteplase Thrombolysis for Acute Non-interventional Therapy in Ischemic Stroke (ATLANTIS)/CT Summit criteria for involvement of $>1/3$ MCAT (129). The same worksheet was used by Mak et al. to reduce subjectivity with the ICE method (130). In 2000, some authors argued that the one third method was not reliable, and a reproducible grading system was needed to improve the overall reading of EICs on NCCT. They developed a quantitative CT score, the Alberta Stroke Programme Early CT Scoring (ASPECTS), and confirmed its reliability, validity and usefulness in estimating EICs. This score divides MCAT into 10 regions in two standardised axial cuts, the first at the level of thalamus and basal ganglia, and the second at the level of corona radiata (See Figure 1 Appendix). The regions are 3 subcortical (Caudate) (Lentiform) and (Internal capsule) and 7 cortical (Insula) (M1, 2, 3 representing anterior, middle and posterior branches of MCAT) and superior to this (M4, 5, 6 representing anterior, lateral and posterior branches of MCAT). A single point is subtracted if an early ischaemic change is detected in a region of MCAT. A score of 0 indicates diffuse ischaemia. A normal scan has a score of 10 (71).

Coutts and colleagues confirmed the reliability of ASPECTS when performed in real time (131). Pexman described ASPECTS as a reliable, robust and practical

method which can be applied to CT in acute stroke and he addressed a number of questions on ASPECTS use, including the determination of cortical M1-6 regions boundaries, the number of ischaemic signs which need to be present in a region to lose a point and the size of the region which needs to be involved to lose a point (132). However, Phan et al. argued that the ASPECTS regions are unequally weighted, with the straitocapsular region having the greatest weight, which might imply that involvement of this region is likely to exclude eligible patients from thrombolysis. In their study, they used the infarct volume of MCAT to examine the internal structure of the ASPECTS template and they suggested incorporation of explicit weights based on the spatial pattern of infarcts (133). Similarly, Wardlaw et al. argued that the ASPECTS score and 1/3 rule do not localise the lesion to particular parts of MCAT (101). Additionally, ASPECTS does not take into consideration the Hyperdense vessel sign which is a major EIC on NCCT and might have prognostic importance. The ASPECTS score was also assessed for its ability to identify acute ischaemic patients who might benefit from thrombolytic therapy by PROACT-II Investigators who confirmed that a baseline ASPECTS score of $<$ or $= 7$ is less likely to benefit from thrombolysis (134), which is the same result which was found by Barber et al. (71). Another study showed increased risk of thrombolytic related parenchymal haemorrhage with low ASPECTS values (124). In a reanalysis of the NINDS trial by baseline ASPECTS, there was no significant difference in the effect of intravenous rtPA given within 3 hours of onset in different strata of severity by ASPECTS score (113). More recently, Hirano and colleagues reanalysed the data from the Japan Alteplase Clinical Trial (J-ACT) using the ASPECTS system. They found that patients with low ASPECTS values (7 or less) have an increased risk of developing ICH (135).

Both scoring systems, ICE and ASPECTS, were compared for their reliability in routine clinical practice. Mak found that in routine clinical practice the one-third MCA method was more reliable than ASPECTS, which had higher potential in detecting more subtle EICs (130). On the other hand, Demaerschalk performed a head-to-head comparison of ASPECTS and ICE and concluded that both were reliable, comparable, easy to learn and quick. He found that ASPECTS allows for a conclusive estimation of the presence of 1/3 MCAT involvement (136). Other less commonly used scales are the International Stroke Trial (IST-3) scale and the

Boston acute stroke imaging scale (BASIS). They score the extent, location and swelling of an ischaemic lesion. The IST-3 scale was assessed in the ACCESS study along with ASPECTS and the 1/3 rule. It showed similar reliability to ASPECTS and the 1/3 rule (101).

2.2.1.5 Significance of EICs on NCCT.

The exact role of EICs in the NCCT in determining the patient's suitability for thrombolysis and prediction of outcome has been debated (125;137). In a review of 14 studies by Wardlaw and Mielke, they found a consistent pattern indicating that presence of EICs was associated with poorer clinical outcome, but there was no evidence that, in the presence of EICs, thrombolysis worsened the functional outcome (106). In contrast, acute stroke patients with normal baseline NCCT seem to have a favourable outcome (74). In a detailed analysis of the relation between each early sign and outcome, Nakano et al. found that cortical sulcal effacement was significantly associated with increased post-thrombolytic leak of contrast with potential tendency to develop into haemorrhagic transformation. On the other hand, loss of insular ribbon and attenuation of lentiform nucleus were not correlated with the risk of haemorrhagic transformation (112). In the NINDS trial, the extent of EICs on the baseline CT was not included in the exclusion criteria for the trial. Investigators found increased risk of sICH in patients with visible signs of "oedema" on their baseline NCCT (42). However, later reanalysis of the NINDS trial with consideration of baseline NCCT prevalence of EICs showed no significant treatment modification effect, but there was a trend for decreased death rate and increased benefit of thrombolysis with favourable baseline NCCT (ASPECTS > 7) (113). The ECASS investigators introduced the concept of exclusion of patients from thrombolysis when they had early major infarct signs involving more than one third of MCAT within 5-6 hours from stroke onset. Although there was an increase in the risk of fatal ICH with an increase in the extent of EICs on pre-treatment NCCT (119), they did not prove the relation of EICs with thrombolysis and outcome (43). In reanalysis of data from ECASS II, authors found no influence of EICs on the effect of rt-PA on functional outcome, but there was substantial increase in the risk of thrombolysis related PH with low ASPECTS score (124). Despite the risk of sICH, the extent of EICs on baseline NCCT is not an independent predictor of outcome

and should not be the only reason to exclude a patient from treatment within the 3-hour window (57;138). The possible limitations of the use of EICs as a predictor of SICH might be due to a lack of agreement among physicians on a universal definition for EICs on NCCT and the old quality of CT scans on which all the reported studies were based (49).

2.2.1.6 Detection of EICs on NCCT.

EICs are prevalent on NCCT in the first few hours following stroke onset. The reported prevalence in the literature ranged from 60-80% (71;113;139). NCCT has shown poor sensitivity for detection of early ischaemia with values being around 75% (115;117;140-146). However, the specificity of these signs is generally good with values being around 90% (75;106;144). In general, it is difficult to determine the exact frequency of EICs because studied sets of scans were subjected to bias when they were selected. This is in part attributed to the relationship of stroke severity and time of admission which varied in the studied groups of stroke patients (bad strokes come to hospital faster and are more likely to be considered eligible for thrombolysis). Among the literature, the reported prevalence and sensitivity varied greatly. In the early 1990s, a study by Von Kummer et al. reported prevalence of 81.8% for hypodensity and CT sensitivity of 82% for ischaemic infarction within the first 6 hours of onset with lower values for shorter time intervals (94). Although this study used CT hard copies (precluding window adjustment by readers) and unclear patient selection methods, the pattern of results was similar to that reported by reanalysis of thrombolytic trials. In ECASS, where patients were enrolled within 6 hours, the prevalence of hypodensity was 46% while focal swelling was 21%. In contrast, patients who were involved in NINDS within 3 hours from onset of stroke had much less prevalence of any EICs at 30%. More broadly, Koga et al. studied the prevalence of each early abnormal sign separately and they reported 37% for loss of insular ribbon and 41% for both hypoattenuation of lentiform nucleus and hemispheric sulcal effacement (105). Similarly, a review by Sarikaya et al. showed the relation of frequency of these signs to the time interval from stroke onset. They found that loss of insular ribbon and attenuation of lentiform nucleus were the most prevalent signs in early stroke with frequency 77% and 82% at 3 hours time interval respectively (103). However, lower prevalence

values were reported in some literature such as that reported by Aronovich et al., who found 28.7% for loss of insular ribbon, 20.7% for lentiform hypoattenuation and 41.3% for effacement of sulci (147). Unlike hypoattenuation, isolated focal swelling had much lower frequency values, such as the 13% prevalence reported by Na et al. (120). It was noted that the ability of observers to detect these changes depends on a number of factors including the time of first scanning, stroke severity, reader's experience and scanner quality (74;94;126;148). A study of a stroke population consisting of 786 patients by Von Kummer et al. reported prevalence of hypoattenuation at 55% by expert readers and 34% by the study investigator. Along the same lines, experts attained a 64% sensitivity level, whereas study investigators achieved 40% only. Also, they found that sensitivity in the first hour of stroke onset was 58%, which is less than that achieved in the next hours (66%)(74). In contrast, a web study by Wardlaw et al. revealed that the speciality of readers and not years of experience was associated with improved detection of EICs. In addition, severe EICs were detected more frequently than mild signs by all readers (121). Suar and colleagues compared CT sensitivity to that of MRI and they found that EICs were present on 33 of 45 scans with sensitivity of 73%, which did not differ significantly from the sensitivity achieved with knowing the affected hemisphere (76%) (117). However, almost the same level of sensitivity had been reported by both Kalafut et al. and Barber et al. with a value at 78% (71;129). A study by Lev et al. sought the effect of using variable window settings on the detection of EICs on NCCT and found that sensitivity increased from 57% to 71% when non-standard soft-copy settings were used. On the other hand, reported specificity kept constant at 100% with different window settings (149).

2.2.1.7 Agreement in assessing EICs on NCCT.

In clinical practice, thrombolysis decisions fortunately do not depend only on detection of EICs because no standardised approach to this issue has yet been agreed on. The ways of assessing the observer agreement on EICs varied greatly among publications in relation to many factors, including statistical analysis, observer's speciality and experience, patient characteristics, clinical data availability, the definition and scoring systems for EICs and CT scan quality and the way of viewing it (Table 2-2).

Von Kummer et al. (94) assessed the inter-observer agreement among neuroradiologists to prove the presence and the ability to recognise EICs. They defined the changes, illustrated them by CT examples and asked readers to recognise them and only to determine the extent of hypodensity on NCCT according to a 20% scale: <20%, 20-40%, 41-60%, 61-80%, >80%. They calculated agreement in different situations, including percentage agreement on early signs of infarction among all readers and with the exclusion of readers in least agreement, percentage agreement with reference, chance adjusted agreement (kappa) for dichotomous ratings for HMCA, focal swelling and hypodensity, ordinal kappa for extent of hypodensity, pairwise agreement between each reader and another, and analysis of readers' responses to determine the clear majority vote and number of agreements with reference. The multiple ways of manipulating data yielded more information on how observers agreed on EICs. For instance, unblinding did not change agreement significantly, exclusion of the least consistent reader improved overall agreement with reference and using large partitions of MCAT rather than smaller ones to estimate the volume of hypodensity increased agreement percentage considerably. In this study, they estimated agreement by 5 different statistical measures (**Table 2-2**) which resulted in different levels of agreement for the same variable under the same conditions. With exclusion of HMCA sign, kappa for multiple raters ranged from 0.55-0.59 indicating moderate agreement according to the Landis and Koch scale. However, the pairwise weighted kappa ranged from 0.32-0.79 indicating fair to substantial agreement. When they estimated extent of hypodensity by rates, they attained low values although kappa values were indicating substantial agreement. Meanwhile, pairwise weighted kappa values were 0.37 to 0.80 which might correlate with the low percentage of overall agreement percentage.

Table 2- 2: Studies of EICs reliability.

Study	Statistics for assessing agreement	Readers	CT scans	Clinical data	EICs evaluated
Von Kummer et al 1996	-Kappa for -multiraters -Ordinal kappa -Pairwise weighted kappa -ICC. -Percentage of overall agreement	6, -Neuroradiologists Reference neuroradiologist -Two sequential sessions	-45, <6hrs -5-10mm slice thickness -Hard copy	Blind/non-blind	HMCA, parenchymal hypodensity, focal brain swelling. + definitions. Extent (increments of 20%)
Lev et al 1999	-Weighted kappa	2, -Neuroradiologists -Two separate sessions (4wks) -Consensus	-30, <6hrs -Standard window width and centre level(80,20 HU) -Variable soft copy settings(1-30HU window) (28-36 HU centre level) - imaging workstation	Blind	Focal hypodensity + 1-5 scales
Wardlaw et al 1999	-Absolute numbers -Percentage of agreements.	15, -Neuroradiologists E -Neurologists E+T -Stroke physicians E -General practitioner -Trainee physicians 1 session	14, <6hrs - hard copy slides	Blind/non-blind	HDMCA LIR, loss of basal ganglia, hypodensity, sulcal effacement, Extent (1\3 rule)
Grotta et al 1999	Balanced pairwise kappa.	16, NINDAS investigators Neurologists Emergency stroke physicians Stroke fallows Radiology fallows Neuroradiologists(reference) One session	70, 3hrs 10mm slices Hard copies	Non-Blind	-Oedema -Mass effect -Loss of Gr-Wt Hypodensity Sulcal effacement Any early change -Extent (1\3rule). Definitions+ illustration course

Study	Statistics for assessing agreement	Readers	CT scans	Clinical data	EICs evaluated
Barber et al, 1999	kappa statistics?	2, Neuroradiologists Consensus	17,6hrs 1-cm trans-axial slices Hard copies	Blind	HMCA Hypodensity Cerebral oedema Definitions Extent (1\3rule)
Marks et al, 1999	ICC Pairwise kappa	3, Neuroradiologists	50,<6hrs	Blind	Hypoattenuation Sulcal effacement HMCA Extent(1\3 rule)
Kalafut et al, 2000	Percentage agreement	3, Neuroradiologists 2sessions	25,3hrs	Blind Non-blind for scans arising disagreement	ATLANTIS criteria sheet Extent (1\3 rule)
Pexman et al, 2001	Balanced pairwise kappa	6, Stoke Neurologists Neuroradiologists 2sessions 3wks	156?, 3hrs 10mm slices Hard copies	Blind Non-blind	Hypoattenuation Focal brain swelling Definition ASPECTS(<,>7) 1\3 rule
Fiebach et al, 2002	Unweighted kappa Pairwise kappa	9, Neuroradiologists Neurologist Residents 2 sessions	54,<6 8mm slices	blind	HMCA LIR, OLN, cortical focal swelling Extent (1\3rule)

Study	Statistics for assessing agreement	Readers	CT scans	Clinical data	EICs evaluated
Saur et al, 2003	Kappa for multiple raters	6, -Neuroradiologists -Neurologists 2 sessions	46, 6hrs(categorised) 2mm 30\80HU 6mm 35\50 HU Hard copies	Blind Non-blind	HMCA Hypoattenuation Cerebral oedema Definitions Regional classification Extent (1\3 rule)
Mak et al, 2003	Percentage agreement Pairwise kappa Prevalence adjusted kappa.	5, -Neuroradiologists -Neurologists -General radiologist	80, <6hrs 5-10mm Hard copies on viewing box	Blind	6 EICs ? Extent (1\3rule) Extent ASPECTS(<,>7).
Demaerschalk et al , 2005	Unweighted kappa ICC.	4, Stroke neurologists	40,<6hrs Hard copies with viewing boxes	Blind	Loss of Gr-Wt Sulcal effacement Subtle lucency 1\3 rule ASPECTS 0-10
Muir et al, 2007	Cohen's kappa statistic with the Fleiss-Cuzick extension for multirater analyses.	5, Neuroradiologists Stroke neurologist Stroke physician	32,<6hrs DICOM viewer software	Blind	Isodense swollen Hypodense swollen Hypodense Extent ASPECTS 0-10
Wardlaw et al, 2010	Calculating the area under receiver operator characteristic (ROC) curves (AUC)	258, Neurologists, geriatricians, general radiologists, neuroradiologists, emergency physicians, family doctors Years of experience <>5,	32 duplicated 63,<6hrs "SMPTE" test Scans stored in digital jacket in jpeg format and uploaded to web site of study with advantage of SMPTE for monitor adjustment.	Blind	HMCA Mild\sever hypoattenuation Mild\sever swelling Definitions Extent 1\3 rule, ASPECTS0-10, IST-3 score

However, investigators did not take the patient's characteristics into account when selecting scans for the study, and also they used a homogenous group of readers and standard CT characteristics, which could leave an open question about their effect on agreement. The short interval between the two viewing sessions might not be enough to eliminate the effect of subconscious memory in reading the unblinded set of scans which could affect the result of agreement too. In addition, estimation of swelling extent, which is more difficult than estimating the extent of hypoattenuation, was not included, and could have further lowered the agreement values. In subsequent studies of agreement, some of these factors were clarified.

Lev and his colleagues sought the effect of changing the window settings of scans on detection of EICs by two neuroradiologists. Although detection improved significantly, agreement did not show the same pattern (0.48 to 0.50). Authors used weighted kappa for two raters to assess agreement on a diagnostic scale rated 1-5 with 1 indicating definite absence of stroke and 5 indicating definite stroke. The idea of this rating scale was different from other ways of rating EICs in that it did not assess the extent of ischaemic change directly. Consequently, the agreement level attained by Lev and his colleagues is difficult to compare with other studies. However, the main concern of the study was to determine the reliability and accuracy of detection of EICs rather than inter-observer agreement (149).

Wardlaw and colleagues considered the effect of speciality and experience in studying how good physicians were in detecting EICs. The authors expressed their results in absolute numbers of observations and the percentage agreement value on EICs was not recorded in the study. They found that inexperienced doctors failed to recognise EICs, while experienced observers missed hypodensity frequently. This might have been due to the poor definition of EICs and their extent in the context of this study. However, the ability of readers to reproduce their results regarding coding scans as normal versus abnormal was good (150).

Grotta and his group provided a broader analysis of agreement between different specialities including a number of physicians who had participated in a NINDS trial. A short training course for readers, stroke severity consideration

when selecting scans and the use of balanced kappa and repeated sampling were all tried to optimise agreement. Even so, the agreement was only fair and not affected by the speciality and experience of readers. This might be related to the low prevalence of EICs in selected scans which affects the values of kappa significantly. Moreover, the compared groups of physicians were small and unequal, which could make comparison questionable (122).

In the studies where the main aim is not to assess the agreement between readers on EICs on the NCCT, the values obtained would be less reliable than those of well-designed studies of agreement. For example, Barber et al. (115) reported kappa value at 0.44, while Kalafut et al. reported 96% agreement on involvement of $>1/3$ of MCAT. In the Kalafut et al. study, there were no clear definitions for EICs involved in the study and it was left up to the reader's discretion (129). Marks et al. (144), in a full approach to EICs on NCCT, reported a similar level of agreement to Barber et al., the results between 3 readers with pairwise kappa values being 0.44, 0.50 and 0.65. Both studies tested neuroradiologists and looked for almost the same EICs but with different definitions and the total number of scans involved in each study.

When Pexman et al. assessed the ASPECTS score versus $1/3$ MCAT rule, they reported pairwise kappa values between different specialities ranging from 0.56 to 0.89 for ASPECTS and 0.20 to 0.64 for $1/3$ rule. However, when the same speciality was considered, the highest agreement was between neuroradiologists (0.89) when using ASPECTS and the lowest agreement again between neuroradiologists (0.52) when using the $1/3$ rule (132). In a study comparing CT and MRI, Fiebach et al. calculated the agreement between experts and novice physicians with results ranging from 0.42 to 0.52 for detection of each infarct sign on NCCT by experts, while novices showed lower agreement in detection of early infarction signs with kappa at 0.38 (151). A similar study was conducted by Saur et al. but with a different way of analysing the data. They reported moderate agreement on EICs with kappa value of 0.57 for the blinded set and a substantial level of agreement with 0.67 for an unblinded set of scans. However, both values had no significant difference statistically. The agreement did not differ significantly between both groups of readers, with 0.65 and 0.60 for neuroradiologists and neurologists respectively. In separate analysis for scans

obtained in the first 3 hours, interrater agreement fell to 0.36. In addition, Suar et al. assessed the intrarater agreement and found that raters did not change their readings of the same scans when presented for the second time with kappa of 1 for each rater and 0.67 to 0.90 for different regions (117). Mak et al. did not specify the EICs which they were assessing and the calculated agreement was for the extent of these changes by comparing 1/3 MCAT rule and ASPECTS scoring systems. Paired kappa ranged from 0.10 to 0.88 by using aspects with an average of 0.44 and from 0.31 to 0.72 by using 1/3 MCAT rule with an average of 0.49. Readers consisted of different specialities and they had a brief training in reading the scans before commencing the study (130). In contrast, Demaerschalk et al. reported a substantial level of agreement (0.72) between stroke neurologists when they used ASPECTS and ICE. Observers scored NCCT from 0-10 using ASPECTS. Hence the ICC was calculated for ASPECTS (0.79). However, investigators did not illustrate EICs and their definitions (136). Muir et al. calculated both interobserver and intraobserver agreement on each sign of early infarction independently. Although observers agreed on hypodensity and isodense swelling poorly, with kappa values 0.15 and 0.08 respectively, the intrarater agreement between individual readers was good (75). The ACCESS study presented more details on observer reliability in the detection of EICs. This was by involving a large number of observers [258] from different specialities and scientific backgrounds, and assessing all the factors related to observers, scans and patients on a changing level of agreement. These included presence of ischaemic sign, time to scan, brain background appearance, speciality, years of experience and time to read the scan. Additionally, they used web technology to present compressed images to readers who had the ability to adjust the screen for better visualisation of scans. The agreement with a reference standard was only reported by using AUC and odds ratios. However, the agreement between readers was not assessed (101).

2.2.1.8 Analysis of agreement variables.

Most of the studies which were conducted to assess the agreement level on EICs had different approaches. Many authors were concerned with how the observers would agree in the presence of a number of variables related to scans, the patient and the readers themselves.

A- Speciality and experience of readers.

Expert neuroradiologists were one of the most tested groups. They generally showed moderate to substantial agreement with almost the same values of kappa reported in several papers, ranging from 0.44 - 0.79 (94;115;129;144;149). Although fair agreement levels with kappa values at 0.32 and 0.35 were reported in some studies, these findings were blamed on the involvement of inconsistent observers, with improved agreement when excluded (94). In ACCESS, investigators found that the highest agreement level with reference standards was achieved by neuroradiologists and followed by stroke physicians. However, they did not assess agreement among the different groups of readers or the totality of participants in the study. The exclusive approach in repeating studies of agreement among expert neuroradiologists might be pointless since other specialties are more frequently involved in taking the rapid treatment decisions, including stroke physicians, general radiologists and emergency physicians. Among stroke physicians, agreement was substantial to perfect in three studies: 0.60, 0.72, 0.85 (117;132;136). However, the studies which involved more than one or two specialties showed only fair to moderate agreement: 0.22-0.43 by Grotto, and 0.44 by Mak (122;130). According to the ACCESS study (101), years of experience in reading stroke scans seem to have no effect on agreement level, but a longer time being spent on assessing the EICs was the main determinant of increasing the odds of agreeing. However, experience in reading stroke scans makes a big difference between experts and novices when agreeing on EICs (151).

In many papers where the readers had a poor performance in reading EICs, authors suggested that training observers on how to recognise EICs would improve overall agreement. A study by Von Kummer et al. showed a significant increase in the number of correct estimates by trained participants. They found that the trained ECASS II investigators reduced the number of falsely included patients in the trial to an extent similar to that found in the study, and the proportions of patients with large infarctions or ICH reduced to 50% in comparison with ECASS I (152).

B- Patient characteristics.

Factors related to patients, such as age, gender, morbidity and NIHSS score, were not considered in the majority of agreement on EICs studies and patients were included in these studies based on their scan findings. Although authors mentioned the age and gender in some studies, they rarely assessed their effect on agreement on EICs on NCCT. However, NIHSS scores were involved more frequently in the inclusion criteria of patients, but also were not correlated with agreement on EICs. In the ACCESS cohort, investigators studied the relation of NIHSS and age with EICs and they found that increasing age increased both detection of EICs and agreement with reference standard, whereas NIHSS scores had no effect (101).

C- Scan quality.

Generally, authors found no effect on agreement level in the presence or absence of clinical data with scans. However, other intrinsic factors related to CT technology were less often mentioned although it was common to blame poor performance on early generations of CT scanners regarding depiction of early signs of infarction. In studies where the effects of scan quality (in terms of noise) and window settings were tested there was no significant effect on agreement, although the sensitivity might change significantly (101;149). The study of effect of matrix size on detection of EICs by Ogura et al. showed the effectiveness of applying reasonable matrix size in the examination of EICs (153). The other intrinsic factor which might affect detectability is the slice thickness of scans. In most studies of agreement by using multidetector scanners, the slice thickness was 5-10mm. Tanaka et al. found that using greater slice thickness improves the detectability of hypoattenuated objects significantly (154). However, the use of both thin and thick slices was recommended by some neuroradiologists to increase diagnostic accuracy in early strokes with offset against the additional time to evaluate (155). In contrast, a longer time to scan, severe ischaemia and old stroke lesions were all associated with increased agreement on EICs. However, white matter changes had a negative impact on agreement (101). More recently, use of modern Digital Imaging and Communications in Medicine (DICOM) image viewers has allowed the readers to manipulate the scan window level and adjust the best view of scan

slices. Moreover, advanced Web tools have helped to save scans in optimal sittings and use them for large-scale studies (75;101;121).

On the other hand, there has been no proof of the superiority of using DICOM technology over hard copies and viewing boxes in practical and research sittings.

D- Statistics of agreement.

Kappa statistics (chance-adjusted-index of agreement) were used predominantly to measure inter-observer variability in assessing EICs on NCCT with reference to Landis and Koch's scale for agreement level in Table 3.4 [Chapter III]. Percentage of agreement, intraclass correlation coefficient (ICC) and ROC analysis were used to a lesser extent. Kappa exists in various forms which should be taken into consideration when analysing data for assessment of agreement. For instance, weighted kappa penalises disagreements in terms of their seriousness (i.e. the degree of disagreement in grading - e.g. two observers scoring a region as a 1 and a 5 respectively is weighted more heavily than two observers scoring a 4 and a 5), whereas unweighted kappa treats all disagreements equally. Consequently, values obtained by the two measures will differ dramatically. Scharf et al. reported a value of 0.19 by unweighted kappa and 0.35 by using weighted kappa which changed agreement from slight to fair (156). In addition, there are different weighting schemes for weighted kappa which produce different values from the same data, including linear and quadratic weightings. The linear weighting is used when the difference between rated categories is significant, whereas quadratic weighting is applied when the difference is not so important. However, the magnitude of kappa along with its interpretation is influenced by other factors which differ markedly among various studies. Among these are prevalence of EICs, bias and non-independence of ratings. Prevalence and/or bias adjusted kappa (PABAK) scores were used in a number of studies shown in Table 2-2. Nevertheless, balanced kappa values should be displayed alongside true kappa values because the former reflect a hypothetical situation in which no prevalence or bias effects are present. For example, Mak et al. calculated both kappa and PABAK with higher values for the second one, e.g. 0.72 to 0.90 respectively.

The previous implementations of kappa are used for two raters, but in the presence of more than 2 raters, Fleiss's kappa for multiraters is employed to assess overall agreement among raters. Generally, there are two forms of kappa for multiraters: fixed-marginal kappa and free-marginal kappa. Unlike Cohen's kappa, there are no weightings; hence the results might be less reliable in some situations when kappa values are low in the presence of good agreement. In this case, the calculation of pairwise weighted kappa for each pair of readers with total average could help to better reflect the true agreement level among raters. In the study conducted by Von Kummer et al. (94), they applied varied forms of kappa to assess the true agreement among raters.

Percentage of agreement does not take into account agreement that would be expected purely by chance. Consequently, the overall agreement rate may be high in the absence of intrinsic agreement between raters. Kalafut et al. applied percentage agreement solely, and the interpretation of results was rather ambiguous in the absence of an appropriate scale (129).

Intraclass correlation coefficient is used with continuous data and it takes into account the variance between observations. ICC may be preferred over Fleiss's kappa to assess multiple raters agreement because it gives more favourable levels of agreement. Marks et al. and Von Kummer et al. used ICC to calculate overall agreement between multiple readers beside weighted kappa for individual pairs.

The Receiver Operator Characteristics (ROC) curve is used mainly to evaluate how accurate a diagnostic test is, whereas the Area under Curve (AUC) evaluates the test's effectiveness. However, this requires a reference standard ("gold standard") to estimate agreement. In the ACCESS cohort, AUC with odds ratios were used to measure the agreement of each group of observers against a gold standard. However, this method is not suitable to assess agreement among raters. In brief, whatever the statistical method used by authors to assess agreement on EICs, it should be interpreted and compared cautiously.

D- Early signs being assessed.

Since the emergence of the concept of early signs of infarction there has been increased interest in their evaluation with concomitant multiplicity in the terms being used to describe these changes. The calculated agreement for early changes varied according to the main focus in individual studies. For instance, Lev et al. measured agreement on focal parenchymal hypoattenuation only, whereas Mak et al., who reported similar results, did not mention that 6 signs were assessed because the main purpose of their study was to compare ASPECTS and the 1/3 rule.

In more than two studies, authors tended to assess two categories of EICs - hypodensity and brain swelling - simultaneously (94;101;115;117;132;144). However, some authors gave different definitions to each category and others used synonyms for brain swelling, such as cerebral oedema (115;117). They measured agreement either for each change alone, or altogether. In other studies, authors adopted a broader evaluation of early infarction signs on the NCCT by involving more than the usual two parenchymal changes (122;136;150;151). For instance, Grotta et al. measured both agreements on and extent of loss of grey-white matter interface, hypodensity and cerebrospinal spaces compression, aiming to assess the performance of experts in reading each change separately. In contrast, Demaerschalk et al. did not record the agreement on each sign they explained to readers because the main focus was on comparing ASPECTS with the ICE method in quantifying EICs.

2.2.1.9 Detection of Penumbra on NCCT.

Imaging of brain ischaemia with positron emission tomography (PET) revealed the physiological characteristics of penumbra. Along the same lines, magnetic resonance diffusion-perfusion mismatch and perfusion CT demonstrated the existence of both grey and white matter penumbral tissue. Basically, penumbra is a hypoperfused tissue with compensatory vasodilation or early post-ischaemic hyperperfusion which was proved to correspond to an area of tissue swelling

without change in X-ray attenuation on NCCT (**Figure 2-5B**) (75;102;120). Moreover, unlike parenchymal hypoattenuation, isodense focal swelling is less likely to progress into infarction with major reperfusion (102). CT attenuation of brain swelling caused by cerebral vasodilatation does not decrease (isodense) and theoretically it might increase due to the relative increase in the blood content of the tissue (increased attenuation on CT). Conversely, brain swelling due to ischaemic oedema causes reduction in CT attenuation as a result of the increased tissue content of water (120). The prevalence of isodense swelling in many studies was not reported and, when assessed, it was very low. For instance, Von Kummer et al. reported a prevalence of 2%, whereas Na et al. reported 13% (119;120). Overall, the depiction of penumbra on NCCT and its distinction from infarct core appearance has been under-evaluated in most of the literature. Detection of this sign in the first few hours after stroke onset on the NCCT seems to be more difficult than the recognition of subtle hypodensity itself. Moreover, estimation of its extent and its separation from hypodensity appears to be complex.

Von Kummer et al. (94) estimated the extent of parenchymal hypodensity alone without the involvement of focal swelling and suggested that brain swelling and hyperdense segments of arteries should not be included in the estimation of the extent of EICs on baseline NCCT to decide eligibility for thrombolysis because of their different pathophysiological background (125). Subsequent studies on isodense brain swelling recommended its exclusion from the ASPECTS score (107). However, studies of EICs and clinical outcome did not exclude the sign of brain swelling from the overall estimated extent of EICs on baseline NCCT (113;124;134). This might be attributed to a number of factors, such as considering tissue swelling and hypoattenuation as a manifestation of the same underlying pathology which is oedema, non-separation between the two forms of swelling associated with early stroke, and the infrequency and subtlety of isolated focal swelling (124). In addition, scoring systems like ASPECTS and 1/3 rule do not differentiate these findings unless the investigator discriminates them on baseline evaluation (119). However, mixing up these two findings when estimating the extent of EICs on pre-treatment NCCT may explain the dramatic recovery from apparently extensive baseline EICs in some cases (134;157). On the other side, some cases with marked isodense swelling without concomitant

hypodensity on baseline NCCT progress to infarction despite successful reperfusion (107).

2.2.1.10 Hyperdense middle cerebral artery sign (HMCA).

This sign is a marker of intraluminal thrombus, most often seen in the MCA, but also reported in other intracranial vessels. It can be seen in the MCA M1 segment as hyperdense linear streaks following the course of M1 from its origin toward the Sylvian fissure (**Figure 2-2c**). Additionally, the MCA dot sign is seen as a circular hyperdensity in M2 and M3 segments as result of occlusion of distal branches of MCA (158) (**Figure 2-6**). Also, occlusion of the internal carotid artery may be displayed on NCCT as a hyperdense ICA sign indicating thrombus within the supraclinoid segment of the distal ICA. Other arteries were also reported as hyperdense PCA (159).

Reported prevalence varied among reports. Barber et al. found it in 5% of patients, while Ozdemir et al. saw it in 35% of NCCT scans (123;160). The HMCA sign has high specificity (100%) but low sensitivity ranging from 24% to 54% (161;162). This might be attributed to the effects of a number of factors, including slice thickness, experience of readers and haematocrit level. For instance, a study by Kim et al. revealed that thin-section slices had higher sensitivity and specificity (up to 100%) for detection of acute thrombus compared to 5-mm slices(163). An added value to thin-slice CT is the ability to assess the length and volume of acute thrombus and quantification of the extent of vascular obliteration (164). In most studies assessing the agreement on early parenchymal changes, authors also reported agreement on the HMCA sign. However, agreement swung from fair to perfect among papers (106). Generally, it has been found that the HMCA sign is associated with severe stroke and poor functional outcome (106;161;165) and sometimes with large embolic infarcts (166). However, there is no evidence to exclude those patients from thrombolysis (161;165). Kharitonova et al. found that the risk of symptomatic ICH after thrombolytic therapy was similar in HMCA and non-HMCA groups of patients (161). In a cohort study of patients who were registered in (SITS-ISTR), there was a good outcome in patients with disappearing HMCA sign after thrombolysis twice as many as patients with persistent sign. Additionally,

authors found that HMCA predicted functional independency and survival independently and the early NIHSS improvement predicted HMCA disappearance (167). Comparably, the HICA sign was found to be associated with severe initial neurological deficit and worse prognosis than HMCA sign even in the presence of thrombolysis (160). On the contrary, the MCA dot sign appeared to be associated with better outcome than HMCA sign (123). All of this was consistent with the sign indicating only the site of occlusion, rather than independently indicating severity.

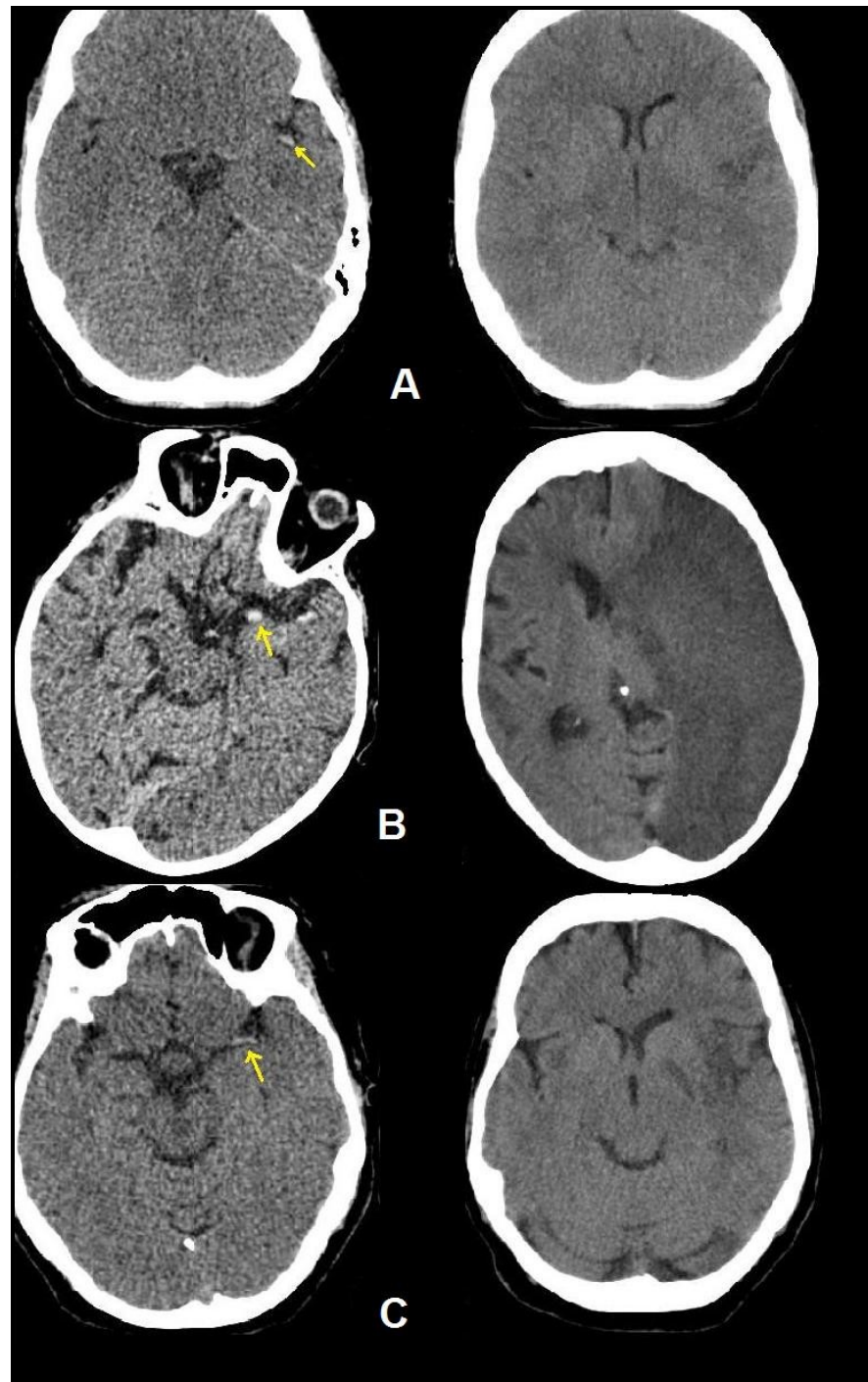


Figure 2. 6: Examples of hyperdense vessel sign in NCCT and tissue fate on follow up (>24 hours) scans. A-MCA “Dot” sign (arrow); seen after 154 minutes after stroke onset in a 41-years-old woman. Patient received rtPA with recanalisation and disappearance of HVS and good outcome after 3 months. B-HICA sign as seen in a 76-years-old woman who presented after 137 minutes from onset with severe stroke and had poor outcome. Follow up scan showed infarction of the whole left hemisphere. C-HMCA sign as seen in a 76-years-old woman after 164 minutes from stroke onset. There was no recanalisation and patient had poor outcome.

2.2.2 Perfusion Computed Tomography (PCT) in acute stroke.

Conventional NCCT is still the primary imaging modality preferred by most emergency departments for the initial evaluation of strokes. However, for detection of early ischaemic changes and stratifying patients for thrombolysis, NCCT faces the problem of the subtlety of EICs. Hence, it has been suggested that the evaluation of cerebral perfusion might aid selection of stroke patients suitable for thrombolysis. In other words, it might help in distinguishing salvageable tissue which is at risk of infarction from that with extensive irreversible ischaemia. PCT imaging has the potential to improve the overall performance of CT for management of early stroke because it visualises the underlying pathophysiology rather than structural signs of brain damage. Thus, it enables depiction of the perfusion deficit on the tissue level. PCT is considered a relatively new technique which allows quantitative and qualitative assessment of cerebral perfusion. It has been found that PCT is useful for non-invasive diagnosis of cerebral ischaemia and it complements NCCT and CT angiography (168). In general, the perfusion technologies are of two major branches, *a diffusible tracer technique* which relies on the rapid passage of a lipophilic agent across the blood brain barrier (BBB) into the brain tissue. Determination of perfusion flow requires determination of the agent's amount intravascularly and in parenchyma. The second branch is *the non-diffusible tracer* technique which involves the use of an agent which remains inside blood vessels and does not pass into brain parenchyma assuming intact BBB. Quantification of perfusion parameters is done through analysis of time-density curves. The last branch represents the technology of perfusion CT(169).

2.2.2.1 PCT technique.

PCT is a rapid add-on examination which takes only a few minutes to perform. PCT generates maps of cerebral perfusion parameters, typically cerebral blood flow (CBF), cerebral blood volume (CBV), mean transit time (MTT) and time to

peak (TTP) (**Figure 2-7**). CBV is defined as the total volume of blood in a given unit volume of brain. This includes blood in large vessels and in the tissue. It is measured by millilitres of blood per 100g of tissue. CBF is defined as the volume of blood moving through a given unit of tissue per unit of time. It is measured by millimetres per 100g of tissue per minute. MTT is defined as the average transit time of blood via a given brain region and it is measured by seconds. TTP is the time from the beginning of contrast injection to maximum enhancement within a region of interest (164;170).

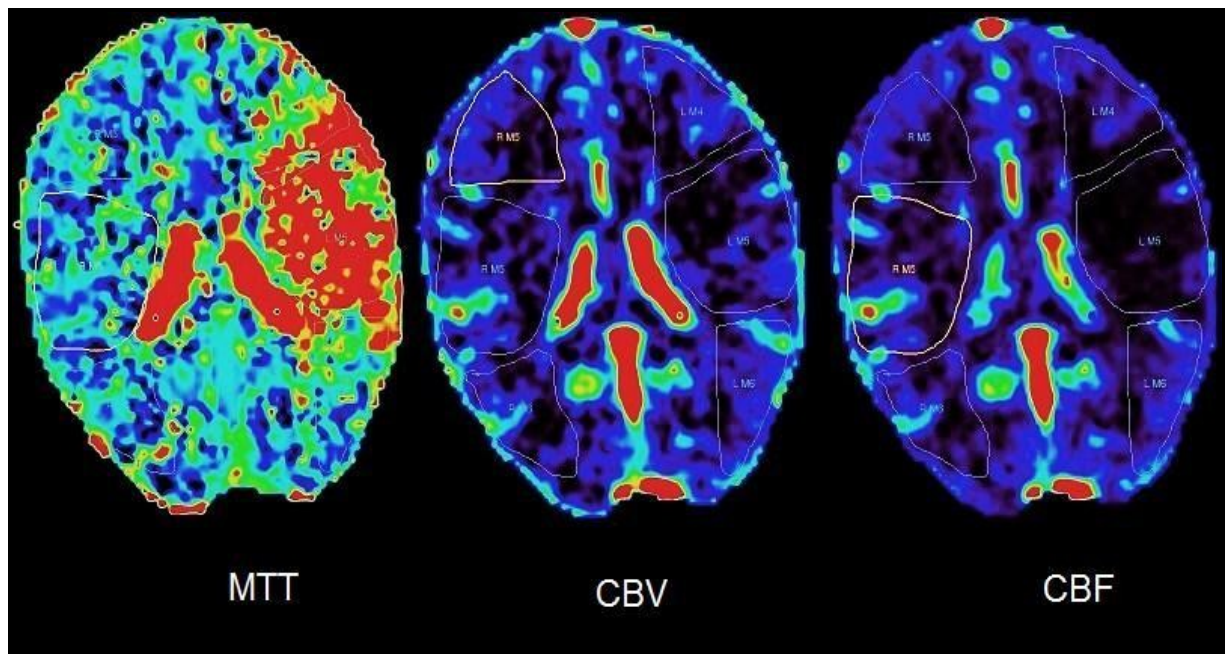


Figure 2. 7: PCT perfusion parameters from patient with acute stroke with left side perfusion defect at 5 hours from symptoms onset showing CBV\CBF or MTT mismatch [ASPECTS areas are plotted on the maps].

Perfusion studies are obtained by tracking transient changes in blood vessel and brain parenchyma during the first pass of intravenously injected iodinated contrast agent (*non-diffusible perfusion technology*), which causes a transient increase in the Hounsfield Units in linear relationship with its concentration in the perfused tissue. Perfusion parameters can be obtained from pixel-to-pixel analysis of density changes over time. These changes can be graphed as regional time-attenuation curves (TAC) for each voxel and from which perfusion parameters can be calculated (**Figure 2.8**). The evolving of high-speed helical/spiral CT scanners having solid-state detectors and a gantry-design (a

high gravitational force generated by fast rotation) with the advantage of software facilitated the accurate measurement of perfusion parameters with rapid analysis and pushed up perfusion CT to the current state. Two tracer kinetic models were described for calculation of the perfusion parameters. These techniques are based on the indicator dilution principle in which the concentration of a known amount of injected contrast material is measured against the time in intracranial vessels. The first one is *the central volume principle* which describes CBF as simply related to CBV and MTT. The accuracy of this method requires an intact blood-brain barrier to preserve contrast material to intravascular spaces. Any leakage to extra-vascular tissue causes spuriously high values of flow parameters. The mathematical approach involved in the calculation of perfusion parameters is called the “*deconvolution*” operation. This method, however, has to meet some conditions to derive perfusion parameters, including a need for a gamma variate fit to evaluate the bolus first pass only to avoid the violation of simple-voxel compartment assumption, and the determination of arterial input function (AIF) to isolate the true tissue response function from the measured parenchymal density curve by mathematical deconvolution.

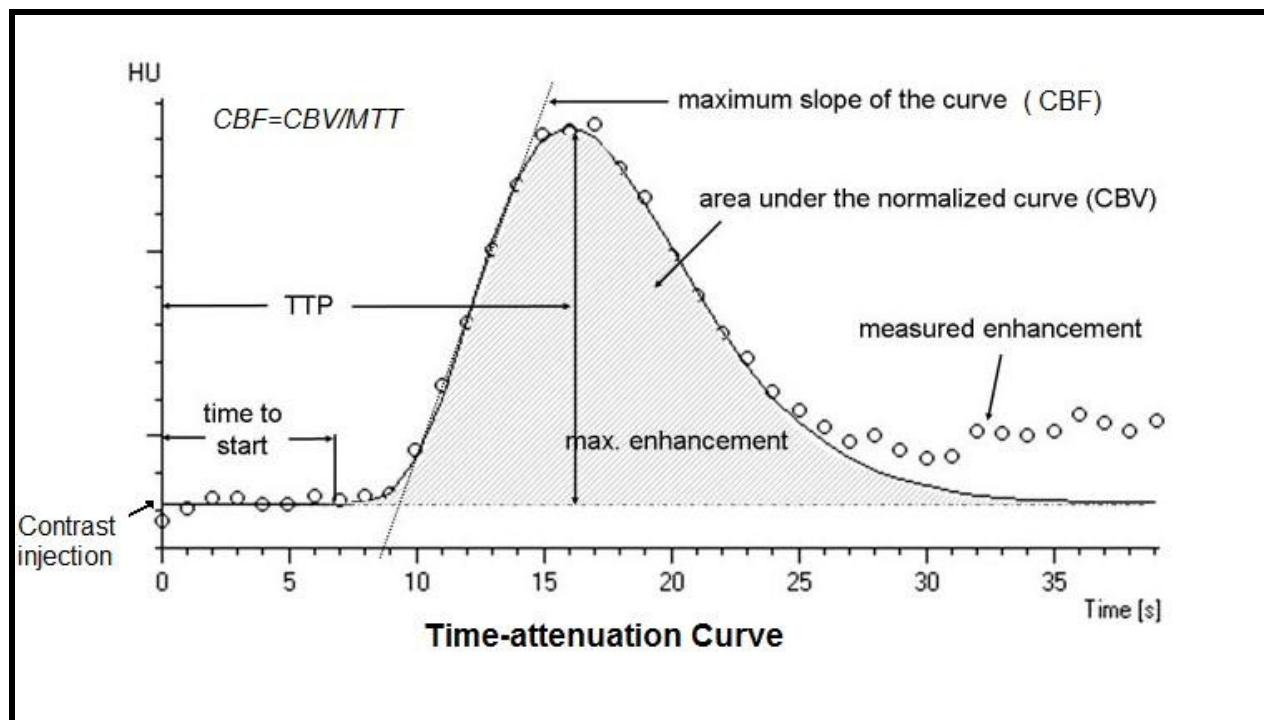


Figure 2. 8: Time attenuation curve plotted from perfusion data of normal brain tissue [modified from Tomandle et al.].

The true AIF into the tissue voxel of interest cannot be measured directly and is usually estimated from a major artery, such as MCA, assuming that this vessel represents the input to the tissue of interest. Any delay or dispersion of bolus will cause errors in the estimation of CBF. However, the potential effect of multiple collateral vessels in maintaining residual perfusion in ischaemic compartments may affect the AIF by the creation of multiple inlets equal to ischaemic voxels which violates the underlying perfusion model assumption.

The second approach is *the maximum slope model* technique, in which CBF is calculated from the maximum slope of TAC, and CBV from the maximum enhancement of TAC in a voxel of interest compared with that of superior sagittal sinus. This is to avoid arterial partial-volume averaging effects. Because the model necessitates that the bolus should be retained temporarily by the capillary network in order to obtain valid values of blood flow, the contrast material is injected at very high rates in this model to achieve rapid arterial rise time within a few seconds. Otherwise, CBF will be underestimated. The mathematical method involved in the calculation of perfusion parameters is called the “*non-deconvolution*” operation which assumes venous outlet to be equal to zero. This simplified and sped up the calculations by this model compared to the “*deconvolution*” operation, which is more demanding and involves complicated and time-consuming processes. Hence, the interpretation of results which relied on the “*non-deconvolution*” method may be less reliable than those reliant on the “*deconvolution*” operation. The very short time span for each curve to peak eliminated the need for gamma variate fitting for calculation of perfusion parameters. Therefore, this approach is insensitive to motion and does not require recirculation correction or operator decisions. On the other hand, due to partial volume effects inherent to 5-10 mm slice thickness, the selective calculation of absolute perfusion parameter values might be inaccurate and comparison of CBV and CBF values in both ischaemic and non-ischaemic hemisphere would be a safer approach. Both illustrated models represent the basis of current multiple software applications for brain CT perfusion (169;171-173). The quantification of CBF by perfusion CT has been tested and studied extensively in animals and humans. In humans, it has been

validated against other functional imaging techniques, such as XeCT, PET and MRI (174-178).

Image acquisition in perfusion CT occurs for a total of 45-60 seconds and up to 90 seconds in a multiphasic approach with scanning at 80kV. However, these parameters have been adjusted to minimise a patient's exposure to radiation. The coverage of brain tissue depends on the width of the CT scanner detector which is limited in the craniocaudal direction in many scanners (but not all) and therefore typically does not allow whole brain assessment. Hence, it is important to pre-determine the target tissue of interest to be covered before starting PCT acquisition (168;179;180). Following data acquisition, the source images are processed in workstation for generation of parametric maps and data processing is accomplished by using special software packages. These tools generate colour-coded maps and time-attenuation curves from which perfusion parameters can be calculated for any area of interest which could be chosen manually by the operator (as was described above). Non-cerebral tissues can be removed by masking using semi-automated "image segmentation" which depends on using thresholds based on attenuation measurements. Calculation of perfusion parameters might be subject to delay and dispersion which can result in underestimation of CBF and overestimation of MTT which can be overcome by the deconvolution technique or by using local AIF estimated from smaller vessels close to ischaemic tissue (168;180). Quantitative analysis may aid the use of threshold values to determine infarct core, penumbra and normal tissue. One suggested operationally defined penumbra is the volume of tissue contained within the region of CBF/CBV mismatch on PCT maps (180). On the other hand, the core has reduced both parameters, CBV and CBF. Quantitative assessment is done by placing regions of interest (ROIs) in suspected ischaemic areas and corresponding locations in the contralateral hemisphere. Relative and absolute values of perfusion parameters in these regions can be obtained. Thresholds were determined for both penumbra and core using relative and absolute values of CBF and CBV. Most papers referred to thresholds derived by Wintermark et al. which assumed cut-off values greater than or equal to a 34% reduction from baseline CBF for penumbra and less than or equal to 2.3-2.5ml/100g CBV for core, while relative MTT above 145% of the normal hemisphere outlined all at-risk tissue (178). Later on, they studied 130 patients having acute stroke and

found that relative MTT was the most accurate parameter characterising the penumbra and absolute CBV the parameter most accurately describing the infarct core (181). However, other parameters with different thresholds might be applied in some centres. Hence, validation of optimal postprocessing and image interpretation procedures is needed (168).

2.2.2.2 Reliability of PCT and its prediction of clinical outcome.

To date, the only imaging technique required before administration of thrombolytic treatment is NCCT. However, the narrow time window has constrained the use of thrombolysis in a larger portion of acutely presenting stroke patients. Hence, there has been increased interest in understanding the core/penumbra mismatch concept by using advanced imaging techniques such as PCT and MRI to extend the time-to-treatment window.

The PCT technique is considered relatively new when compared to MRI, therefore its clinical applications are less thoroughly reported in the literature. Hamberg et al. found that PCT had the potential to provide the earliest indication of vascular occlusion and its distribution and it might be easily applied in the clinical studies concerned with vascular pathophysiological changes. In a study of post-cardiac surgery patients in intensive care units to evaluate PCT feasibility in hyperacute stroke, Bisdac et al. found greater sensitivity of PCT in detecting and mapping of ischaemic stroke in ICU patients in whom NCCT findings were inconsistent with the severity of clinical condition (182). Similarly, the use of visual interpretation of PCT maps in clinical settings was validated by Muir et al. (183). The diagnostic accuracy of PCT in the detection of secondary infarction to vascular spasm following aneurismal subarachnoid haemorrhage was assessed and demonstrated high sensitivity for prediction of clinically relevant spasm (184;185). Bisdas et al. compared the performance of PCT with diffusion-weighted MR imaging (DW-I) in hyperacute strokes and they found sufficient assessment by both with good correlation with admission and follow up scores (186). Earlier, Wintermark et al. compared quantitative PCT with qualitative

diffusion and perfusion MRI in emergency settings and found equivalence in both imaging modalities regarding identification of penumbra in acute stroke patients (187). Similarly, Na et al. investigated multiphase PCT (covering the whole or most of the brain) by comparison with DWI and PW-I in regard to the prediction of tissue outcome and final infarct volume, infarct growth and clinical severity. They found that the PCT mismatch was highly specific for tissue at risk and strongly predictive of infarct growth and concluded comparable utility to DW-I and PW-I in early stroke assessment (188). Eastwood et al. studied the correlation of abnormalities seen on PCT with their volumes as seen on DW-I and PW-I in acute stroke patients. They reported good correlation of CBF and MTT parameters on PCT with the full volume of abnormality, however CBV had lower correlation with full volume on PW-I(189).

Although PCT has shown the ability to predict clinical outcome and final infarct volume, the accuracy and validity of PCT parameters in estimating the extent of ischaemic tissue in acute stroke patients is debated (**Figure 2-9**). In addition, the decision about the best perfusion parameters to estimate ischaemic tissue volume and predict its outcome has not yet been agreed. Nonetheless, there have been continuous efforts in evolving post-processing and interpretation of perfusion maps. Schaefer et al. sought the usefulness of PCT maps in predicting final infarcted tissue and found that PCT was able to distinguish hypoperfused tissue likely to infarct from tissue likely to survive. They suggested that CBF was a good parameter in differentiating penumbra into two compartments: penumbra that infarct and penumbra that recover with reported values of 0.19, 0.34, 0.46 for core, infarcted penumbra and recovered penumbra respectively. In other words, independent of recanalisation status, ischaemic tissue with >66% reduction in CBF was predicted to infarct, whereas ischaemic tissue with < 50% reduction in CBF was predicted to survive and >75% reduction in CBF corresponded to the core. They called for avoidance of overestimation of tissue that is going to infarct depending on visual estimation of TTP/CBV ratios. However, CT/CBV lesions were typically non-reversible and had a strong correlation with final infarct size (190). Similarly, Dr Konstas and Dr Lev in their commentary review, stated that salvageable penumbra was overestimated by benign oligoemia by using the traditional cut-offs for MTT and CBF (173). Muir et al. reported the relation of recanalisation to the fate of

ischaemic tissue by using TTP and CBV on PCT maps and found that in recanalised patients the final infarct volume was correlated with initial CBV volume but not with TTP, while in patients in whom there was no recanalisation the final infarct volume correlated with initial TTP and not CBV (183). Along the same lines, Gasparrotti et al. found that patients with large TTP/CBV mismatch ratio and small core on baseline PCT had a favourable outcome and the core size was the strongest predictor of clinical outcome as was measured by CBF on perfusion maps (191).

Among thrombolysis trials which used the mismatch concept to assign patients to thrombolysis was the Desmoteplase in Acute Ischemic Stroke (DIAS II) trial. This trial was the only one reported to date that used PCT along with MRI to select patients based on core/penumbra mismatch with inclusion of scans which showed at least 20% penumbra (59). However, the DIAS II trial did not confirm the results from the preceding DIAS I and DEDAS trials that selected patients based only on MRI mismatch (58;192). In the DIAS II trial investigators reported some inconsistent results between MRI and PCT. One of these was because of the limited brain coverage by PCT which caused profound differences in mismatch volumes with MRI. In addition, PCT showed a reverse change in core lesion volume at day 30 compared to MRI in which a median percentage increase in core lesion volume on MRI was seen compared with a similar decrease on CT.

PCT parameters have high sensitivity and specificity to predict infarction. Murphy et al. reported the sensitivity and specificity of CBV and CBF for infarction at 97% (193). Nabavi et al. reported higher predictive values for PCT than CTA and NCCT in testing MOSAIC score (defined later) (194). Similarly, Lin et al. sought ASPECTS accuracy on PCT maps for MCA stroke patients with evidence of complete arterial recanalisation and found that ASPECTS delineated perfusion maps with higher accuracy and sensitivity than CTA and NCCT (195). However, in another study by Fiorella et al. there was insufficient agreement between 3 CT technologists to include quantitative values of perfusion parameters into clinical decision making despite the high degree of correlation between the parenchymal regions of interest derived from CBV, CBF and MTT maps. Therefore, they recommended that with optimisation of post-processing

parameters, the degree of variability between assessors might be improved (196).

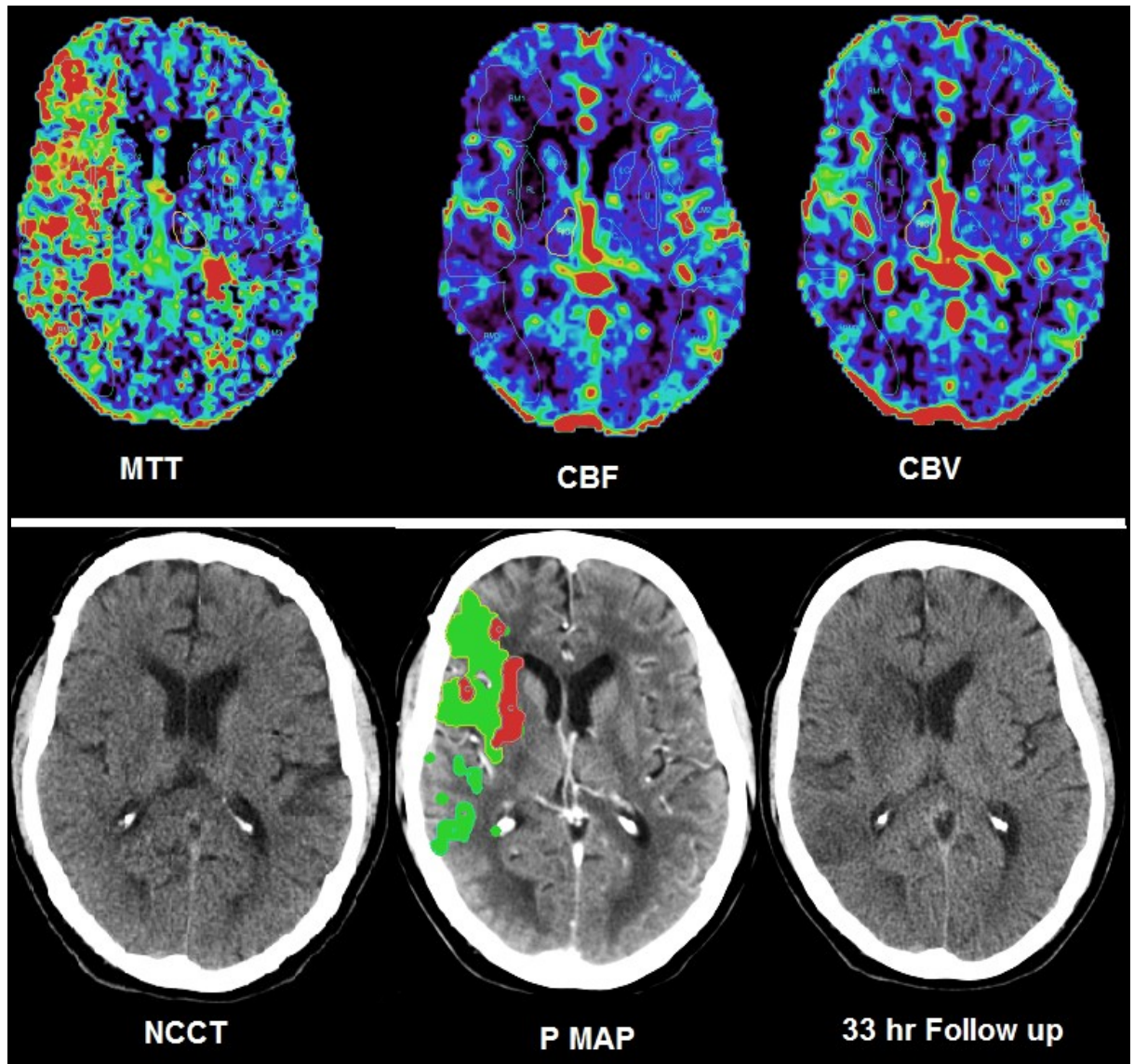


Figure 2. 9: Perfusion maps with baseline NCCT and 33-hours follow-up scans showing EICs in a 65 years-old patient with acute stroke. Scanning was done within 3 hours of symptoms onset and accomplished in 17 minutes and rtPA was infused and recanalisation approved. Visually, MTT delineates a total ischaemic area of $>2/3$ of right hemisphere [M1-M3] areas with different levels of CBV\CBF ratio. Areas with severe reduction of both CBV and CBF and areas with a slightly decreased CBF and normal CBV ended in infarction while areas with normal CBF and normal or increased CBV recovered.

2.2.2.3 Comparison of PCT with PMR.

Because the general principles underlying the computation of perfusion parameters are the same for both PCT and PMR, the overall clinical applicability of both is similar (168). However, PCT has benefits over PMR in that it has widespread availability and relative ease of scanning, particularly in the presence of attendant monitors or presence of absolute contraindications to MRI scanning. Speed of scanning, which adds no more than 5 minutes to NCCT scanning, and low cost are other pros of PCT (86). The most important potential advantage is the linear relationship between contrast concentration and attenuation on PCT, which allows quantitative measurement of perfusion parameters. In PMR maps, the contrast concentration is not linearly related to T2 effect which makes absolute measurements of perfusion parameters difficult (168). In addition PMR has susceptibility effects from adjacent tissue, whereas PCT has greater spatial resolution (180).

Being widely available with simpler methodology and greater degree of quantification, PCT has the potential to increase patient access to new treatment and clinical trials (86). Unlike PMR, PCT has relatively limited coverage, which must be sufficient in making treatment decisions in acute strokes. However, source images from CTA, which depict core tissue, cover entire brain volume and are available immediately at scan completion (180). A second disadvantage of PCT is its low sensitivity to detect microbleeds which are easily seen by MRI, although the relevance of the latter has not been proved either. In addition, the patient is exposed to risk of radiation (increased risk of cancer and genetic effect and skin burns) and there are adverse effects of iodinated contrast (contrast-induced nephropathy and increased risk of hyperthyroidism) (168;180).

Despite the fact that post-processing of PCT and CTA images may be manually demanding, they can still be rapidly and reliably constructed (180). However, the role of MRI in acute stroke triage has been evaluated more than PCT. Therefore, although PCT seems to be promising in the treatment of acute strokes in many small studies, its validation in clinical practice is not yet been proved in large patient cohorts.

2.2.2.4 Multimodal evaluation of acute stroke

A multimodal approach incorporating the three modalities of CT - NCCT, PCT and CTA - may offer advantages for early imaging of stroke patients. Despite this, NCCT is still the preferred modality for initial evaluation of patients presented with acute stroke [for the reasons illustrated earlier in this chapter]. Nabavi et al. evaluated a score system based on a multimodal approach to patients in the acute stage using a scoring system termed the MOSAIC score (0-8), which sums scores from each of the 3 CT components: presence and amount of early signs of infarction on non-contrast CT (NCCT; 0 to 2 points), stenosis (>50%) or occlusion of the distal internal carotid or middle cerebral artery on CTA (0 to 2 points), and presence and amount of reduced cerebral blood flow on 2 adjacent PCT slices (0 to 4 points). The predictive value of this score was evaluated in respect to final infarct size and 3 months clinical outcome by use of mRS and BI scores. Throughout the analysis, MOSAIC's score was superior to all single CT components with respect to the various outcome measures (194). Similarly, Kloska et al. reported higher sensitivity of 78.9% when using the multimodal approach than each single CT component alone (197). Along the same lines, Scarif et al. found that, although the PCT and CTA increased the scan time from onset to diagnosis from 2 minutes to 10 minutes, the sensitivity to detect ischaemia increased significantly among observers. Moreover, the inter-observer agreement, which was fair to moderate when using NCCT, rose to a substantial level (156). More recently, a larger study which recruited 191 acute stroke patients by Hopyan et al. showed that the addition of PCT in approaching acute stage patients improved stroke diagnosis even by inexperienced scan readers over that achieved with NCCT alone or a combination of NCCT and CTA. Furthermore, it improved intra- and inter-observer agreement up to a substantial level (69). However, the diagnostic performance of the multimodal CT approach has not been evaluated against the performance of MRI for infarct detection.

2.2.3 Computed Tomography Angiography (CTA) in acute stroke

An important aspect in acute stroke is the evaluation of intra- and extracranial vasculature status. Vascular imaging helps localisation of the site of arterial occlusion, thrombosis or stenosis which may be crucial to determine the type of therapy. It has been found that intravenous thrombolysis appeared more efficacious for distal than proximal thrombus and that mechanical thrombectomy and intra-arterial thrombolysis might be more efficacious for treatment of large vessel occlusion (198). CTA can be defined as a fast, volumetric CT examination performed with a time-optimised bolus of contrast material for the opacification of vessels (199). It relies on continuous scanning while the patient is moving through the X-ray beam. In addition to the acquisition of axial cuts, surface or 3-D rendering, multi-planar reformatting and maximum intensity techniques can be performed. CTA scanners can cover the entire region from common carotids up to the circle of Willis in a single data acquisition.

Wildermuth et al. evaluated the feasibility of CTA in acute ischaemic stroke patients and they reported a high diagnostic accuracy compared with digital subtraction angiography (DSA) and Doppler ultrasonography (DU). They stated that patients with autolysed thrombi, occlusion of the internal carotid artery bifurcation, and poor leptomeningeal collaterals may have little potential for benefit from thrombolytic therapy (200). The sensitivity of CTA for detection of extracranial carotid artery stenosis ranged around 90%. A study by Berge et al. found that CTA was comparable to DSA, which is the gold standard for diagnostic vascular imaging, in the diagnosis of significant carotid artery disease (201). CTA has been found to be very sensitive for detection of very-high-grade stenosis which should be distinguished from the total lumen occlusion because of different therapy plans (202). However, single-slice CTA were found insufficiently robust concerning plaque composition with moderate predictive value for detection of plaque ulceration (203). In addition to its vascular visualisation, CTA source images (CTA-SI) were suggested as a useful added-on examination tool in the assessment of ischaemic tissue status. It can be rapidly obtained after NCCT in emergency settings, and, unlike PCT, it covers the entire

brain and does not require postprocessing. Scharman et al. found that a combination of NCCT, CTA and CTA-SI were comparable to DWI by MRI in predicting final infarct volume (177). Camargo et al. compared the reliability of both NCCT and CTA-SI, and they found that CTA-SI was more sensitive in detection of early ischaemia and more accurate in the prediction of final infarct volume (204). The reliability of CTA for the detection of intracranial occlusions was also very high in several studies with reported sensitivities up to 100% in some papers. In contrast, it has lower sensitivity for detection of intracranial stenosis than those for occlusion which might be due to its low estimation of heavy atheromatous calcifications (205;206). However, Bash et al. stated that CTA sensitivity was not compromised by extensive atheromatous calcifications when appropriate window settings were used. In the same study, CTA appeared superior to MRA with a higher sensitivity and positive predictive value than 3D TOF MRA for both intracranial stenosis and occlusion(207). Additionally, CTA spatial resolution is twice that for MRA because it is less susceptible to motion, pulsation, slowness and other artefacts. Post-processing time is similar in both methods.

In general, vascular imaging at an early phase of the stroke is recommended to triage patients to the best therapy and to determine prognosis (208). Sims et al. have found that thrombus location on CTA influenced subsequent patient outcome and recommended that CTA can safely and rapidly support the stratification of stroke patients based on location, degree and presence of vascular occlusion (209). More recently, Gonzalez et al. argued that lack of arterial occlusion information in several stroke classification systems might have contributed to the poor progress in stroke treatment and there was a need for a refinement of stroke evaluation instruments, particularly the NIHSS and ASPECTS scores which did not involve the occluded vessel assessment. They claimed that current thrombolytic trials (DIAS III and DIAS IV) support this suggestion because they use CTA as a critical component of patient selection. In their study, they evaluated the performance of a combination of Boston acute stroke imaging scale (BASIS), which includes arterial occlusion evaluation, and NIH stroke scale (NIHSS). They found that the combined instrument was substantially more powerful in predicting outcomes of acute stroke patients than any single classification method (210). Although CTA is a non-invasive approach with high

levels of accuracy it has some disadvantages related to the use of substantial amounts of intravenous contrast material which may limit its use in patients with contrast allergy and renal dysfunction. In addition to this, there is the risk of exposure to ionising radiation.

2.3 Magnetic resonance imaging (MRI) in early stroke

Since the emergence of thrombolytic therapy as a treatment for acute stroke, MRI has offered an alternative to CT for the evaluation of acute stroke. MRI is used to image the intensity of the cerebral parenchyma and its anatomic structure. Similar to CT, MRI is employed in acute stroke to exclude haemorrhage and stroke mimics, and detect ischaemic tissue. To meet this demand and perform a thorough evaluation of ischaemia, a combination of conventional MRI, MR angiography (MRA) and diffusion- and perfusion-weighted MRI techniques can be used. The conventional MRI sequences typically used in acute stroke include T1-weighted spin-echo, T2-weighted fast spin-echo, fluid-attenuated inversion recovery, T2*-weighted gradient-echo, and gadolinium-enhanced T1-weighted spin-echo sequences. In the first few hours after stroke onset, conventional MRI is less sensitive than DW-MRI and it may result in false negative findings. Conventional MRI (two T₂-weighted sequences, a T₁-weighted sequence, and a "balanced" pulse sequence with the use of a high-resolution data acquisition matrix) techniques were insufficient to detect EICs until 8-12 hrs after symptom onset (140;211). However, subsequent development of fast-echo gradient technique and diffusion imaging along with clinically available echo-planar imaging which is resistant to patient motion, have permitted a rapid and very sensitive MR imaging protocol in early stroke.

The appearance of ICH on MRI depends on its age and the MRI sequence used. Conventional MRI T1 and T2-weighted sequences are sensitive to detection of subacute and chronic blood and less sensitive to acute haemorrhage within the first 6 hrs. As blood is extravasated into the brain parenchyma, haemoglobin

becomes deoxygenated. Deoxyhaemoglobin is a paramagnetic substance which produces a non-uniform magnetic field causing signal loss and darkening on T2 sequence images. In a study by Kidwell and colleagues, the gradient recalled echo (T2*-Sensitive) sequence was found to be equivalent to NCCT in detecting acute haemorrhage. On the other hand, DWI has unproven reliability in the detection of early parenchymal haemorrhage. Kidwell et al. sought the reliability of MR GRE in detecting acute cerebral haemorrhage and found that MRI was superior to CT in detecting chronic microbleeds which were not visualised on NCCT (92). More recently, a study by Boulanger et al. found that patients with < 5 micro haemorrhages were not at increased risk of developing symptomatic ICH (without thrombolysis). However, they were at increased risk of recurrent disabling or fatal stroke (212). Despite this, NCCT is still considered the gold standard for exclusion of haemorrhage by most clinicians (as illustrated earlier in section 2.2.1.1).

The most important sequence of MRI for demonstration of acute ischaemia is DWI. It is based on the detection of restricted diffusion as water moves from extra- into intra-cellular spaces. Ischaemic tissue on DWI is readily visible as brighter areas than normal brain tissue. DWI has the ability to detect very small infarcts and those in the posterior fossa: it also shows changes within minutes of stroke onset. Numerous authors consider DWI as the most sensitive and specific technique for imaging acute ischaemic stroke. Current DWI employs an echo-planar technique with very short image acquisition time and high sensitivity to signal changes (213). Gonzales et al. sought the accuracy of DWI in the diagnosis of stroke in the first 6 hours of stroke onset and reported very high sensitivity and specificity up to 100% in comparison to conventional MRI and NCCT (18% and 45% respectively). The very high sensitivity reported by Gonzalez et al. might be due to unadjusted time interval between conducting the CT and MRI (214). However, Fiebach et al. performed a randomised crossover comparison of DWI and NCCT and demonstrated a higher sensitivity and specificity for DWI than NCCT (151). Other conditions which cause restricted diffusion, such as infection and inflammatory diseases, may mimic ischaemia on DW images. Additionally, areas with reversible ischaemia and increased blood volume appear normal on a DWI map. Therefore, perfusion-weighted MRI was recommended along with DWI to detect areas with reversible ischaemia (penumbra).

Warach et al. combined DWI and PWI during same session to report the presence of penumbra within the mismatch area between the two maps. Thus, the acute hyperintensities on the DWI represented ischaemic core areas, whereas surrounding areas of perfusion deficits corresponded to penumbral tissue, according to the postulation of Warach et al. (215). Lovblad et al. found a strong correlation between the DWI lesion and stroke severity, clinical outcome, and final infarct volume which means that the larger perfusion deficit than DWI lesion could be a qualitative marker for potential infarct expansion (216). Despite this, it cannot predict how much expansion actually occurs and the inability to truly quantify MRP restricts its ability to define accurate thresholds (107). However, MRP remains very sensitive to ischaemic lesions which makes it useful as a triage technique for patient management, but its specificity in accurately predicting tissue outcome and final infarct volume is poor (217;218). Moreover, most MRP investigations have not resulted in consensus as to which perfusion parameter is the most accurate predictor of tissue fate. On the other hand, several authors suggested the visual mismatch estimation rather than using a quantitative method. Luby et al. compared the performance of qualitative mismatch evaluation against the quantitative method and they reported no difference. In addition, qualitative mismatch selection had high sensitivity, specificity and positive predictive values among neurologists (219). In (Desmoteplase in Acute Ischemic Stroke-phase II) DIAS II trial, investigators used MRI as the mismatch concept by visual inspection for the first time as an entry criterion to thrombolyse patients and as a primary efficacy end point and they reported a significant difference between treated and untreated patients up to 9 hours post ictus (192). These results were approved later on by investigators of DEDAS (58). In general, despite these different methods applied by using MRI in the acute stage of strokes and their effectiveness in predicting tissue fate and clinical outcome, there has been a lack of definitions of ischaemic changes and clinical outcome on which the accuracy of MRI parameters is based. Additionally, time to reperfusion has not been taken into account when evaluating MRI methods.

As part of the MRI protocol for stroke, MR angiography (MRA) is a helpful tool for the detection of intra- and extra-cranial vasculature. Unenhanced MRA showed sensitivity of up to 93%, while enhanced MRA had higher sensitivity of up

to 97%. However, MRA showed a high sensitivity for the detection of cerebral aneurysms > 3mm (220). The MRI protocol for the evaluation of acute stroke patients consists of conventional MRI, DWI, PWI and MR angiography which usually takes 15 minutes, a bit longer than CT protocol. However, the two modalities were proven to be useful to approach acute stroke patients, and currently both have a role in patients' evaluation depending on local clinical circumstances and constraints, such as available technology and staff experience (221).

2.4 Other functional imaging techniques are used for evaluation of acute ischaemia

2.4.1 Positron Emission Tomography (PET).

PET is the gold standard for the quantification of CBF and cerebral tissue oxygen consumption. Penumbra tissue appears on PET as an area of reduced CBF and increased oxygen extraction fraction (OEF). Heiss et al. found a significant correlation between the volume of hypoperfusion areas on PET and patients' clinical outcomes (35). However, PET is confined to research with limited clinical application because of the arterial sampling techniques required for absolute quantitative CBF values are relatively contraindicated with standard systemic thrombolysis (70).

2.4.2 Single-photon emission computed tomography (SPECT).

This technique depends on injected radioisotope which binds to certain blood compounds and diffuses through the intact blood brain barrier and can be

metabolised by brain tissue. Acquisition of data takes a bit of a long time in comparison with standard techniques of stroke evaluation which renders SPECT unsuitable for clinical settings (72). SPECT provides semiquantitative measurements of CBF which can be performed rapidly. However, its limitations include tracer preparation, expense and low spatial resolution in comparison with CT and MRI (64). Additionally, the subtracted data is physiologic and not anatomic like MRI and CT.

2.4.3 Xenon-enhanced computed tomography scan (Xe-CT).

This technique depends on inhalation of the inert gas Xenon in a known concentration and tracing the subsequent changes in tissue density. This technique was approved in both animal and human models for accuracy in the detection of ischaemia with strong correlations(222). A study by Firlik and colleagues reported sensitivity to detection of EICs up to 100%. Additionally, they found that CBF values less than 15ml were associated with the development of severe oedema and poor outcomes (223). Generally, there has been little literature relating to XeCT imaging, which limits the involvement of the technique in routine clinical settings. In addition, Xenon has anaesthetic effects which might affect its administration in acute patients.

Chapter III : Methodology

3.1 Study design

This study was conducted retrospectively on CT scans of stroke patients, who were recruited to ongoing studies at an academic stroke centre. The study consisted of three stages: stage I, the consensus stage, and stage II. Finally, an analysis of perfusion parameters of scans and the fate of tissue compartments on follow-up scans was done (figure 3-1). CT scans were categorised into two separate groups: the first set of scans for stage I, and a second set of scans for stage II. In addition, there was a small set of CT examples for the consensus stage.

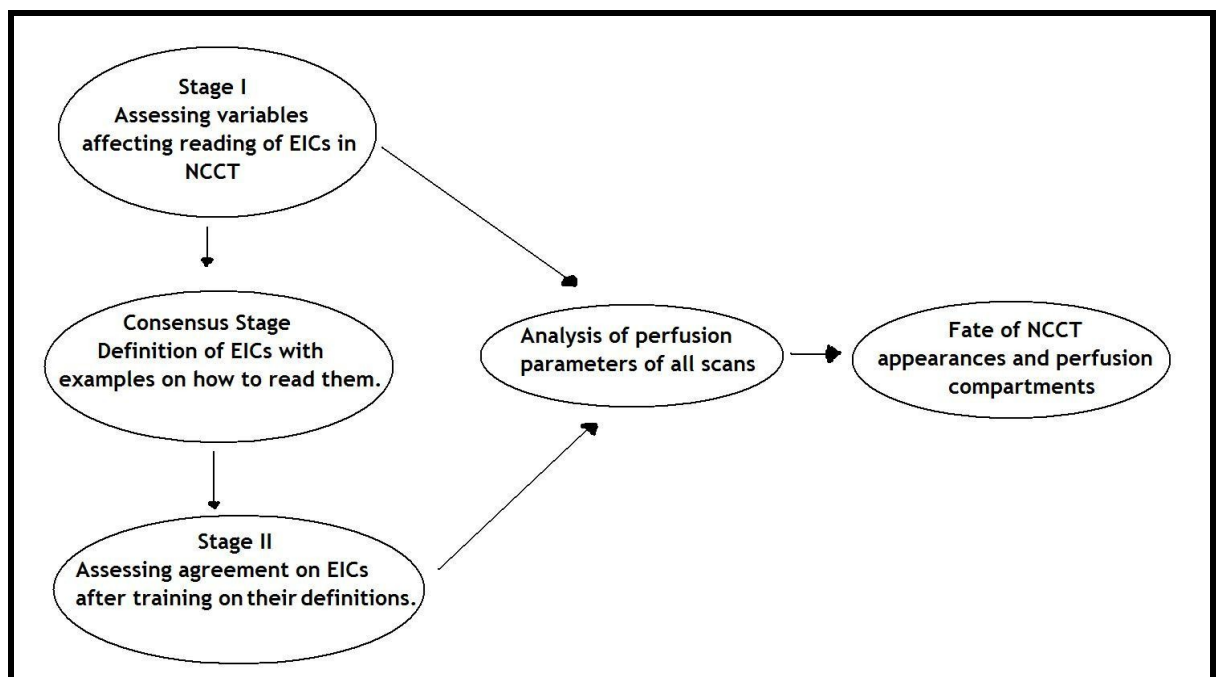


Figure 3. 1: Study design.

3.2 Patients

The target population was patients with acute ischaemic stroke recruited to one of two studies at an academic stroke centre, namely the Multicentre Acute Stroke Imaging Study (MASIS / Wyeth) and Post Stroke Hyperglycaemia (POSH). Study inclusion and exclusion criteria for both studies are listed in table 3.1.

Demographic data, including age, gender, domestic circumstances, alcohol and smoking status, were collected from eligible patients. On admission, time of onset of symptoms, time of hospital arrival and time of first scanning were reported and the patient's risk factors and concomitant medications were also assessed. The pre-morbid modified Rankin Scale (mRS) and NIH Stroke Scale (NIHSS) for each patient were taken. Almost all eligible patients had acute multimodal CT scanning, including NCCT, CTA and PCT, and repeat scanning at 24-72 hours after a stroke.

In MASIS, patients had MRI and MRA as the main follow-up imaging technique, while CT modalities were seldom used. Conversely, NCCT and CTA were the main follow-up imaging tools for POSH patients. In both studies, the time of onset of acute NCCT, perfusion and angiography scanning were all recorded. In addition, patients had outcome assessments on day 7 with the NIHSS, and day 30 with the mRS.

Eligible patients were those who presented within 6 hours of stroke onset and had acute NCCT, perfusion imaging and follow-up NCCT and angiography. Patients were not stratified according to age, gender and NIHSS score. Prevalence of EICs on CT was not taken as a determinant for involving patients in the study.

Inclusion criteria	Exclusion criteria
Presented within the first 6 hours	Non-stroke diagnosis
Proven diagnosis of acute stroke	Inability to lie in a recumbent position
	Intercurrent illness limiting surviving up to a month.
	Coma
	Renal failure
	Known allergy to contrast media

Table 3. 1: Inclusion and exclusion criteria for both; MASIS and POSH studies.

3.3 Readers

Targeted observers were stroke neurologists and neuroradiologists with different levels of experience. They were invited to the study by e-mail or by meeting face to face to illustrate the study purpose, and their role in it (See Appendix; tables 1,2,3). The study set out to include observers of varying experience and professional background. No trainee neuroradiologists were available to participate at the time of the study. All readers except one were either medical staff or members of research teams at Southern General Hospital. When the consensus was ready, all were sent invitations to read the consensus set of scans and further their participation in the second stage of study. Only 5 readers agreed to continue, while the other 4 apologised. Six new readers responded positively to the consensus invitation and agreed to participate in the second stage. All participants except two were either member of medical staff or research teams at Southern General Hospital.

3.4 CT Scans

Scans of eligible patients, including acute and follow-up NCCT, PCT and CTA, were loaded into the MiStar software package [Version 3,2,63 DICOM 3.0 Conformance software] for processing. Each scan was anonymised and coded by serial numbering according to their groups starting from number 01. Coding of scans was arbitrary and was not randomised. Acute NCCT scans were saved in Joint Photographic Experts Group (JPEG) format for the purpose of gathering the targeted slices, which contain the 10 ASPECTS regions only. These slices were collected in one image of a maximum 6 slices by loading onto the Paint program and resaved as (JPEG) file (figure 3-2). The size of the slices was adjusted at about 400*400 as measured by the program, for equalisation of appearance. The slices of one scan were reduced to be shown in 2-4 images. Scan resolution for providing the best viewing window for readers was optimised for grey-white matter differentiation on MiStar software before being formatted by Paint. PCT scans were all processed by MiStar using Stroke Mode and slices of interest (ASPECTS areas) were all saved in (JPEG) format. Follow-up NCCT scans were viewed on MiStar and stored in (JPEG) files for revision.

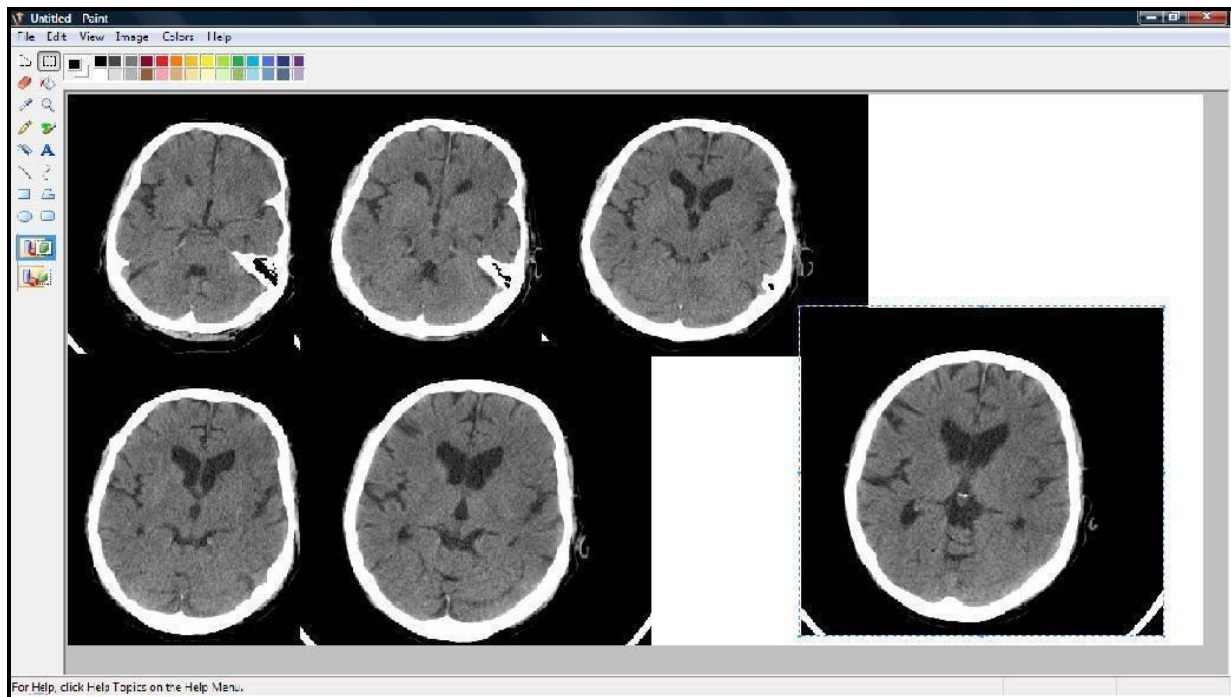


Figure 3. 2: Recollection of CT scan slices in one image maximum 6 slices and minimum 3 slices.

3.5 Reading the scans

Targeted changes to be read were isodense swelling and hypodensity. The ASPECTS score anatomical template was used to read EICs in this study (see Appendix; figure 1). The Hyperdense vessel sign was not included in the detailed assessment in this study, but was added as extra information with assessments in the first stage of the study. Therefore, EICs hereafter always refer to isodense swelling and hypodensity but not the Hyperdense vessel sign. Readers were asked to classify the ischaemic changes into 10 areas according to ASPECTS template. In the first set, the posterior and anterior cerebral artery territories were added to ASPECTS areas. However, this study mainly included scans from patients with middle cerebral artery occlusion; hence, the posterior and anterior areas were rarely involved in any ischaemic changes and their incorporation in analysis of agreement caused misleading results i.e very high values of free marginal kappa although readers were not agreeing on the presence of abnormality in the area. Therefore, responses to these areas were

excluded from the analysis of first stage results and they were not involved in the second stage of the study. A reference standard for the presence or absence of EICs in each region was not done in this study for purpose of comparing these classifications with their correspondent areas on PCT in the next stages of the study and finding out how the perfusion changes of acute ischaemia on PCT be interpreted by observers on NCCT. The classification as hypodense, isodense, both, or normal was defined by the majority interpretation of readers. The cortical and subcortical white matter was all considered in reading each ASPECTS area.

Survey Title	Created	Modified	Design	Collect	Analyze	Actions
SCAN-28	October 11, 2010 16:48	1 year ago				9 Clear Transfer Delete
SCAN-12	October 10, 2010 16:56	1 year ago				9 Clear Transfer Delete
SCAN-38	October 11, 2010 16:59	1 year ago				9 Clear Transfer Delete
SCAN-40	October 11, 2010 17:01	1 year ago				9 Clear Transfer Delete
SCAN-29	October 11, 2010 16:49	1 year ago				9 Clear Transfer Delete
SCAN-21	October 11, 2010 03:10	1 year ago				9 Clear Transfer Delete
SCAN-13	October 10, 2010 16:58	1 year ago				9 Clear Transfer Delete
SCAN-14	October 10, 2010 16:59	1 year ago				9 Clear Transfer Delete
SCAN-10	October 10, 2010 16:51	1 year ago				9 Clear Transfer Delete
SCAN-27	October 11, 2010 03:06	1 year ago				9 Clear Transfer Delete

Showing 11 - 20 of 43

« 1 2 3 4 5 6 7 8 9 10 »

Figure 3. 3: Scans on Survey Monkey.

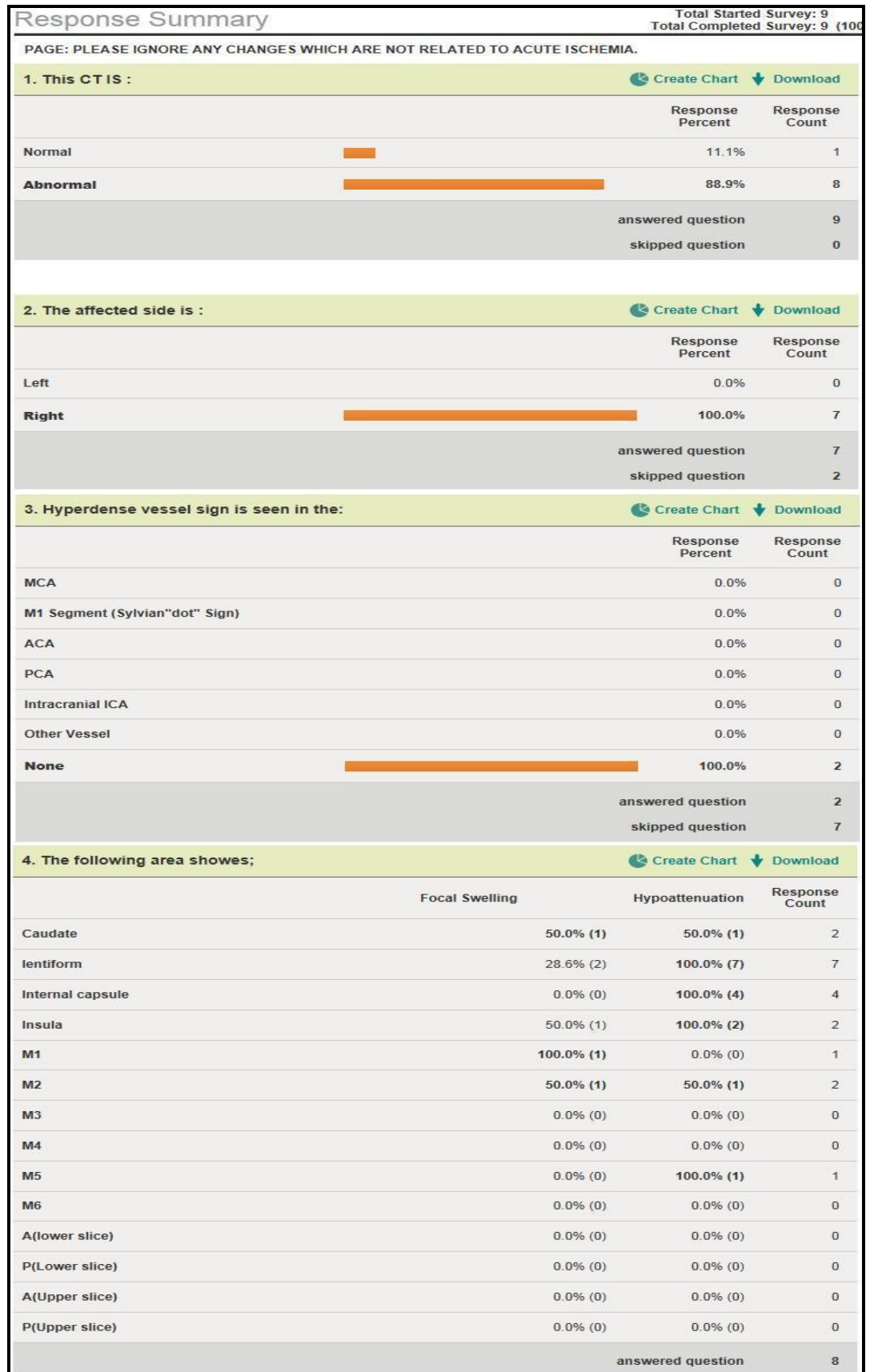


Figure 3. 4: Responses of readers to one survey (one scan).

3.6. Presentation of scans to readers

Presentation of scans to readers was done by the creation of the web-based survey tool Survey Monkey. A basic account was the model used for loading the set. It permits a limited number of questions (up to 10 per survey) with a limited number of responses. Therefore, the scan slices were gathered in one image with priority to slices containing the ASPECTS template regions. An example of scans loaded to the survey with the questionnaire is shown in **Appendix figures 2 and 3**. Images on Survey Monkey have no adjustment exposure tool; therefore, changing contrast to enhance the grey-white matter interface was not possible and readers couldn't change the window settings of loaded slices for best viewing of EICs. Each scan had its own survey with a web link.

Each survey was named with its scan number. The order of surveys and their links was not correlated with their numbers (**figure 3-3**). A total of 40 surveys were created on Survey Monkey, with 40 web links for all scans of the first set. They were organised in an arbitrary way but avoided repeating similar scans in adjacent places. Thirty two surveys were created for second set scans. Readers were sent survey links via e-mail together with ASPECTS template as a PDF file (**Appendix figure 1**). Each link connects to a scan in the set. Responses from all readers to each scan were collected by survey collector tool with the possibility of browsing each response individually (**figure 3-6**). The survey does not match the responses to each reader's e-mail, but it gives the time of starting response to scan and the time last modified. However, the time at end was dependent on the last second the reader closed the survey, so the whole interval is not always indicative of the real time spent by the reader on reading the scan.

3.7 Stage I of the study (First Set of Scans)

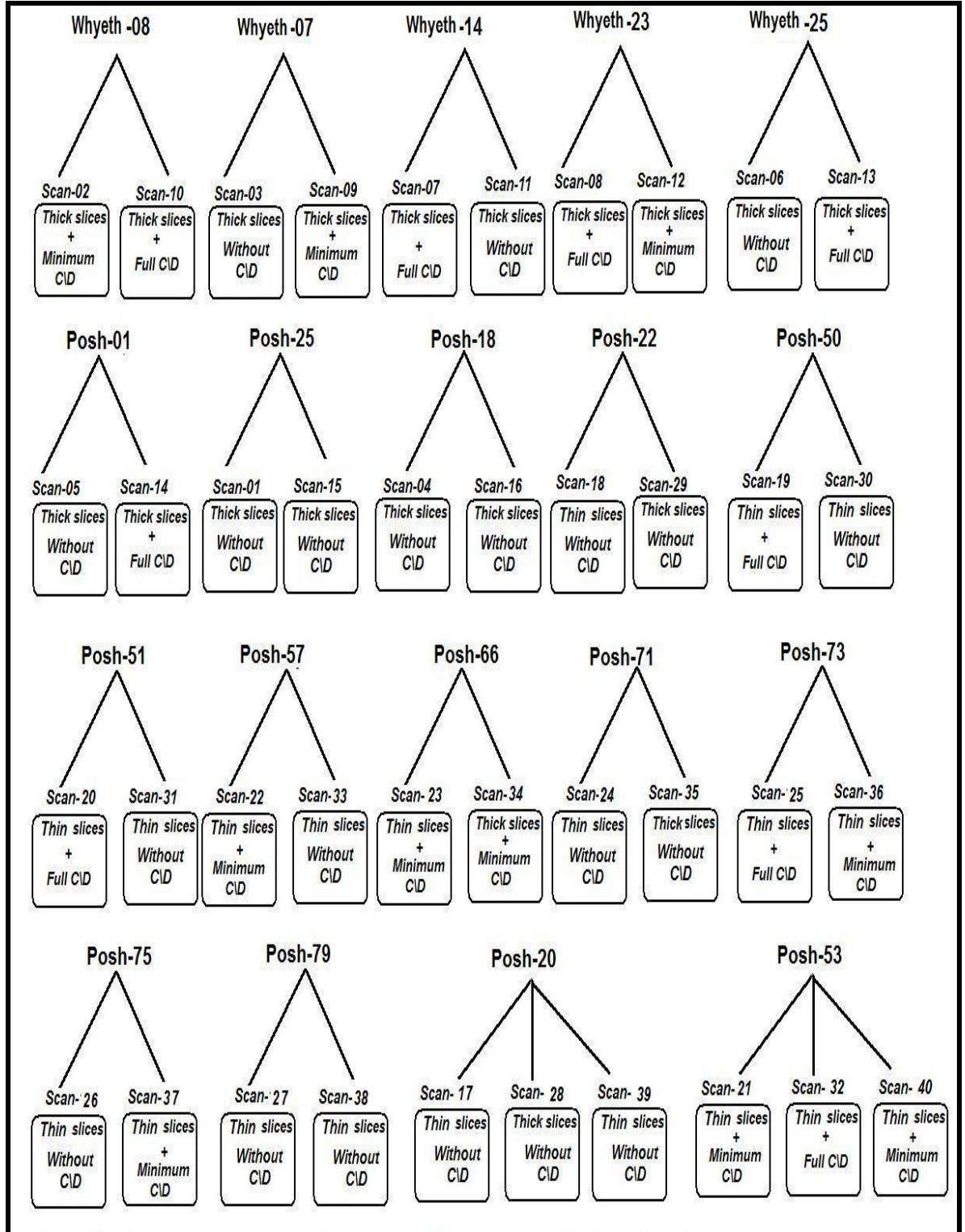


Figure 3. 5: Schematic drawing of repetition process with scans coding [C/D Clinical Data].

The aims of this stage of the study were:

- 1- To assess the effect of the number of variables on reading EICs: hypodensity and isodense swelling on NCCT.
- 2- To assess intra-observer agreement.
- 3- To assess the untrained group of readers.
- 4- To evaluate Hyperdense vessel sign.

In the first stage, scans from 19 patients were used to assess inter- and intra-observer agreement. Two out of the total number of patients had non-stroke diagnosis at the final evaluation. They were added to the first set in order to assess the ability of readers to recognise normal appearing brain tissue from an ischaemic one at the time of the presentation. Therefore, 17 scans were only involved in all subsequent analyses of agreement, perfusion and fate.

All 19 scans were repeated, making a total of 40 scans, and presented to readers as the first set of scans. Readers were not informed of any duplicate scans. Seventeen scans were presented twice, and two scans were presented three times within the set. The repetition process aimed at changing the slice thickness and clinical information with scans. Additionally, some scans were repeated without change to assess intra-rater reliability. Readers were not given any training or illustration of EICs before their participation in the study.

3.7.1 Study Variables

In this stage of the study, 4 main variables were assessed for their effect on reading EICs on acute NCCT. These include slice thickness of scans, knowing clinical information, readers' experience and readers' speciality. Other situations, such as affected hemisphere, normality of scans, intra-rater agreement and Hyperdense vessel sign were also measured with this set of scans. The effect of other factors on reading the scans like old infarcts, white matter diseases and atrophic and atherosclerotic changes, which are intrinsic factors related to brain parenchyma, were not assessed in this study though they were found to affect the observer reading of EICs. This was because this study is mainly concerned with seeking agreement on isodense swelling among group of

readers rather than seeking the agreement on hypodensity or both changes together which have been more likely to be mixed with other chronic brain changes. Additionally, this study introduces defining criteria for isodense swelling and hypodensity which differentiate them from each other and recognise each one as a separate entity from any other change. And for purpose of testing the defined criteria before and after training these factors were cancelled and readers were asked to focus on acute ischaemic changes.

A- Slice thickness

Scans were adjusted to two levels of slice thickness: 5mm (thick) and 0.9mm (thin). For scans which were stored in thin slices, MPR reformatting by MiStar was done to generate thin slices. In total, there were 20 scans with thick slices and 20 scans with thin slices. Of these, 4 scans were presented twice within the set with fixed clinical information, changing their slice thickness from thin to thick. **Figure 3-6** shows an example of these scans in thick slices and thin sliced forms.

B- Clinical information

Observers read the scans with and without any knowledge of the patient's presentation. In total, 20 scans were shown without concomitant clinical information, which means that readers should judge normality of scan and recognise the affected side before they look for EICs. The other 20 scans were presented with their clinical information, which states that readers know the affected hemisphere and they just need to distinguish ischaemic changes. From the total number of these scans, there were 8 scans shown without clinical data and then repeated with clinical data with fixation of their slice thickness. Scans with clinical information were further subdivided into two groups according to the amount of provided clinical information: scans with full clinical data and scans with minimum clinical data.

Full clinical data show the detailed symptoms and signs of the patient on presentation, whereas minimum clinical data is just a hint of the affected hemisphere. Examples of these are as follows:

Example 1; full clinical data

Scan-10. A 76-year-old woman with breast cancer presents with partial left facial paralysis, left upper limb weakness, mild sensory loss and severe hemi-inattention.

Example 2; minimum clinical data

Scan-02. A 79-year-old woman presents with left side symptoms.

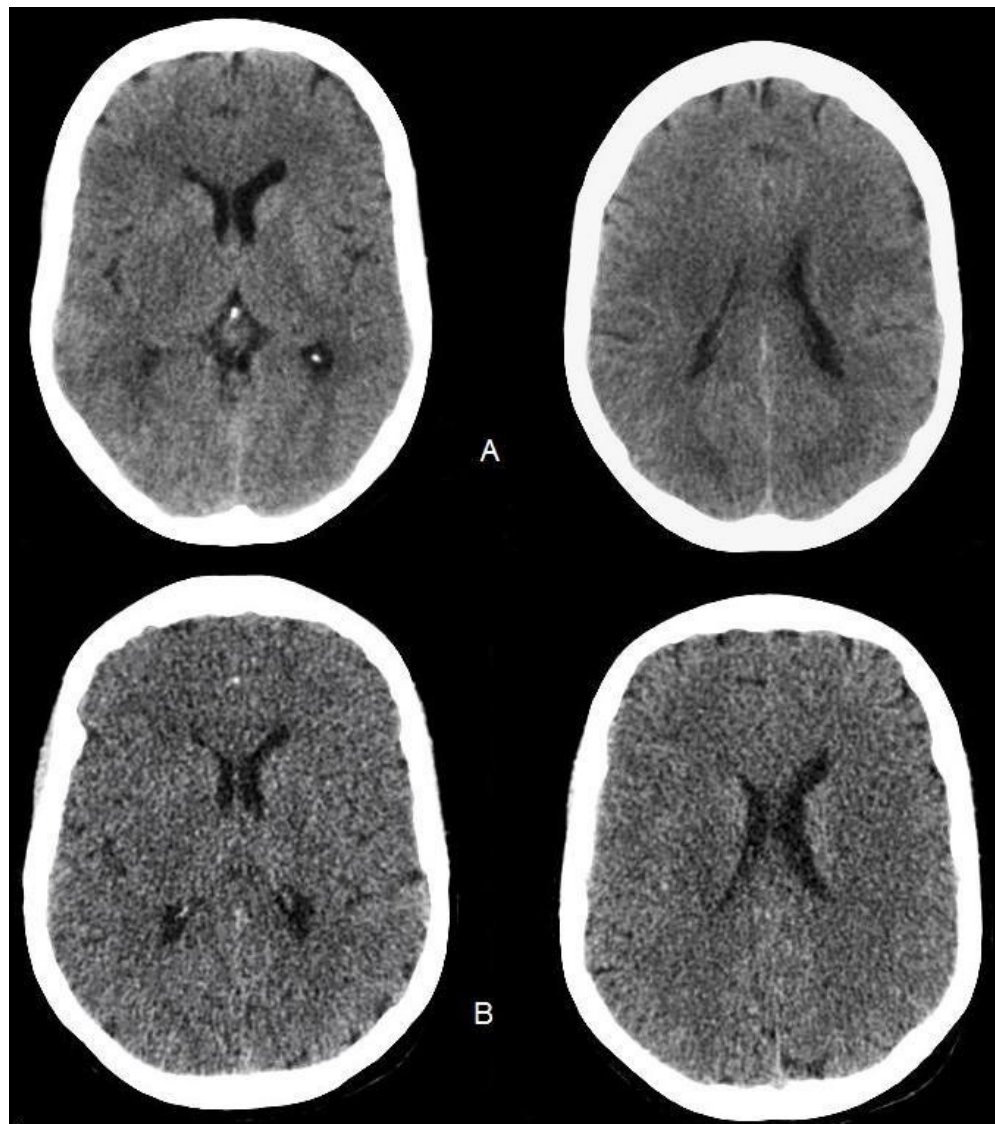


Figure 3. 6: Same scan with thick slices(A) and thin slices(B). In both situations, the ganglionic and supraganglionic levels of ASPECTS template are only shown.

In total, 11 scans were with minimum clinical data and 9 scans with full details. Categorisation of scans regarding the amount of clinical data available was not stratified according to the prevalence of EICs or severity of stroke, and the number of scans which had full or minimum C\I was according to the availability of clinical details from the studies' files.

C- Readers' experience and speciality.

Two specialities and two experience levels were investigated in this study to seek their effect on agreement. Specialities which were involved in acute stroke management were mainly targeted in this study, including stroke neurologists and neuroradiologists. Their experience was classified into two categories: expert readers, who are consultant doctors who have spent many years in reading scans from stroke patients, and trainee readers, who are doctors still training to read scans from stroke patients. In total, there were 7 stroke neurologists, 2 neuroradiologists, 5 experts and 4 trainees.

D- Affected side and normality of scan

Because this set included normal scans and scans without clinical information, the ability of readers to agree on the normal scans and the ischaemic hemisphere was also assessed. Two scans from non-stroke patients were included within the set. Both presented without any clinical information, but one was with thick slices and one was with thin slices. Both were duplicated and hence there were 4 normal scans within the first set of scans. Readers' agreement on the affected hemisphere for all abnormal scans (36) and for scans without clinical information (16) was assessed separately.

E- Intra-observer agreement

For assessment of intrinsic reliability of readers in reading EICs, the number of scans with different presentations was repeated without change. There were in total 5 scans and with repetition they were shown 10 times within the first set.

This CT is : <input type="radio"/> Normal <input type="radio"/> Abnormal		
2. The affected side is : <input type="radio"/> Left <input type="radio"/> Right		
3. Hyperdense vessel sign is seen in the : <input type="radio"/> MCA <input type="radio"/> M2 Segment Sylvian "dot" Sign <input type="radio"/> ACA <input type="radio"/> PCA <input type="radio"/> Intracranial ICA <input type="radio"/> Other vessel <input type="radio"/> None		
4. The following area shows:		
	Focal Swelling	Hypoattenuation
Caudate	<input type="checkbox"/>	<input type="checkbox"/>
Lentiform	<input type="checkbox"/>	<input type="checkbox"/>
Internal capsule	<input type="checkbox"/>	<input type="checkbox"/>
Insula	<input type="checkbox"/>	<input type="checkbox"/>
M1	<input type="checkbox"/>	<input type="checkbox"/>
M2	<input type="checkbox"/>	<input type="checkbox"/>
M3	<input type="checkbox"/>	<input type="checkbox"/>
M4	<input type="checkbox"/>	<input type="checkbox"/>
M5	<input type="checkbox"/>	<input type="checkbox"/>
M6	<input type="checkbox"/>	<input type="checkbox"/>
A(lower slice)	<input type="checkbox"/>	<input type="checkbox"/>
P(Lower slice)	<input type="checkbox"/>	<input type="checkbox"/>
A(Upper slice)	<input type="checkbox"/>	<input type="checkbox"/>
P(Upper slice)	<input type="checkbox"/>	<input type="checkbox"/>
		<input type="button" value="Done"/>

Table 3. 2; First set questionnaire.

3.7.2. First set questionnaire

Readers were asked to answer 4 questions on each scan in the first set. The questionnaire template is illustrated in **table 3-1**. If they answered yes to any of choices, they had to tick the corresponding box of choice. An absence of a tick mark means that the reader thinks the choice is absent and the scan is normal. In the first two questions, readers had to decide whether the scan was normal or abnormal and, if abnormal, which side was affected? The next two questions are related to ischaemic changes which they have to detect when the scan is abnormal. They had to look for a Hyperdense vessel sign and localise it to a cerebral artery. Then they had to recognise isodense swelling and hypodensity and localise them to each ASPECTS region. Readers were asked not to report any changes which were not related to acute ischaemia. The time required to complete the whole set of scans was open but with a maximum of 4 weeks. Thereafter, readers were sent regular reminders. Time recorded by the survey, together with contact e-mails from readers, helped to identify each reader personally.

3.8 Consensus stage (consensus set of scans).

The aims of this stage were as follows:

- 1- To seek consensus among readers on definitions of isodense swelling and hypodensity.
- 2- To build up general steps in reading EICs on NCCT.
- 3- To distinguish clearly between isodense swelling and hypodensity.

Scans which had the highest level of agreement on EICs were used to illustrate the appearances of isodense swelling and hypodensity and were employed to derive definitions for these appearances. Other scans from stroke studies were also used to give examples of these changes. The definitions of isodense swelling and hypodensity and their signs on NCCT were taken from previous literature,

mainly publications from Von Kummer et al. and Wardlaw et al. These definitions were collected and organised for the purpose of illustration and differentiation between both changes (see **Appendix; figures 4a-e**).

3.8.1 Appearances of EICs

Scans which attained good agreement in the first stage were analysed on MiStar software. During this stage, the NCCT and PCT of each case were analysed. Their NCCT and PCT scans were both loaded to the viewer at the same time for the purpose of matching the appearances of EICs on NCCT with penumbra-gram on PCT. MiStar's "penumbra gram" [the generation of "penumbra gram" will be described with PCT later] displays areas with penumbral perfusion thresholds in a green colour, while areas with core perfusion are in red. Because the axial orientation of some patients differed between the NCCT scan and PCT scan, NCCT slices for these cases were reformatted by the MPR tool to match the axial orientation of PCT slices.

Visual comparison of areas was the main method of analysis. Additional methods included:

- 1- Densitometry; measurement of Hounsfield Units for areas on NCCT corresponding to core and penumbra. On MiStar, this is displayed as statistical information for each ROI(region of interest) pixel. The mean HU value of each ROI was reported for the comparison process. However, the determination of the exact difference in HU readings between isodense swelling and hypodensity is not the main purpose of study and the reported values were mainly to support the visual comparison findings.

- 2- Histogram; this is displayed dynamically for the chosen ROIs. It is a plot of pixels against HU values. Thresholds can be adjusted according to the desired range to minimise artefact and obtain clearer curves for comparison.

On the penumbragram slice, ROIs were drawn on penumbra areas automatically by choosing the “Grow by Threshold” button and on core areas too, and then copied onto the NCCT corresponding slice, and finally mirrored onto the contralateral hemisphere. This was done to find out how penumbra appeared on an NCCT scan. Structural changes within ROIs were compared with normally appearing contralateral tissue in respect to: changes in radiolucency, narrowing and loss of CSF spaces, and loss of grey-white matter interface. Areas which showed deviation from normal appearance had densitometries and histogram measurements. ROIs were also drawn manually when the automatically generated ROIs were large and disorganised or when samples were from abnormal regions, and normal and abnormal white matter were tested.

For purposes of comparison, and because there were few scans with good agreement on either isodense swelling or hypodensity from the first set, other scans from ongoing studies with large core or penumbra, and with mixture of both, were also added to the analysis. **Figures 3-7,8,9 and 10** show examples of a scan with large penumbra, a scan with large core and a scan with mixed core and penumbra tissues. The way of visual comparison was also illustrated in those figures with reference to densitometry readings and histogram appearance in normal and abnormal hemispheres. Other examples of consensus analysis are shown in **appendix figures 7,8,9,10**.

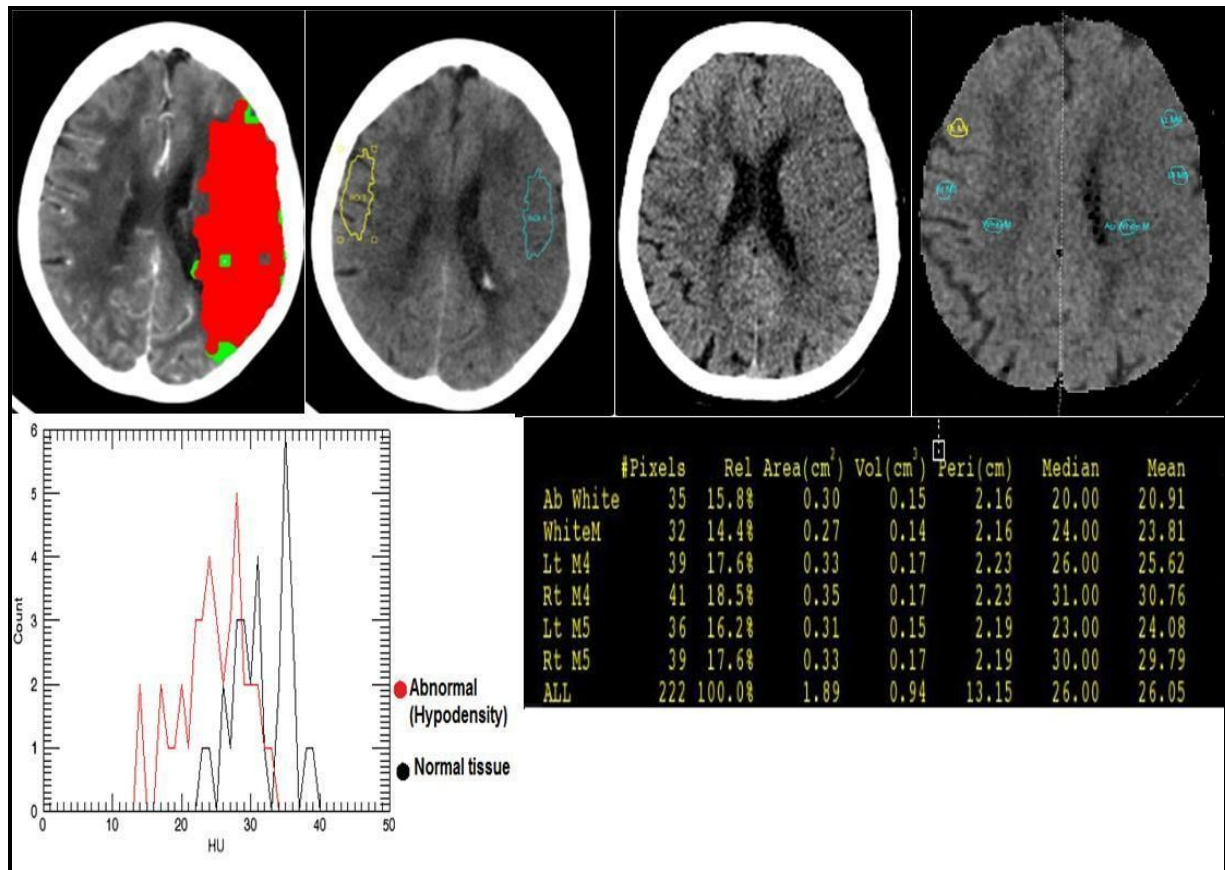


Figure 3. 7: Core appearance analysis. Upper: from left to right; Penumbra-gram, ROI, Acute NCCT, Histogram thresholds. Lower; Right: densitometry readings with averages of HU units in each ROI. Left: Histogram.

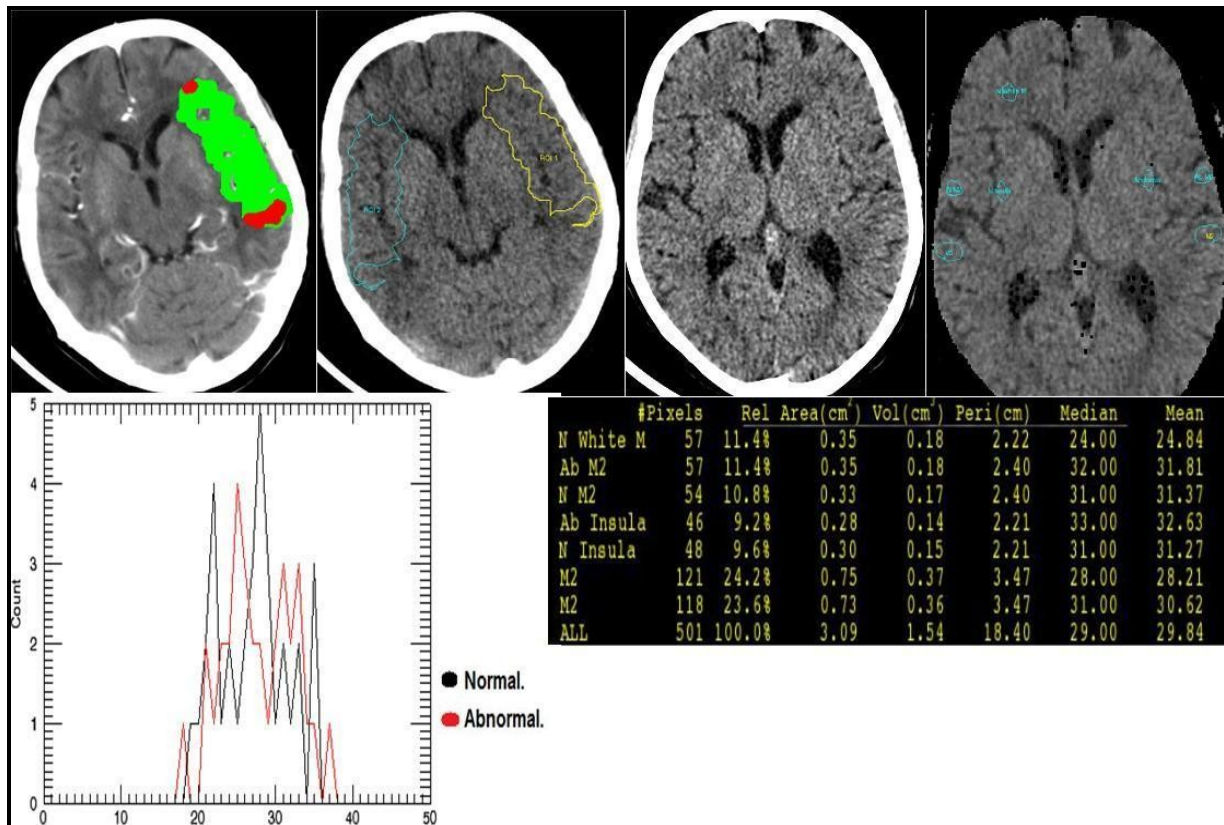


Figure 3. 8: Penumbra appearance analysis. Upper: from left to right penumbra gram, ROIs, NCCT, Histogram thresholds. Lower; Left; Histogram Right; densitometry readings.

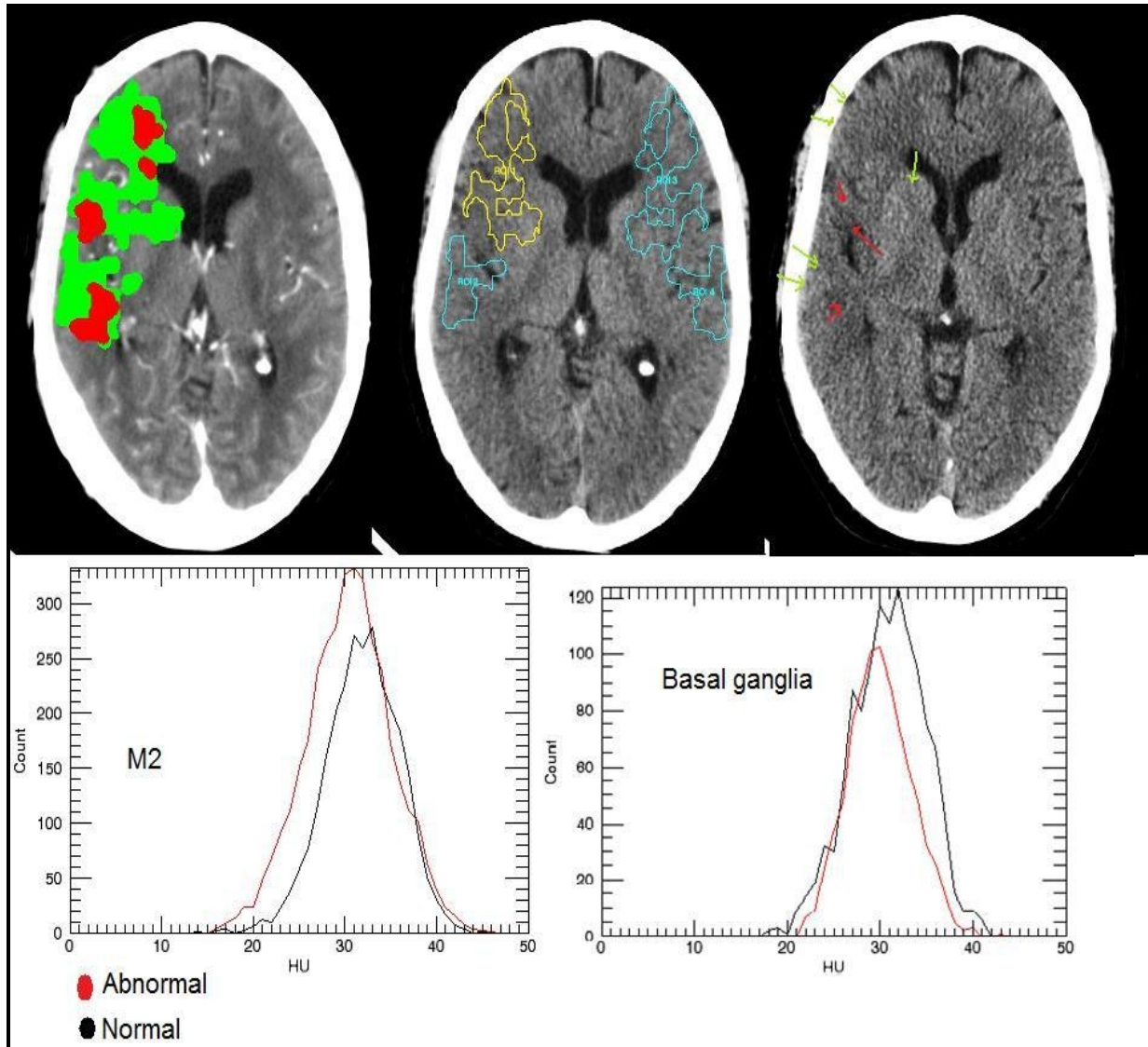


Figure 3. 9: Appearance of areas with mixed penumbra and core tissues. Red arrows indicate on NCCT and green arrows indicate penumbra areas.

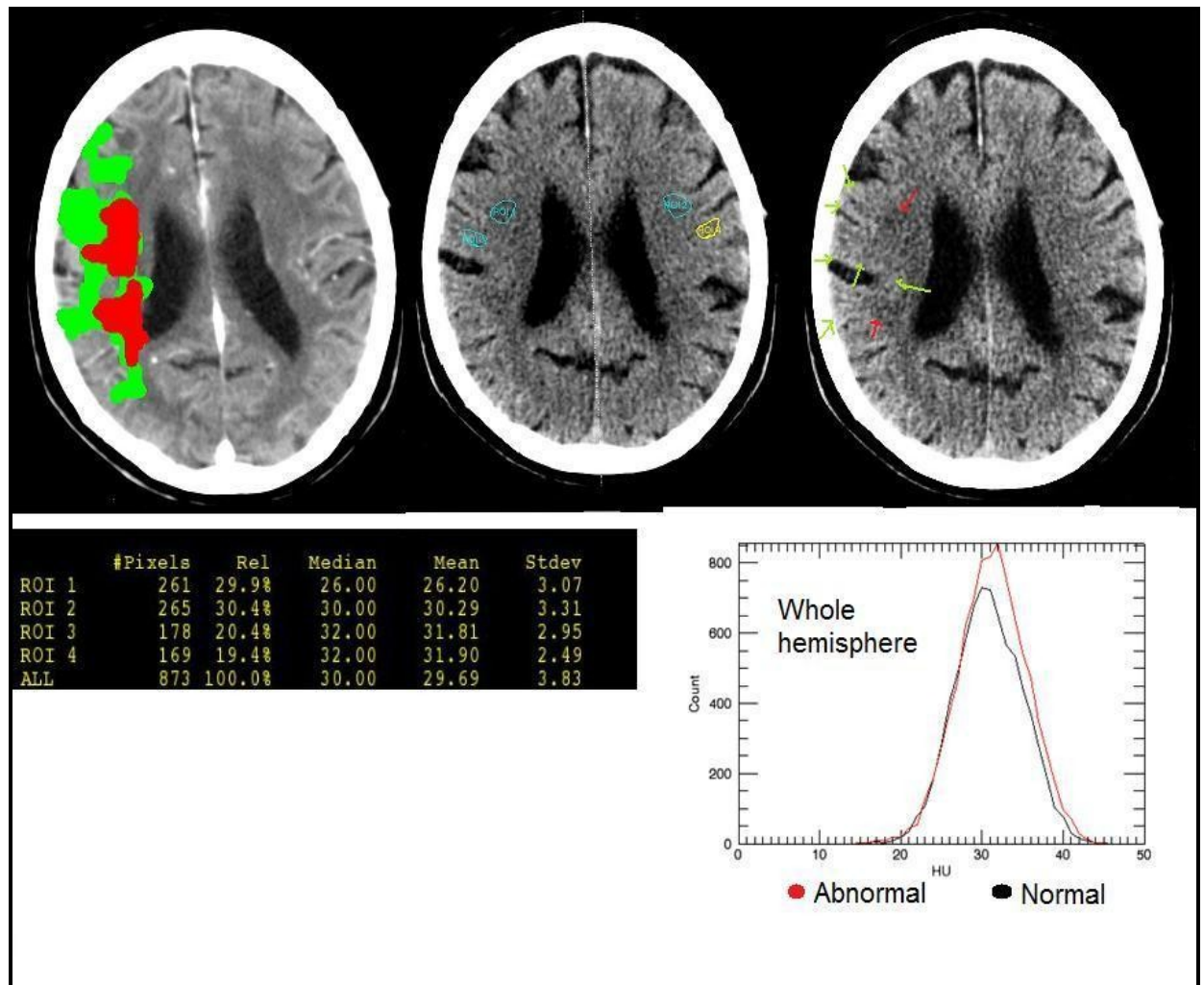


Figure 3. 10: Scan with mixture tissue. Samples from affected areas show low HU for core areas and similar HU values for penumbra and normal tissue. Green arrows show areas of penumbra (isodense), Red arrows show areas of core (hypodensity).

3.8.2 Definition of isodense swelling and hypodensity

Definitions for both isodense swelling and hypodensity were derived from the above analysis and from the definitions given by Von Kummer et al. and Wardlaw et al, as well as publications from Na et al, Muir et al. and Koga et al.

Hypodensity; Increased radiolucency of brain structures relative to other parts of the same structure, or to its contralateral counterpart that could be recognised visually.

Hypodensity signs on NCCT scan are;

1- Complete loss of differentiation between grey-white matters (**CDGW**); complete loss of cortical ribbon due to decreased attenuation of grey matter. There should be no distinction between density of cortex and underlying white matter, and the density should be equal to, or less than, contralateral white matter.

2- The disappearing basal ganglia sign (**DBG**) and Obscuration of lentiform nucleus (**OLN**); loss of the normal contour of basal ganglia, or decreased attenuation of parts, or whole, lentiform nucleus, with loss of precise delineation of the area and blurring of its margins so that its differentiation from contiguous white matter structures is impossible.

3- Loss of insular ribbon (**LIR**); loss of the usual slightly increased attenuation of insular cortex with reduced precision in delineation of grey-white interface at its lateral margins.

4- Cortical sulcal effacement (**CSE**); decreased contrast density with loss of precise delineation of grey-white matter interface at the margins of the cortical sulci.

Isodense swelling; brain swelling without concomitant hypoattenuation.

This might be associated with the following signs on the NCCT:

1- Partial loss of differentiation of grey-white matter interface (**PDGW**); loss of grey-white matter interface. Cortical ribbon is not well recognised if compared to contralateral hemisphere; however, the cortex is still brighter than subcortical tissue and is less dense than contralateral white matter.

2- Cortical sulcal effacement (**CSE**); a localised mass effect. It can appear as a reduced number of sulci and the straightening of brain outer contour in affected areas.

- 3- Obscuration of Sylvain fissure (**OSF**); narrowing or obliteration of Sylvain fissure.
- 4- Loss of insular ribbon (**LIR**); reduced precision in delineation of grey-white interface at its lateral margins.

The reading of both on the NCCT depends on recognising two signs:

- 1- The changes in the grey-white matter interface; complete disappearance with hypodensity and partial disappearance with isodense swelling.
- 2- Brain swelling; local swelling with normal density is isodense swelling and not hypodensity.

The signs which are stated for each change were gathered in this way in order to lessen any confusion which might arise with regard to the many names for EICs. The appearance of these signs with each change is illustrated with definitions.

3.8.3 Consensus between readers

Definitions of EICs with their signs and with illustrative examples were collected in a PowerPoint presentation and saved as a PDF file (see Appendix for the complete consensus presentation). The appearances of the changes were generally categorised into two: hypodensity and brain swelling. Then, more specific definitions were stated on presentation. Readers were also given an illustration of how to use these definitions when reading the scans.

Readers who agreed to participate in the study were sent an e-mail and the PDF file of consensus presentation. They were asked to go through the definitions and the illustrative examples and, if they agreed to participate further in the study, they would be sent the second set of scans. Readers who disagreed with any element of the proposed definitions were able to reply for clarification of any issue.

Most the readers who had a positive reply were satisfied with the consensus set. Two readers sought clarification of the partial and complete loss of gray-white matter.

3.9 Second stage of the study (second set of scans)

The aim of this stage was to:

1. Assess trained group of readers.
2. Assess the effect of training on reading EICs.
3. Assess the effect of training in relation to experience and speciality.

In this stage, NCCT scans from 32 patients were involved. There was no repetition of any of the scans within the set. All scans were presented with similar variables: thick slices (5mm) and minimal clinical information. An example of minimum data is as follows:

A 90-year-old man presented with RIGHT SIDE symptoms.

3.9.1. Second set questionnaire

In this stage, the questionnaire consisted of one question, as illustrated in **table3-2**, which shows the questionnaire template. Readers were asked to read each ASPECTS region and categorise it as normal, isodense swollen or hypodense. A tick at an area in any box for hypodensity or isodense swelling means that the reader saw the change at that area. Absence of any tick for an area means it was normal. If they thought the scan was normal, they had to tick the next icon as designed in the questionnaire. For the purpose of identifying each reader, they were given codes and were asked to sign their codes at the end of each scan. Additionally, readers were asked not to report any changes which were not related to acute ischaemia. The time required to complete the reading of the whole set of scans was determined at 15 working days and readers

were offered a £10 Amazon voucher if they completed reading the scans in time!
The identity of each reader was known from the code.

The following area shows:		
	Hypodensity	Focal swelling
Caudate nucleus	<input type="checkbox"/>	<input type="checkbox"/>
Lentiform nucleus	<input type="checkbox"/>	<input type="checkbox"/>
Internal capsule	<input type="checkbox"/>	<input type="checkbox"/>
Insula	<input type="checkbox"/>	<input type="checkbox"/>
M1	<input type="checkbox"/>	<input type="checkbox"/>
M2	<input type="checkbox"/>	<input type="checkbox"/>
M3	<input type="checkbox"/>	<input type="checkbox"/>
M4	<input type="checkbox"/>	<input type="checkbox"/>
M5	<input type="checkbox"/>	<input type="checkbox"/>
M6	<input type="checkbox"/>	<input type="checkbox"/>

In this SCAN:

There is no Hypodensity or Focal swelling.

Reader code is :

C E F N K H M T Z

Table 3. 3; Second set questionnaire.

3.10. Analysis of perfusion parameters for all scans

The aims of analysing the perfusion scans are to:

- 1- Compare CBF, CBV and MTT for all ASPECTS regions of an affected hemisphere with those of the normal hemisphere.
- 2- Correlate NCCT appearances as categorised by readers with perfusion categories.
- 3- Compare perfusion parameters of the three NCCT appearances.

3.10.1 Perfusion CT scans

PCT scans of all cases from both first and second stages were loaded onto MiStar for analysis.

Each scan was loaded onto the CT perfusion analysis programme/ stroke module. Viewer image parameters were all adjusted automatically except for the time interval, which was entered manually for each scan at 2 seconds. Arterial input (AIF) and venous output functions (VOF) were also adjusted manually and penumbra map processing then applied. Displayed perfusion maps on the main screen are: CBF, CBV, MTT, Delay Time, raw CTA image, function curves, penumbra gram, mean arterial and venous enhancement maps, mean arterial and venous phase maps and mean baseline map. Maps of interest for ROIs analysis in this study were MTT, CBV, CBF and penumbra gram.

Perfusion thresholds for penumbra and core were set in relative values (given as percentage of normal tissue of contralateral hemisphere). The programme calculates this automatically. However, penumbra MTT threshold (minimum) was adjusted manually to 145% of normal tissue MTT, and then applied to all scans automatically. Core CBV threshold was also adjusted manually to be 2ml/100g and then it was applied automatically to all scans. Other perfusion parameters' thresholds were kept constant as measured by the programme.

To avoid the presence of blood vessels on the true values of perfusion parameters, adjustment of maps by 'Masking by Threshold' effect was used. The highest threshold value for the CBV map was set at 90 in order to exclude all pixels with absolute CBV > 9ml\100g, this in turn excluded all blood vessels from the map prior to any analysis.

3.10.2 Measurement of perfusion parameters

ROIs corresponding to each ASPECTS area were selected manually from two slices selected to correspond to the ganglionic and supra-ganglionic ASPECTS templates. Sizes of penumbra and core as displayed by the penumbra-gram were also considered when choosing these slices with preference of the largest one. Loading the slice into the ROI analysis was done with “all maps of current slice” choice for the purpose of measuring all parameters of the same area at once.

The first step in the analysis was the determination of core and penumbra readings for each scan, which was done using the penumbra-gram. A manually-drawn ROI on penumbra was grown automatically using the “grow by threshold” choice from the menu. The same was done with the core area (**figure 3-12**). Subsequently, the programme displays readings from all perfusion maps of the same slice. Secondly, ASPECTS regions were drawn manually on both hemispheres using the contrast CTA map as anatomical reference. Data from those areas were exported to a folder and saved as a text file. The exported statistical information for each parameter per ASPECTS region included: median, mean, standard deviation, maximum and minimum values. They were all absolute values. Calculated mean was the measure used for comparing areas in this study. In addition, each perfusion map was saved as a jpeg file.

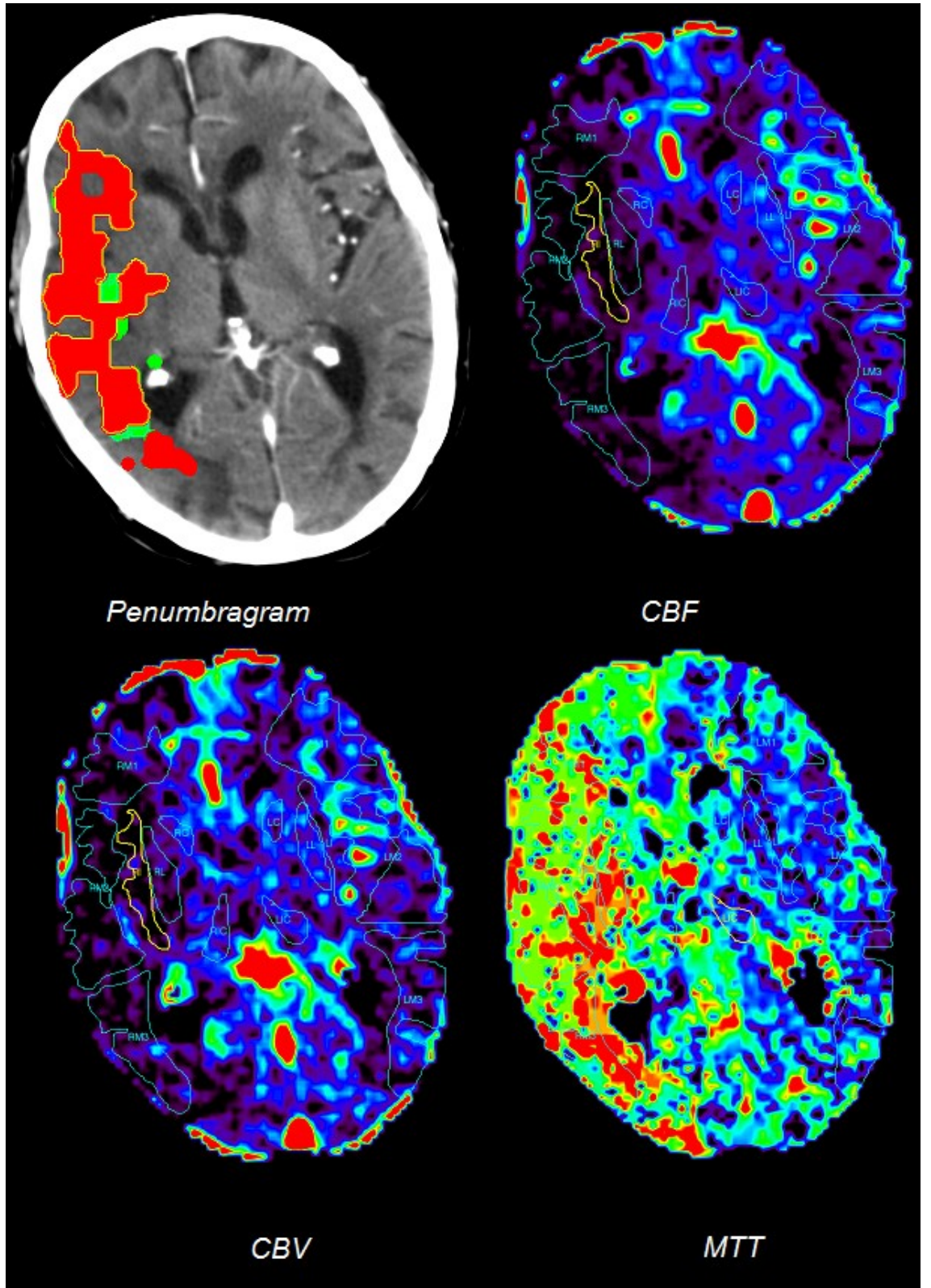


Figure 3. 11; Perfusion maps with ASPECTS regions.

3.11. Cerebral angiography

The aim of the angiography was to assess a vessel's patency after 24 hours from the onset of a stroke. Recanalisation was determined from either study-specific database information, or from neuroradiology clinical reports.

3.12. Follow-up NCCT scan

The aims of assessing follow-up scans were to:

- 1- Determine fate of ASPECTS regions on acute NCCT.
- 2- Compare fate of perfusion categorised compartments with fate of NCCT appearances as categorised by readers.

A total of 49 follow-up NCCT scans were loaded onto the MiStar DICOM and exported to a folder as jpeg files. The comparison process was carried out visually for each ASPECTS area on acute NCCT, which was compared directly with its corresponding area on the follow-up scan and categorised as either normal or infarcted. Examples of this are illustrated in **figure 3-13**.

Each ASPECTS region was classified into three compartments:

- 1- Baseline (<6h) NCCT appearance: normal, isodense swelling, hypodense or both (hypodensity and isodense swelling).
- 2- Perfusion CT categorisation; normal, core, penumbra or both (penumbra and core).
- 3- 24 Follow-up NCCT; normal or infarcted and mixed fate (part is infarcted and part is normal).

Comparison between the three classifications was carried out for the purpose of determining the fate of each ASPECTS area categorised by perfusion or readers.

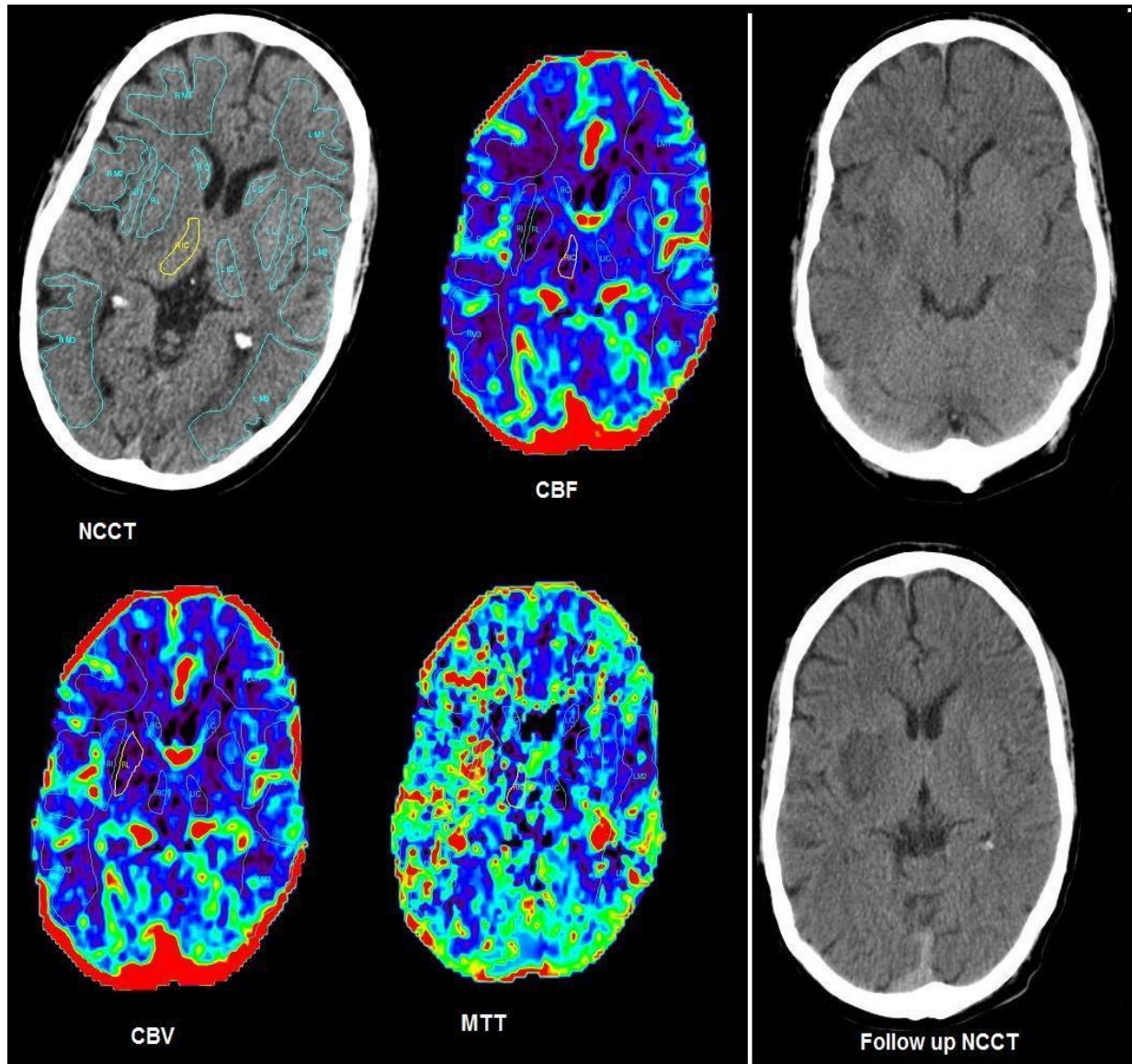


Figure 3. 12: Correlation of ASPECTS area's categories with their fate on follow up NCCT scan. In this example parts of lentiform nucleus and insula ended in infarction.

3.13. Statistical analysis

Data analysis was carried out by using MedCalc Statistical Software Package Version 12.2.1(224). Microsoft Excel was used to collect all data in a spreadsheet. Online calculations for some measures were done with StatTool Programme(225) and *Online Kappa Calculator* (Randolf stat)(226).

3.13.1 Collection of data

All collected data were stored in spreadsheets and created by Microsoft Excel. These included:

1- Readers' responses to each scan on Survey Monkey from both sets of scans. These were loaded as the response from individual readers for each single scan and each category of ASPECTS regions (isodense swollen or hypodense). Absence of response to any category meant a normal appearance and was shown as = 0. Positive response=1.

2- ASPECTS score of each scan; this was calculated as total score 0-10 and trichomatous score, 0-2, 3-7, 8-10. Responses of readers were categorised by ASPECTS into three categories as follows:

- Total ASPECTS score; the overall response of readers to EICs which they see on each scan, e.g. the total score given by a reader to a scan considers only the normality of an area, regardless of the type of change in it. If the area was normal it was given 0 and if it was abnormal it was given 1. In other words, this category represents the value of ASPECTS score when there is no differentiation of isodense swelling from hypodensity, which is currently used to read the scans.
- Hypodensity; responses to the presence of hypodensity were the only responses considered in calculating the total ASPECTS of the scan. Areas with positive hypodensity were given 1, and areas that were normal or had isodense swelling were given 0.
- Isodense swelling; responses to seeing isodense swelling in ASPECTS areas were the only responses used to calculate the total

ASPECTS of the scans. Areas which showed isodense swelling were given 1, while areas with hypodensity or isodense swelling were given 0.

Further classifications of scores according to experience, speciality, slice thickness of the scans, clinical information was also carried out.

3- Counts of readers' responses; number of responses to ASPECTS areas categories (either isodense swelling or hypodensity) were summed separately. Further classification according to experience, speciality, slice thickness of the scans, and clinical information was also done.

4- Responses to Hyperdense vessel sign; positive=1 absence response=0.

5- Tissue compartments; ASPECTS areas as categorised by readers; normal, isodense swelling and hypodensity, and by perfusion parameters; normal, penumbra and core.

6- ASPECTS areas fate; for each scan, either normal or infarcted. Added canalisation status for each scan.

7- The mean value of CBF, CBV and MTT for each area was categorised as isodense swollen or hypodense and with their contralateral counter area.

3.13.2 Agreement

Kappa statistics were the main tool of measuring inter-observer agreement. The percentage of total agreement and intraclass correlation coefficients was used to a lesser extent for the purpose of comparison of agreement levels. The main analysis of agreement was done by pairwise kappa, which converted agreement into measurable data for statistical testing.

Weighted Cohen's kappa (quadratic weights) was used to calculate pairwise kappa for each pair of readers. This is because the study used ASPECTS scoring 0-10, which has different levels of importance between its categories. Pairwise Kappa was measured with readers' responses to total ASPECTS, hypodensity and isodense swelling, and for first stage and second stage data separately. For the

first set of variables, pairwise kappa was further calculated for each pair of readers by dividing data according to experience, speciality, slice thickness of scans, clinical information, and for the three categories of ASPECTS. Average pairwise kappa was used to evaluate the agreements by individual readers.

Fleiss's Kappa for multiple raters was used to measure inter-observer agreement among all readers on each EIC category. It was employed in two forms: fixed marginal kappa [XMK] and free marginal kappa [FMK]. XMK or intraclass correlation coefficient were used to add clarification of the agreement level. Trichotomised ASPECTS scores and the count of responses to each ASPECTS area were used. Some 95% confidence intervals for FMK and XMK were calculated; however, CI of FMK was very wide and not included in the results.

Weighted Cohen's kappa (linear weights) for two raters with 95% confidence interval was used to calculate intra-observer agreement in two situations:

- On all ASPECTS areas using trichotomous scoring; kappa was calculated for total ASPECTS, hypodensity and isodense swelling.
- On each single area using count of responses. Kappa was calculated for isodense swelling and hypodensity.

Level of agreement was determined by using Landis and Koch's scale for agreement level **Table 3.4**.

κ	Interpretation
< 0	Less than chance agreement
0.01 – 0.20	Poor agreement
0.21 – 0.40	Fair agreement
0.41 – 0.60	Moderate agreement
0.61 – 0.80	Substantial agreement
0.81 – 1.00	Almost perfect agreement

Table 3. 4: Landis and Koch's scale for agreement level.

Intraclass correlation coefficient ICC was calculated with ASPECTS scores 0-10 and with trichomatous ASPECTS.

The percentage of overall agreements (POA) was used for measuring agreement on Hyperdense vessel sign with XMK.

Pairwise kappa was calculated by using the MedCalc programme(224), while linear Cohen's kappa, XMK and ICC, were calculated by using the online *StatTool* programme(225) [<http://www.stattools.net/StatToolsIndex.php>]. FMK was calculated by *Online Kappa Calculator* [<http://justusrandolph.net/kappa/>] (226). POA were calculated by Microsoft Excel.

3.13.3 Tissue compartments and fate

Absolute numbers with proportions were used to express the results of tissue fate and the matching of NCCT appearance with perfusion category. Prediction statistics included calculation of sensitivity and specificity, likelihood ratios and predictive values. They were calculated for the whole set and for trained and untrained groups of readers. Odds ratio was used for hypodense versus isodense swollen areas, and for recanalized versus non-recanalized isodense areas.

3.13.4 Statistical significance testing

All tests of significance were calculated by using the MedCalc programme. The t-test for independent samples and for paired samples was used to evaluate the significance in difference in agreement level for most compared samples. However, the Mann-Whitney test (independent samples) and Wilcoxon test for paired samples were used instead of the t-test when samples were small or were not normally distributed. Testing the significance of a difference in agreement among more than two samples was done by ANOVA. One-way analysis of variance was used with normally distributed samples and Kruskal-Wallis test for samples which were not normally distributed.

Chi-square tests were used to test the statistical significance of categorical data in relation to the fate of different compartments in relation to recanalization status. One-way analysis of variance was used to test the

difference between the three perfusion parameters: CBF, CBV, MTT for EICs and normal tissue.

3.13.5 Study graphs

Almost all graphs were generated by the MedCalc programme. Descriptive graphs of agreement results were done by using three types of graphs. Multiple line graphs were used to plot the data from compared groups, such as pairwise kappa values and average pairwise kappa values. Mean in the graphs were plotted either as red dots or as a horizontal line. Multiple variables graphs were used to plot all paired agreements for each reader and also to plot all paired agreements for the same reader before and after training. Agreement among all readers in each set of scans by kappa for multiraters was plotted by graphs generated on Microsoft Excel. A line trend graph was used to present XMK reported on each ASPECTS area by trained and untrained observers. A column chart was used to present the results of HVS as a comparison between thin and thick slice scans.

Tissue compartment categorisation and fate results were presented as stacked columns generated by Microsoft Excel. Each stack column represented the frequency and proportion of each classified group within each category. A data comparison graph was used to present a comparison of each perfusion parameter across the three NCCT appearances. The box and whisker with minimum and maximum value plot was used to represent data.

3.14 Ethical considerations

Ethical approval from the Multicentre Research Ethics Committee for Scotland had already been given for the MASIS (REC reference; 07\MRE00\96) and POSH studies. Study consent included use of anonymised imaging data for further analyses. Patients in both studies were coded and the identity of each patient was not provided.

Chapter IV (Results): Agreement.

4.1 Epidemiology data

1- Patients' Data.

Data	Frequency	Mean	Standard deviation	Interquartile range
Number of patients	49 patients	-	-	-
Patients' average age		70.2 years	11.5 years	-
Number of males	28 patients	72.3 years	8.3 years	-
Number of females	21 patients	67.8 years	14.5 years	-
Heart disease	22 patients	-	-	-
NIHSS	(Median)15	-	-	Lower=9 Upper=19
Diabetes Mellitus	9 patients	-	-	-
Average onset of scanning	-	174min	-	-
Average onset of perfusion scanning	-	187 min	-	-
Treated patients.	36 patients	-	-	-
Onset of follow up	-	30 hours	-	-

Table 4. 1 Patients' data.

2- ASPECTS Areas Data.

Data	Frequency of isodense swelling	%	Frequency of Hypodensity	%	Mixed EICs	%	Normal	%
All Scans	20	40.8%	24	48.9%	-	-	-	-
1 st set Scans	5	29.4%	8	47.1%	-	-	-	-
2 nd set Scans	15	46.8%	16	50%	-	-	-	-
ASPECTS Areas on NCCT	38	7.7%	49	9.7%	14	2.8%	390	79.5%

Table 4. 2: frequency and proportion of EICs as categorised by readers on all scans and in each set. And frequency and proportion of ASPECTS areas as categorised by patients on NCCT.

Data	Frequency of Penumbra	%	Frequency of Core	%	Mixed core and penumbra	%	Normal	%
ASPECTS Areas on PCT	86	17.5%	94	19.1%	27	5.5%	283	57.7%
1 st set Scans	30	17.6%	25	(14.7%)	3	(1.7%)	-	-
2 nd set Scans	56	17.5%	69	21.5%)	24	7.5%)	-	-

Table 4. 3: frequency and proportion of ASPECTS areas as categorised by perfusion CT. These are for the whole set and for each set.

Data	Total infarcted areas	Total normal areas	Mixed fate
All ASPECTS areas	154 (31.4%)	336(68.5%)	23*(14.9%)
Areas with mixed EICs	10 (71.4%)	2 (14.3%)	2 (14.3%)
Areas with mixed core \ penumbra	9(34.6%)	-	17(65.7%)

Table 4. 4: frequency and proportion of ASPECTS areas fate on follow up NCCT [* this is the percentage from totally infarcted areas and not from all areas].

A total of 51 patients from both studies, MASIS and POSH, were included in this study. **Table 4.1** represents epidemiological data of 49 patients who were included in the subsequent analysis of this study. All had a final diagnosis of acute middle cerebral artery ischaemic stroke except five patients, in whom; acute posterior ischaemic infarction was the final diagnosis. In the first stage, there were nine readers involved: three expert stroke neurologists, four trainee stroke neurologists, and two expert neuroradiologists. 11 readers participated in reading the second set of scans after they were trained on the consensus set. Among the 11 readers, there were four expert stroke neurologists, four trainee stroke neurologists, two expert neuroradiologists and two trainee neuroradiologists. In total, 47 PCTs were included in the analysis. Two scans from the first set were excluded because they were normal, and two scans from second set had perfusion MRI and not perfusion CT which were analysed by different mode.

Tables 4.2, 3 and 4 demonstrate all information on ASPECTS areas as were categorised by readers and PCT with their final fate.

3- Hemispheric Involvement of the Scans.

Data	Total	% of correctly detected	Overall kappa	Added clinical information
Normal scans	4 (10%)	36%	0.08	-
Abnormal scans	36 (90%)	76%	0.42	78%
Right hemispheric stroke	42%	67%	0.56	K 0.64
Left hemispheric stroke	58%	77%	0.46	K 0.61

Table 4. 5: statistics of involved scans and hemispheres [K; kappa].

The data on normality of scans in total and percentage of readers who were correctly recognising the abnormality is demonstrated in Table 4.5. The effect of addition of clinical information on correct answers of readers is also presented.

4.2 Intraobserver Agreement

ASPECTS category	Kappa (COHEN'S)	95% CI
Total score	0.96	0.73 to 1
Hypodensity	0.84	0.49 to 0.99
Isodense Swelling	0.74	0.59 to 1

Table 4. 6. Intraobserver agreement for individual readers using trichotomised ASPECTS.

Area	Hypodensity	Focal swelling
Basal ganglia	Kappa=0.9446	Kappa=0.6341
Insula	Kappa=0.9275	Kappa=1.0000
MCA Territories	Kappa=0.9275	Kappa=0.9091

Table 4. 7: Cohen's kappa for intraobserver agreement on regions of ASPECTS template using tables of counts.

As can be seen from Tables 4.6 and 7, the intrinsic agreement of individual readers on the three categories of ASPECTS and on ASPECTS areas by using the repeated scans within the whole set was substantial to perfect agreement.

4.3 Effect of Scan's Factors on Interobserver Agreement

	Free marginal kappa for multi-raters (FMK)			Intra-class correlation coefficient (ICC)		
	Total score	Isodense swelling	Hypodensity	Total score	Isodense swelling	Hypodensity
Blinded	0.52	0.69	0.59	0.48	0.20	0.45
Unblinded	0.38	0.60	0.55	0.41	0.11	0.37
Full C\D	0.36	0.49	0.51	0.49	0.11	0.44
Minimum C\D	0.40	0.69	0.58	0.34	0.093	0.33
Thick slices	0.45	0.68	0.54	0.54	0.13	0.50
Thin slices	0.60	0.61	0.60	0.38	0.15	0.32

Table 4. 8 Overall interobserver agreement among the nine readers on each category of EICs by using trichotomous ASPECTS.

ASPECTS category	Total score		Hypodensity		Isodense swelling	
	APK	P Value	APK	P Value	APK	P Value
Blinded	0.45	0.34	0.39	0.53	0.14	0.089
Unblinded	0.38		0.35		0.05	
Full C\D	0.46	0.05	0.42	0.16	0.11	0.26
Minimum C\D	0.32		0.32		0.05	
Thick slices	0.50	0.01	0.46	0.01	0.06	0.55
Thin slices	0.34		0.31		0.1	

Table 4. 9: Comparison of average pairwise kappa (APK) of each group of variables across the three ASPECTS categories. [significance level is at $P < 0.05$]. [C\D clinical data]

As can be seen from Table 4.8, overall interobserver agreement among the nine readers by using free marginal kappa for multiraters was different from that by ICC across the three ASPECTS categories.

Analysis of agreement between each observer, [**Appendix tables 15, 16 and 17**] yielded paired agreements ranging from very poor to perfect agreement. Linear distribution of paired agreements in blinded and non-blinded sets of scans showed closely related curves with crossing over at some points as it is illustrated in **Figure 4.1**. In **Table 4.9**, the average kappa across the three categories of changes ranged from poor to moderate for blinded set and from poor to fair for non-blinded set. The values of APK were higher in the blinded set than the non-blinded set. Despite this, it can be seen that there is no statistically significant difference.

In **Figure 4.2**, the linear distributions of paired agreements in both sets appeared close to each other for isodense swelling and hypodensity while they were separated in a large area for Total score. As is reported in **Table 4.9**, average pairwise kappa for set with full data indicated moderate agreement for Total score and hypodensity and poor agreement for isodense swelling. In contrast, the set with minimum clinical data had fair agreement on Total score and hypodensity and very poor agreement on isodense swelling. Although the detailed clinical information on patient presentation seemed to enhance interobserver agreement, the difference in level of agreement between the two sets of scans along the three categories is statistically not significant.

It is clear from **Table 4.9** that average pairwise kappa declined from moderate for scans with thick slices to fair for scans with thin slices when readers agreed on Total score and hypodensity, whereas it was poor for both sets when readers agreed on isodense swelling. In **figure 4.3** curves in Total score and hypodensity categories were separated apart with thick slices set in positive direction and thin slices set in negative direction whereas in isodense swelling category they overlapped with each other. The agreement level on Total score and hypodensity for scans with thick slices shows a statistically significant difference from that for thin slices. However, agreement on isodense swelling did not change significantly when thick slices were used instead of thin slices scans. When scans had thick slices, readers agreed more consistently than when the set were with thin slices where readers showed very poor agreements and even no agreement at all. In case of isodense swelling, the great portion of agreements was in the no agreement zone and the few remaining pairs deviated

greatly from the average in a positive direction [full statistical measures for the variables are presented in [Appendix Table 18].

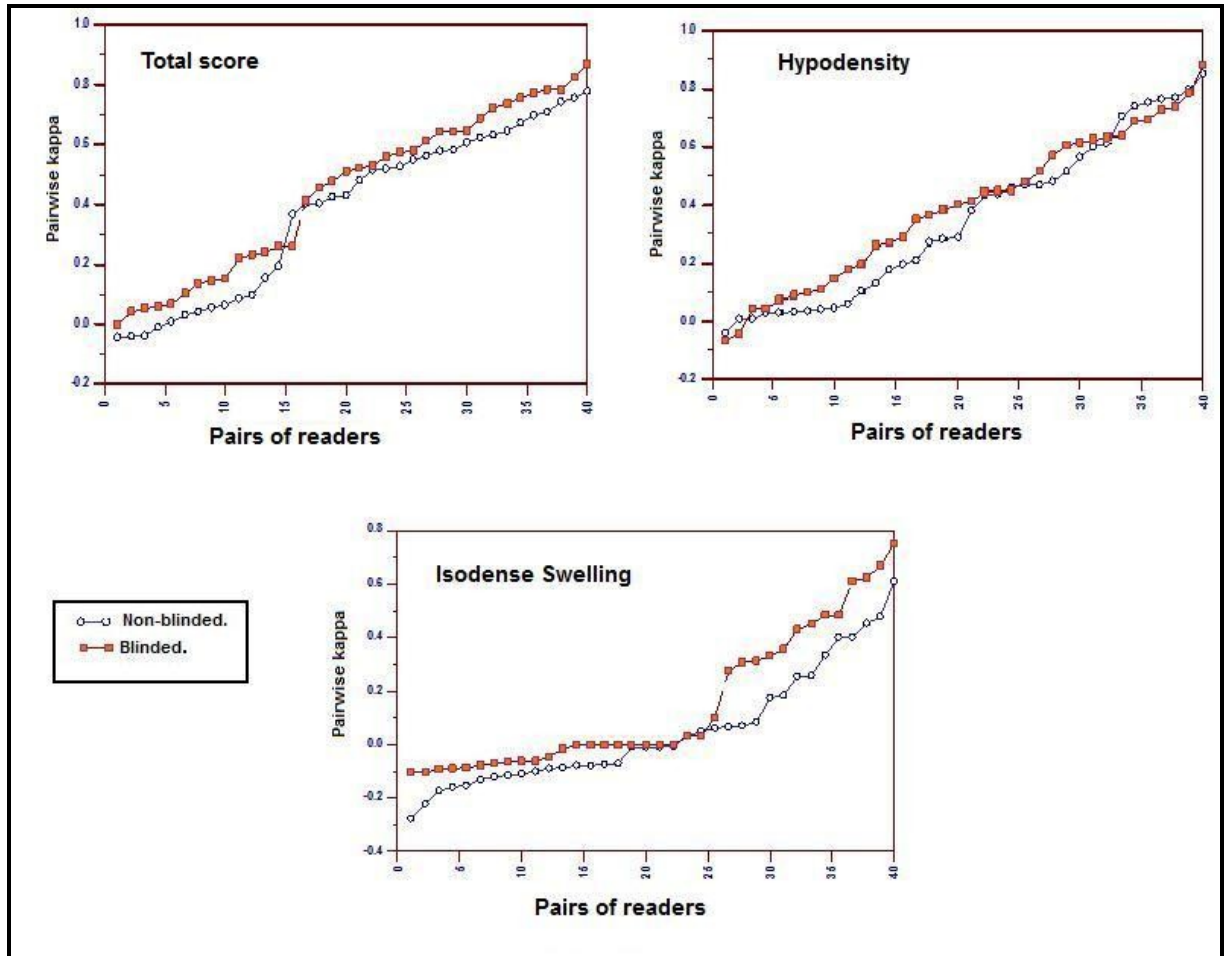


Figure 4. 1:Linear distribution of pairwise kappa in relation to clinical data for each category of ASPECTS.

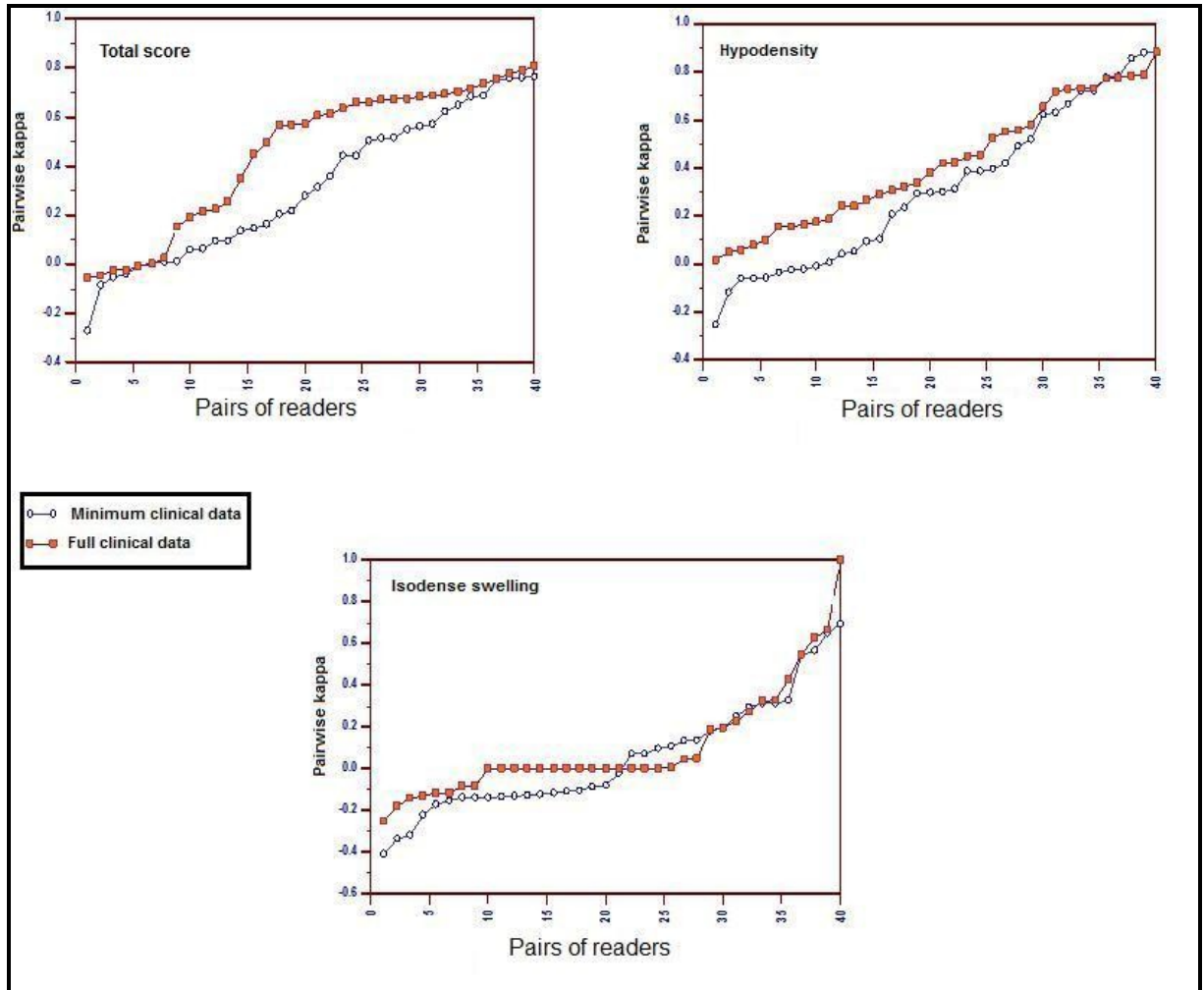


Figure 4. 2: Linear distribution of pairwise kappa in relation to amount of clinical data for each category of ASPECTS.

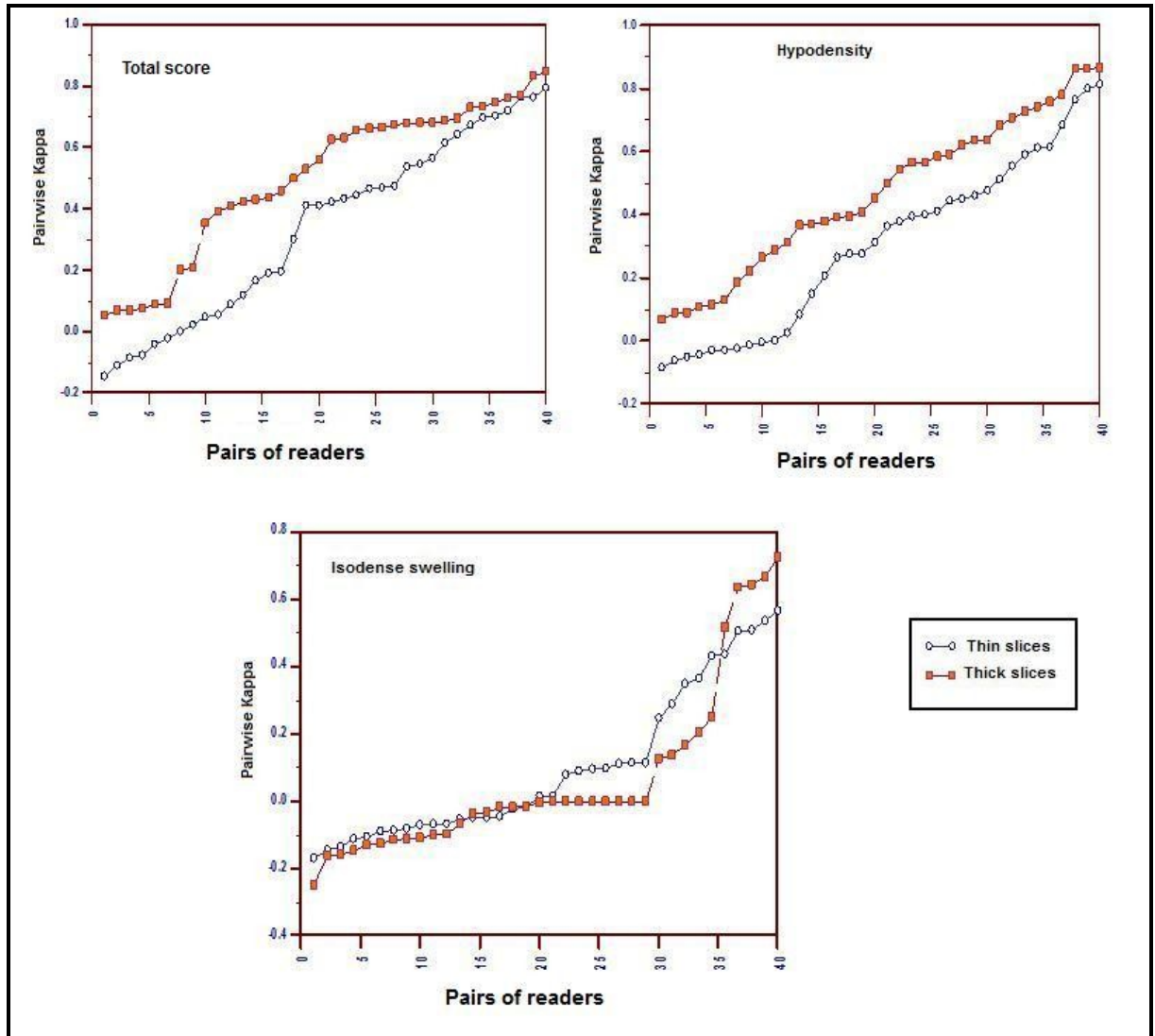


Figure 4. 3: Linear distribution of pairwise kappa in relation to slice thickness for each category of ASPECTS.

4.4 Effect of Training on Interobserver Agreement

4.4.1 Trained Group Versus Untrained Group

In this section, the interobserver agreement will be calculated in relation to training by dividing the groups into trained and untrained

A-Comparison of Interobserver Agreement on EICs Between Trained and Untrained Groups of Readers

Group	Trained group			Untrained group		
parameter	Total score	Isodense swelling	Hypodensity	Total score	Isodense swelling	Hypodensity
FMK	0.39	0.50	0.57	0.44	0.63	0.57
XMK	0.26	0.20	0.29	0.26	0.10	0.25
ICC	0.42	0.055	0.37	0.42	0.40	0.15

Table 4. 10. Overall interobserver agreement on each category of ASPECTS. for trained versus untrained readers as measured by free marginal kappa (FMK), fixed marginal (Fleiss's Kappa) (XMK) and intraclass coefficient (ICC).

Group	Trained group of readers				Untrained group of readers				Significance P<0.05	
	APK	CI*	SD**	variance	APK	CI*	SD**	variance	t- test	P value
Total score	0.42	0.38- 0.45	0.14	0.021	0.41	0.32- 0.49	0.25	0.066	0.16	0.87
Hypodensity	0.37	0.31- 0.43	0.21	0.046	0.37	0.29- 0.45	0.24	0.06	0.15	0.88
Isodense swelling	0.30	0.25- 0.35	0.18	0.033	0.093	0.019- 0.16	0.21	0.047	4.77	0.0001

Table 4. 11: The difference of average pairwise kappa of each category of ASPECTS for trained and untrained groups of readers [* Confidence interval, ** standard deviation].

From **Table 4.10** it can be seen that calculation of overall agreement by three different agreement measurements yielded different results among the two groups of readers. FMK gives the highest values of kappa whereas using XMK gives a very low agreement levels. In contrast, by using ICC, agreement had similar trend to pairwise kappa analysis.

In reference to average pairwise kappa in **Table 4.11**, trained and untrained readers agreed moderately on Total score and fairly on hypodensity. However, trained readers agreed fairly on isodense swelling whereas untrained readers agreed very poorly on isodense swelling. The difference in agreement on isodense swelling between the trained and untrained readers was statistically significant. In **Figure 4.4** the linear curves represents the paired agreements given by observers in each group; red boxes are trained readers and blue circles are untrained readers. The vertical axis represents the ascending values of kappa. In the first figure; each red sequer represent paired agreement of two trained observers on total aspects score and each blue circle represents paired agreement of two untrained readers on total aspects score. Paired agreements in each group were sorted in descending order to exhibit the points of crossover between both groups. AS it can be seen, the linear curves crossover when readers were agreeing on Total score and hypodensity, whereas they were separated from each other when readers agreed on isodense swelling with trained readers'

agreements were in positive direction of kappa scale. However, both curves widened apart from each other as they sloped down kappa scale for Total score and hypodensity with a higher level of agreements given by the trained group. Paired agreements that were given by trained readers appeared more consistent with less variation than those given by untrained readers across the three categories of ASPECTS. A great portion of paired agreements given by untrained readers was poorer than predicted to occur by chance, which reflects the absence of agreement among a considerable number of untrained readers on isodense swelling. On the other hand, agreements by the trained group had considerable portion above the average level with agreements up to a substantial level [Appendix table 19].

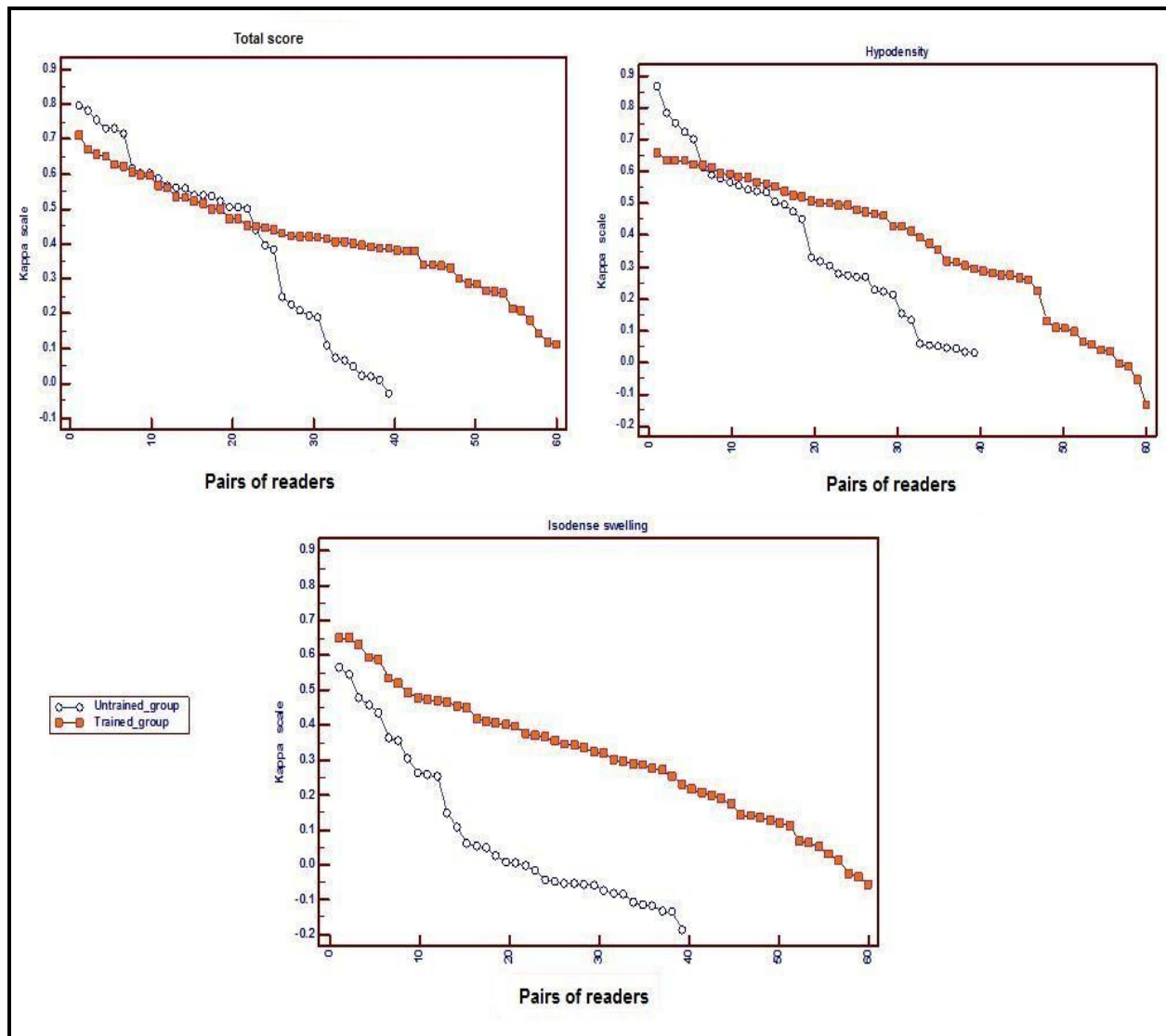


Figure 4. 4: Linear distribution of pairwise kappa in each group of readers for each ASPECTS category.

B- Does the effect of training differ among individual readers ?

Group	Trained group of readers		Untrained group of readers		Significance P<0.05	
	Mean APK	variance	Mean APK	variance	Mann-Whitney test	P value
Total score	0.42	0.006	0.41	0.03	109	0.65
Hypodensity	0.37	0.02	0.38	0.02	114	0.94
Isodense swelling	0.30	0.009	0.09	0.02	4.04*	0.0012

Table 4. 12: Comparison of average pairwise kappa (APK) for each reader in the trained and untrained groups across the three studied categories[* t.test].

As is reported in **Table 4.12**, the overall average agreement on Total score was moderate in both groups with a statistically insignificant difference between trained and untrained readers ($P>0.05$). In **Figure 4.5**, paired agreements of untrained readers showed wide variation across kappa scale whereas paired agreements of trained readers appeared more consistent and less variable. Only one untrained reader had strong consistency of agreements with others with good agreement level except for one odd value. One untrained reader showed a cluster of very poor agreements with others. This can be also extracted from **Figure 4.8**, which shows an almost linear relationship between APK of trained readers with a very steady decline in the level of agreement and a steep drop of APK of untrained readers after an almost linear steady course. This sudden drop in the untrained group occurred because of two readers who showed much less than the average level of agreement than others in their group. The distribution of average agreements of readers around their mean in each group had the same explained pattern.

The pattern of paired agreements on hypodensity by each reader in both groups appeared as that given to Total score. This is illustrated in **Figure 4.6**. However, as can be seen in **Figure 4.4**, the almost linear steady course showed steep decline in agreement for both groups, this time with deviation of one untrained reader and two trained readers. The average agreement of five untrained readers was moderate while three others had fair average agreement

and the last reader agreed poorly on average. In the trained group, seven readers had moderate average agreement while three had fair agreement and only one agreed poorly. Even so, it is clear from **Figures 4.8** that the performance of readers in both groups tended to be similar. This can be explained by the absence of a statistically significant difference in agreement between the two groups as seen in **Table 4.12**.

Untrained readers agreed in general very poorly or did not agree at all with each other on isodense swelling when compared with trained readers, who showed a range of agreement up to a substantial level. This can be noted from the distribution of agreements of each reader in **Figure 4.7**. In the untrained group, there were three clusters of no agreement or very poor agreement with wide variation in agreements given by other readers. In contrast, trained readers showed variability in their agreements except for one reader who showed clustering at a very poor level of agreement. In reference to APK, there were three untrained readers who had no agreement with others on average, and three untrained readers showed fair average agreement with borderline kappa at 0.22. The last three readers showed poor average agreement with a various range from 0.09 to 0.20. Therefore, it is clear that all APKs of trained readers are higher than those of untrained readers. This can be seen in **Figure 4.8**, which shows higher values of APK for trained readers with an almost linear relationship and very steady decline across the kappa scale. Agreements of untrained readers were below those by the trained group and although it started constant for the first three readers, it showed a rapid decline in agreement for all subsequent groups. Unlike the untrained group, all the trained readers had fair average agreement except two readers; one showed moderate and one showed poor agreement on average. Therefore, it can be said that, in general, untrained readers agreed poorly on isodense swelling whereas the trained group agreed fairly. The difference in the level of agreement between the two groups is statistically significant as seen in **Table 4.12** [pairwise kappa and APK by each reader in each group and for the three categories are in **Appendix tables 20-25**].

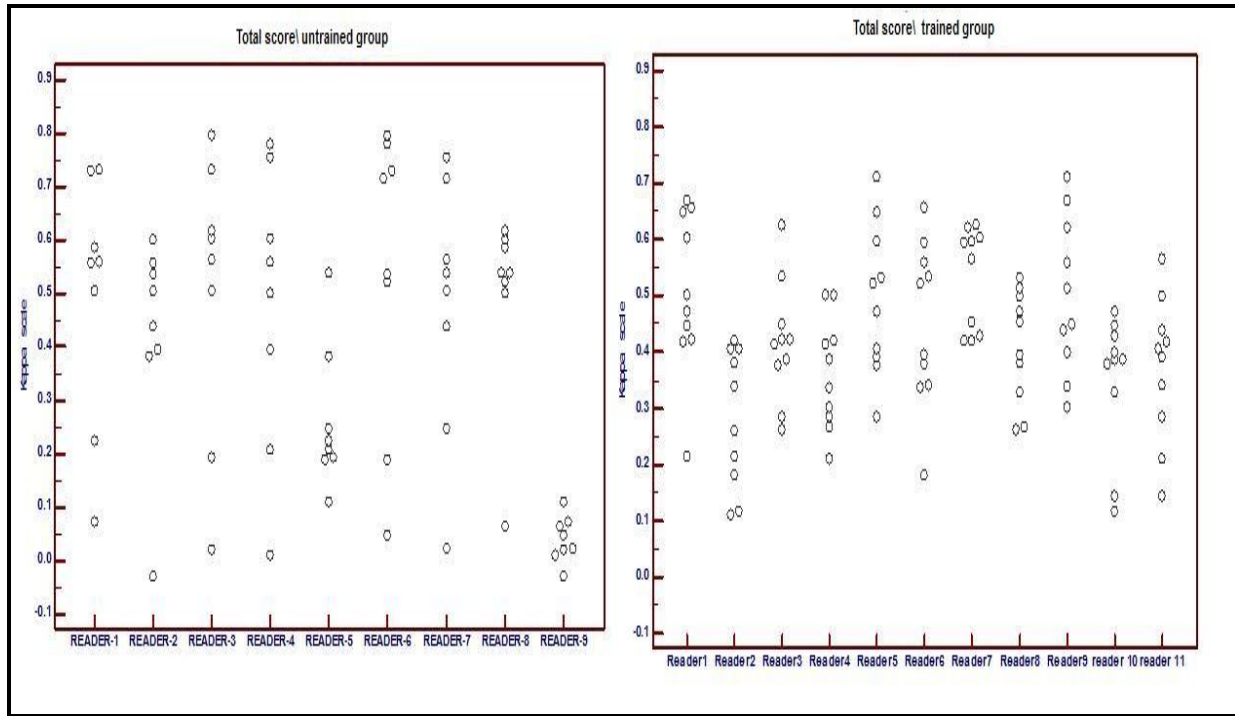


Figure 4. 5: Plot distribution of pairwise kappa on both changes of each reader in trained and untrained group.

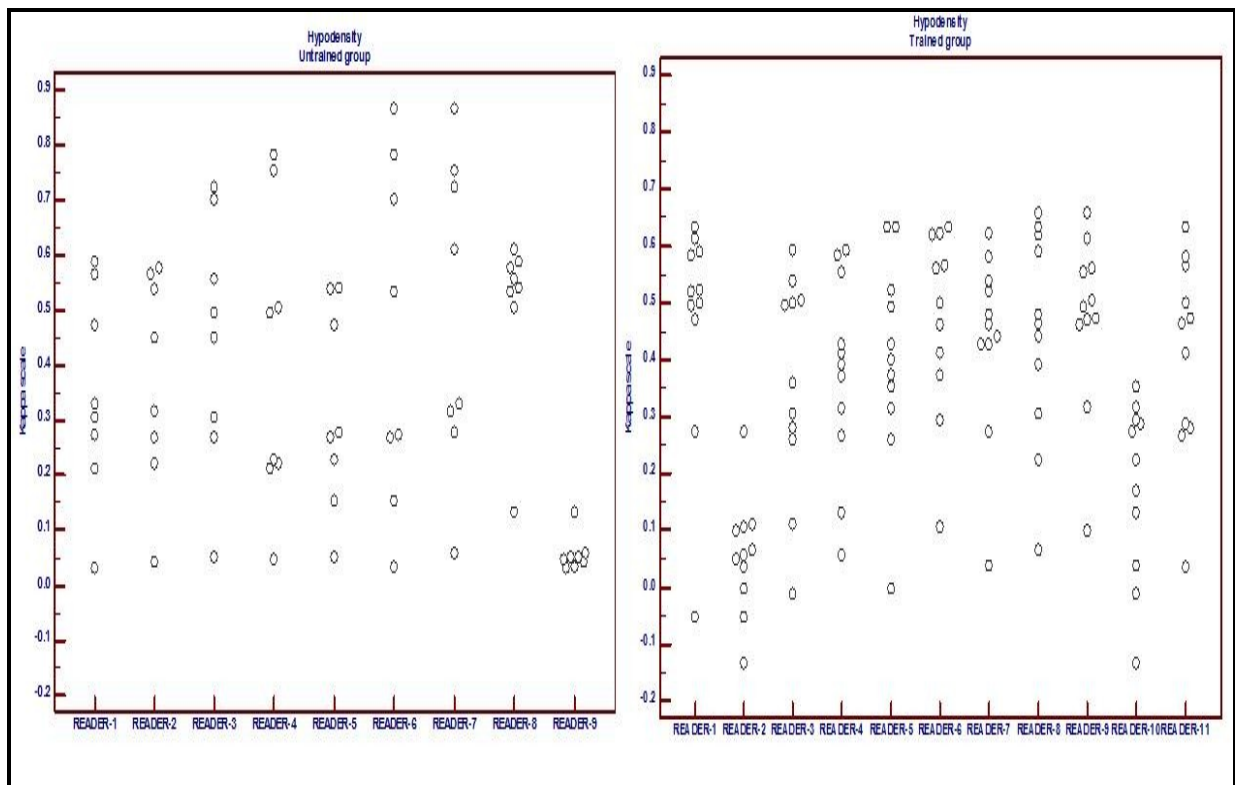


Figure 4. 6: Plot distribution of pairwise kappa on hypodensity of each reader in trained and untrained group.

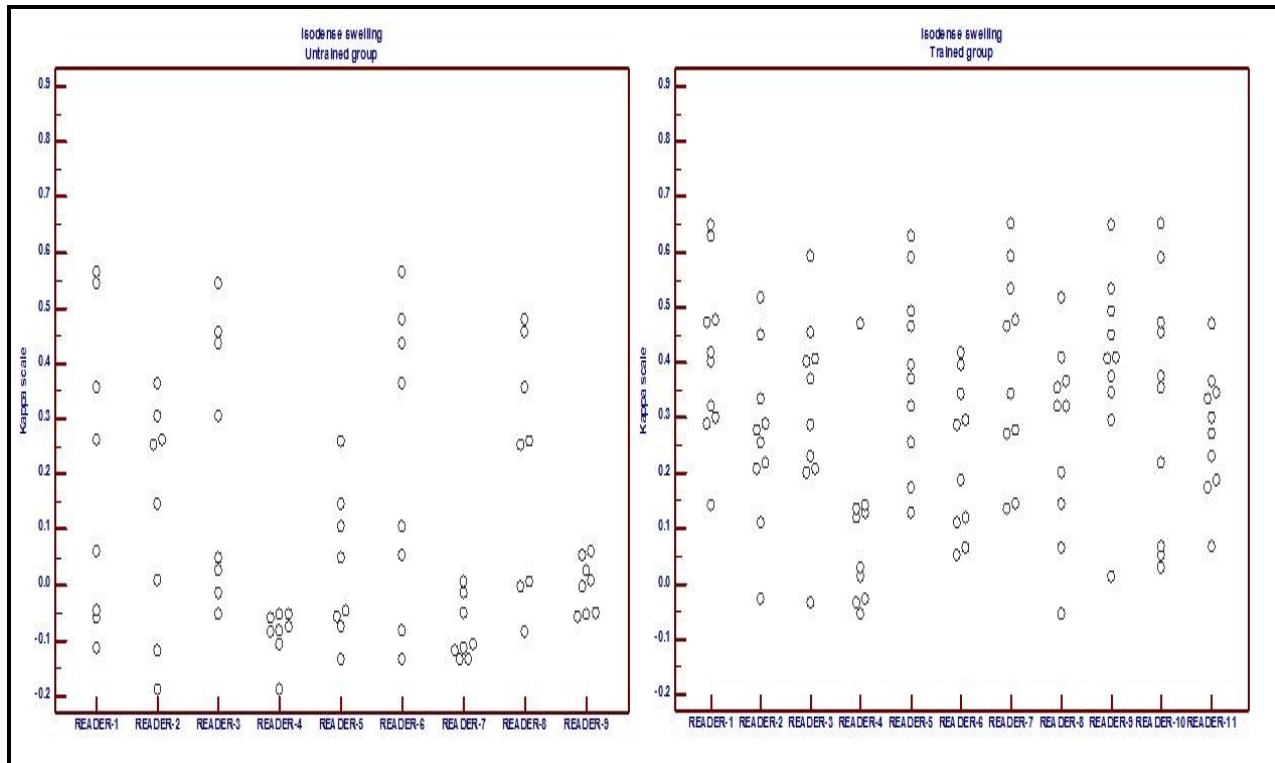


Figure 4. 7: Plot distribution of pairwise kappa on isodense swelling of each reader in trained and untrained group.

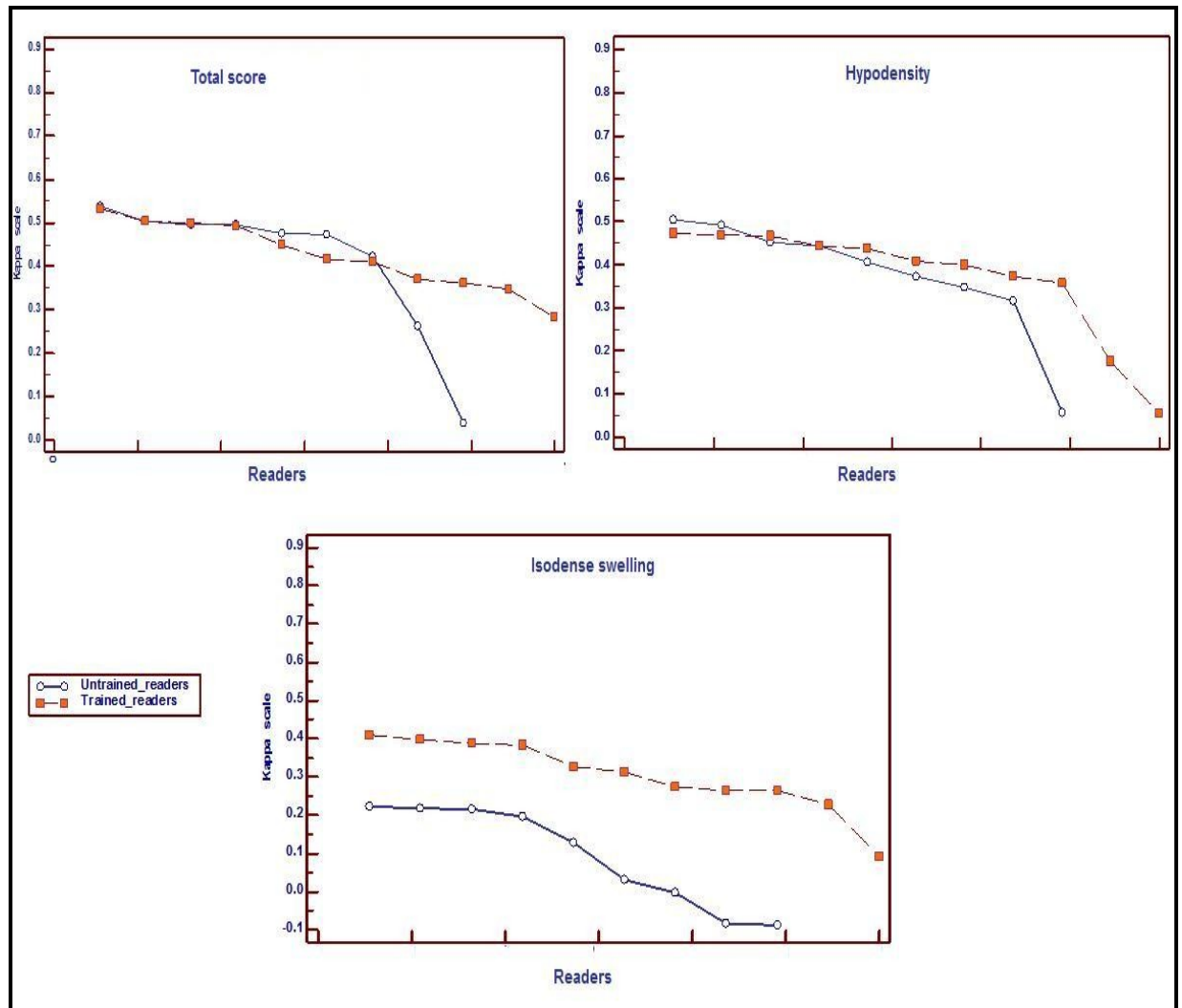


Figure 4. 8: Linear distribution of APK of each trained and untrained reader on each studied category of EICs.

C- Comparison of Interobserver Agreement of Trained and Untrained Groups After Exclusion outliers.

Four untrained readers and six trained readers were excluded because they had the least average agreement in their group. Therefore, the two new groups to be compared consist of five readers each.

Group	Trained group of readers		Untrained group of readers		Significance P<0.05	
	Mean APK	variance	Mean APK	variance	Mann-Whitney test	P value
Total score	0.60	0.005	0.62	0.002	23	0.42
Hypodensity	0.48	0.002	0.48	0.003	27	1.0
Isodense swelling	0.50	0.001	0.40	0.004	2.29*	0.021

Table 4. 13: Comparison of average pairwise kappa (APK) for each reader in the trained and untrained groups across the three studied categories [* t.test].

The most noticeable change after exclusion of outliers is that the average agreement increased in both groups [Appendix tables 27-31]. Although untrained readers had a higher average kappa value than trained readers when agreed on Total score, they did not differ significantly as is shown in Table 4.13. It is also clear from Figure 4.10 that the readers in both groups agreed in an almost identical line. The pattern of agreements given by readers in both groups is similar as is illustrated in Figure 4.9 despite trained readers showing variability in their agreements more than untrained readers.

The agreement level on hypodensity in both groups improved from fair to moderate with the preclusion of inconsistent agreements. All readers in the two sets agreed moderately with different variability, which appeared to be higher for untrained readers. This is illustrated in Figure 4.9, where agreements of trained readers appeared more consistent than agreements of untrained readers. However, only one untrained reader showed good consistent agreements with a good moderate level. Comparing the difference between the two groups yielded no statistical significance and assumed high similarity between the means of both as illustrated in Table 4.13.

Agreement on isodense swelling rose from very poor to moderate agreement among untrained readers and from fair to good moderate among trained readers. However, the difference in agreement between trained and untrained groups is

still statistically significant even with the exclusion of inconsistent readers. This can be explained by the pattern of agreements given by readers in both groups. In **Figure 4.10** the curves of APK in both groups are separated from each other and there is no overlap with higher values for trained readers. Moreover, the variations in agreement among untrained readers are also higher than variations among trained readers. This can be also noted from **Figure 4.9**.

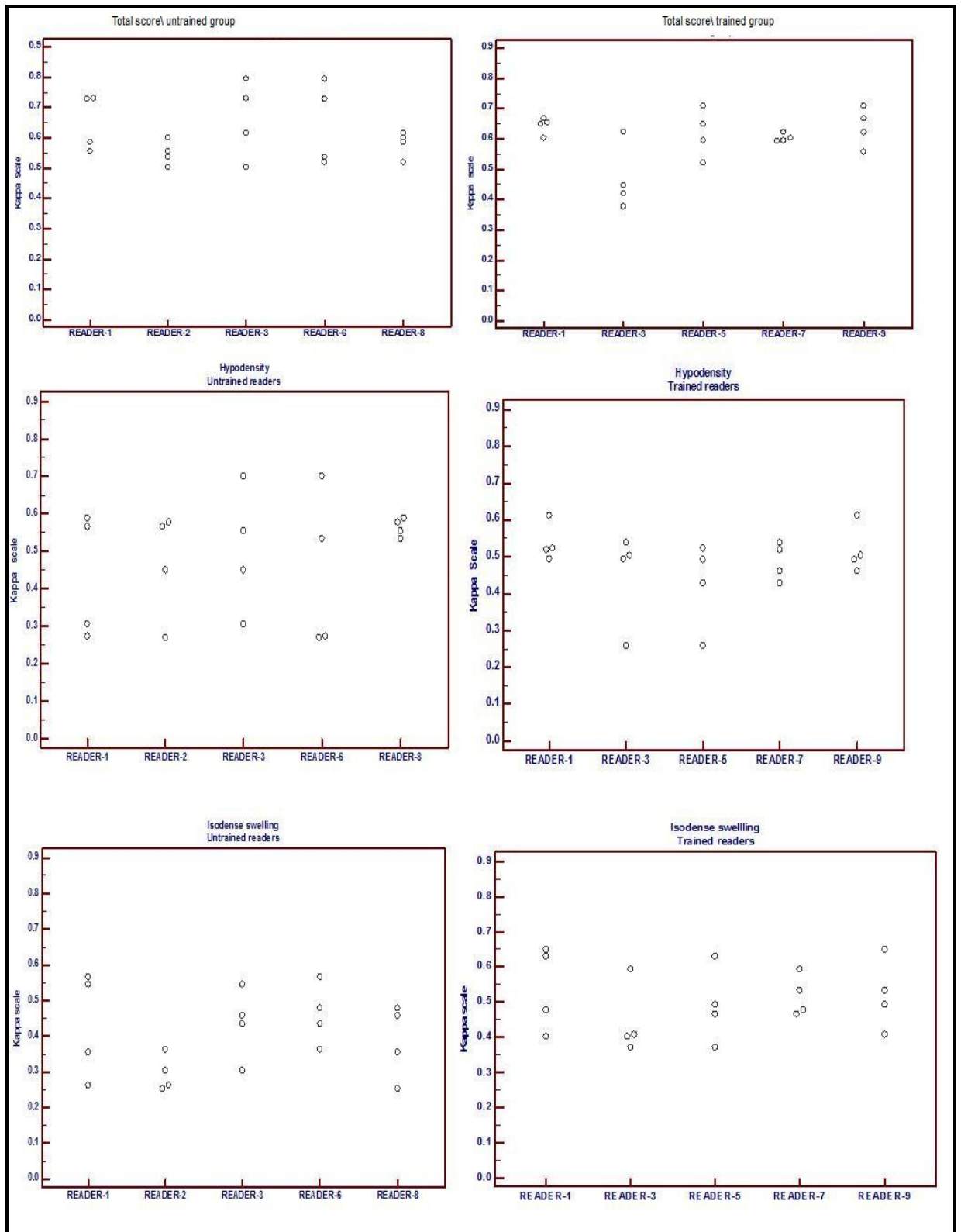


Figure 4. 9: Plotting of pairwise kappa of each reader in trained and untrained groups after exclusion of outliers for the three categories of EICs.

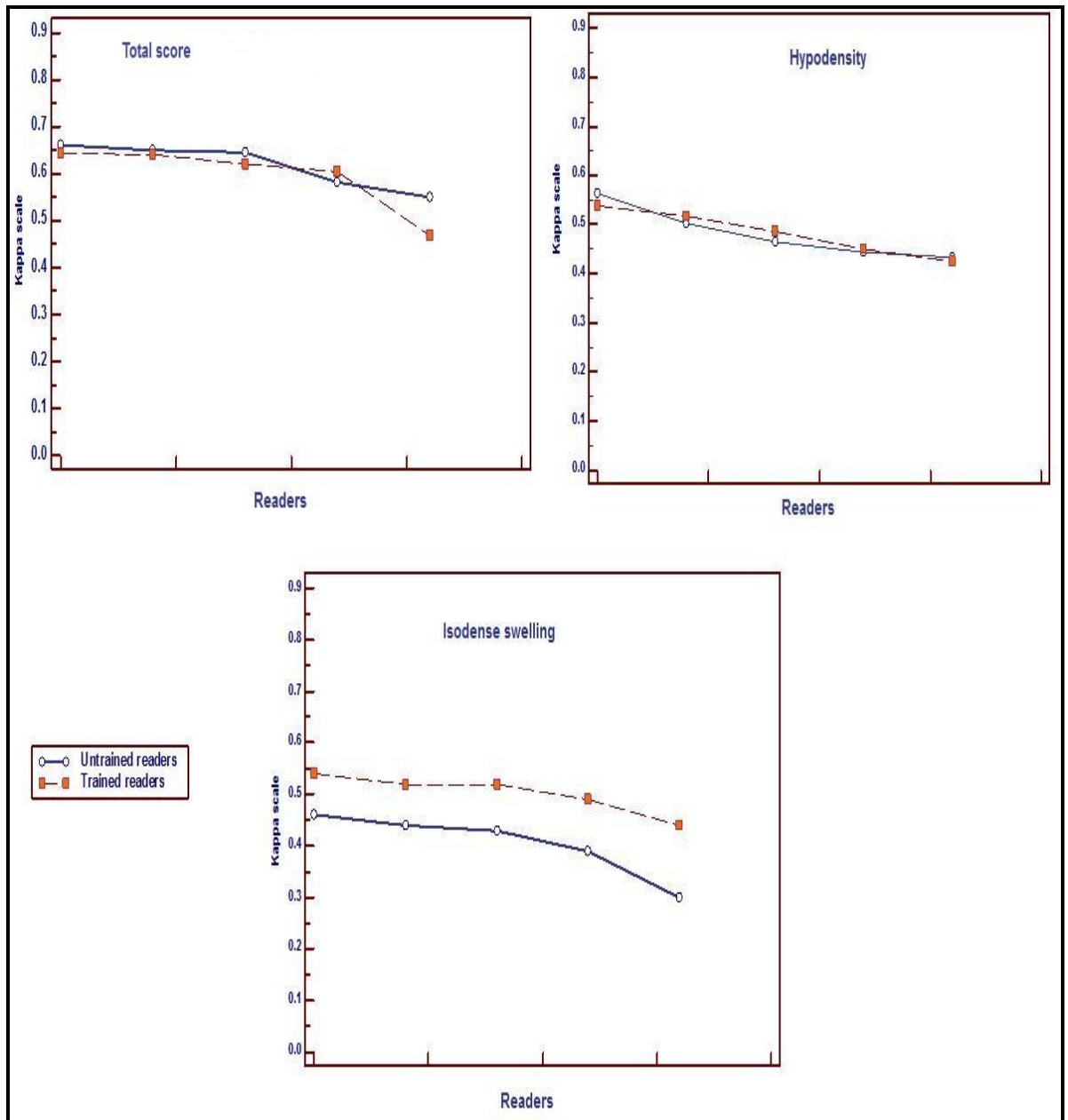


Figure 4. 10: Linear distribution of average pairwise kappa of each reader in the trained and untrained groups for the three categories of EICs after exclusion of outliers.

4.4.2 Pre- and Post-Training Groups of Readers (same readers).

A- Comparison of Pre- and Post-Training Interobserver Agreement on EICs for the Whole Group.

Scan's set	Pre-training				Post-training				Significance P<0.05	
	APK	CI	SD	variance	APK	CI	SD	variance	t-test	P value
Total score	0.61	0.52-0.72	0.13	0.017	0.36	0.23-0.48	0.17	0.030	13.12	0.0001
Hypodensity	0.42	0.28-0.58	0.20	0.041	0.34	0.15-0.52	0.25	0.067	2.2	0.06
Isodense swelling	0.20	0.008-0.49	0.28	0.078	0.19	0.077-0.30	0.15	0.025	0.40	0.69

Table 4. 14: Comparison of average kappa before and after training across the three ASPECTS categories.

As is illustrated in **Tables 4-14**, readers who participated before and after consensus generally had better performance before they were trained on recognising EICs. Their average agreements were substantial on Total score before training and dropped to fair after training with a significantly different level of agreement. This is demonstrated in **Figure 4.11**. In addition, there was a higher variation of agreements when readers were trained.

For hypodensity, readers agreed moderately before training and fairly after training. Despite this, the difference in pre-and post-training performance is statistically insignificant as shown in **Table 4.14**. In **Figure 4.11**, it is clear that there was an overlapping in the pattern of agreements in the two situations with higher values for the pre-training set. The paired agreements showed less variability before the consensus.

Readers agreed poorly on isodense swelling before and after training with no statistically significant difference as seen in **Table 4.14**. However, readers agreed more consistently on isodense swelling after training [see **Appendix Tables 32 and 33**, for pairwise kappa for each reader].

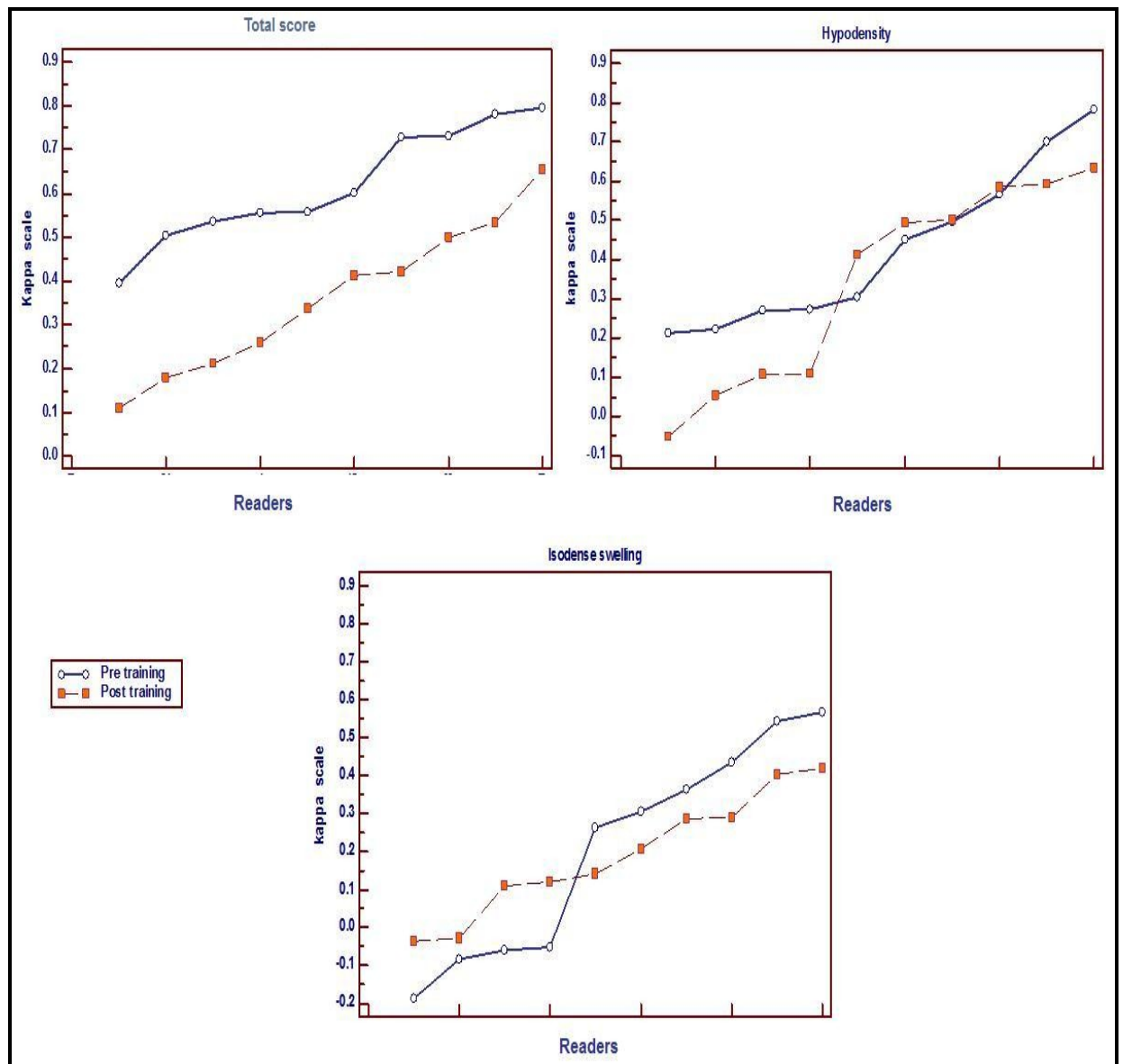


Figure 4. 11: Linear distribution of pairwise kappa before and after training for each category of ASPECTS.

B- Comparison of Pre- and Post-Training Interobserver Agreement on EICs for Each Reader.

READERS	Total score			Hypodensity			Isodense swelling			ANOVA	
	Pre	Post	Sig-level	Pre	Post	Sig-level	Pre	Post	Sig-level	F-ratio	P value
READER-A	0.71	0.45	P>0.05	0.51	0.41	P>0.05	0.32	0.31	P>0.05	1.6	0.25
READER-B	0.49	0.19	P<0.05	0.37	0.057	P<0.05	0.18	0.14	P>0.05	5.2	0.004
READER-C	0.66	0.45	P>0.05	0.49	0.42	P>0.05	0.31	0.22	P>0.05	2.8	0.044
READER-D	0.58	0.34	P>0.05	0.43	0.41	P>0.05	-	0.05	P>0.05	7.8	<0.001
READER-E	0.64	0.42	P>0.05	0.34	0.41	P>0.05	0.096 0.33	0.23	P>0.05	1.9	0.13

Table 4. 15: ANOVA analysis of each reader response before and after training with reference to average pairwise kappa of each ASPECTS category.

Scan's set	Pre-training	Post-training	Significance P<0.05
Parameter	APK	APK	P value*
Total score	0.70	0.48	0.0312
Hypodensity	0.46	0.54	0.3125
Isodense swelling	0.22	0.22	0.8438

Table 4. 16: Comparison of average kappa pre- and post- training after exclusion of reader B. [* Wilcoxon test].

From **Table 4-15**, it is clear that all average agreements on Total score were higher before training. Agreement on hypodensity showed less change, with a moderate level for most readers before and after training. However, one reader had fair agreement before training and dropped to very poor after training. Most readers agreed on isodense swelling similarly before and after training with levels ranging between fair and poor agreement. Changes in pre- and post-training agreements of each reader on each ASPECTS category are illustrated in **Figure 4.12**. As seen in **Table 4.15**, the changes in agreement level before and after training has no statistical significance for all readers except for reader B, who showed a significant change in agreement on both changes and hypodensity before and after training.

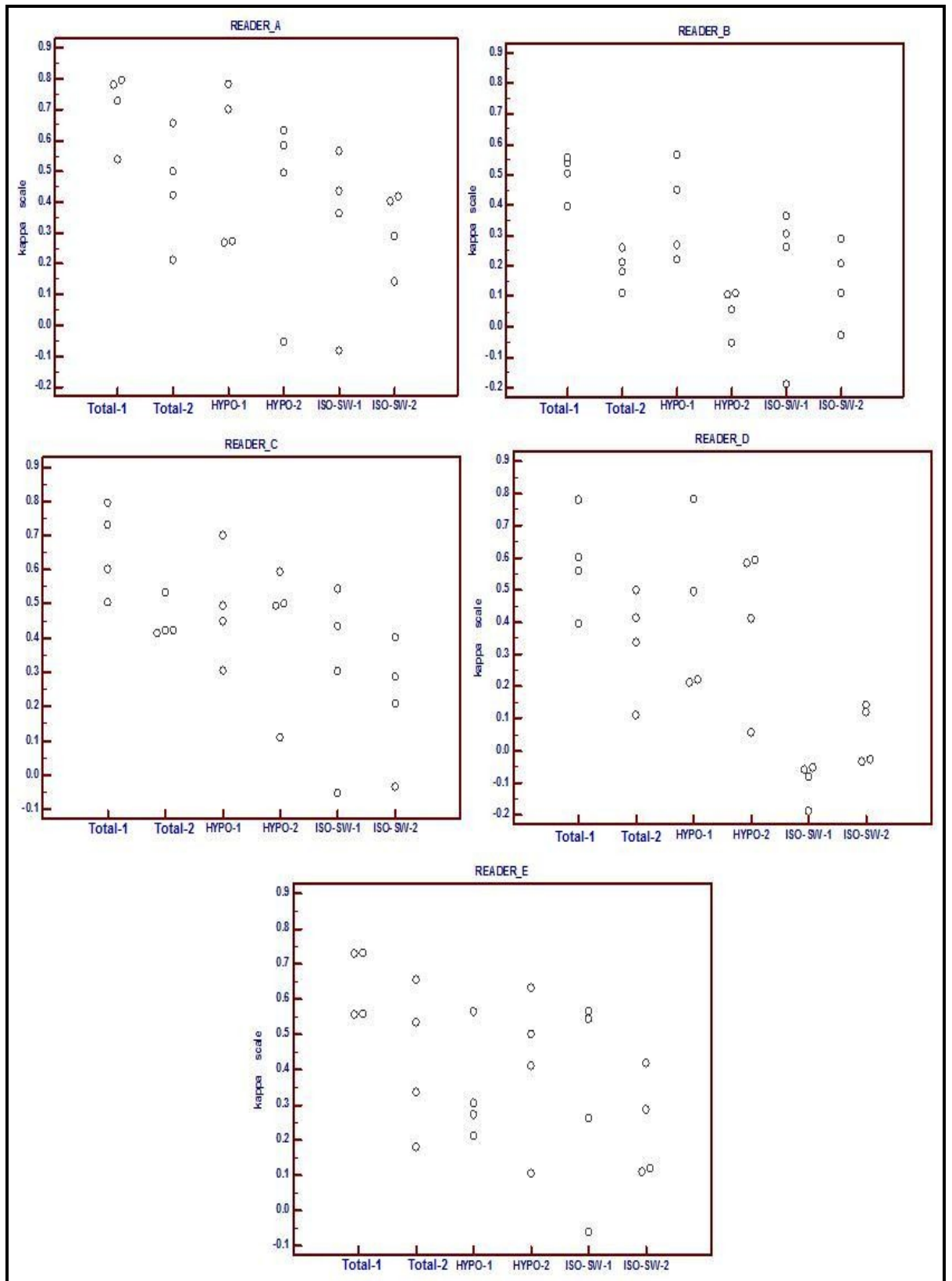


Figure 4. 12: Distribution of pre- and post-training pairwise kappa of each reader for the three EICs categories.

When reader B was excluded from analysis, the resulted levels of agreements is shown in **Table 4.16** with reference to average pairwise kappa of paired agreements for Total score isodense swelling and hypodensity.

From **Figure 4.13**, it is clear that curves in hypodensity and isodense swelling categories crossed each other whereas those for Total score separated apart widely. The pre-training agreements for hypodensity and isodense swelling showed wide variability, and the post-training agreements appeared more consistent with fewer variables.

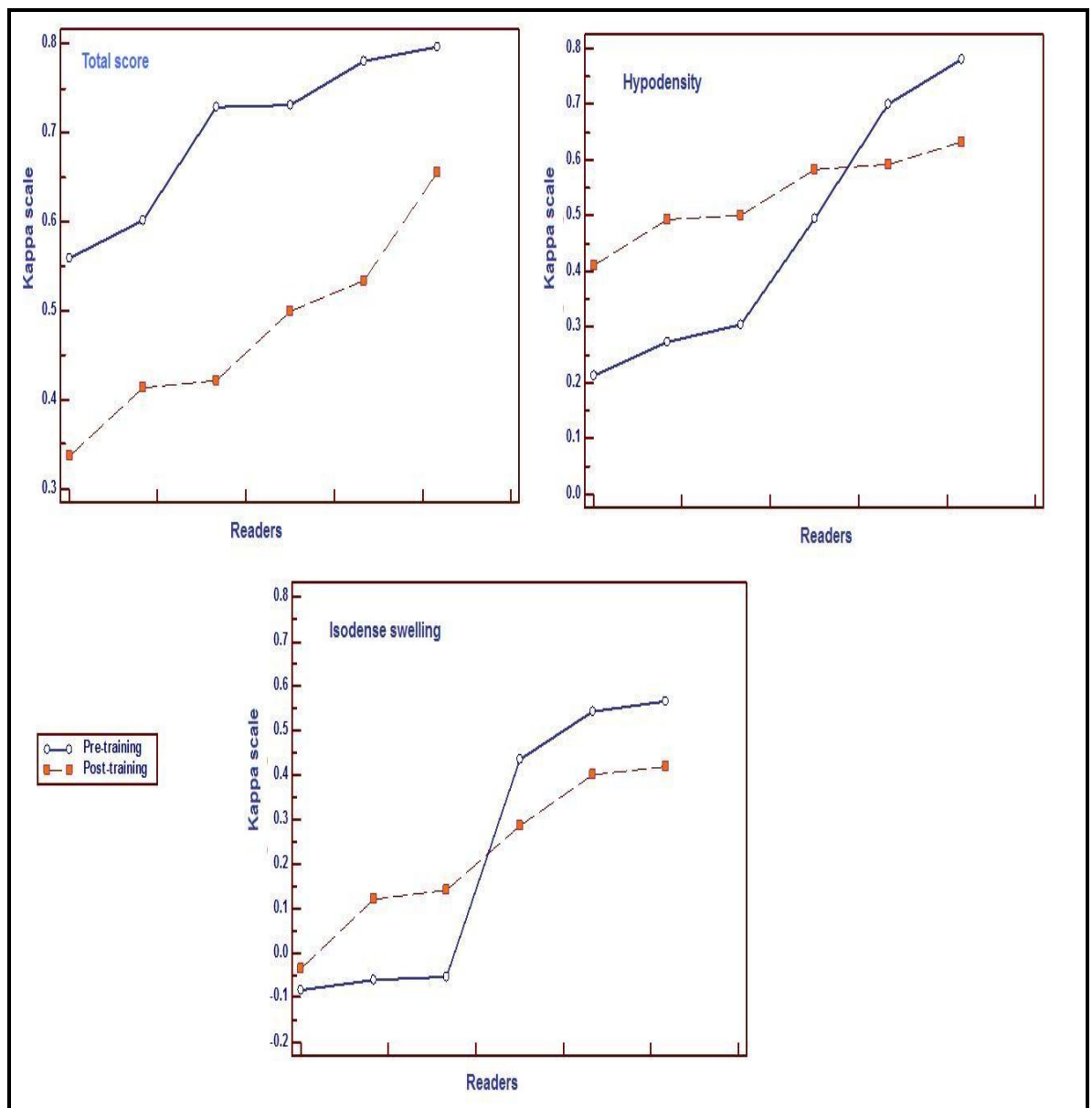


Figure 4. 13: Linear distribution of average pairwise kappa of pre and post trained readers after exclusion of reader B across the three EICs categories.

4.5 Effect of Speciality and Experience on Interobserver Agreement

4.5.1 Readers' Speciality

Group	Neuroradiologists	Stroke neurologists	Significance P<0.05
Parameter	APK	APK	P value*
Total score	0.30	0.49	0.09
Hypodensity	0.33	0.45	0.09
Isodense swelling	0.24	0.36	0.09

Table 4. 17: Comparison of average pairwise kappa of neuroradiologists and stroke neurologists (* Kruskal-Wallis test).

Parameter	Neuroradiologists*			Stroke neurologists**		
	Trained	Untrained	P Value	Trained	Untrained	P value
Total score	11.67	21	0.13	0.46	0.51	>0.05
Hypodensity	11.50	20	0.13	0.41	0.45	>0.05
Isodense swelling	8.33	0	0.13	0.35	0.30	>0.05

Table 4. 18: Comparison of average pairwise kappa of neuroradiologists and stroke neurologists before and after training for each ASPECTS category (* Kruskal-Wallis test, ** one-way ANOVA).

Table 4-17 presents comparison of interobserver agreement between neuroradiologists and stroke neurologists. Generally, neuroradiologists agreed fairly on the three categories whereas stroke physicians agreed moderately on Total score and fairly on isodense swelling. Although stroke physicians performed

better than neuroradiologists, this has no statistical significance with $P > 0.05$ across the three categories of ASPECTS. **Table 4.18** presents the comparison in relation to training in each speciality. It is clear that the performance of each speciality before training had no statistically significant difference from the performance in the post-training group.

4.5.2 Readers' Experience.

1- Interobserver Agreement Comparison Between Experts and Trainees.

Untrained	Experts			Trainees			Significance $P < 0.05$	
	APK	Median	variance	APK	Median	variance	MWT*	P value
Total score	0.61	0.58	0.021	0.26	0.16	0.056	30	0.02
Hypodensity	0.55	0.60	0.066	0.30	0.30	0.055	35	0.09
Isodense swelling	0.04	-0.068	0.25	0.096	0.17	0.028	75	0.31

Table 4. 19: Comparison of average pairwise kappa of untrained experts and trainees (* MWT Mann-Whitney test).

Trained	Experts			Trainees			Significance $P < 0.05$	
	APK	SD	variance	APK	SD	variance	T test	P value
Total score	0.36	0.15	0.023	0.44	0.12	0.015	1.44	0.16
Hypodensity	0.28	0.25	0.062	0.44	0.17	0.031	1.82	0.08
Isodense swelling	0.24	0.20	0.04	0.30	0.17	0.029	0.18	0.42

Table 4. 20: Comparison of average pairwise kappa between trained experts and trainees (MWT Mann-Whitney test).

Tables 4.19 and 20 demonstrate comparison between experts and trainees when they were untrained and trained. Generally, experts had better performance than trainees in untrained group with the only statistically significant difference in agreement on Total score. On the other hand, in the trained groups, trainee readers had better performance than experts. However, these differences were statistically insignificant across the three categories.

2- Interobserver Agreement Comparison Between Trained and Untrained readers in relation to experience.

Experts	APK		ANOVA		
Parameter	Untrained	Trained	P value	F ratio	P value
Total score	0.61	0.36	<0.05	10.37	P < 0.001
Hypodensity	0.56	0.29	<0.05	10.37	P < 0.001
Isodense swelling	0.04	0.24	<0.05	10.37	P < 0.001

Table 4. 21:Comparison of average kappa of trained experts with that of untrained experts across the three categories of ASPECTS.

Trainees	APK		Kruskal-Wallis one-way analysis*		P value
Parameter	Untrained	Trained	Untrained	Trained	
Total score	0.26	0.44	26.5	39.8	>0.05
Hypodensity	0.30	0.44	28.8	39.9	> 0.05
Isodense swelling	0.096	0.30	11.50	27.7	< 0.05

Table 4. 22: Comparison of average kappa of trained with that of untrained trainees across the three categories of ASPECTS [* values are the average rank by Kruskal-Wallis].

Tables 4-21 and 22 present the average pairwise kappa values of untrained and trained experts and trainees with test of significance.

Untrained experts agreed substantially on Total score and moderately on hypodensity whereas trained experts agreed fairly on both categories. These differences in performance had statistical significance as is illustrated in Table 4.21. However, trained experts agreed fairly on isodense swelling whereas untrained experts agreed very poorly. This showed statistical significance as is clear in Table 4.22.

In general, trained trainees performed better than the untrained trainees. The average agreement of trained trainees were moderate on Total score and hypodensity and fair on isodense swelling, while the untrained trainees had fair agreement on Total score and hypodensity and very poor agreement on isodense swelling. These differences in trainees' performance were only statistically significant regarding agreement on isodense swelling as is clear from Table 4.22.

4.6 Overall Interobserver Agreement on Each Area of ASPECTS.

ASPECTS AREA	Isodense Swelling				Hypodensity			
	Untrained readers		Trained readers		Untrained readers		Trained readers	
	FMK	XMK	FMK	XMK	FMK	XMK	FMK	XMK
Caudate Nucleus	0.78	0.01	0.92	0.008	0.66	0.29	0.68	0.21
Lentiform Nucleus	0.70	-0.003	0.81	0.02	0.47	0.34	0.395	0.23
Internal Capsule	0.85	-0.003	0.95	0.06	0.72	0.09	0.62	0.03
Insula	0.71	0.01	0.46	0.10	0.43	0.19	0.359	0.24
M1	0.60	0.006	0.51	0.14	0.63	0.34	0.67	0.30
M2	0.50	0.08	0.28	0.14	0.56	0.10	0.511	0.28
M3	0.65	0.08	0.41	0.19	0.66	0.11	0.586	0.20
M4	0.65	0.12	0.51	0.18	0.66	0.24	0.643	0.13
M5	0.50	0.12	0.33	0.20	0.56	0.13	0.5272	0.15
M6	0.59	0.12	0.40	0.23	0.66	0.18	0.72	0.18

Table 4. 23: Overall agreement on isodense swelling for each ASPECTS region among all readers in the trained and untrained groups [free marginal kappa (FMK) and Fleiss's kappa (XMK)].

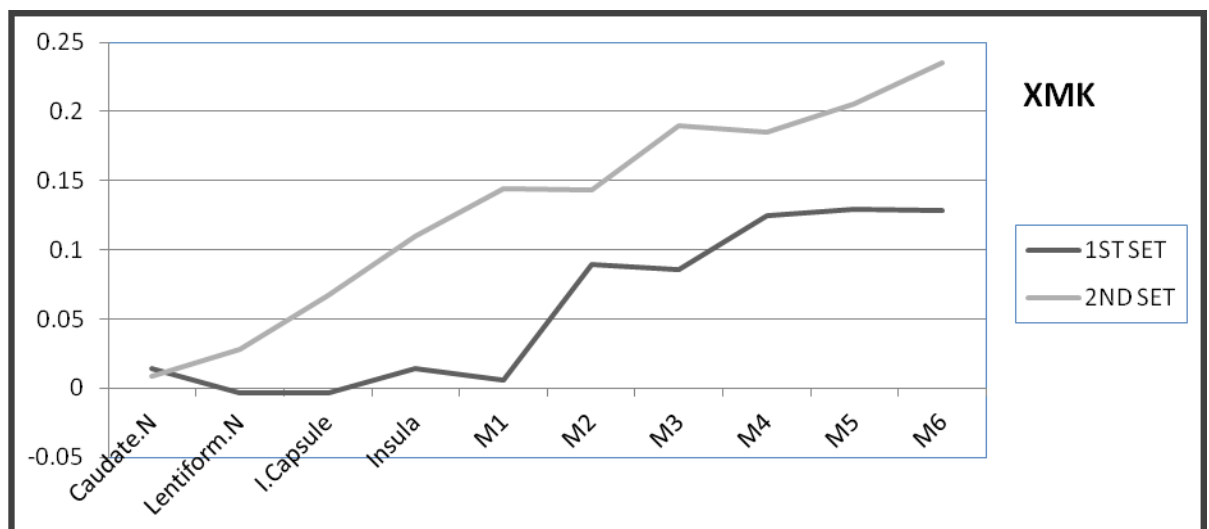


Figure 4. 14: Linear distribution of overall Fleiss's kappa (XMK) values on isodense swelling for each ASPECTS area in untrained (first set) group and trained (second set) group.

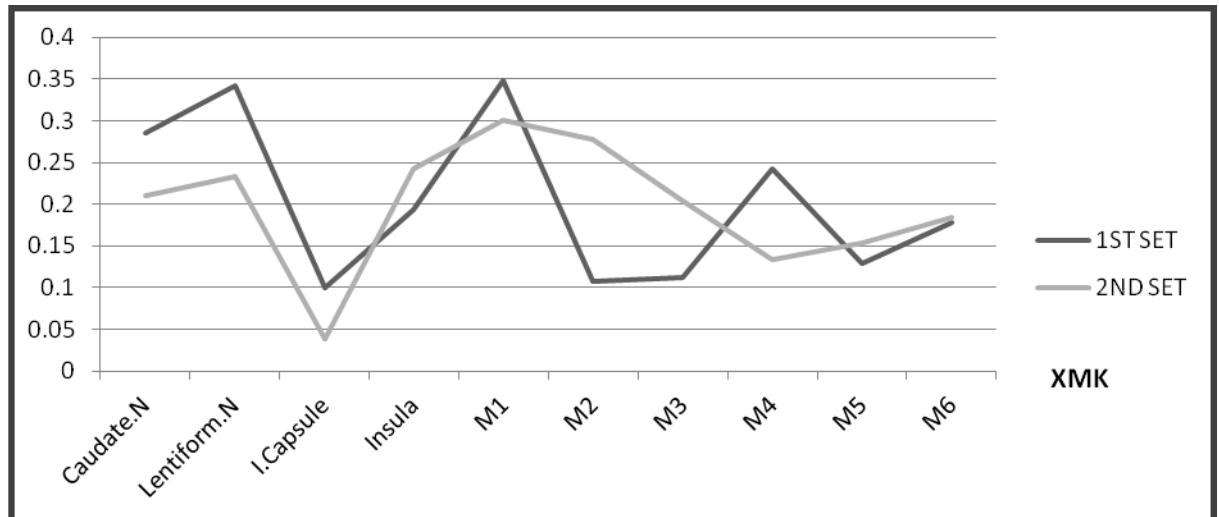


Figure 4. 15: Linear distribution of overall Fleiss's kappa values on hypodensity for each ASPECTS area in untrained (first set) group and trained (second set) group.

The overall agreement on isodense swelling and hypodensity for each ASPECTS area by using FMK and XMK with 95% confidence intervals are presented in **Table 4.23**.

Figures 4-14 and **15** show the trends of agreement on areas of ASPECTS template. In **Figure 4.14** it is clear that agreement on isodense swelling appeared to improve gradually in both groups as it moves out from subcortical areas toward cortical areas. In **Figure 4-15**, agreement on hypodensity showed improvements and worsening in both subcortical areas and cortical areas. However, in upper cortical areas agreement on hypodensity dropped in both sets when compared to the other ASPECTS areas. In both figures, readers showed very poor agreement or no agreement on the internal capsule area. However, agreement on isodense swelling for the second set appeared to be better than that for the first set, whereas agreement on hypodensity overlapped in both sets.

4.7 Hyperdense Vessel Sign (HVS)

Parameter	Presence	Category of HVS	Thick slices scan			Thin slices scan		
			Overall	MCA	Dot Sign	Overall	MCA	Dot Sign
Fleiss's kappa	0.42	0.58	0.25	-	-	0.31	-	-
% of positive responses	38.9%	0.3-19.8%	25%	0.1%	83%	52%	71%	16%

Table 4. 24: Fleiss's kappa (XMK) and percentage of positive responses for presence of hyperdense vessel sign and its categorisation and in relation to thick and thin slices scans.

Table 4.24 summarises some data collected on HVS. However, of the positive responses on HVS, 51% were on MCA, 38% on "Dot" sign and 11% on the rest of the intracranial arteries including PCA, ACA and ICA. The responses of observers varied with changing the scans' slice thickness. The positive responses on MCA sign on thick slices were very low in comparison with thin slices scans. In contrast, positive responses on "Dot sign" were low on thin slices scans and soared on thick slices scans. Differences in responses on HVS categories are illustrated in **Figure 4-16** with reference to absolute numbers of responses on each category in both sets of scans.

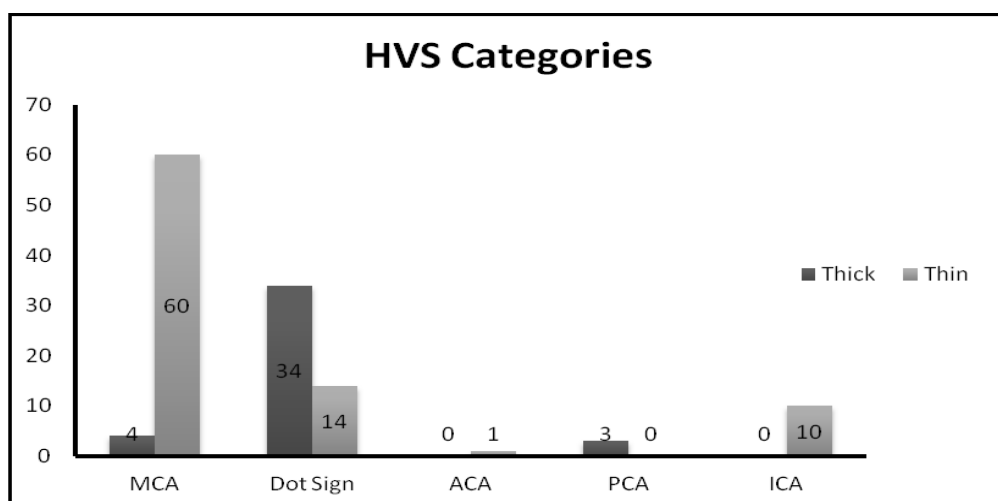


Figure 4. 16: Number of responses on each HVS category on thick and thin slices scans.

Chapter V (Results): Tissue fate

5.1 Consensus results

5.1.2 Notes from comparison of acute NCCT and PCT in consensus analysis*¹

The comparison process yielded the following findings;

1- Areas with core appeared uniformly hypoattenuated on NCCT, with radiolucency equal to or less than that of normal white matter. On densitometry and histogram, they were different from normal tissue too. Samples from these areas had lower HU values than contralateral areas. Graphically, curves from normal and hypoattenuated areas were separated from each other on the histogram (**figure 3-7**).

2- Areas with penumbra appeared isodense with an equivalent radiolucency to that of normal tissue. These areas had similar densitometry readings and histogram to that of normal areas. HU values were almost the same in normal and isodense areas, and curves overlapped on each other (**figure 3-8, 9 Basal ganglia**).

3-When penumbra and core occurred in the mixture, which was the commonest finding on penumbra grams, they appeared in a patchy manner (**figure 5.1**). When core tissue predominates, penumbra tissue appears as normal or hyperattenuated areas surrounding or dispersed across hypodense areas, and when penumbra tissue predominates, core areas appears as dark patches within isodense areas (**figure 3-9**).

4-In the case of mixed findings, the ROI of the whole ASPECTS area gives slightly deviated curves from normally appearing tissue (**figure 3-9 M2**). HU values of affected ASPECTS area are difficult to judge because of the interrelationship between core and penumbra within these areas. However, if hypodense patches and isodense patches were compared

¹ -* Some of Figures in the next two sections are found in chapter III.

with contralateral normal areas, they have values similar to that described in point 1 and 2 respectively (figure 3-10).

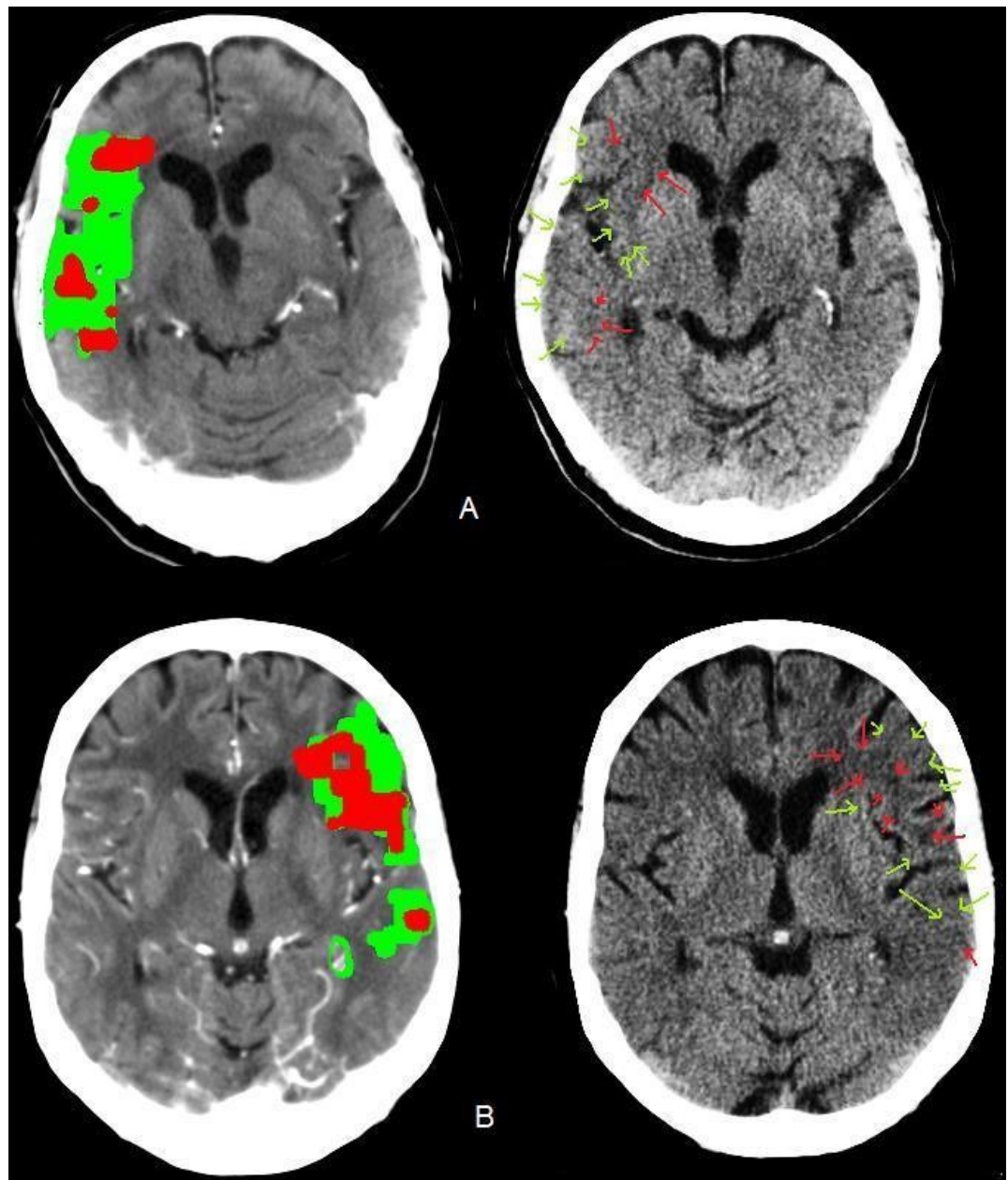


Figure 5. 1: Scans with mixed penumbra and core tissue. Green arrows: penumbra [isodense swelling] red arrows [hypodensity].

5-Structural changes within ROIs, regardless of radiolucency changes, included narrowing or obliteration of CBF spaces. This might appear as complete obliteration, reduction of the number of sulci and cisterns, decreased depth of cortical sulci and partial or complete effacement. For example, in figure 3-7, there is complete effacement of cortical sulci; in figure 3-10, there is narrowing of some cortical sulci; in figure

3-8, there is narrowing of Sylvian fissure; and in **figure 3-9** there is obliteration of Sylvian fissure and cortical sulci. Straightening of the brain outer contour, as in **figure 3-8**, might also occur in conjunction with underlying swelling.

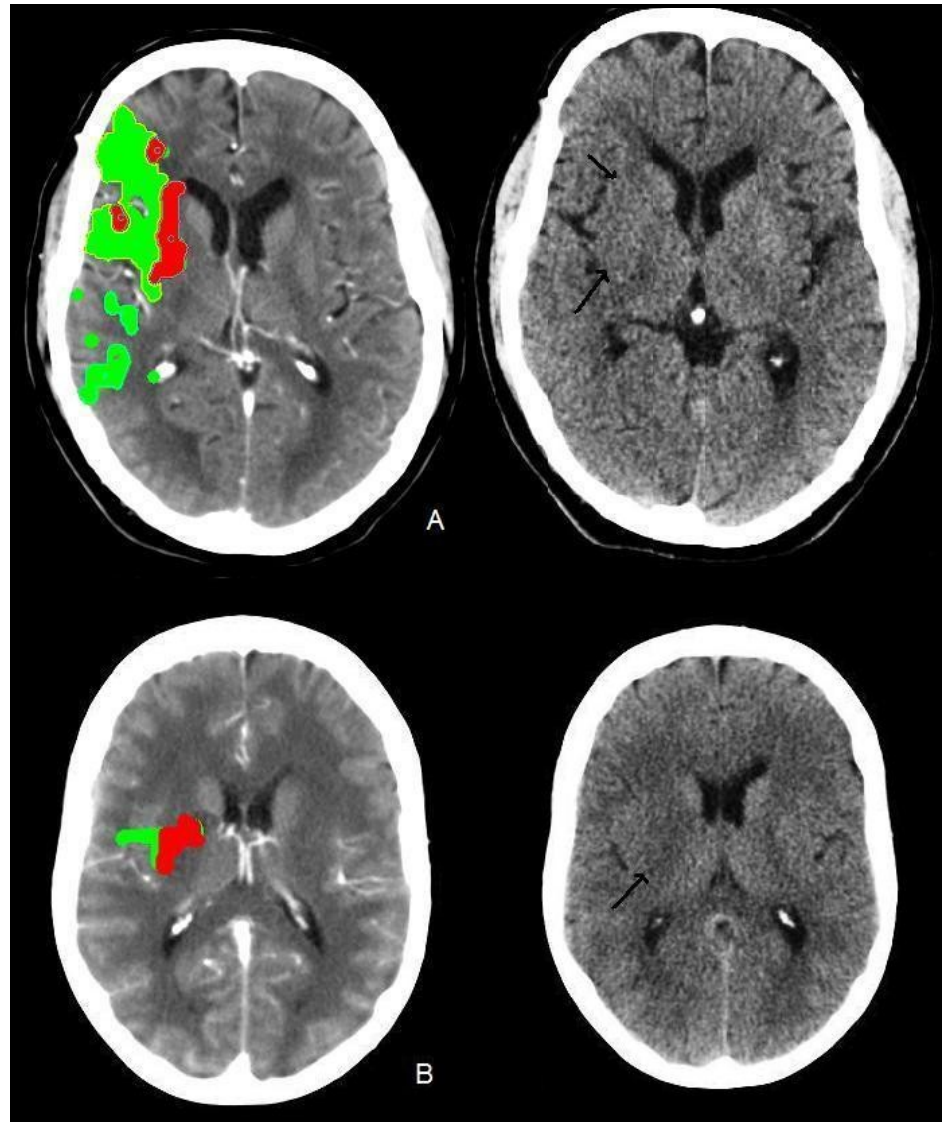


Figure 5. 2:Obscuration of lentiform nucleus[black arrows].

6-Another structural change was distortion of the normal delineation of grey-white matter. Hypodensity compatible with the core was associated with complete loss of differentiation between grey and white matter, with decreased radiolucency as in **figure 3-7**. In contrast, areas with penumbra showed incomplete loss of delineation, which appeared as mixing of bright and dark areas together, as in **figure 3-9** and **figure**

5.1 A. Penumbra areas might also retain the grey-white matter interface as normal, as in **figure 3-8** and some areas in **figure 3-10**, or with its deviation in an outer direction as in **figure 3-9**.

7-The same distortions in cortical grey-white matter can occur in insular ribbon. Loss of insular ribbon might be complete as in **figure 3-9** or partial as in **figure 5.1 A**.

8-Distortion of the normal contour of basal ganglia, mainly the body of lentiform nucleus. The borders between lentiform nucleus and adjacent structures become blurred and it is difficult to differentiate its contour. In **figure 5.2 A**, it is difficult to draw borders between the insula and lentiform nucleus. In **figure 3-9**, there is incomplete loss of shape with retained brightness. In **figure 5.2 B**, there is complete distortion with hypodensity.

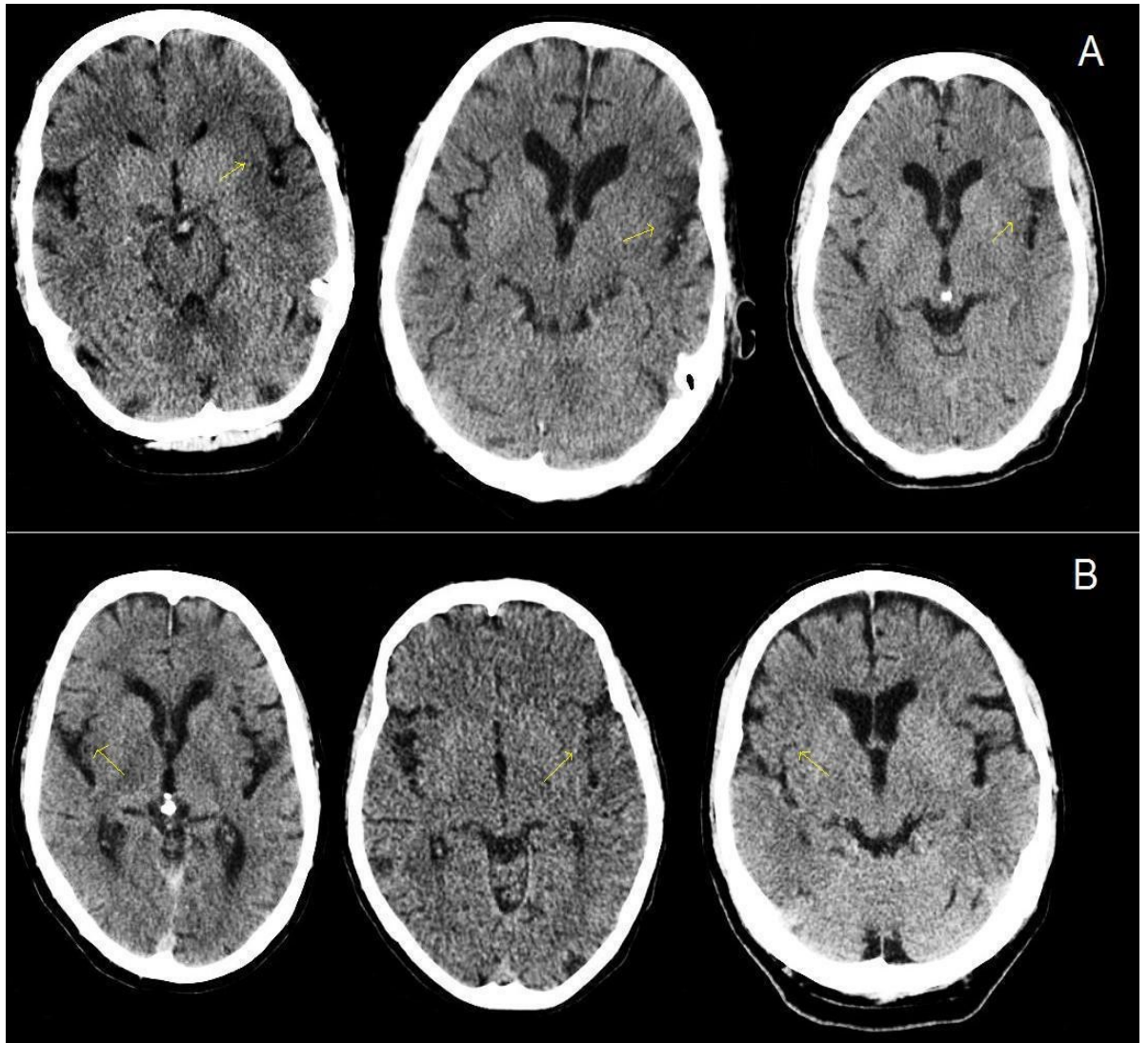


Figure 5. 3: Example of loss of insular ribbon sign A; With evident core by PCT.
B; With evident Penumbra by PCT.

5.1.2 Conclusions from comparison process

Core tissue on NCCT appeared in all examples as dark areas in comparison with ipsilateral normal tissue and the contralateral hemisphere, i.e. decreased radiolucency [hypodensity, hypoattenuation]. The degree of density on the grey-scale seemed to be in level with normal white matter or lower. This change in

radiolucency might be associated with the manifestation of brain swelling as a narrowing of CSF spaces, e.g. sulcal effacement. In other words, if hypodensity occurs as a uniformly dark area, it will very likely be core tissue. When core occurred in lentiform nucleus, it caused distortion of its shape making it difficult to differentiate it from contiguous structures. It might appear as a uniform dark patch, or a uniform loss of its lighter appearance (**figure 5.2**). Core in the insula caused loss of its characteristic ribbon shape. This might include loss of the small area of light and the zigzag path of insular region with increased darkness, and it can be associated with local swelling manifestations, such as the narrowing of Sylvian fissure when compared with contralateral hemisphere (**figure 5.3 A**).

Penumbra tissue appears on the NCCT as similar in appearance to normal tissue, or is slightly lighter when compared with contralateral hemisphere. The slight hyperattenuation occurs in a mixture with isodensity and not solely in all examples; however, it is not very common and cannot be used to distinguish penumbra from adjacent normal tissue. Appearance of penumbra can be distinguished on the NCCT by evidence of local swelling. In **figure 3-8**, isodensity is associated with the narrowing of Sylvian fissure. In **figure 3-10**, isodensity is associated with effacement of cortical sulci. These findings can be applied on insular ribbon, which shows isodensity with a narrowing of Sylvian fissure, as in **figure 5.3 B**. In some instances, the characteristic zigzag of insula might be distorted when compared with contralateral insula, as in **figure 5.3 B** [left and middle slices]. Penumbra affecting basal ganglia is difficult to recognise, although partial isodense distortion of lentiform nucleus contour might indicate penumbra rather than core, as in **figure 3-9**.

Predominance of core or penumbra alone seems to have a distinguishable appearance on NCCT as a uniform dark area and isodense swollen area respectively. Moreover, determination of their extension is attainable. However, when they occur in a mixture, the appearance also becomes a mixture of normally appearing tissue, isodense swelling and hypodensity; its reading on the NCCT also becomes rather confusing because of its similarity with normally appearing contralateral hemisphere. In this situation, foci of hypodensity might be difficult to recognise, particularly in cases with diffuse atherosclerotic

changes that had a similar density to acute ischaemic changes. However, hypodensity patches will most likely be surrounded by penumbra rather than normal tissue in this case.

Brain swelling, which is associated with acute ischaemia, occurs with both hypodensity and isodense swelling. Penumbra on the NCCT is always associated with swelling, whereas the core may or may not be associated with swelling on NCCT.

5.2 Fate of tissue categories

5.2.1 Fate of Tissue Compartments as Categorised by Readers

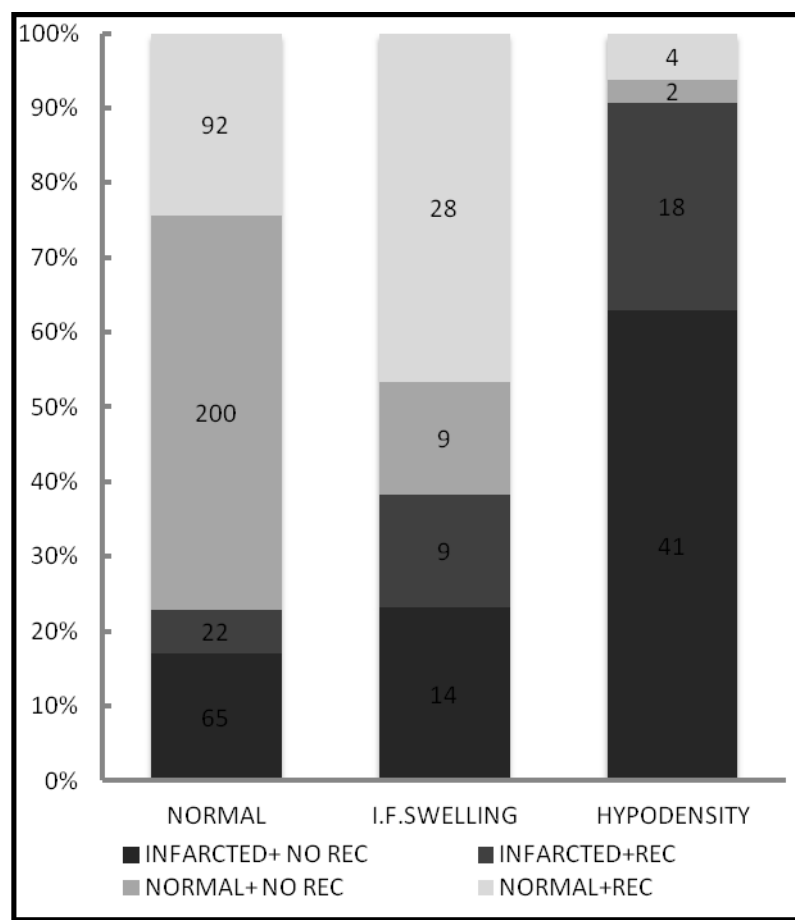


Figure 5. 4: The proportion and frequency of each NCCT appearance category in relation to fate and recanalisation [I.F. swelling, isodense swelling; REC, recanalisation].

EICs	Chi-square	Contingency coefficient	Significance level
Isodense swelling fate	27.2	0.22	P < 0.0001
Hypodensity fate	110.3	0.42	P < 0.0001
Normal appearance fate	96	0.40	P < 0.0001

Table 5. 1: Chi-square test for classification of NCCT appearances fate in relation to recanalisation.

Risk of infarction	Hypodense areas versus isodense swollen areas	Non-recanalized versus recanalized Isodense swollen areas
Odds ratio	11.9	4.8
95% CI	4.4 to 32.6	1.5 to 14.9
Significance level	P < 0.0001	P = 0.006

Table 5. 2: The odds of developing infarction in isodense swollen areas with confidence interval and p values.

As is presented in **Figure 5.4**, the categorisation of readers to NCCT appearances yielded the following: 11.9% of overall ASPECTS areas were classified as isodense swollen, 12.8% as hypodense and 75.1% as appearing normally.

Of isodense swollen areas, 38.3% were infarcted and 61.6% returned to normal. Recanalisation was associated with normalisation of 46.6% of the total areas categorised as isodense swollen and 75.6% of totally recanalised areas. In contrast, absence of recanalisation was associated with infarction of 23.3% of the total areas categorised as isodense swollen and 60.8% of total infarcted isodense swollen areas. Correlation between isodense swelling and infarction in relation to recanalisation is statistically significant with p value <0.05 as can be seen in **Table 5-1**. However, the contingency coefficient is only 22%, which indicates a weak relationship.

It was found that 90.7% of areas categorised by readers as hypodense ended in infarction and only 9.3% were normal on follow-up scans. Of the total infarcted hypodense areas, 69.4% were infarcted with absence of recanalisation and 30.3% infarcted in its presence. The association of hypodense areas with fate of

infarction in relation to recanalisation is statistically significant with $P < 0.05$ and has a relation strength of 42%.

Areas categorised as normally appearing by readers remained normal on follow-up scans in 71.1% of the total. However, the infarcted normally appearing areas occurred in 74.7% of totally non-recanalised areas. This relation between normally classified tissue, infarction and recanalisation status has statistical significance with P value < 0.05 and it showed a strength of 40%.

From **Table 5.2**, it is clear that the hypodense areas had 11.9 times the odds as isodense swollen areas to infarct. This shows statistical significance with $p < 0.05$ and the 95% CI does not contain the null value. In isodense swollen areas, persistent occlusion increased the odds of infarction by 4.8 times when compared with state of evident recanalization with 95% CI empty of the null value and statistical significance of $p=0.006$.

5.2.2 Fate of Tissue Compartments as Categorised by Perfusion Parameters

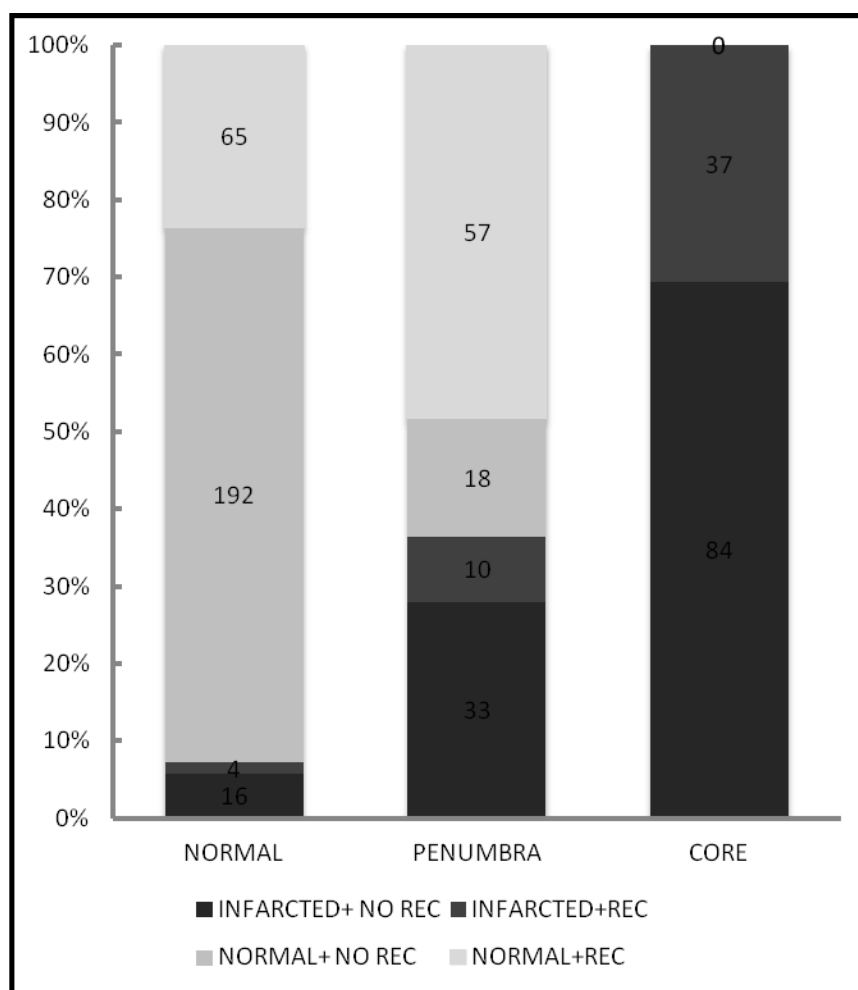


Figure 5. 5: Distribution of proportion and absolute numbers of areas fate for penumbra, core and normally appeared tissue [I.F.swelling: isodense swelling, REC: recanalisation].

Tissue compartment	Chi-square	Contingency coefficient	Significance level
Penumbra fate	64.2	0.33	P < 0.0001
Core fate	287	0.59	P < 0.0001
Normal tissue fate	256.2	0.57	P < 0.0001

Table 5. 3: Chi-square test for classification of tissue compartments according to fate and recanalisation.

Risk of infarction	Core areas versus penumbra areas	Non-recanalized versus recanalized penumbra areas
Odds ratio	422	10.5
95% CI	25.5 to 6953	4.3 to 26
Significance level	P < 0.0001	P < 0.0001

Table 5. 4: The odds of developing infarction in isodense swollen areas with confidence interval and p values.

From **Figure 5.5**, it can be seen that 53.6% of the total studied ASPECTS areas had normal perfusion parameters, 23.6% had core parameters and 22.8% displayed penumbra perfusion thresholds.

Of the penumbra areas, 63.5% returned to normal on follow-up scans while 36.3% were infarcted. In absence of recanalisation, penumbra ended in infarction in 75% of totally infarcted salvageable tissue and normalisation of only 25%. In areas with evident recanalisation, 85.1% of penumbra tissue returned to normal perfusion status and 14.9% were infarcted while in areas without recanalisation, 64.7% of penumbra ended in infarction and 35.2% returned to normal perfusion. The classification of penumbra according to fate and recanalisation was statistically significant with $p < 0.05$, albeit the strength of relation was only 33%. No core areas returned to normal on follow-up scans and 100% of areas categorised as core ended in infarction. However, the percentage of infarcted core areas with recanalisation was lower than that without evidence of recanalisation. Classification of the fate of core areas in relation to recanalisation status was statistically significant with $p < 0.05$ and good relation strength of 59%.

Results showed that 92.8% of normally perfused remained normal on follow-up scans and only 7.1% of normally perfused areas ended in infarction. The proportion of infarcted normal areas was lower in the presence of recanalisation compared with those in its absence. This classification of normal tissue fate had statistical significance with good relation at 57.6%. In **Table 5.4**, core areas are 421.7 times more likely to infarct than the penumbra regions with high statistical significance. However, non-recanalised penumbra areas had 10.4

times the odds to infarct than the recanalised penumbra areas with 95% CI being empty of the null value and high statistical significance.

5.3 Relation of NCCT Appearances with Perfusion Categories

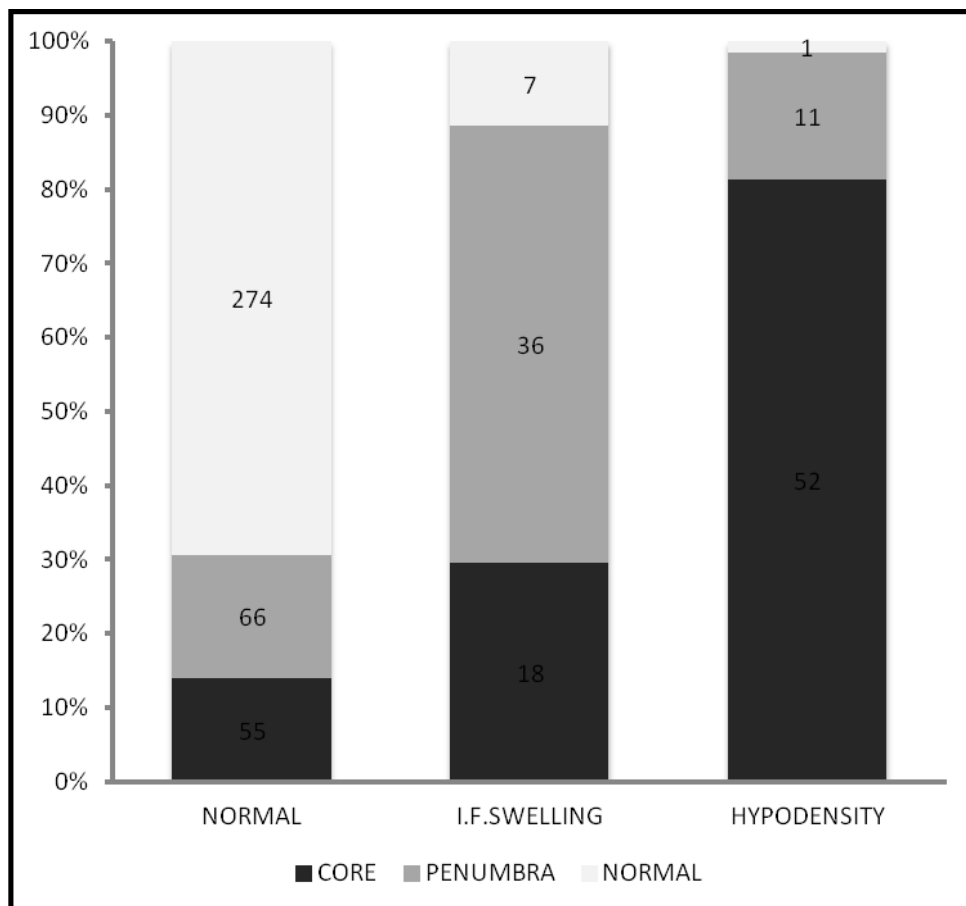


Figure 5. 6: Proportion and frequency of each perfusion categorised areas in relation to NCCT appearances [I.F.Swelling, isodense swelling].

NCCT category	Chi-square	Contingency coefficient	Significance level
Isodense swelling matching	68.6	0.34	P < 0.0001
Hypodensity matching	137.4	0.46	P < 0.0001
Normal appearance matching	158.4	0.48	P < 0.0001

Table 5. 5: Chi-square test for relation of NCCT appearances with perfusion categorised areas.

Figure 5-6 demonstrates the NCCT appearances as categorised by readers and their correspondent perfusion category. Generally, readers were correctly matching the perfusion category in 69.6% of the total matched areas, and the most common correct match was for normally appearing tissue to normal perfusion followed by hypodensity to core, and then isodense swelling to penumbra. Of the total mismatched categories, classification of penumbra as normal on NCCT was the most common with 41.7% followed by core as normal with 34.8%. In only 6.9% was penumbra categorised as hypodensity and in 11.8% core as isodense swelling of the total mismatch. In general, normally perfused areas were not commonly coded as isodense swollen or hypodense by readers with only 2.8% of total. However, readers categorised normally perfused areas as isodense swelling more frequently than as hypodensity.

Fifty-nine per cent of the areas named isodense swelling by readers had penumbra perfusion and 29.3% had core perfusion. The correlation of isodense swelling with perfusion categories is statistically significant with $p < 0.05$ and a strength of 34%.

Of hypodense areas, 81.2% had core perfusion and 17.2% had penumbra perfusion. This classification had statistical significance as is seen in **Table 5.5** with strength of 45.7%

In addition, 69.2% of normally categorised areas were normally perfused tissue on PCT while 16.7% were penumbra and only 13.9% were core. As demonstrated in **Table 5.5**, the correlation between normal appearance on NCCT and its perfusion category on PCT has a high statistical significance with p value < 0.05 and strength of relation at 48.3%.

5.4 Prediction of Tissue Perfusion and Fate by NCCT Appearances

1- Isodense Swelling

	Penumbra	Core	infarction
Sensitivity	31.86%	14.40%	13.61%
Specificity	93.86%	89.11%	88.96%
Positive Likelihood Ratio	5.19	1.32	1.23
Negative Likelihood Ratio	0.73	0.96	0.97
Positive Predictive Value	59.02%	29.51%	38.33%
Negative Predictive Value	83.22%	76.69%	67.12%

Table 5. 6: Predictive statistics of isodense swelling to penumbra, core and infarction.

From **Table 5-4** it is clear that isodense swelling is generally a low-sensitivity sign for penumbra, core and infarction. However, it had the highest predictive values for penumbra when compared to core and the final fate of infarction. Although sensitivity to penumbra is low, it is higher than that for core and infarction. Additionally, in case of absence of isodense swelling on NCCT, there is a good probability of absence of penumbra with a negative predictive value up to 83.2%. The positive likelihood ratio of 5.19 indicates an increased likelihood of penumbra when isodense swelling is seen on the NCCT but with a negative likelihood ratio of 0.73 that absence of isodense swelling can't exclude presence of penumbra. On the other hand, prediction of core by isodense swelling appears less likely when compared with penumbra prediction findings.

Isodense swelling appears to be a specific sign of penumbra with a value up to 93.8% and its presence on NCCT can indicate penumbra. A rather high specificity to core was also found, however, exclusion of normal tissue from calculation yielded specificity to penumbra of 74% and to core of only 23%. The positive predictive value is not as high as specificity, with only 59% probability of penumbra when isodense swelling is reported on NCCT. For prediction of fate, the pattern was more similar to the prediction of core with a very low sensitivity and a rather high specificity. However, this might reflect that isodense swelling is in general less likely to infarct. A positive predictive value of only 38.3% and a

positive likelihood ratio of 1.23 are both indicative of very low probability of infarction in isodense swollen areas. This is also supported by the high negative likelihood ratio of 0.97, which indicates that absence of isodense swelling does not exclude infarction.

2- Hypodensity

	Core	Penumbra	infarction
Sensitivity	41.60%	9.73%	34.91%
Specificity	96.96%	86.98%	98.21%
Positive Likelihood Ratio	13.69	0.75	19.49
Negative Likelihood Ratio	0.60	1.04	0.66
Positive Predictive Value	81.25%	17.19%	90.77%
Negative Predictive Value	83.99%	77.63%	74.94%

Table 5. 7: Predictive statistics of hypodensity to core, penumbra and infarction.

As is presented in **Table 5.7**, hypodensity is not so sensitive to core with sensitivity of only 41.6%. However, there is a good probability of 83.9% of absence of core when hypodensity is not seen on NCCT, as can be concluded from the negative predictive value. In addition, hypodensity seems to increase the likelihood of core significantly with a positive likelihood ratio of 13.69. On the other hand, a negative likelihood ratio of 0.60 is not adequate to make the absence of hypodensity on NCCT an exclusion sign for core. In contrast, hypodensity is highly specific for core and had good probability to be a core with the positive predictive value of 81.25%.

The prediction of penumbra by hypodensity is generally very poor, as can be seen from the statistics in **Table 5.7**. Although hypodensity showed a rather high specificity to penumbra, the positive likelihood ratio and positive predictive value were very low and indicate decreased likelihood of penumbra. In contrast, hypodensity had prediction values for infarction that were almost similar to those for core. It is a very specific sign for infarction too. In case of positive hypodensity on NCCT, there is a significantly increased likelihood of infarction

with a positive likelihood ratio of 19.49 and a positive predictive value of 90.7%. However, hypodensity is not as sensitive as a sign to infarction, with a low negative predictive value and high negative likelihood ratio that makes it likely to miss many areas that are going to infarct.

3-Prediction of Perfusion Categories by NCCT Appearances as Categorised by at Least Four Readers

	Isodense swelling to penumbra	Hypodensity to core
Sensitivity	42.11%	50.00%
Specificity	93.63%	96.97%
Positive Likelihood Ratio	6.61	16.50
Negative Likelihood Ratio	0.62	0.52
Positive Predictive Value	64.86%	84.00%
Negative Predictive Value	85.27%	85.91%

Table 5. 8: Predictive statistics of hypodensity and isodense swelling in case of agreement by at least four readers.

Table 5.8 presents prediction statistics of both hypodensity and isodense swelling for core and penumbra respectively, when agreement on seeing them on NCCT was made by at least four readers. It can be noted that there is a general increase in power of prediction of both changes when compared to those presented in **Tables 5.6 and 5.7**. Although sensitivity of both changes was improved, they are not high enough to make hypodensity and isodense swelling sensitive signs to correspondent perfusion category. Specificity and predictive values have not changed greatly. However, the likelihood ratios were improved in favour of increased likelihood of penumbra with positive isodense swelling and core in the case of positive hypodensity.

4- Comparison of Prediction Between Trained and Untrained Groups.

NCCT category	Isodense swelling to penumbra		Hypodensity to core	
	Trained	Untrained	Trained	Untrained
Predictive parameter				
Sensitivity	41.25%	9.09%	39.58%	48.28%
Specificity	92.51%	96.43%	97.61%	95.83%
Positive Likelihood Ratio	5.51	2.55	16.56	11.59
Negative Likelihood Ratio	0.64	0.94	0.62	0.54
Positive Predictive Value	62.26%	37.50%	86.36%	70.00%
Negative Predictive Value	84.01%	81.82%	80.86%	90.20%

Table 5. 9: Predictive statistics of isodense swelling and hypodensity for the scans of trained group and scans of untrained group.

By dividing the scans into two groups in relation to status of readers, trained versus untrained, for the purpose of comparing prediction statistics, there were differences in the level of predictive power of each early ischaemic change to correspondent perfusion characteristics on PCT.

As can be seen from **Table 5.9**, isodense swelling had higher sensitivity to penumbra when scans were read by trained readers than untrained readers. Although the value is generally low (41.25%), it differs from the very low value attained by untrained readers (9.1%). In contrast, specificity was high in both groups but with a higher value among untrained readers. Trained readers attained better values of positive predictive value and positive likelihood ratio for penumbra than those achieved by untrained readers who showed much lower values. However, the negative predictive value and negative likelihood ratios were almost similar in both groups.

For hypodensity prediction of core, prediction power appeared generally almost similar in trained and untrained groups. A higher sensitivity level of 50% was achieved by the untrained readers compared with only 39.5% by the trained group. However, good specificity with more than 90% was attained by both

groups. Trained readers had a higher positive likelihood ratio and positive predictive values than untrained readers, who achieved better values of negative likelihood ratio and negative predictive value.

5.5 Comparison of Perfusion Parameters Across the Three NCCT Appearances.

Perfusion parameter	CBV(ml\100g)		MTT seconds		CBF(ml\100g\min)	
	Mean	P value	Mean	P value	Mean	P value
Isodense swelling	2.5	P >0.05 x Normal P <0.05 x hypodensity	9.9	P <0.05 x Normal P >0.05 x hypodensity	19.1	P <0.05 x Normal P <0.05 x hypodensity
Hypodensity	1.2	P <0.05 x Isodense swelling P <0.05 x Normal	10.3	P >0.05 x Isodense swelling P <0.05 x Normal	8.1	P <0.05 x Isodense swelling P <0.05 x Normal
Normal appearance	2.3	P >0.05 x Isodense swelling P <0.05 x Hypodensity	6.1	P <0.05 x Isodense swelling P <0.05 x Hypodensity	24.6	P <0.05 x Isodense swelling P <0.05 x Hypodensity

Table 5. 10: Comparison of averages of mean transient time MTT, cerebral blood volume CBV and cerebral blood flow CBF across the three NCCT appearances.

Table 5-10 presents one-way ANOVA comparison between averages of the relative values of perfusion parameters matched with the three appearances of EICs on NCCT. Although areas of isodense swelling had higher average CBV values than that of normal tissue, it did not differ significantly from it. Hypodensity had very low CBV values in comparison with isodense swollen and normal areas with statistical significance at p value < 0.05. In Figure 5-7, the bulk of CBV values for isodense swelling located above that for normal and hypodense areas. Values for normal areas appeared more consistent with close minimum and maximum values to median value. However, CBV values for isodense swelling and hypodensity had a wide range around the median.

The MTT values for both isodense and hypodense areas prolonged significantly compared to those of normal tissue with statistically significant difference which is demonstrated in **Figure 5-8** as well. However, hypodense areas had the most prolonged MTT values among the three categories with no statistically significant difference from that of isodense swelling.

In CBF maps, isodense swelling had a statistically significant low CBF value compared to normal tissue and statistically significant high value compared to hypodense areas. This difference is also illustrated in **Figure 5-9**. The hypodensity compartment showed very low CBF with most values being less than 10ml\100g\min and deviated significantly from values of normal tissue.

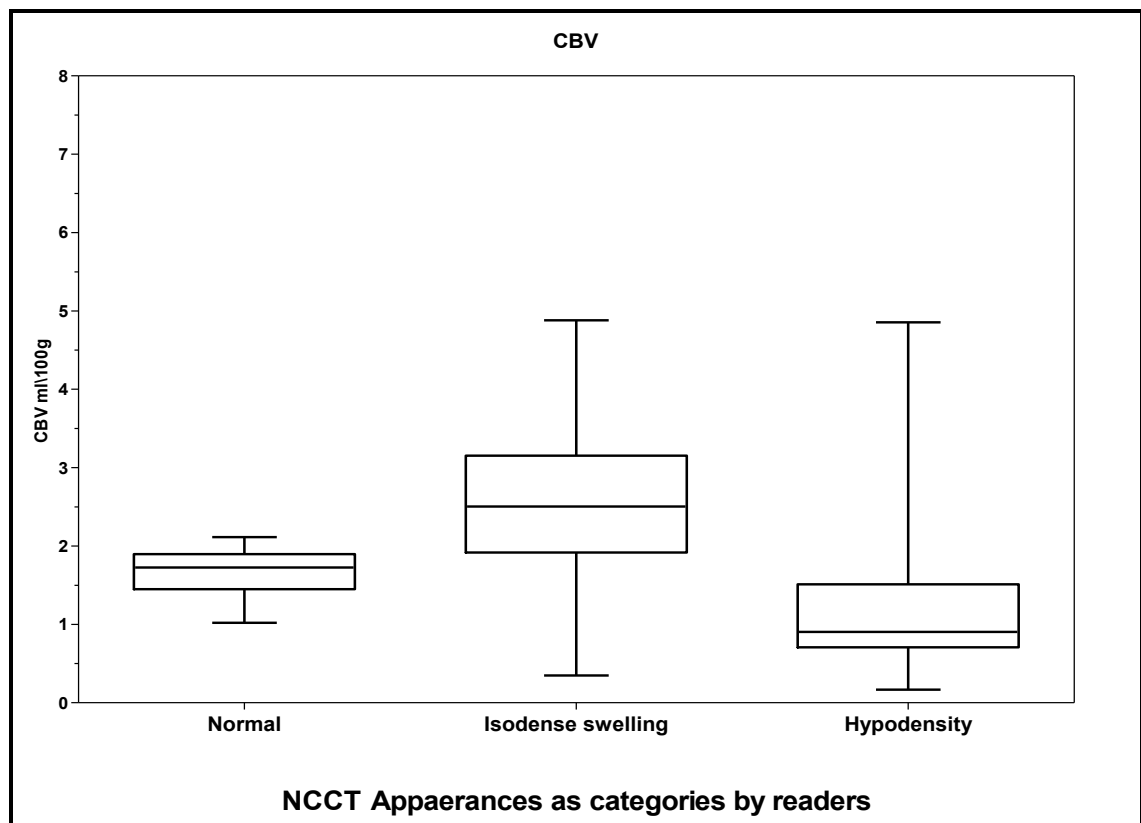


Figure 5. 7: Box and whisker plots of CBV values with minimum and maximum values for the three NCCT categories: hypodensity, isodense swelling and normal tissue.

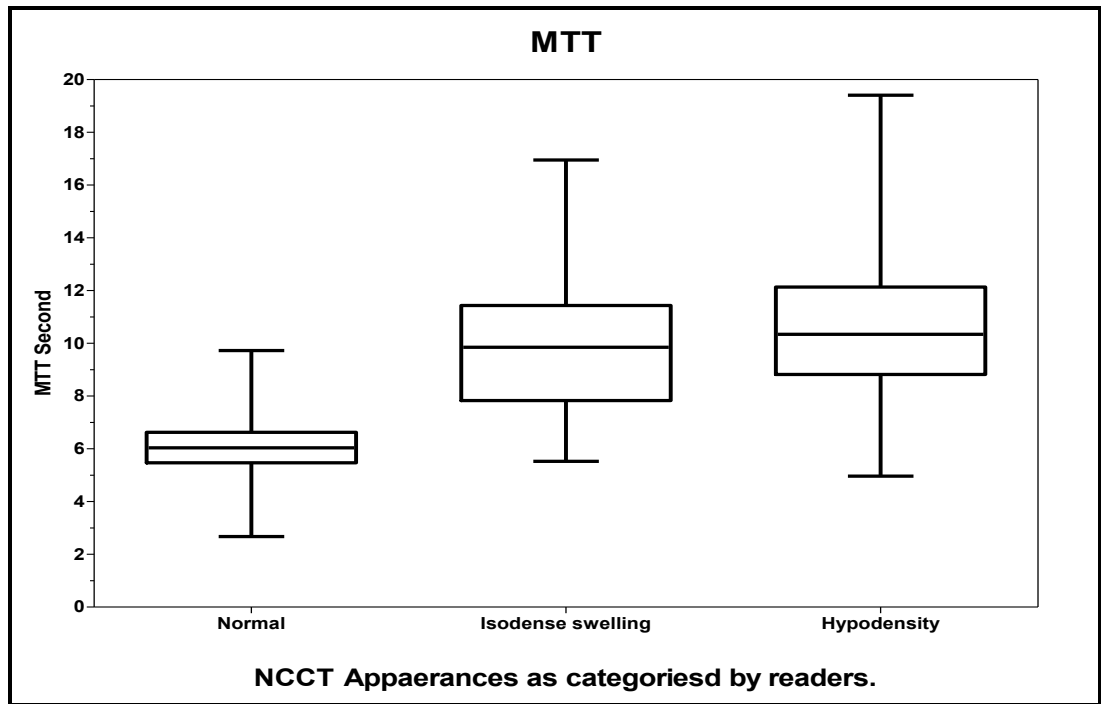


Figure 5. 8: Box and whisker plots of MTT values with minimum and maximum values for the three NCCT categories: hypodensity, isodense swelling and normal tissue.

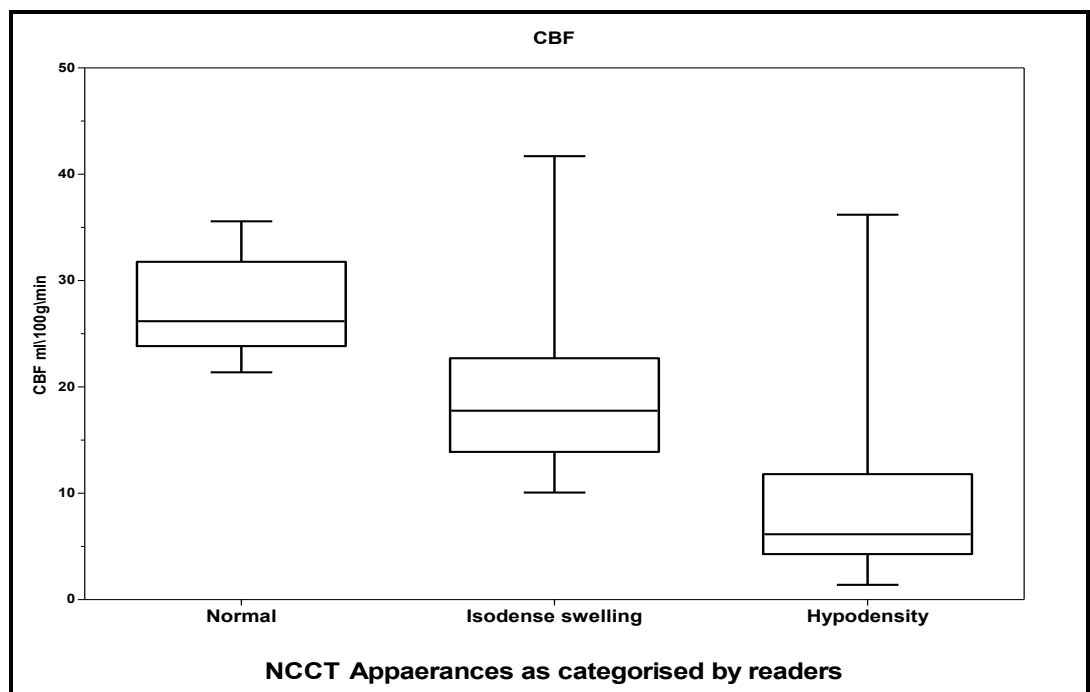


Figure 5. 9: Box and whisker plots of CBF values with minimum and maximum values for the three NCCT categories: hypodensity, isodense swelling and normal tissue.

Chapter VI: Discussion

6.1 Discussion.

Both isodense swelling and hypodensity are prevalent on NCCT within the first six hours of stroke onset, representing the distinct changes that occur in the acute stage of ischaemia and signify different pathophysiological status of ischaemic brain tissue. It was previously described that isodense swelling is more likely to represent penumbra, whereas hypodensity is more likely to represent the core. The results of this study confirm these observations. The prevalence of EICs depends on the inclusion criteria for the study from which the scans are taken, hence their prevalence varied among reports in the literature. I reported 41% prevalence of isodense swelling in this study, which is higher than that reported in the previous studies. However, this percentage includes scans reviewed after training, so this might be a consequence of the study rather than a difference in either the patient population or the observers' prior beliefs. Hypodensity showed prevalence within the range of the previous reported values. Although there were a few studies which reported prevalence of isodense swelling as distinct from hypodensity; the figure that appears in this study differed from the figures reported in those studies (119;120) of high prevalence for hypodensity and low for isodense swelling, in that hypodensity had a rather low prevalence and isodense swelling had a high prevalence. This might be attributed in part to the increased recognition of isodense swelling at the expense of hypodensity which can be noticed when the first and second sets of scans are compared (from 29.4% in first set scans to 46.8% in second set scans). The trained group were able to recognise more areas with isodense swelling than the untrained group without much change in the diagnosis of hypodensity. The reduction of sensitivity and improvement of specificity of hypodensity in relation to core can also be noted after training, so it may be that the introduction of a clearer definition for isodense swelling also caused readers to re-classify abnormal areas as swelling rather than hypodensity.

Hypodensity has been recognised as indicative of tissue infarction since the introduction of CT in the 1970s. Less marked radiolucency has been recognised

in association with brain CT in more acute stages of stroke within a few hours of onset as imaging has been undertaken at earlier time points, and particularly because clinical trials followed by clinical practice have focused on thrombolytic drug therapy delivery. Recognition of its prognostic relevance - either indicating more extensive or more severe ischaemia - has been reflected in exclusion criteria for major stroke trials for more than 15 years (43).

Over time, improved recognition of early ischaemic parenchymal changes can be noted in the increase in prevalence on reanalysis of thrombolysis trials; for example, from 31% to 52% in the NINDS trial dataset. The focus of the previous research and its detection was illustrated in many papers which involved reliability studies on EICs in acute ischaemia. However, defining radiolucency becomes more complex in very acute stroke and with advances in CT technology. Differences between grey scale shades for hypodensity and normal brain tissue on NCCT are difficult to perceive, but despite this both experienced and less experienced CT readers in this study recognised hypodensity in a similar number of scans to what the literature would predict.

Authors have referred to the favourable fate of isodense swelling compared to hypodensity (75;107), but a clear definition of isodense swelling has been lacking, and the specific influence of isodense swelling on a patient's outcome has not been evaluated separately from hypodensity. Most systematic approaches to EIC recognition, such as ASPECTS and the "rule of thirds", do not distinguish hypodensity from isodense swelling.

Tissue that is both swollen and hypodense is likely to be due to ischaemic oedema and occurs in conjunction with decreased radiolucency and featured by effaced sulci and loss of CSF spaces in general, with local mass effects. In contrast, isodense swelling is proposed to be a manifestation of congested blood vessels due to local hyperaemia without any change in density, or sometimes increased density. Mass effects also appear in association with this swelling as effacement of sulci. This appearance is usually exclusive for isolated forms of isodense swelling; however, mixed isodense swelling with hypodensity occurs as islets of bright areas either surrounding boundaries or dispersed within the dark patch of hypodensity.

In 1997, von Kummer et al (119) mentioned focal swelling without hypodensity appeared in 2% of the scans which showed swelling and interpreted this as a reflection of the compensatory vasodilatation in ischaemic areas. This sign was not subsequently analysed. Additionally, they reported two other types of swelling associated with small hypodensity in 35% of scans and with large hypodensity in 92% of scans. These two types were included for the determination of the extent of hypodensity on acute NCCT by the rule of thirds. However, Von Kummer et al. did not illustrate whether these swellings were oedema due to ischaemia or a mixture of isodense swollen areas with hypodensity. These findings by Von Kummer et al. indicate that the prevalence of isodense swelling might be greater than the very low values reported by previous studies if the mixture of hypodensity and isodense swelling was further assessed and the components treated separately. This type of mixed isodense swelling is not uncommon and more likely to be found on NCCT based on the theory of ischaemic penumbra which states that penumbra tissue occurs in the ischaemic zone surrounding the infarct core. In this study, the high frequency of isodense swelling might also be due to reporting of the mixed type of isodense swelling.

The ASPECTS system measures EICs as one change without taking into consideration its type in the total score value. Adaptation of ASPECTS to hypodensity or isodense swelling can be done as in this study. Separation of EICs by ASPECTS can yield different score values and consequently different tissue fate predictions. For example, one patient involved in this study had a total ASPECTS of two, ASPECTS including hypodensity only was eight, and ASPECTS including isodense swelling only was four. The total and isodense swelling ASPECTS predicted unfavourable outcomes, whereas hypodensity ASPECTS predicted a favourable outcome. This patient had a good clinical outcome on day 30, with a Rankin scale of one. However, the exact effect of isodense swelling on patient's outcome has not yet been clarified yet. The three forms of ASPECTS were measured separately in this study in regard to assessment of agreement among readers. The first form was total ASPECTS, which represented the usual way of reading the scans by treating hypodensity and isodense swelling as a one ischaemic change, while the second was for hypodensity alone and the third was for isodense swelling alone. The way of reading scans by readers

showed various patterns of agreement with each form of ASPECTS in response to the different variables of this study. In general, the total score and hypodensity forms of ASPECTS had similar trends in readers' agreements across the different assessed compartments of the study, which reflects the underestimation of isodense swelling and superiority of hypodensity recognition by readers.

The originally described ASPECTS system has the disadvantage of undefined boundaries meaning their determination is therefore subjective. Ischaemic changes are not exclusive to a region when they develop, but commonly affect adjacent areas and do not necessarily involve changes throughout all of an anatomical region. Therefore, abnormal ASPECTS areas, particularly cortical ones, may not reflect the exact size of ischaemic change; however, they do reflect the presence of an abnormality. Moreover, they might have a mixture of findings beside the normal tissue with unclear separation in their proportions. Therefore, analysis of findings within areas of ASPECTS might help in the estimation of final infarct volume, as has been seen in the mixed fate of some of ASPECTS areas in this study. However, there was a discrepancy in the final fate of areas diagnosed as having both hypodensity and isodense swelling on NCCT and penumbra and core on PCT. Most ROIs of mixed hypodensity and swelling on NCCT ended in infarction, whereas ROIs containing mixed penumbra and core on PCT had a variable fate that included both infarction and normality. This might have arisen from the small number of mixed areas detected on NCCT and the definition of tissue category that relied upon the majority view of readers rather than on expert or consensus review. Therefore, a larger sample and a consensus on final diagnosis of changes on NCCT might result in a different pattern of tissue ROI outcomes for ROIs of mixed change.

Although ASPECTS has the flexibility to read hypodensity and isodense swelling in acute ischaemia, it does not include the Hyperdense Vessel Sign, which may have prognostic value (161). The Hyperdense Vessel Sign is distinct from brain parenchymal changes (isodense swelling and hypodensity). Detection of the HMCA sign is improved by using thin slice instead of thick slice CT scans. Similar results were found by Kim et al who reported increased sensitivity with thin slices scans (163). However, the MCA "dot" sign appeared more often on thick slices than on thin slices. The increased depiction of "dot" signs on thick

slices could be attributed to the perpendicular courses of MCA branches in Sylvian fissure and M3 area to the coronal direction of CT slices, which gives more chances for thrombosed segments to be visualised in a number of slices beyond the scope of 5mm. This might also be the reason behind the very poor recognition of proximal MCA occlusions on thick slices, which has a horizontal course in coronal direction making its visualisation in reconstructed thick sections very unlikely (the partial volume effect).

The ability of readers to recognise isodense swelling on NCCT has been studied in only a few instances. Na et al. sought mainly the physiological background of isodense swollen areas on NCCT by using diffusion and perfusion-weighted MRI and they mentioned that the two readers in their study agreed moderately on IS with kappa 0.50. A later study by Muir et al. found very poor interobserver agreement among 5 readers with kappa 0.08. Other studies were not clear on their definition of swelling and might have involved both types of swelling at the same time. The patterns of interobserver agreement for isodense swelling were not examined by any of the studies found in the literature search. Therefore, the results of this study cannot be directly compared to any other.

In this study, the interobserver agreement on isodense swelling varied greatly in relation to the different factors that were assessed. Among all untrained readers, agreement was as poor as previously reported with average pairwise kappa 0.093 (75), but among the most consistent trained readers, agreement was similar to that found by Na et al. (120), with mean pairwise kappa 0.50. The level of agreement also differed according to the type of statistical measure used to assess agreement. This can be seen when the free marginal kappa and Fleiss's kappa in this study were used to assess agreement on isodense swelling. By the first measure, agreement was high, and almost perfect on some occasions, while, at the same time, Fleiss's kappa gave very poor levels of agreement. The approach of agreement using pairwise kappa for pairs of readers gives full information on the pattern and strength of agreement. This was used by Von Kummer et al (94) for assessment of interobserver agreement on the EICs along with other statistical measures and it gave detailed information on how readers agreed on EICs. The same approach was also taken by Grotta et al. to assess variability among and within groups of readers.

Studying the factors that were previously mentioned in the literature as modifying factors for agreement can help the overall understanding how readers are affected in their interpretation of NCCT findings in acute stroke. However, we did not include the effect of intrinsic factors related to brain factors like old infarcts and atherosclerotic changes on observers agreement because I were concerned mainly with testing the training of how to read the changes and differentiate them from each other on the observer agreement in detecting isodense swelling and to less extent how other general controllable factors can improve or worsen the agreement. Although agreement on isodense swelling was poor in the set of scans that were used to assess the effect of slice thickness and clinical data on interobserver agreement, trends in readers' agreement can be identified.

Unlike previous results, readers in this study had better interobserver agreement when they were unaware of the affected hemisphere. This discrepant result could be in part due to the effect of slice thickness where the thin slices comprised most of the scans that were presented with clinical data. Other factors that might have affected the performance of readers include that readers were aware that scans were taken from acute stroke patients and, therefore, were more attentive to EICs on NCCT. In addition, because scans were repeated within the set with changing variables, the effect of the subconscious memory recalling scans cannot be eliminated. However, when scans were provided with clinical information, greater detail of clinical data was associated with better agreement compared to limited information restricted to identifying the affected side. Despite this, the provision of clinical data had no statistically significant effect on observer agreement. This in itself might explain why clinical data sometimes increased agreement level but other times had no effect on it when assessed in previous studies (94;132;150). In general, knowing clinical data might improve reading of scans, but it does not seem to be essential for detection of acute ischaemia. however, clinical information is still important in routine practise for early diagnoses of acut cerebral ischaemia.

Lev et al. used fixed slice thickness of scans for evaluation of the effect of soft-copy (variable window settings; width and centre level) in their review of detection of EICs (149). In this study, I found that with fixed window width,

changing the slice thickness from 0.9mm to 5mm increased the interobserver agreement on hypodensity and total ASPECTS significantly. This result supports the conclusions of Tanaka et al (154). Agreement on the presence of isodense swelling was non-significantly better on thin slice scans, but the very low prevalence of this finding reported in the first stage of the study means that this finding must be considered with caution. Therefore, although the 5 mm slices improve interobserver agreement on hypoattenuation and total score, it is not clear if this, or the opposite, is true for isodense swelling. Additionally, thick slices might reduce recognition of the Hyperdense Sylvian “dot” sign. Overall, variation in presentation of scans in regard to slice thickness and window width will affect detection of EICs; hence, the recommendations by Dr Francesca Ng et al. (155) to routinely use both thin and thick reconstructions is supported by the results of this study.

In previous studies there has always been an emphasis on the importance of training on the performance of readers. Von Kummer et al. found a significant increase in performance of ECASS II investigators after training in reading acute NCCT scans. He suggested that careful CT reading by ECASS II investigators might have contributed to a reduction in ICH incidence in patients recruited to that trial (152) compared to previous studies. In addition, it was suggested by Muir et al (75) that the poor agreement on isodense swelling might have been due to a lack of defining criteria that can distinguish between isodense swelling and hypodensity. In this study I sought the effect of consensus on definitions for EICs among readers on the level of interobserver agreement. As was found in chapter 4, training had a generally positive effect on the agreement on isodense swelling and there was a significant increase in interobserver agreement and a decrease in variability of agreements among pairs of observers. Additionally, training was associated with increased prevalence of isodense swelling and sensitivity to penumbra. The same scenario was observed by Von Kummer when training ECASS II investigators on recognition of EICs (152). At the same time, recognition of hypodensity showed no significant change between trained and untrained readers. Using average pairwise kappa for each reader in both groups helped to detect individuals who agreed poorly with all other observers, which will reduce the overall agreement level. The presence of inconsistent agreements might mask the true level of agreement. Exclusion of observers with consistently weak

agreement increased agreement across the three studied categories of ASPECTS score, as expected, and allowed better clarification of effect of training. This was also done by Von Kummer et al. (94) when assessing the agreement on EICs.

However, evaluation of the same group of readers before and after training revealed a different pattern of results. Those readers showed a drop in interobserver agreement on the total ASPECTS and hypodensity after training, with performance similar change in isodense swelling. This discrepant result was due in part to the inconsistent performance of one reader who was unconvinced of the defining criteria developed in the consensus stage. When this reader was excluded, there was a general improvement in the level of agreement in both stages as well as increased post-training agreement on hypodensity, with comparable agreement on isodense swelling before and after training. A significant difference in agreement on the total ASPECTS in favour of the pre-training set of scans persisted; however, the very high levels of agreement that were achieved before consensus might reflect familiarity with the established use of ASPECTS in defining areas as normal or abnormal, with deterioration in performance being a consequence of the introduction of a more detailed breakdown of the usual assessment into more categories. Using different sets of CT scans in both stages of study might also have caused this result. In general, this outlying performance of some readers compared to the general results of the whole group might be attributed to a number of factors, including the predominant composition of this group being expert readers who showed more conservative responses at the consensus stage, and observer fatigue (this group read 72 scans in total). In comparison, other observers were trainees who participated only once in the study. In general, although training of the same participants had a contradictory effect on the agreement level, training reduced the variability in agreement and increased consistency in the performance of readers, particularly for isodense swelling.

The medical speciality of readers had no effect on agreement in this study compared to the previous studies by Wardlaw et al which showed that neuroradiologists are better than non-neuroradiologists in reading the scan (101;121) Although neuroradiologists showed less interobserver agreement in comparison with neurologists, they agreed well on hypodensity. However,

neuroradiologists showed very reserved decisions in categorising areas as being isodense swollen; therefore, they had very poor agreement on isodense swelling. However, fewer neuroradiologists participated in comparison with stroke neurologists and so within the group comparisons of agreement were less reliable because there were only two neuroradiologists in training. Overall, these results are consistent with other studies which found no significant difference in performance of different specialities (117;122;150). On the other hand, the experience of readers affected their responsiveness to training in this study. Trainee readers exhibited poorer interobserver agreement compared to experts when there was no training on recognition of EICs and showed significant differences to experts regarding total ASPECTS. This result is similar to that obtained by Fiebach et al, who showed generally lower agreement among novices than experts(151) and differs in that after training, trainees' general level of agreement became higher than that of experts. However, this is not the case for isodense swelling, which had very poor agreement before training in both groups and improved significantly in both after consensus, although trainees achieved higher agreement than experts. In fact, experts appeared more conservative in their response to consensus definitions than did trainees. This might explain the significant drop in their agreement on total ASPECTS and their agreement on hypodensity after consensus. As was found by ACCESS authors, years of experience in reading the scans might not be a determinant of agreement by readers, but might influence their response to training.

As can be seen from the interobserver agreement data on individual ASPECTS areas, readers showed very poor agreement on isodense swelling in ganglionic areas, including caudate nucleus, lentiform nucleus and internal capsule. The final area appeared to be the least recognised area of ASPECTS either before or after training, and in general it had, a perfect agreement level by using the free marginal kappa which reflects the area being considered to be of normal appearance by most readers. In general, subcortical areas appear to be very difficult to assess for isodense swelling, therefore, they have the poorest level of agreement of the ASPECTS areas. This is due to the anatomical nature of subcortical areas of very small areas in a narrow space with overlapping boundaries which render their differentiation from each other difficult sometimes. Also, subcortical areas may be affected by beam hardening artefact

effect and variable skull thickness. Additionally, the definition of isodense swelling given in consensus does not involve features that distinguish isodense swelling in these areas. However, cortical areas had a higher level of agreement on isodense swelling which reflects the fact that it is easier to see it in these areas. In reference to training, isodense swelling recognition had the same trend pre- and post-training with continuation of restricted recognition of isodense swelling on cortical areas. In contrast, hypodensity could be seen in any ASPECTS region.

Readers had almost perfect intraobserver agreement on both isodense swelling and hypodensity and were able to reproduce their readings effectively. This was also compatible with findings by Muir et al. (75) and Saur et al. (117) who both reported high values of intraobserver agreement. However, the effect of subconscious memory on repeated scans within the set could not be entirely disregarded in the interpretation of the high intraobserver agreement level. Nevertheless, the high levels of intrinsic agreement of readers indicate good consistency in interpreting EICs by single readers.

ROIs defined by the majority of readers as exhibiting isodense swelling were of normal appearance on follow-up NCCT in 62% of cases: of these, 76% were associated with recanalization. In 38% of ROIs with isodense swelling, there was tissue infarction at follow-up. In contrast, 90% of areas that were categorised as hypodense proceeded to infarction. The data in this study showed that categorisation of an ASPECTS area as hypodense rather than as isodense swollen was associated with odds of infarction greater than eleven, and in isodense swollen ROIs, the absence of recanalization was associated with odds of infarction up to four times higher. Consequently, this might mean that a patient with an acute stroke with isodense swollen areas on NCCT might benefit from thrombolysis more than a patient with hypodense areas. ROIs categorised by perfusion characteristics had very similar outcomes to those based on NCCT EIC features. Penumbra had a normal fate in 63% of its regions and 76% of them gained normality with reperfusion, while core regions all went on to infarction irrespective of recanalization. Penumbra ROIs increased odds of infarction up to 10 times in the absence of recanalization.

The perfusion patterns of areas categorised as isodense swollen varied. Only 59% had penumbra characteristics, while the remainder, had mainly “core” perfusion. Recognition of core as isodense swollen areas on NCCT rendered the specificity of isodense swelling for abnormal perfusion (either penumbra or core) high in this study. The specificity of isodense swelling for core was only 23% compared to 74% for penumbra after the exclusion of ROIs categorised as normal, which is a situation more relevant to clinical practice. Penumbra tissue was predominantly categorised as being of normal appearance by readers, As might be expected, therefore, sensitivity of isodense swelling for penumbra is low in this study, although it is higher (31.9%) than that reported by Muir et al. at (17.4%)(75). This high missing rate of penumbra could be due to two factors; first, a lack of consensus on isodense swelling definition among readers which appears in the soaring of sensitivity from only 9% before training up to 41% after training; secondly, considerations of the maximum number of votes for categorisation of areas in this study which appears in an increased sensitivity of up to 42% when the maximum vote was adjusted to just four readers. Along the same lines, a high portion of core areas are also categorised as normally appearing, reflected in low sensitivity of hypodensity for core perfusion in this study. However, the likelihood ratios for hypodensity being associated with core perfusion and subsequent infarction (13.6 and 19.4, respectively) confirm that the recognition of hypodensity on NCCT is strongly associated with core, rather than penumbral, perfusion. The sensitivity of hypodensity to core decreased after training whereas specificity increased after training. This in part might be attributed to increased recognition of mixed areas which had both hypodensity and isodense swelling. Additionally, reducing the vote threshold increased the sensitivity to 50% and also other predictive statistics to core.

Perfusion parameters of ASPECTS areas as categorised by readers as isodense swollen, hypodense or normally appearing, indicating their different pathophysiological states. Areas of isodense swelling had high CBV values, reduced CBF and prolonged MTT, whereas hypodense areas corresponded with substantially reduced CBV and CBF and prolonged MTT. These enhance the correlation of isodense swelling with penumbra and hypodensity with core. However, normal-appearing regions generally had normal perfusion parameters. The high CBV values found in isodense swollen areas are consistent with the

hypothesis that swelling reflects engorged blood vessels due to local hyperaemia, with brightness in these areas being due to blood protein content. These findings support the findings of previous studies which combined NCCT with MRI (107;120) and PCT (75;102). Thus, NCCT gives gross information on the changes of perfusion parameters in response to ischaemia while PCT provides a more sophisticated assessment of acute ischaemic regions, allowing a further classification of hypoperfused tissue on the basis of outcome prediction. Some isodense swollen areas had non-penumbra perfusion characteristics on PCT, although it showed prolonged MTT but normal CBV and CBF. These areas could represent benign oligoemic areas, although this is not defined by perfusion thresholds for PCT. This reflects the general criticism that the thresholds that are defining penumbra on PCT might not be robust and valid because they do not distinguish it from oligoemic tissue. However, benign oligoemia might appear on NCCT as isodense swollen areas and can be mistaken for penumbra. In this study, areas which had prolonged MTT but normal CBV and CBF were categorised as normal tissues on PCT. However, they might be blamed for the small proportion of normal tissue which progressed into infarctions, as shown previously.

This study confirms the feasibility of using web technology as a tool for clinical research in imaging. This enhances recommendations stated by ACCESS group on benefits of web technology in reading the scans (101).

6.2 Limitations of the study

Because of the study design, fatigue and subconscious memory effects cannot be excluded from affecting the performance of readers and they may have affected the results to some extent.

On a 4cm detector-width CT scanner, as used here, perfusion CT covers a limited volume of brain tissue; therefore, some scans had very low slices for the

upper cortical regions of ASPECTS with loss of complete coverage of perfusion of vertex areas which limited the complete evaluation of areas.

Presentation through a web-based interface meant that readers were not able to change window settings to adjust the scan contrast.

The consensus stage assembled individual reader comments and feedback but did not include a meeting of all readers. This could be less strong than face-to-face group presentations for convincing readers about the definitions adopted.

ASPECTS areas have no clear boundaries and ischaemic change might happen in-between areas which could be considered by some readers to happen in two areas and by others to be involved in one area. Subjectivity in reading areas' boundaries cannot be eliminated from affecting the agreement levels in this study.

6.3 Conclusions

- Penumbra tissue can be seen on acute NCCT scans as isodense swollen areas.
- Isodense swelling is a distinctive feature of acute ischaemia and is different from hypodensity, and it is prevalent on acute NCCT scans within the first few hours post stroke onset; it represents ischaemic tissue at risk of infarction but whose fate is variable, predominantly determined by recanalisation status.
- Isodense swelling can be defined in NCCT scans as areas without changed density or with a slight increase in density with evidence of local swelling. It might appear isolated or mixed with hypodensity as bright areas either surrounding or dispersed through the dark patch of hypodensity.
- Isodense swelling should not be mixed with hypodensity in estimating the extent of EIC on NCCT and should be withdrawn from ASPECTS when reading hypodensity.
- More than half of isodense areas recover, particularly with restoration of reperfusion.

- Absence of recanalization increases the risk of infarction of isodense areas fourfold.
- Reliability in detection of isodense swelling is good with perfect intraobserver agreement, moderate interobserver agreement and high specificity for penumbra.
- Interobserver agreement on EICs is affected by CT technology where thick slices scans appears to improve agreement on hypodensity and detection of hyperdense “dot” sign, and worse detection of HMCA sign.
- Different statistical measures of agreement result in different levels of agreement and the analysis of paired agreements between individual readers is the most reliable way in concluding the accurate level of agreement, determination of inconsistent observers and performing the statistical significance testing.
- Experience of readers in reading the scans does not affect agreement but it affects the response of readers to training.
- The area of brain tissue involved with EICs affects the level of agreement and should be considered when measuring EICs by using the ASPECTS template.
- The sensitivity of isodense swelling to penumbra is still low together with sensitivity of hypodensity to core, which indicates a high missing rate and the need for further improvements in approaching them on NCCT.
- Training is effective in improving the overall performance of reading acute NCCT and reducing the missing rate of EICs.
-
- Isodense swelling has perfusion characteristics of penumbra when its regions on NCCT were matched with their correspondents on perfusion maps, and this study confirms results published previously on the different pathophysiology of isodense swelling and hypodensity.
- This study adds confirmation to the validity of the ASPECTS system as a robust searching tool of EICs in acute stroke. It is flexible and can be adapted to measure each ischaemic change separately with good reliability. However, it does not measure the hyperdense vessel sign.

Appendix

Dear (reader)

I am a Libyan doctor doing an MSc and I am looking at the interpretation of acute CTs, specifically the swelling versus hypodensity issue. I am just e-mailing you to know if you would be willing to participate in the study to send you the first set of the scans? . They come as links in email that take you to a short online questionnaire about each scan, and there are about 40 in all at this stage. Once we complete this set, which supposed to finish on December 15, the plan is to identify what is generally agreed to represent swelling and do some "training" for consistency, then have a second look at agreement. Your participation will be very important to me and your opinion on scans of great value.

Kind Regards

Dear participant

Thank you for participating in the CT reading study seeking to determine agreement on isodense swelling and hypodensity in acute stroke. Links to the [first] set of scans and score sheets are listed below:

1. <http://www.surveymonkey.com/s/9H9QLMT>
2. <http://www.surveymonkey.com/s/VH78JJ3>
3. <http://www.surveymonkey.com/s/V6WQGQ8>
4. <http://www.surveymonkey.com/s/VHB3NLF>
5. <http://www.surveymonkey.com/s/VB5QNGC>
6. <http://www.surveymonkey.com/s/8BK5GFH>
7. <http://www.surveymonkey.com/s/SW2VLCG>
8. <http://www.surveymonkey.com/s/SWJ5MWH>
9. <http://www.surveymonkey.com/s/SWR5Q7N>
10. <http://www.surveymonkey.com/s/SWTGG2X>
11. <http://www.surveymonkey.com/s/SW3D5FX>
12. <http://www.surveymonkey.com/s/SWHY58L>
13. <http://www.surveymonkey.com/s/SWZXPHC>
14. <http://www.surveymonkey.com/s/RNQZ7MX>
15. <http://www.surveymonkey.com/s/SSVMR6R>
16. <http://www.surveymonkey.com/s/SSDG55J>
17. <http://www.surveymonkey.com/s/SSQL3X5>
18. <http://www.surveymonkey.com/s/SSRWNWD>
19. <http://www.surveymonkey.com/s/SST3WYJ>
20. <http://www.surveymonkey.com/s/SSFH2K>
21. <http://www.surveymonkey.com/s/VH5F27P>
22. <http://www.surveymonkey.com/s/SRJPZJC>
23. <http://www.surveymonkey.com/s/SRFC5S7>
24. <http://www.surveymonkey.com/s/V62367K>
25. <http://www.surveymonkey.com/s/VP5CKNH>
26. <http://www.surveymonkey.com/s/STD96FF>
27. <http://www.surveymonkey.com/s/STCPGZ3>
28. <http://www.surveymonkey.com/s/STQBFWF>
29. <http://www.surveymonkey.com/s/STTS2ZS>
30. <http://www.surveymonkey.com/s/STXTW6M>
31. <http://www.surveymonkey.com/s/STBKF2M>
32. <http://www.surveymonkey.com/s/VBFW8CF>
33. <http://www.surveymonkey.com/s/SML57LM>
34. <http://www.surveymonkey.com/s/VHXXRBV>
35. <http://www.surveymonkey.com/s/SMDZ7BQ>
36. <http://www.surveymonkey.com/s/SMSK6SC>
37. <http://www.surveymonkey.com/s/SMTV8WW>
38. <http://www.surveymonkey.com/s/RSKNGJM>
39. <http://www.surveymonkey.com/s/RS75RT9>
40. <http://www.surveymonkey.com/s/RS2BPKX>

These links are uniquely tied to this survey and your email address. Please do not forward this message.

Note; if the scans are not clear, you can change the zoom level of the scans by a click on the zoom zone at the right corner of your computer.

Thanks for your participation!

Table 1: First set invitation e-mails.

Dear Participant

Thank you for participating in the CT reading study for the second time. It was most generous of you to put aside some of your time to finish the first set of scans. I do really appreciate your assistance and look forward to receiving your response on the second set of CT scans.

As with the first set of scans, I am seeking to determine agreement on isodense swelling and hypodensity in acute stroke. However, this time I am first circulating a short power point presentation [**attached**] that is intended to establish a common definition for these CT appearances based on the responses to the first set of scans. I would be grateful if you could read through this presentation, in particular the distinction between **partial** and **complete** loss of grey-white matter differentiation, before confirming that you are ready to review the second set of scans. Please send an email to confirm that you have read through the presentation: after this is received, links to the second set of scans will be sent, with an ASPECTS template also included with clarification of its regions. Note; **There is the incentive of a £10 amazon gift voucher for each set of scan reads that is completed within 15 days!**

I am looking forward to hear from you.

Kind Regards

Table 2: Consensus invitation e-mail.

Dear participant

Thanks for your participation.

Your reader code is [] please sign it at the end of each score sheet.

Please read the clinical information before reading the scan. We hinted the affected hemisphere by body side. **Right side symptoms = Left hemisphere stroke.**

The deadline for completing the survey is; dd/mm/yy.

There is the incentive of a £10 amazon gift voucher for each set of scan reads that is completed within this time limit!.

Aspects score sheet is attached.

Here are the links to the [second] set of scans and score sheets are listed below;

- 1- <http://www.surveymonkey.com/s/H93GS3S>
- 2- <http://www.surveymonkey.com/s/H9PG2W2>
- 3- <http://www.surveymonkey.com/s/HDV79MK>
- 4- <http://www.surveymonkey.com/s/HD98P23>
- 5- <http://www.surveymonkey.com/s/HDYZJQB>
- 6- <http://www.surveymonkey.com/s/HDJ75X2>
- 7- <http://www.surveymonkey.com/s/HDWML89>
- 8- <http://www.surveymonkey.com/s/HDR7BCV>
- 9- <http://www.surveymonkey.com/s/HDX9GNM>
- 10- <http://www.surveymonkey.com/s/HDF6BTY>
- 11- <http://www.surveymonkey.com/s/HDHG7KF>
- 12- <http://www.surveymonkey.com/s/HDPF5Q8>
- 13- <http://www.surveymonkey.com/s/HY899B8>
- 14- <http://www.surveymonkey.com/s/HYV6DN3>
- 15- <http://www.surveymonkey.com/s/HY9SZZN>
- 16- <http://www.surveymonkey.com/s/HYCNDPP>
- 17- <http://www.surveymonkey.com/s/HYW8C2G>
- 18- <http://www.surveymonkey.com/s/HYTL2ND>
- 19- <http://www.surveymonkey.com/s/HYXP2R>
- 20- <http://www.surveymonkey.com/s/HY3H2PJ>
- 21- <http://www.surveymonkey.com/s/HYH8Z8P>
- 22- <http://www.surveymonkey.com/s/HYP5MBM>
- 23- <http://www.surveymonkey.com/s/HYZYJX3>
- 24- <http://www.surveymonkey.com/s/H2K98JW>
- 25- <http://www.surveymonkey.com/s/H28X2Q5>
- 26- <http://www.surveymonkey.com/s/H2VR57F>
- 27- <http://www.surveymonkey.com/s/H2DQSYG>
- 28- <http://www.surveymonkey.com/s/H227NBL>
- 29- <http://www.surveymonkey.com/s/H2C6P2Q>
- 30- <http://www.surveymonkey.com/s/H2WSQZF>
- 31- <http://www.surveymonkey.com/s/H2SG9GH>
- 32- <http://www.surveymonkey.com/s/H2XVVML>

These links are uniquely tied to this survey and your email address. Please do not forward this message.

Thanks for your participation!

Table 3: Second set invitation

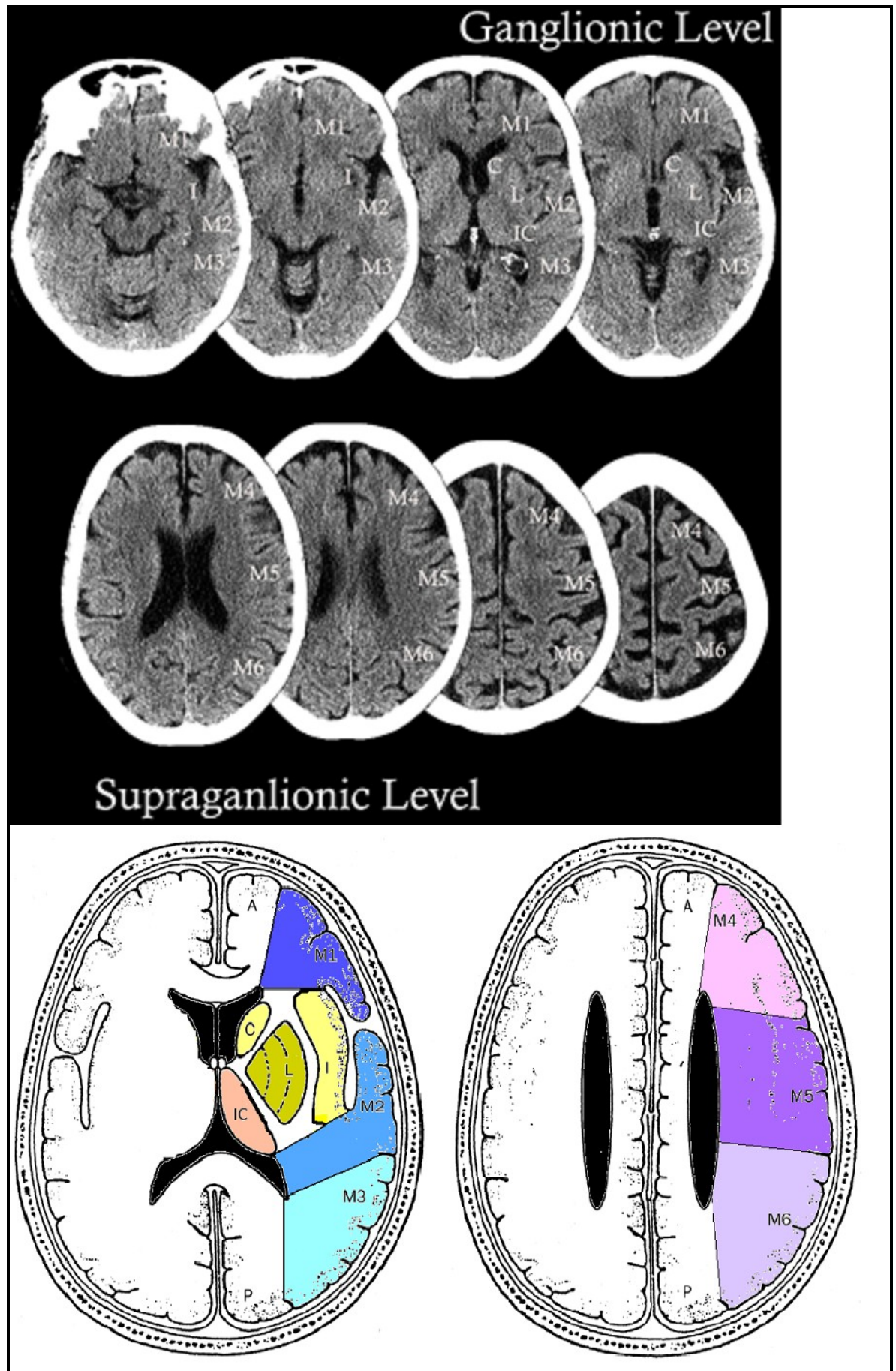
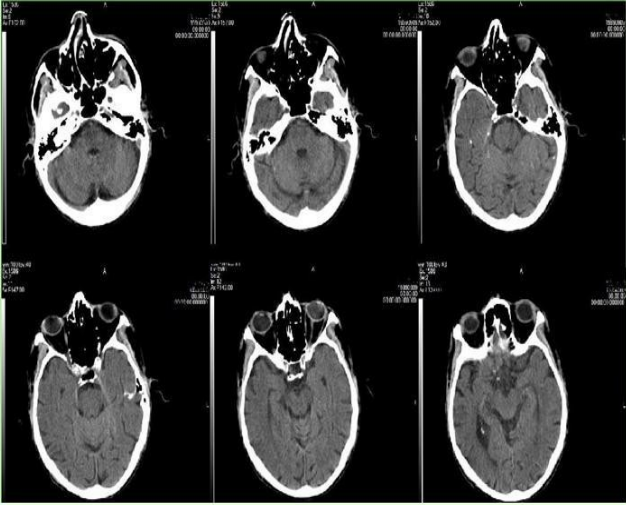


Figure 1; ASPECTS template [Supraganglionic level image is loaded from the official web site for description of ASPECTS(227)]

SCAN-12

1. Please, ignore any changes other than acute ischemic changes

A 79-year-old man presents with right side symptoms.



1. This CT is:

- Normal
- Abnormal

2. The affected side is:

- Left
- Right

3. Hyperdense vessel sign is seen in the:

- MCA
- M1 Segment (Sylvian 'dot' sign)
- ACA
- PCA
- Intracranial ICA
- Other vessel
- None

4. The following area shows:

	Focal Swelling	Hypodensitiation
Caudate	<input type="checkbox"/>	<input type="checkbox"/>
Isthmiform	<input type="checkbox"/>	<input type="checkbox"/>
Internal capsule	<input type="checkbox"/>	<input type="checkbox"/>
Insula	<input type="checkbox"/>	<input type="checkbox"/>
M1	<input type="checkbox"/>	<input type="checkbox"/>
M2	<input type="checkbox"/>	<input type="checkbox"/>
M3	<input type="checkbox"/>	<input type="checkbox"/>
M4	<input type="checkbox"/>	<input type="checkbox"/>
M5	<input type="checkbox"/>	<input type="checkbox"/>
M6	<input type="checkbox"/>	<input type="checkbox"/>
A(lower slice)	<input type="checkbox"/>	<input type="checkbox"/>
P(lower slice)	<input type="checkbox"/>	<input type="checkbox"/>
A(upper slice)	<input type="checkbox"/>	<input type="checkbox"/>
P(upper slice)	<input type="checkbox"/>	<input type="checkbox"/>

Done

Powered by SurveyMonkey
Create your own surveys online

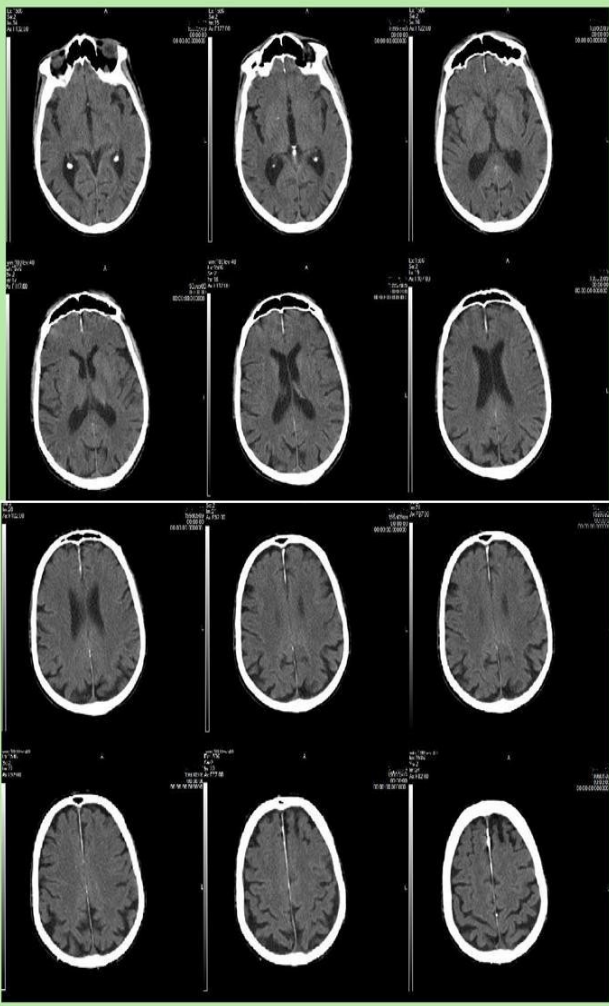
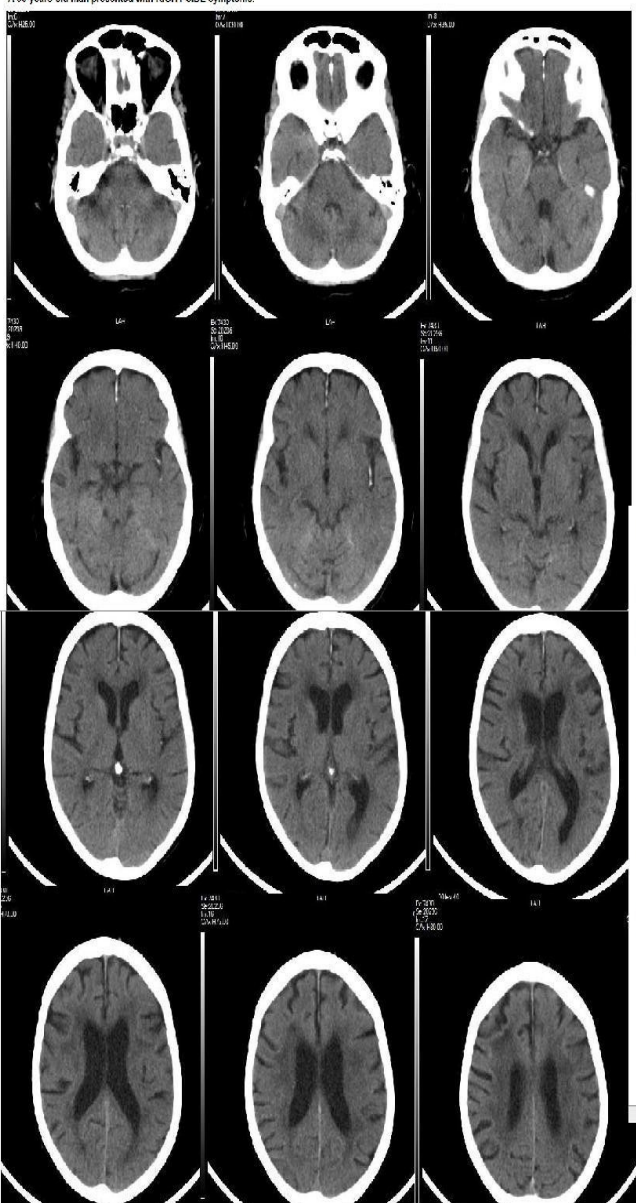
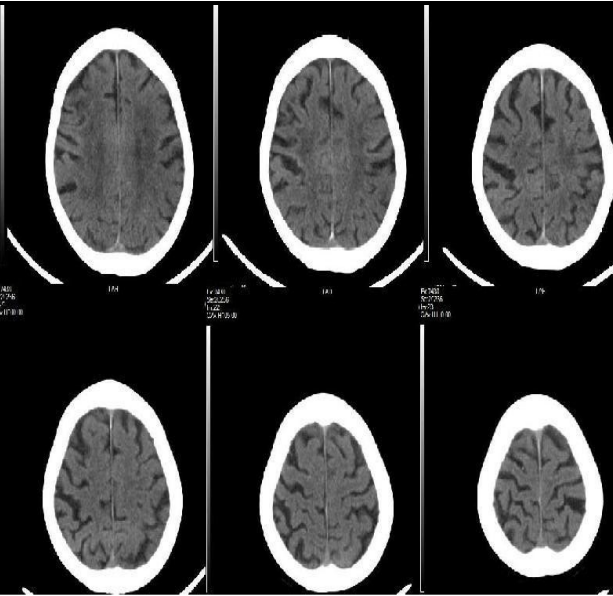


Figure 2: Example of a scan from first set loaded to Survey Monkey.

SCAN-4

Please ignore any changes which are not related to acute ischaemia.

A 90-years-old man presented with RIGHT SIDE symptoms.

The following area shows;

	hypodensity	local swelling
Caudate nucleus	<input type="checkbox"/>	<input type="checkbox"/>
Caudate head	<input type="checkbox"/>	<input type="checkbox"/>
Internal capsule	<input type="checkbox"/>	<input type="checkbox"/>
Insula	<input type="checkbox"/>	<input type="checkbox"/>
M1	<input type="checkbox"/>	<input type="checkbox"/>
M2	<input type="checkbox"/>	<input type="checkbox"/>
M3	<input type="checkbox"/>	<input type="checkbox"/>
M4	<input type="checkbox"/>	<input type="checkbox"/>
M5	<input type="checkbox"/>	<input type="checkbox"/>
M6	<input type="checkbox"/>	<input type="checkbox"/>

In this SCAN;

There is no Hypodensity or Focal swelling

Reader code is ;

C E F A K H M I Z

Powered by SurveyMonkey
© 2015 SurveyMonkey Inc. All rights reserved.

Figure 3: Example of a scan from second set loaded to Survey Monkey.

Figure 4: a to e, are the slides of consensus power point sheet presented to readers.

Consensus set of scans

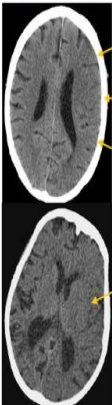
Definitions of early ischemic changes.

A-Brain swelling

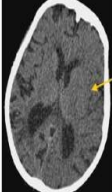
- Circumscribed effacement of cortical sulci, swelling of gyri and / or compression of ventricles. It can be recognized by comparing sulci and cisterns on both hemispheres. In early phase of acute ischemia, it might be associated with hypoattenuation or it might occur without concomitant parenchymal hypoattenuation and then it is called Isolated (isodense) Focal Swelling.

Brain swelling signs on non-contrast CT scan are ;

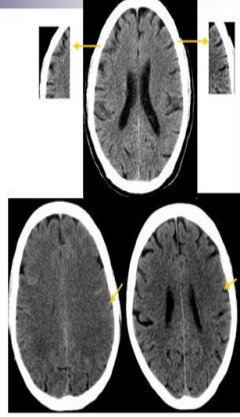
1- Cortical sulcal effacement (CSE); Reduced number of sulci and straightening of brain outer contour in the affected area, usually with loss of precise delineation of the grey-white matter interface at the margins of the cortical sulci, corresponding to a localised mass effect.



2- Obscuration of Sylvian fissure (OSF); Narrowing or obliteration of Sylvian fissure.



3- Partial loss of differentiation of gray-white matter interface (PDGW); loss of grey-white matter contrast due to expansion of swollen white matter into effaced sulci. Cortical ribbon is not well recognized if compared to contralateral hemisphere but the cortical margin is still brighter than subcortical tissue and neither is less dense than contralateral white matter.



4-Compression of ventricles (COV); Obliteration or decrease in size due to mass effect. [It is not common in early stroke].

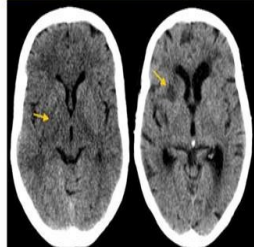


B- Hypodensity

- Increased radiolucency of brain structures relative to other parts of the same structure or to its contralateral counterpart that could be recognised visually.

■ *Hypodensity signs on non-contrast CT scan are ;*

1- The disappearing basal ganglia sign (DBG) and Obscuration of lentiform nucleus (OLN) ; loss of the normal contour of basal ganglia. Or decreased attenuation of parts or whole lentiform nucleus with loss of precise delineation of the area and blurring of its margins so that its differentiation from contiguous white matter structures is impossible.



2-Loss of insular ribbon (LIR); loss of the usual slightly increased attenuation of insular cortex with reduced precision in delineation of gray-white interface at its lateral margins.

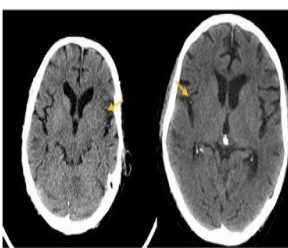
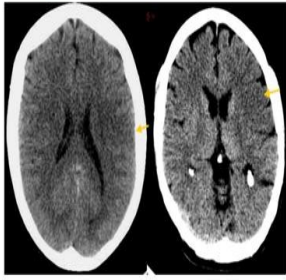


Figure 4a; Consensus sheet.



4-Complete loss of differentiation of grey-white matter interface (CDGW); Complete loss of cortical ribbon due to decreased attenuation of gray matter. There should be no distinction between density of cortex and underlying white matter, and the density should be equal to, or less than, that of contralateral white matter.

Isolated focal swelling;

Any of the following signs on non-contrast CT;
 1- Partial loss of differentiation between grey-white matter interface.
 2- Effacement of sulci and straightening of brain outer contour.
 3- Narrowing of sylvian fissure or ventricles.
 None of those accompanied by hypodensity.

Examples of isolated focal swelling;

Example-1

- 1- Straightening of outer contour of LT hemisphere.
- 2- Obliteration of Sylvian fissure.
- 3- Partial loss of grey-white matter differentiation. Mainly seen in posterior part of M1 and in M2



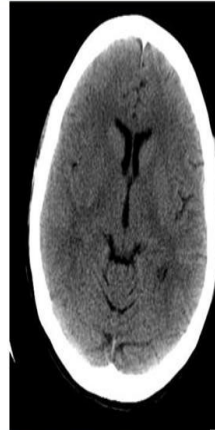
Example-1

- 1- Straightening of outer contour of LT hemisphere.
- 2- Obliteration of Sylvian fissure.
- 3- Partial loss of grey-white matter differentiation. Mainly seen in posterior part of M1 and in M2



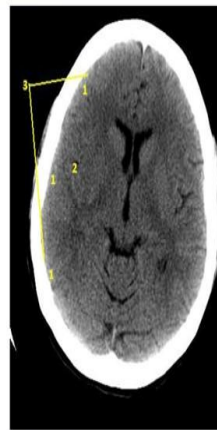
Example-2

- 1- Partial loss of differentiation between gray-white matter interface in M1, M2 and M3.
- 2- Obliteration of Sylvian fissure.
- 3- Straightening of outer contour of RT hemisphere.



Example-2

- 1- Partial loss of differentiation between gray-white matter interface in M1, M2 and M3.
- 2- Obliteration of Sylvian fissure.
- 3- Straightening of outer contour of RT hemisphere.



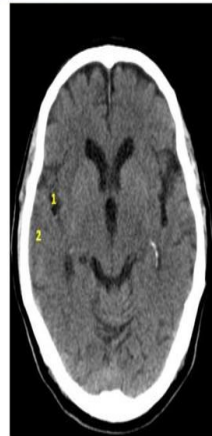
Example-3

- 1- Narrowing of RT Sylvian fissure
- 2- Effacement of sulci in M2 with partial loss of gray-white matter interface.



Example-3

- 1- Narrowing of RT Sylvian fissure
- 2- Effacement of sulci in M2 with partial loss of gray-white matter interface.



Example-4

Effacement of sulci in left M4 and M5.



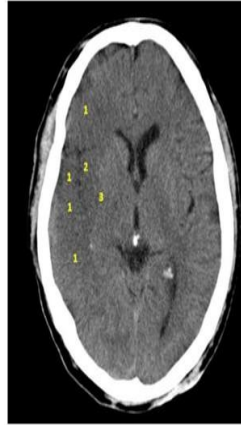
Figure 4b; Consensus sheet.

<p>Example-4</p> <p>Effacement of sulci in left M4 and M5.</p> 	<p>Example-5</p> <p>Effacement of sulci with reduction of the number of cisterna in the RT M4, M5 and M6 when compared with contralateral hemisphere.</p> 	<p>Example-5</p> <p>Effacement of sulci with reduction of the number of cisterns in the right M5 and M6 when compared with contralateral hemisphere.</p> 
<p>Examples of Hypodensity;</p>	<p>Example-1</p> <ol style="list-style-type: none"> 1- Complete loss of grey-white matter differentiation with decreased attenuation in both in Lt M1 and M2. 2- Effacement of sulci. 3- Loss of insular ribbon. 4- Obscuration of lentiform nucleus. 	<p>Example-1</p> <ol style="list-style-type: none"> 1- Complete loss of grey-white matter differentiation with decreased attenuation in both in Lt M1 and M2. 2- Effacement of sulci. 3- Loss of insular ribbon. 4- Obscuration of lentiform nucleus. 
<p>Example-2</p> <ol style="list-style-type: none"> 1- Complete loss of grey-white matter differentiation with decreased their attenuation in Lt M5. 2- An effacement of sulci. 	<p>Example-2</p> <ol style="list-style-type: none"> 1- Complete loss of grey-white matter differentiation with decreased their attenuation in Lt M5. 2- Effacement of sulci in M5 and M6. 	<p>Example-3</p> <ol style="list-style-type: none"> 1- Complete loss of grey-white matter differentiation with decreased attenuation in right M1, antero-medial part of M2 and medial part of M3. 2- Loss of insular ribbon 3- Obscuration of lentiform nucleus. 

Figure 4c; Consensus set

Example-3

- 1- Complete loss of grey-white matter differentiation with decreased attenuation in right M1, antero-medial part of M2 and medial part of M3.
- 2-Loss of insular ribbon
- 3- Obscuration of lentiform nucleus.



Example-4

- 1- Complete loss of grey-white matter interface with reduced attenuation in M4, M5 and M6.
- 2- Effacement of sulci.



Example-4

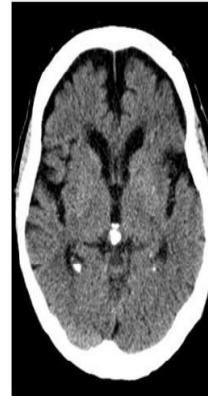
- 1- Complete loss of grey-white matter interface with reduced attenuation in M4, M5 and M6.
- 2- Effacement of sulci.



Reading the Scans;

Example-1

- Left hemisphere stroke;
- 1- Complete loss of gray-white matter interface in most of M1 with straightening of its lateral contour.
 - 2- Loss of insular ribbon, mostly in its anterior part.
 - 3- Narrowing of Sylvian fissure.
 - 4- Partial loss of gray-white matter with sulcal effacement in M2 and M3.



Example-1

- Diagnosis;**
- Hypodensity, M1-Insula.
 - Isolated focal swelling, M2-M3.



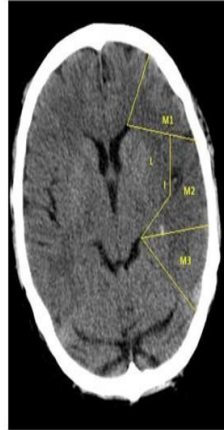
Example-2

- Left hemisphere stroke;
- 1- Complete loss of gray-white matter interface with reduced attenuation and sulcal effacement in M2.
 - 2-Loss of insular ribbon.
 - 3- Obscuration of parts of lentiform.
 - 4- Obliteration of Sylvian fissure.
 - 5- Partial loss of gray-white matter interface and sulcal effacement in posterior part of M1 and anterior part of M3.



Example-2

- Diagnosis;**
- Hypodensity, M2-Insula-Lentiform.
 - Isolated focal swelling, M1-M3.

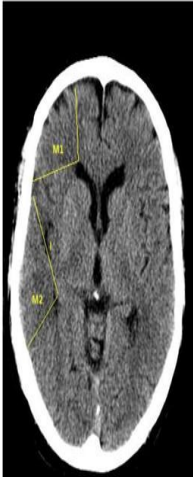
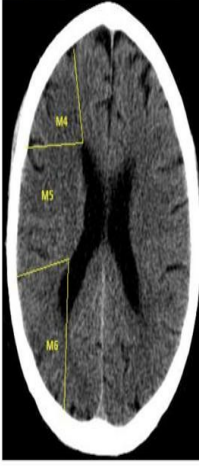
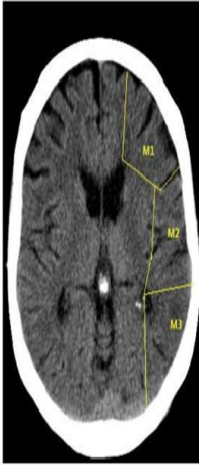
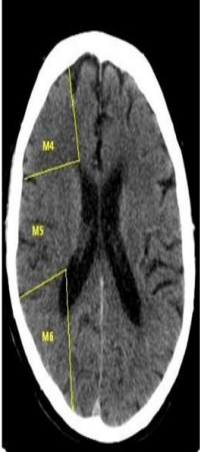


Example-3

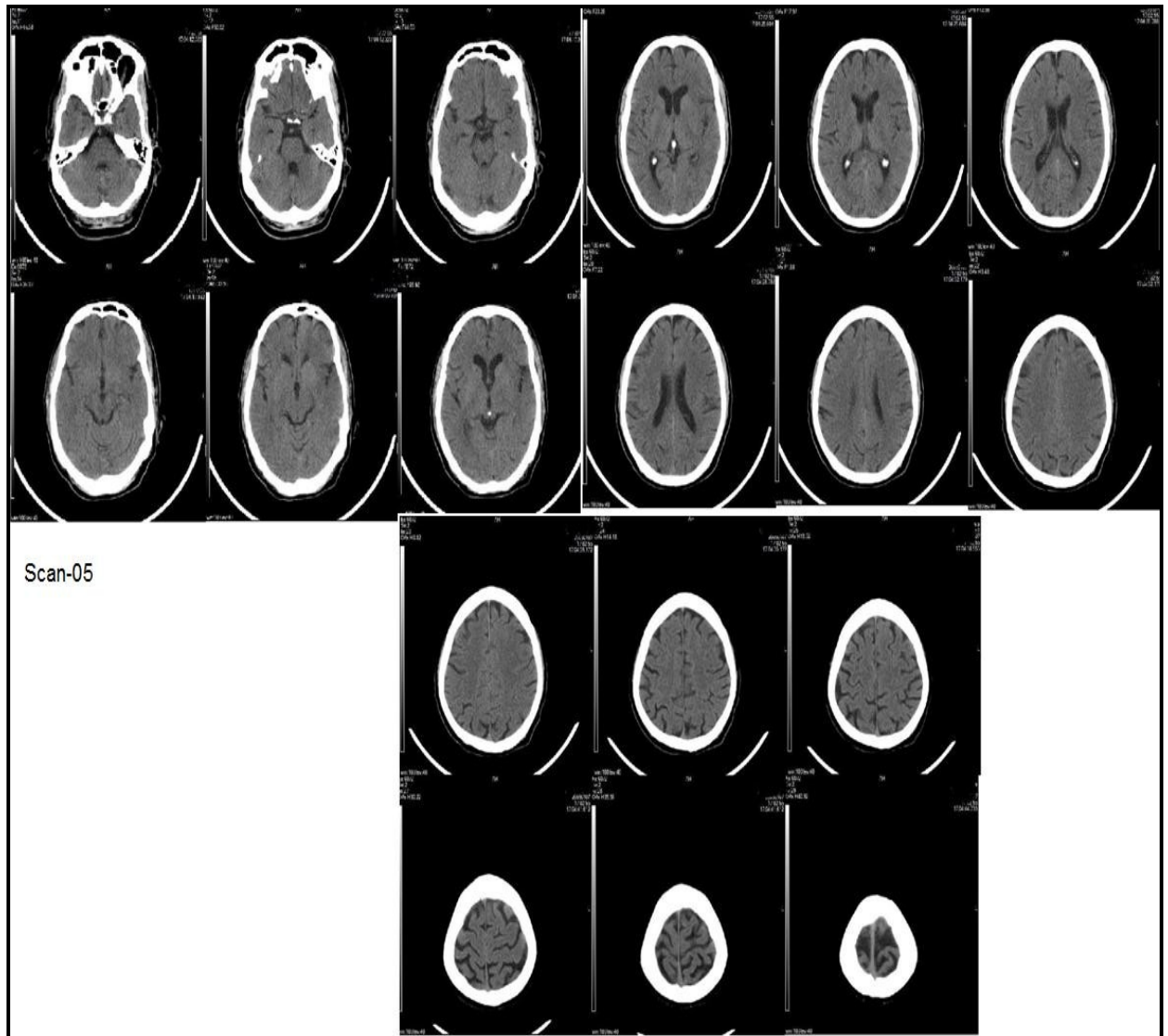
- Right hemisphere stroke;
- 1- Partial loss of grey-white matter interface with sulcal effacement in M1, anterior and lateral parts of M2.
 - 2- Reduced attenuation and poor delineation in postero-medial part of M2.
 - 3- Loss of most of insular ribbon.

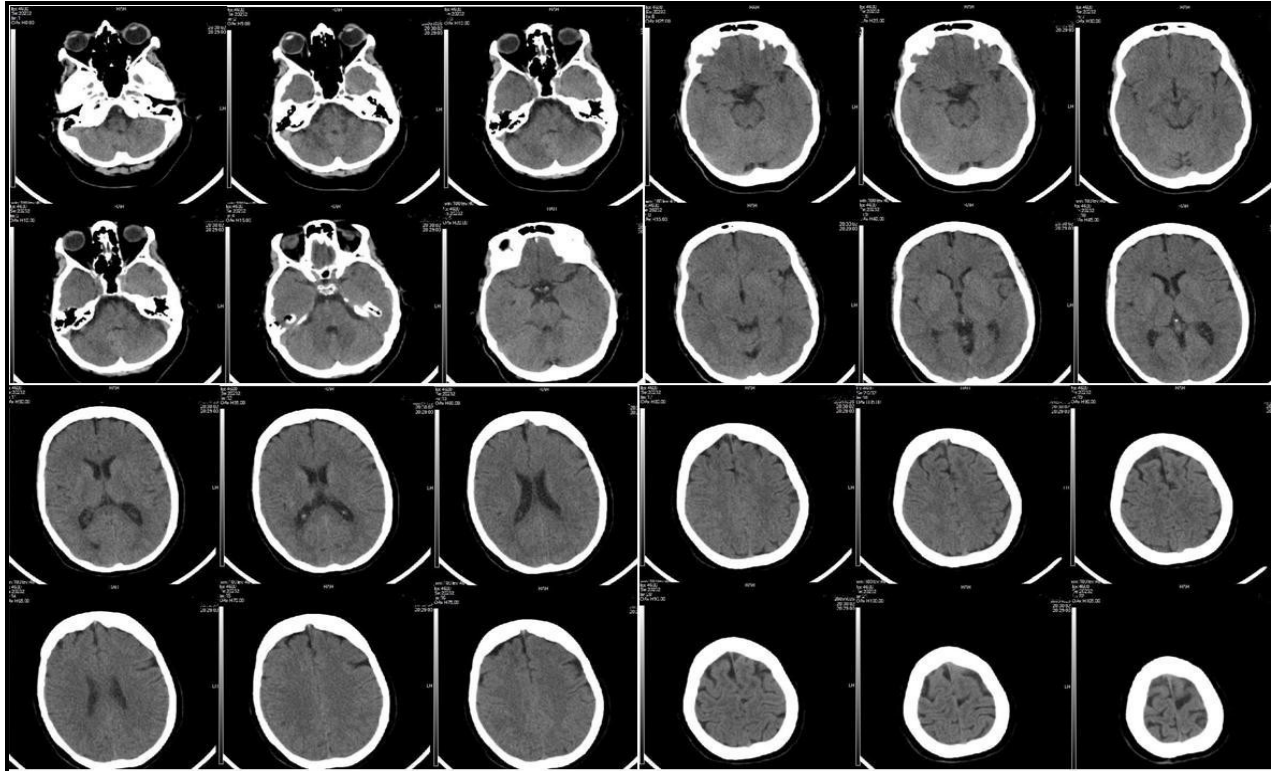


Figure 4d; consensus set.

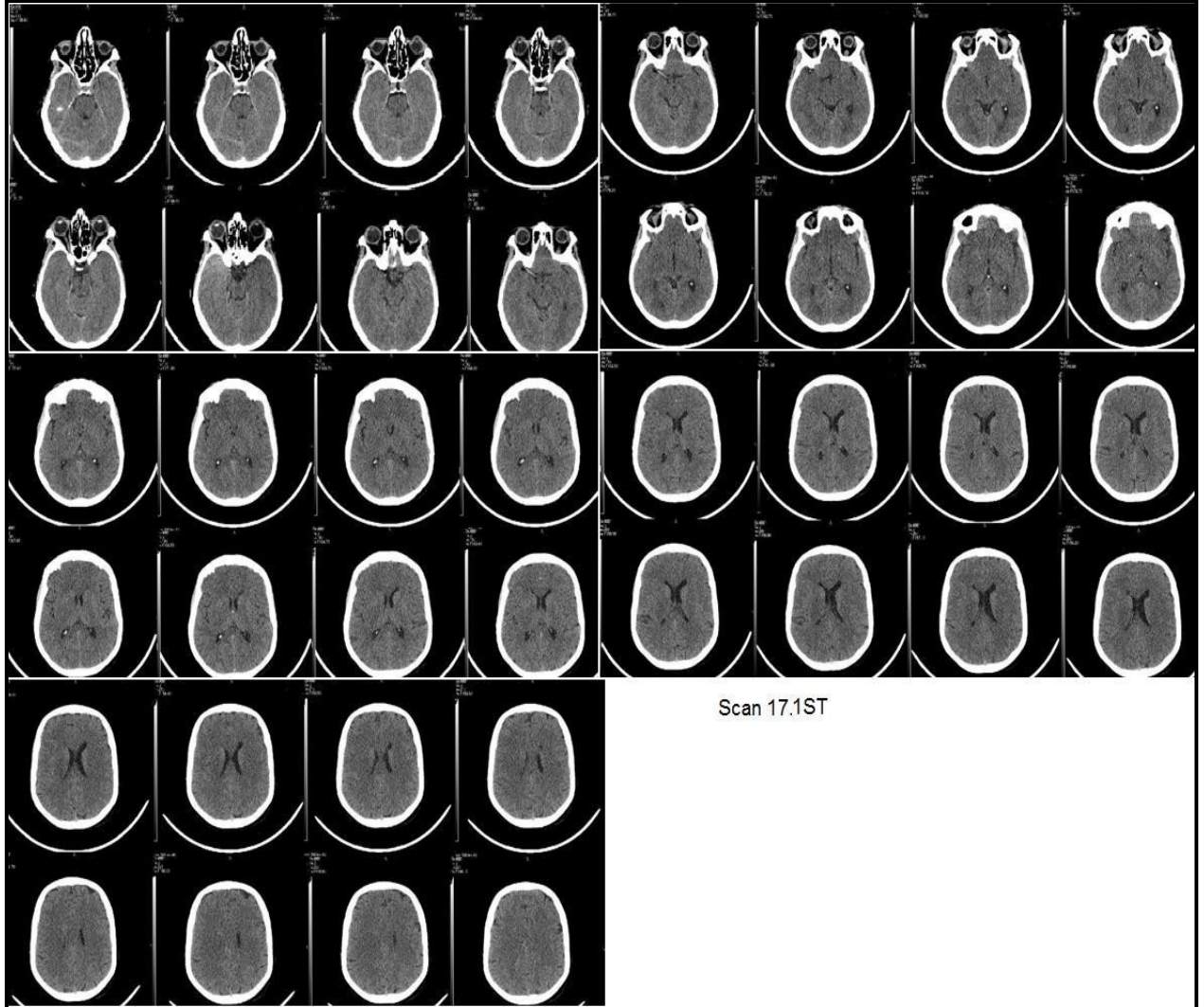
<p>Example-3</p> <p>Diagnosis;</p> <p>Hypodensity; M2-Insula.</p> <p>Isolated focal swelling; M1-M2.</p> 	<p>Example-4</p> <p>Right hemisphere stroke;</p> <ol style="list-style-type: none"> 1-Complete loss of grey-white matter interface with reduced attenuation in almost all M4, anterior part of M5 and most of M6. 2- Partial loss of grey-white matter interface in posterior part of M5 and the most antero-lateral part of M6. 3- Cortical sulcal effacement in M4, M5 and M6. 	<p>Example-4</p> <p>Diagnosis;</p> <p>Hypodensity; M4-M6-M5.</p> <p>Isolated focal swelling; M5-M6.</p> 
<p>Example-5</p> <p>Left hemisphere stroke;</p> <ol style="list-style-type: none"> 1-Complete loss of grey-white matter differentiation and reduced attenuation in almost all of M1 and anterior part of M3. 2- Partial loss of grey-white matter interface in M2 and the most posterior part of M3. 3- Cortical sulcal effacement in M1, M2 and M3. 	<p>Example-5</p> <p>Diagnosis;</p> <p>Hypodensity; M1-M3.</p> <p>Isolated focal swelling; M2-M3.</p> 	<p>Example-6</p> <p>Right hemisphere stroke;</p> <ol style="list-style-type: none"> 1- Cortical sulcal effacement in M4, M5 and M6. 2-Partial loss of grey-white matter interface in M5, middle parts of M4 and parts of M6. 
<p>Example-6</p> <p>Diagnosis;</p> <p>Isolated focal swelling; M4-M5-M6.</p> 	<p>Figure 4e; Consensus set.</p>	

Figure(s) 5: First set scans.

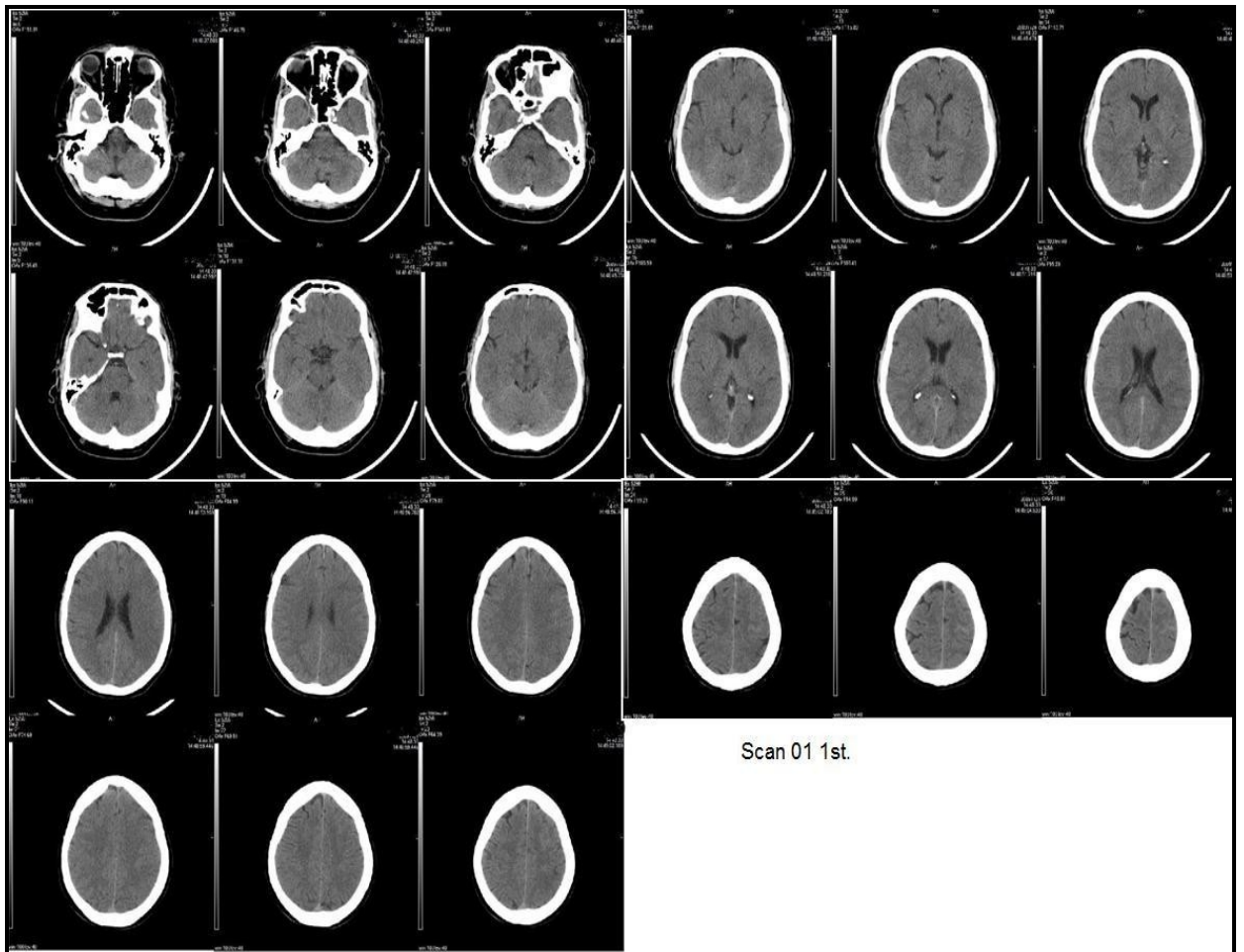
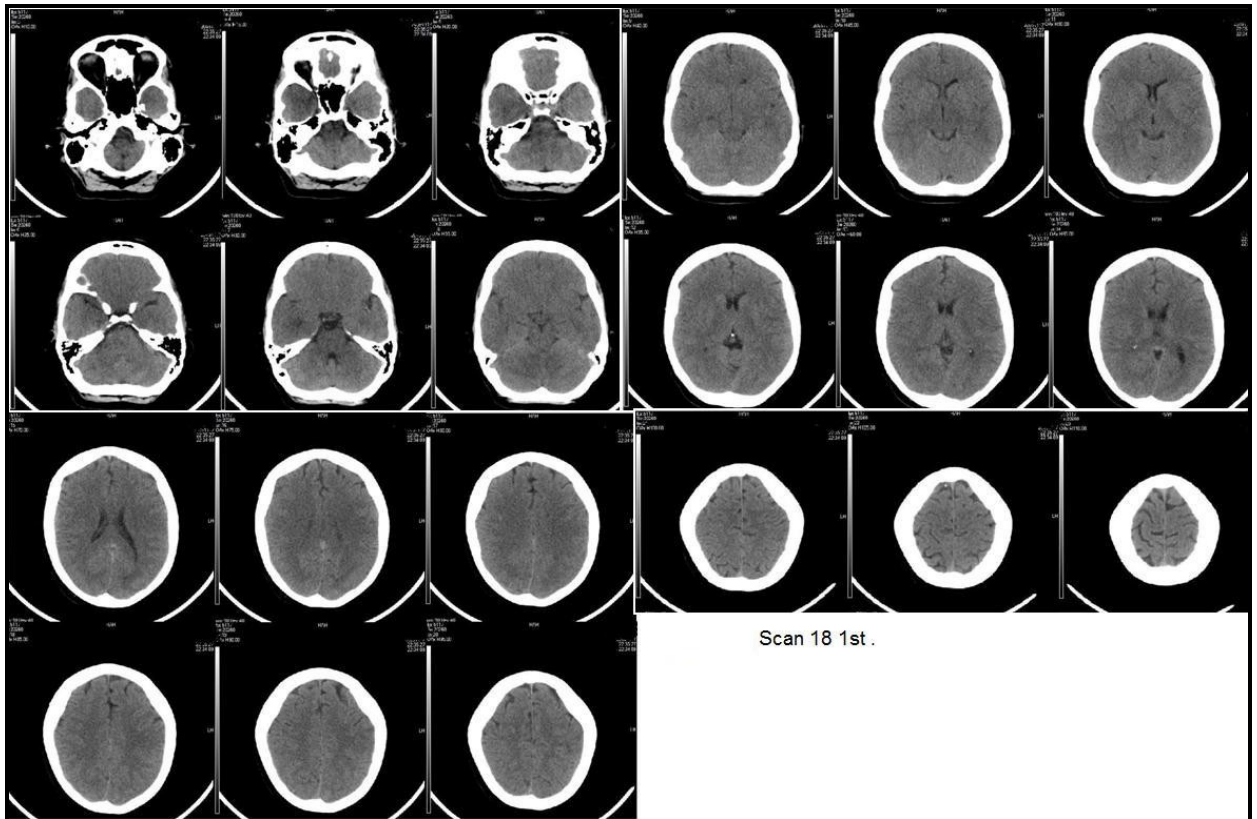


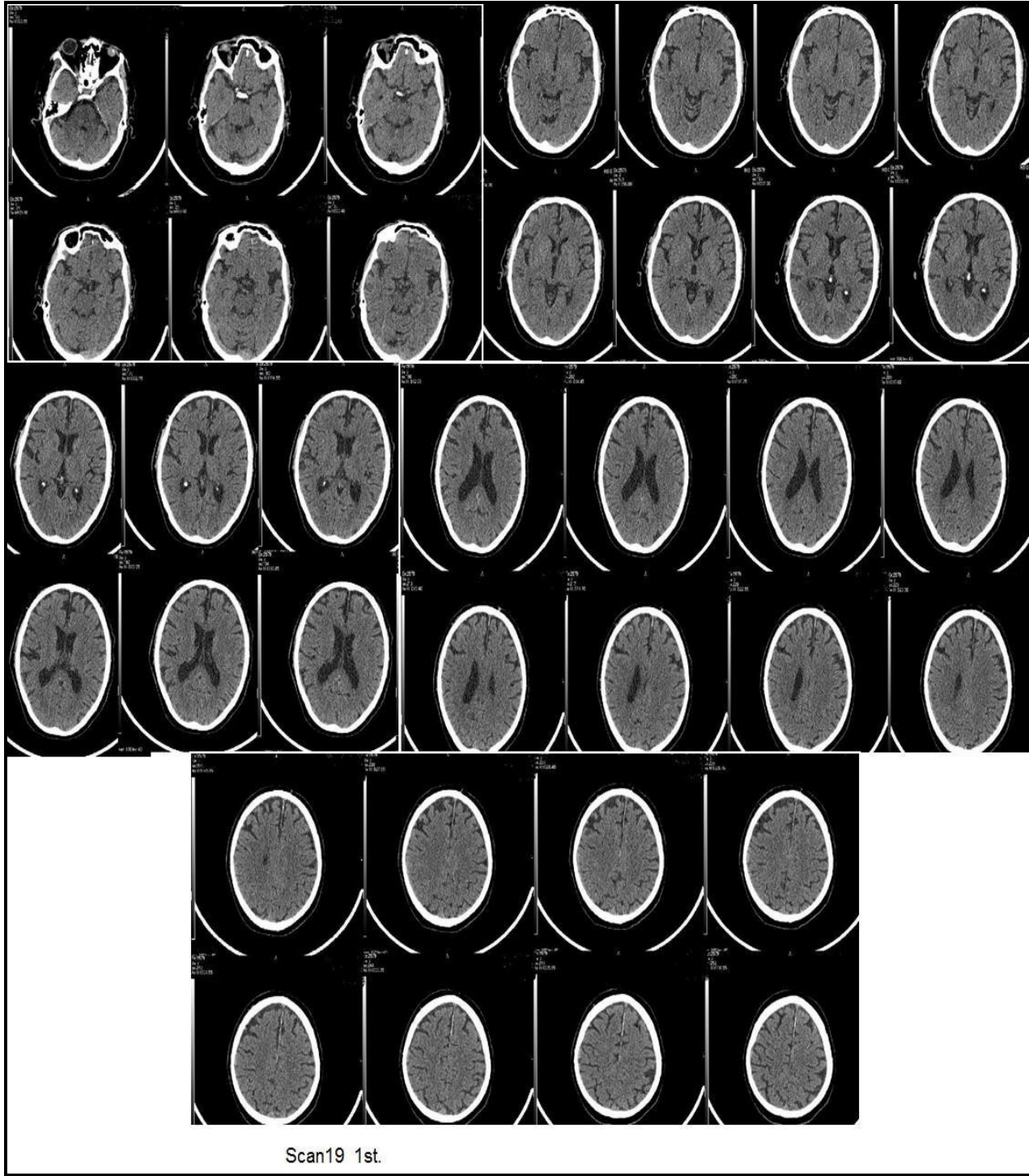


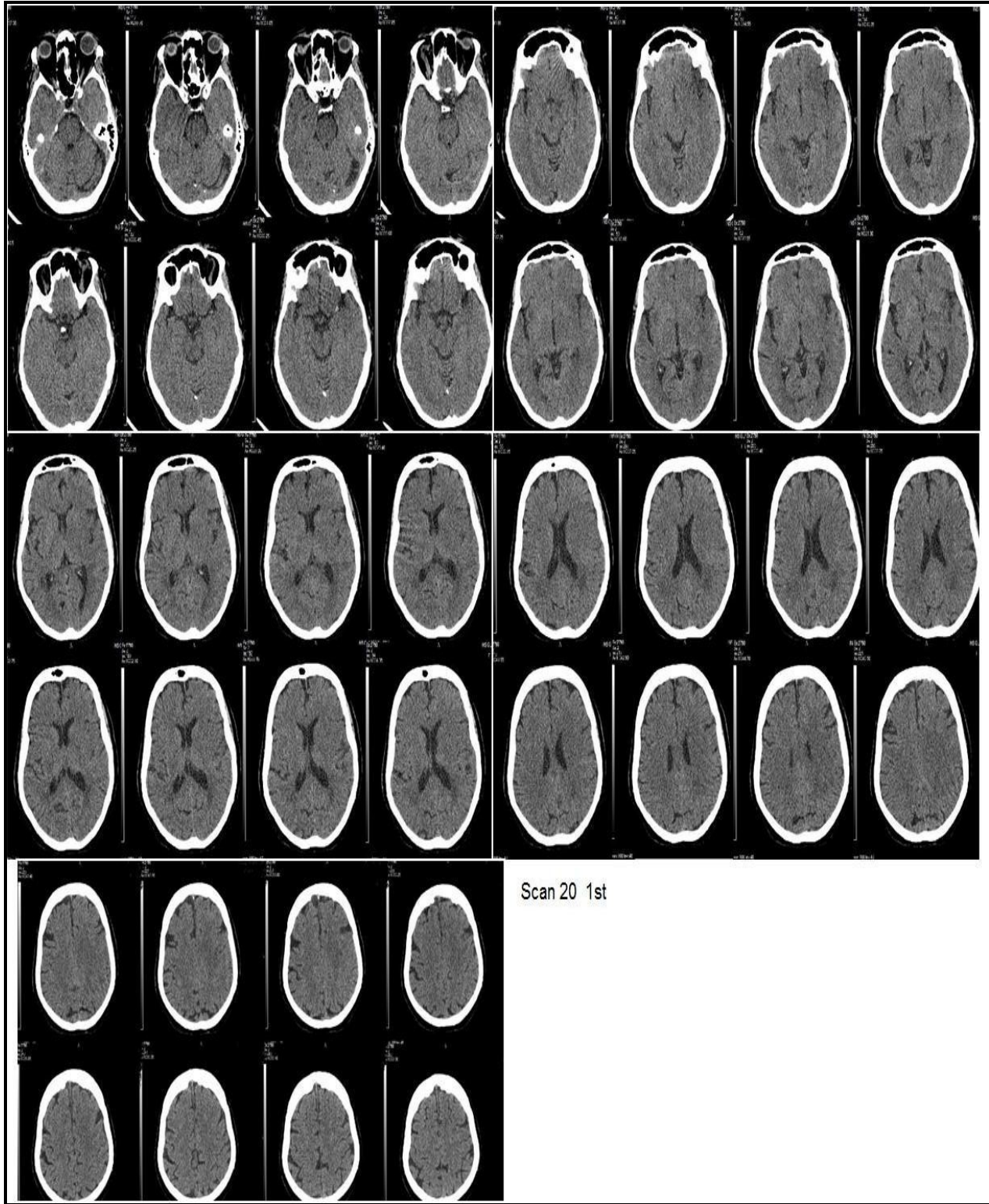
Scan-04

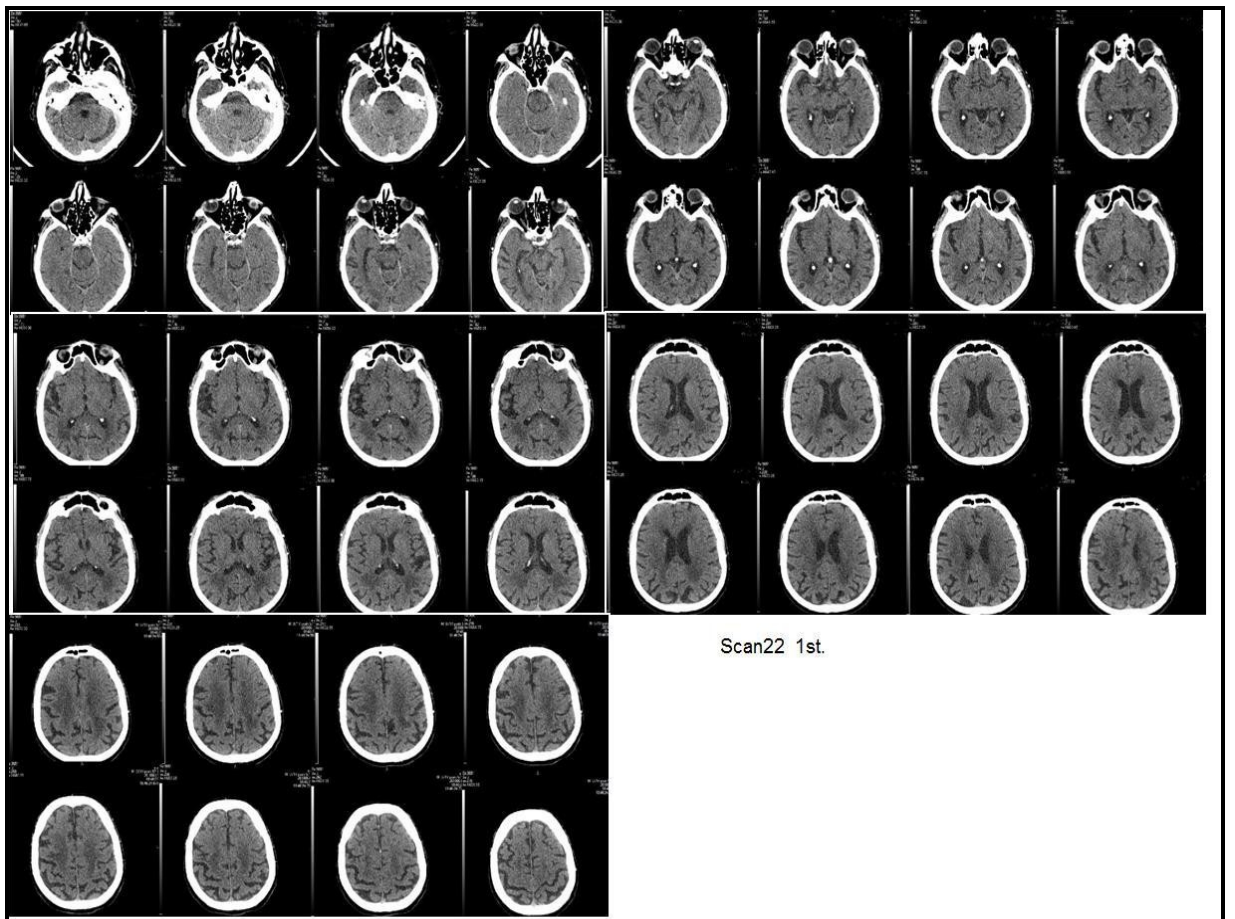
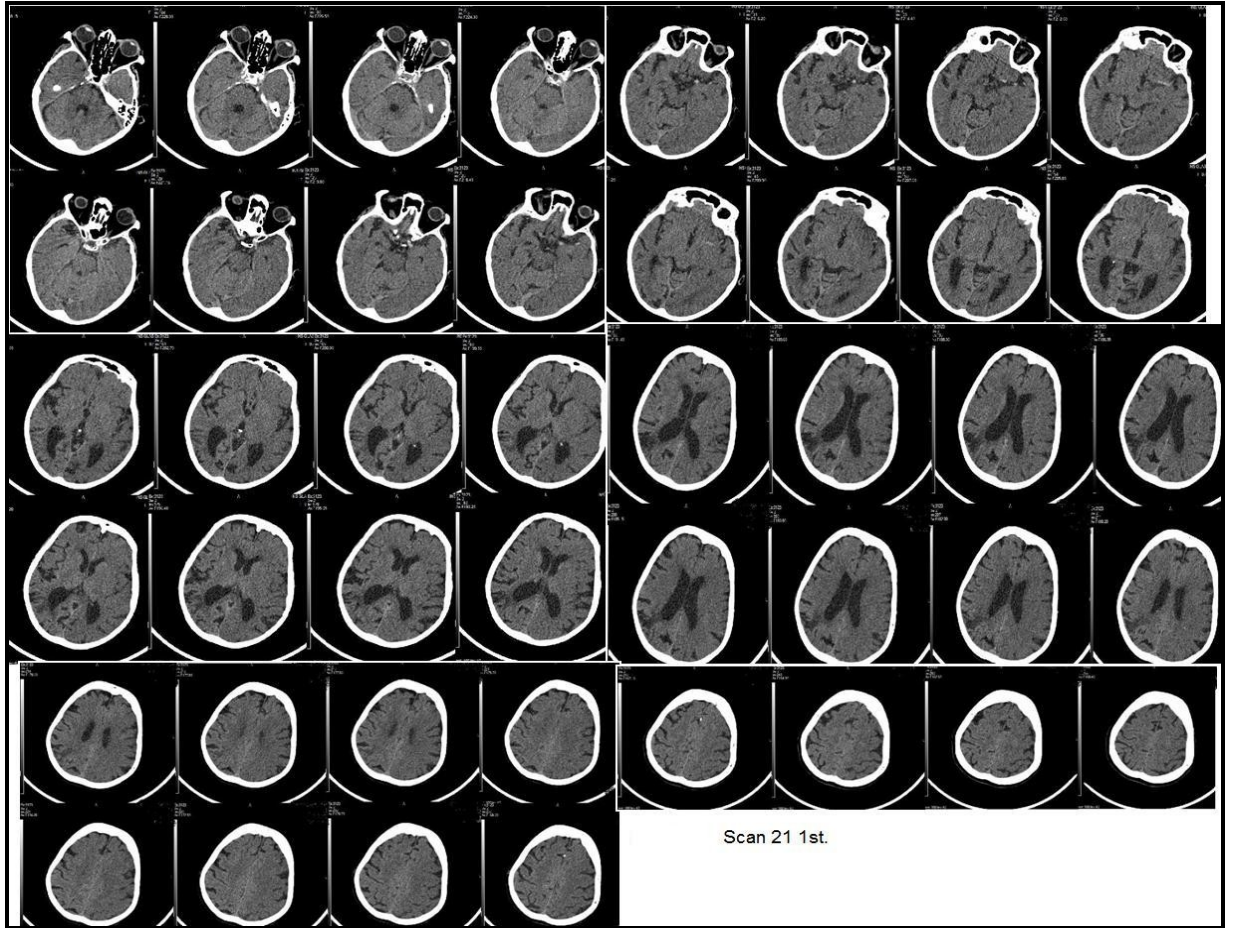


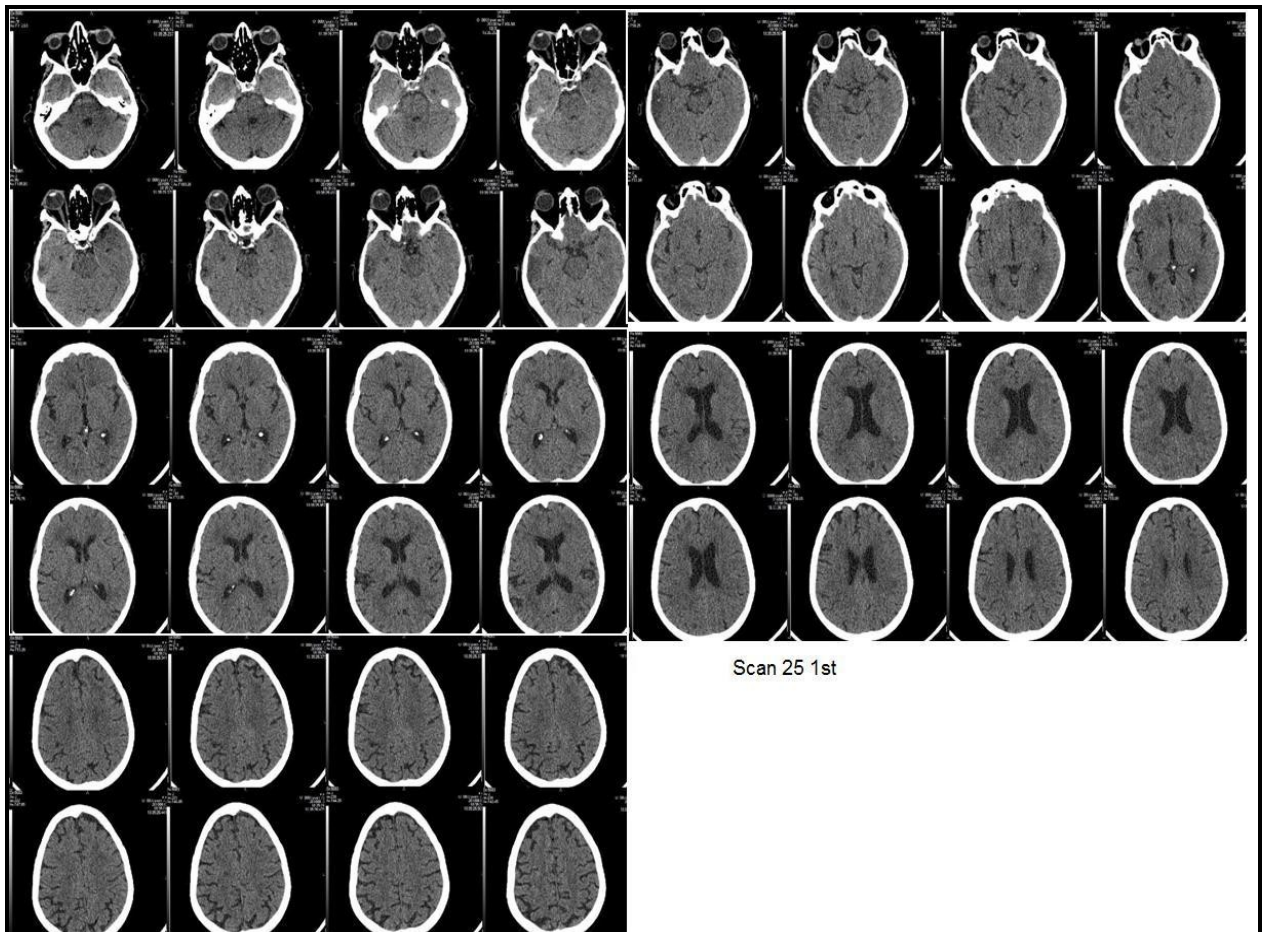
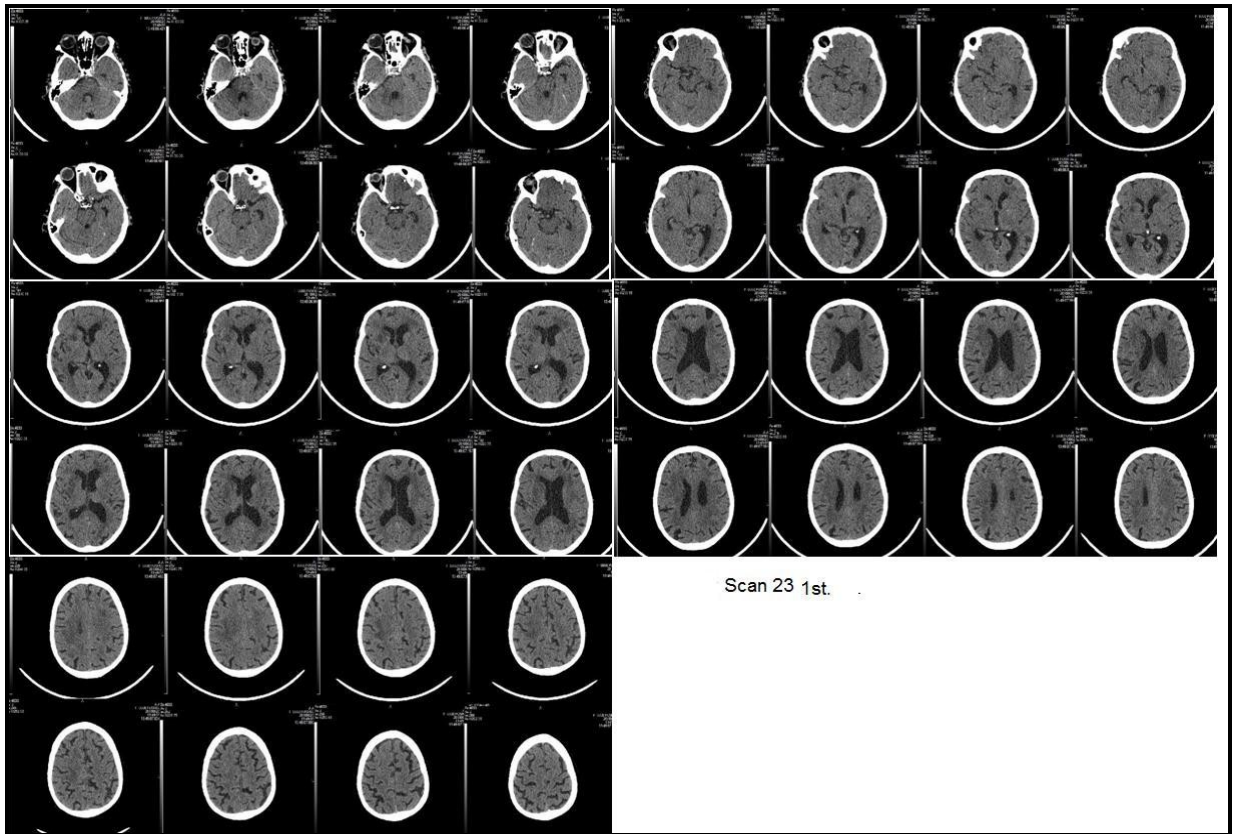
Scan 17.1ST

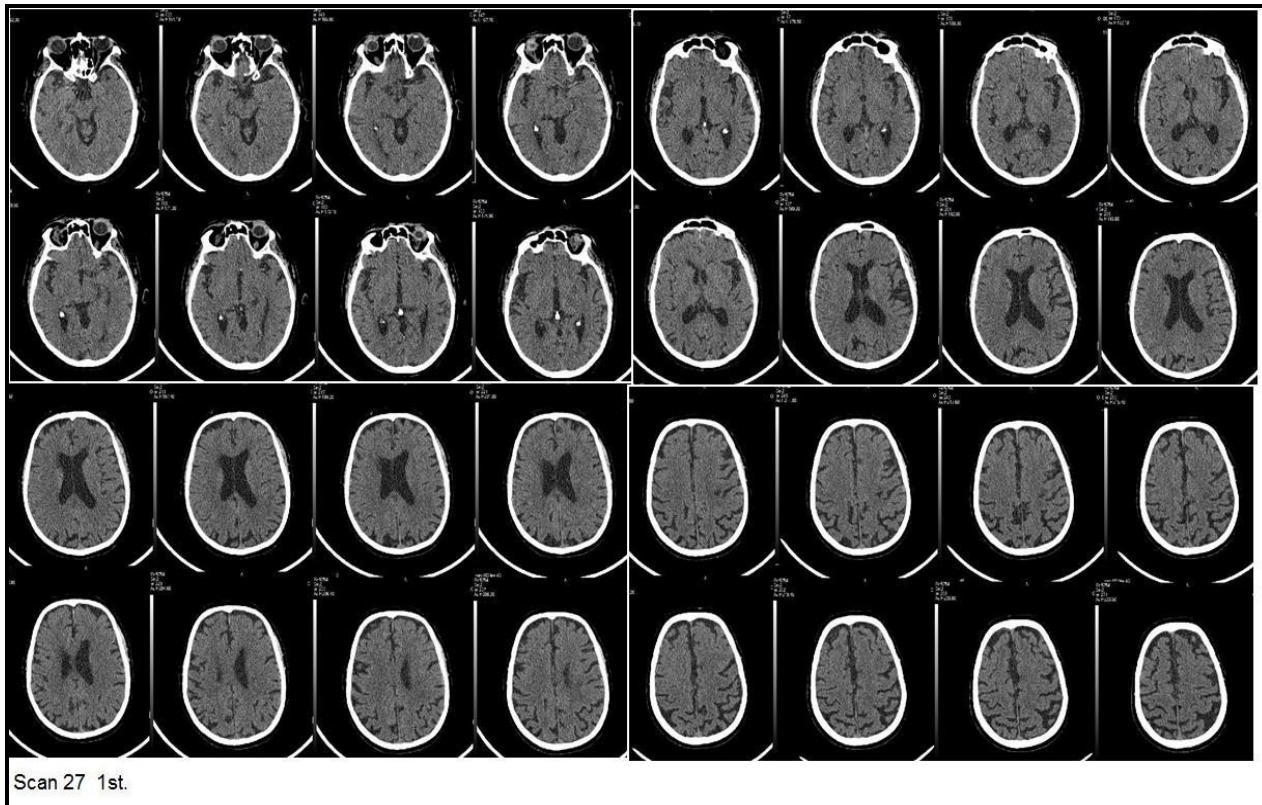
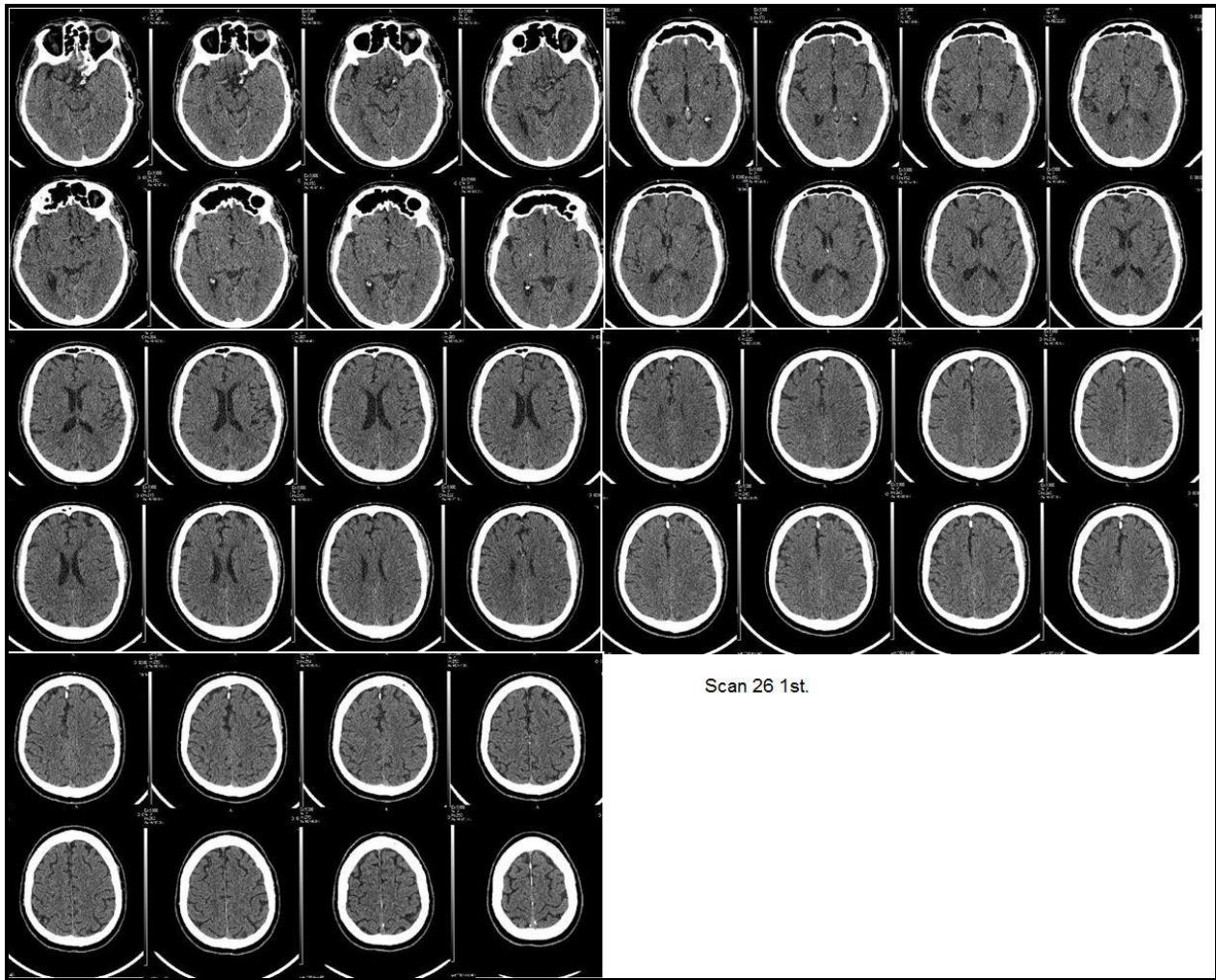


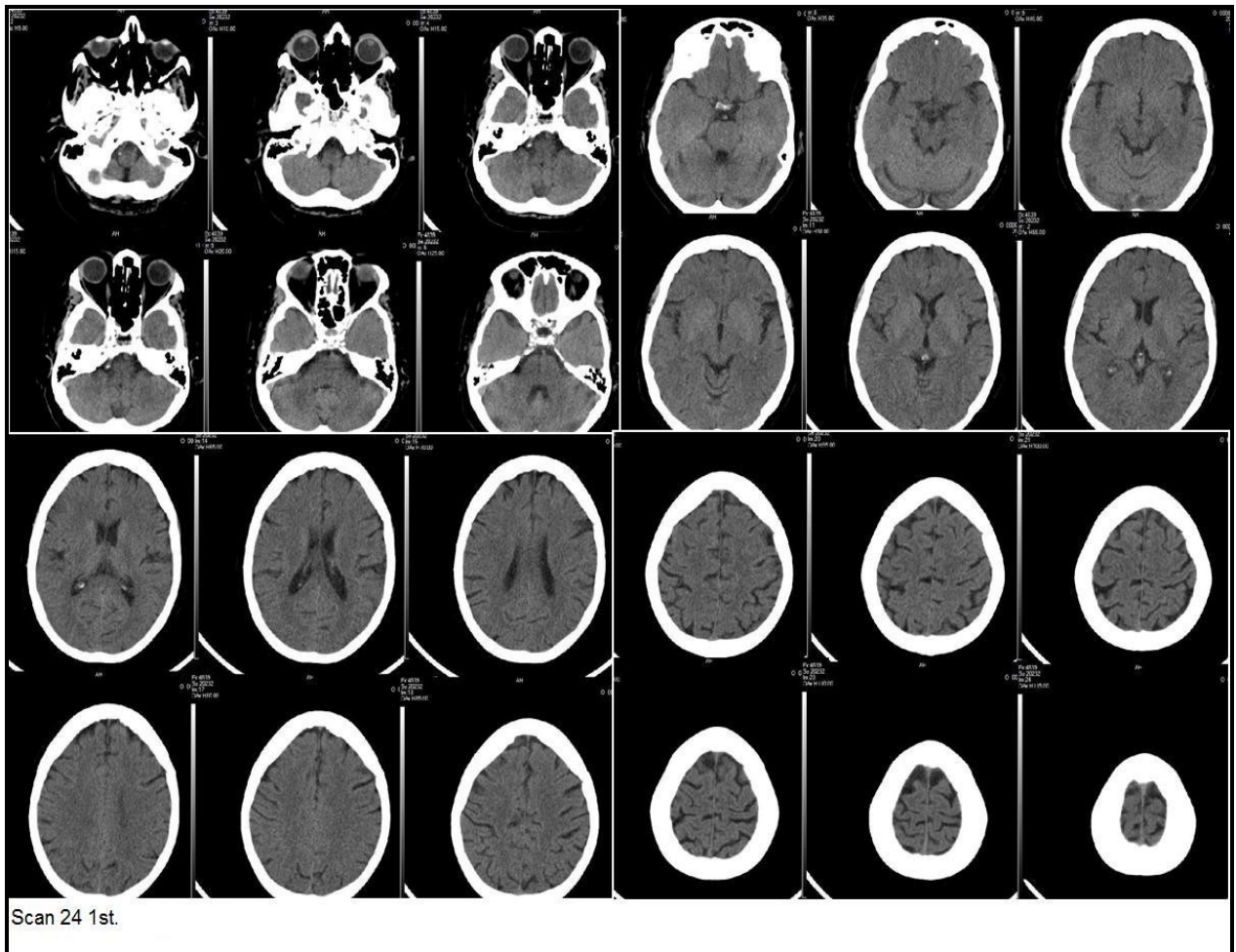
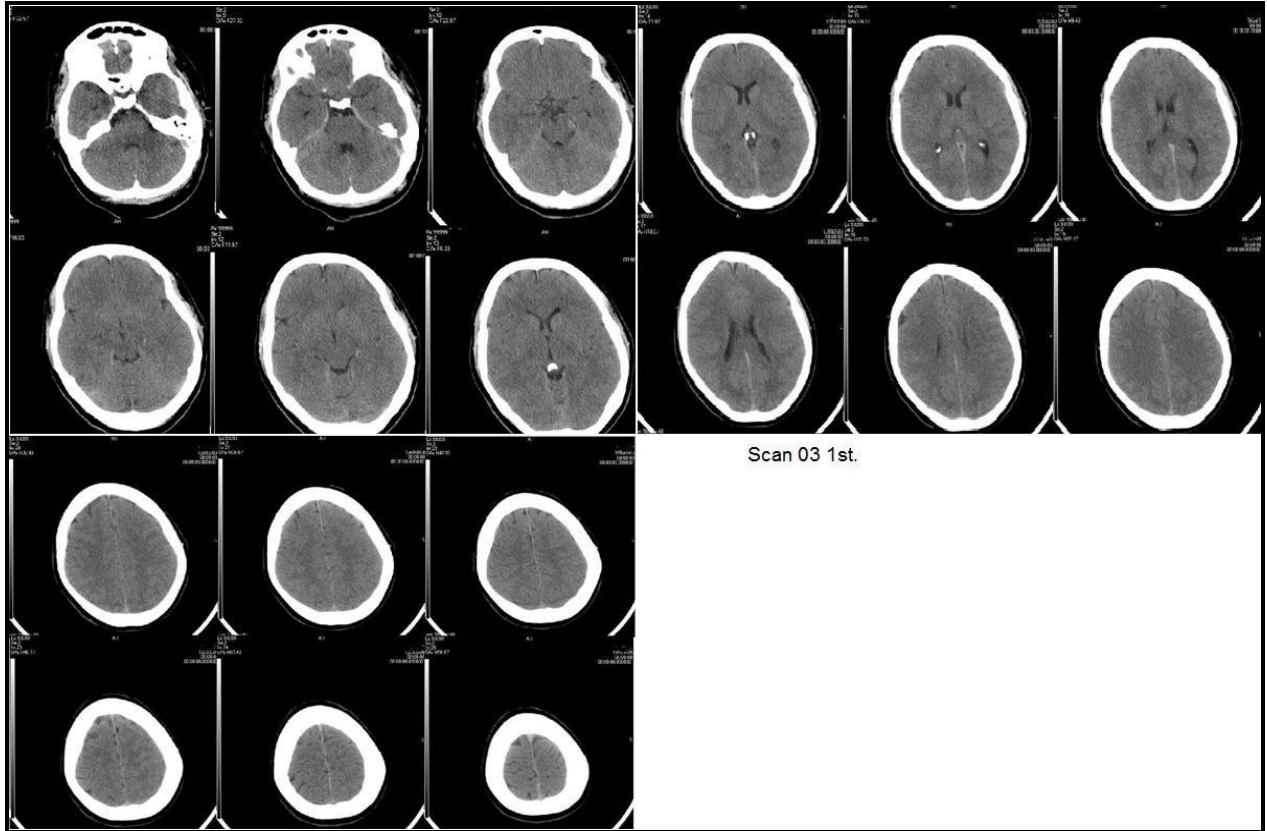


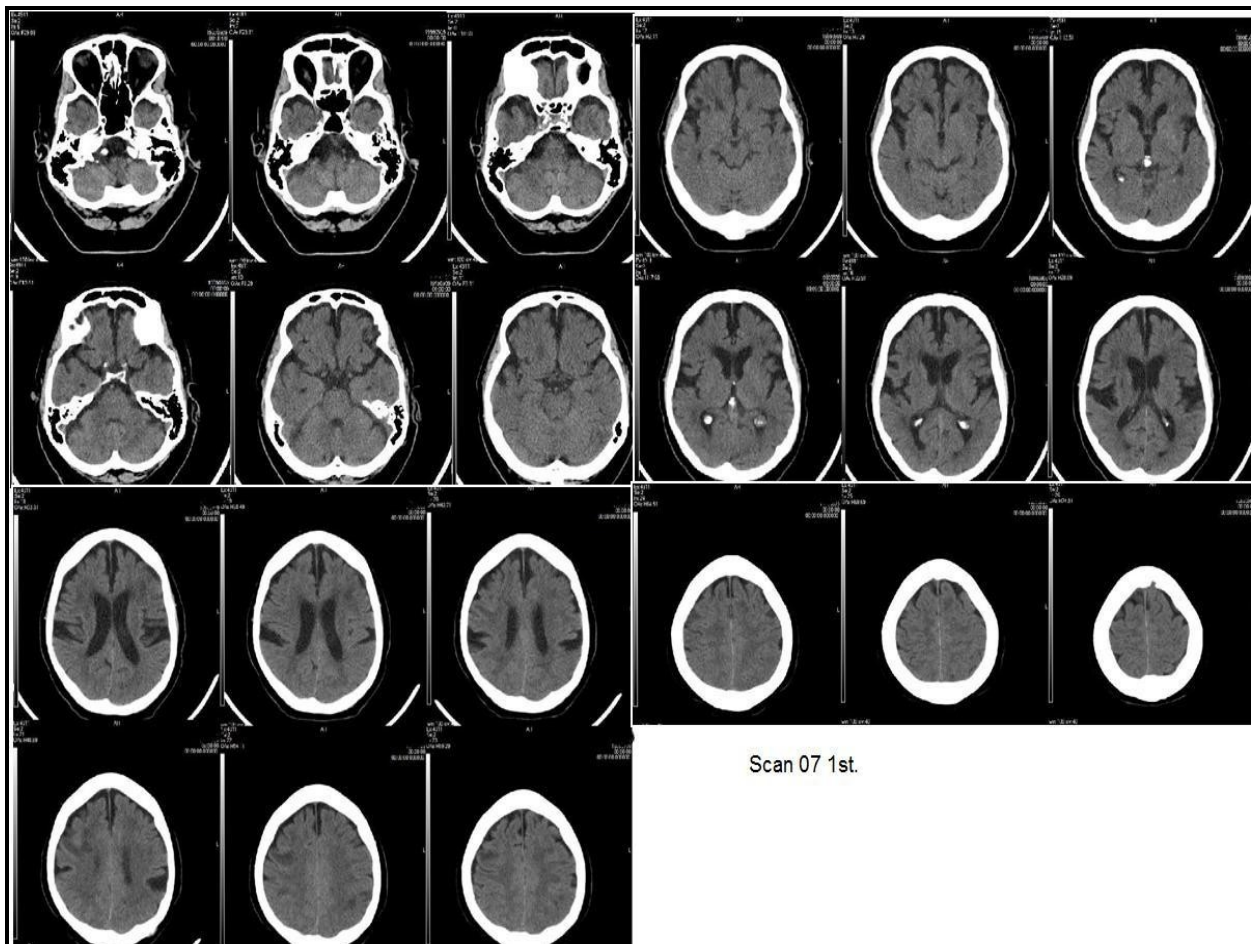
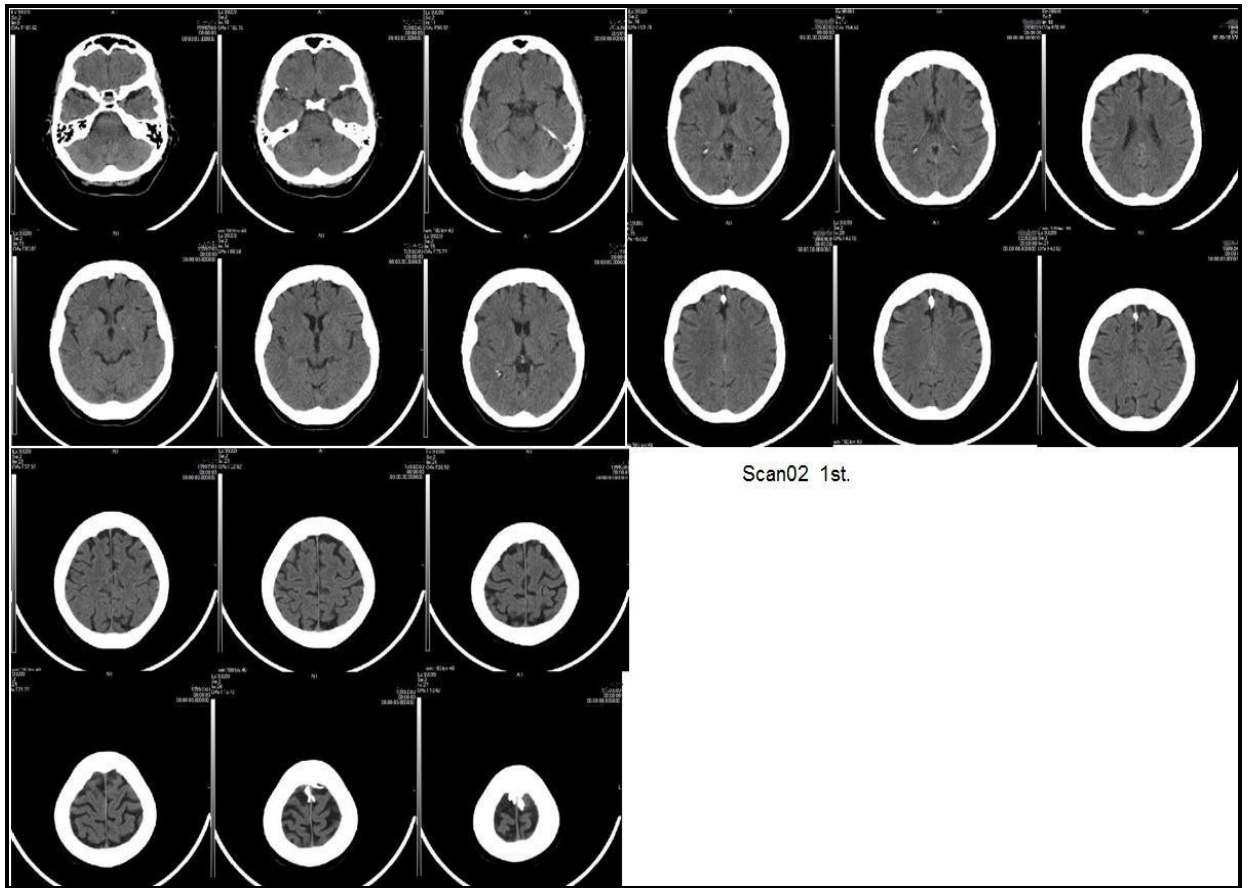


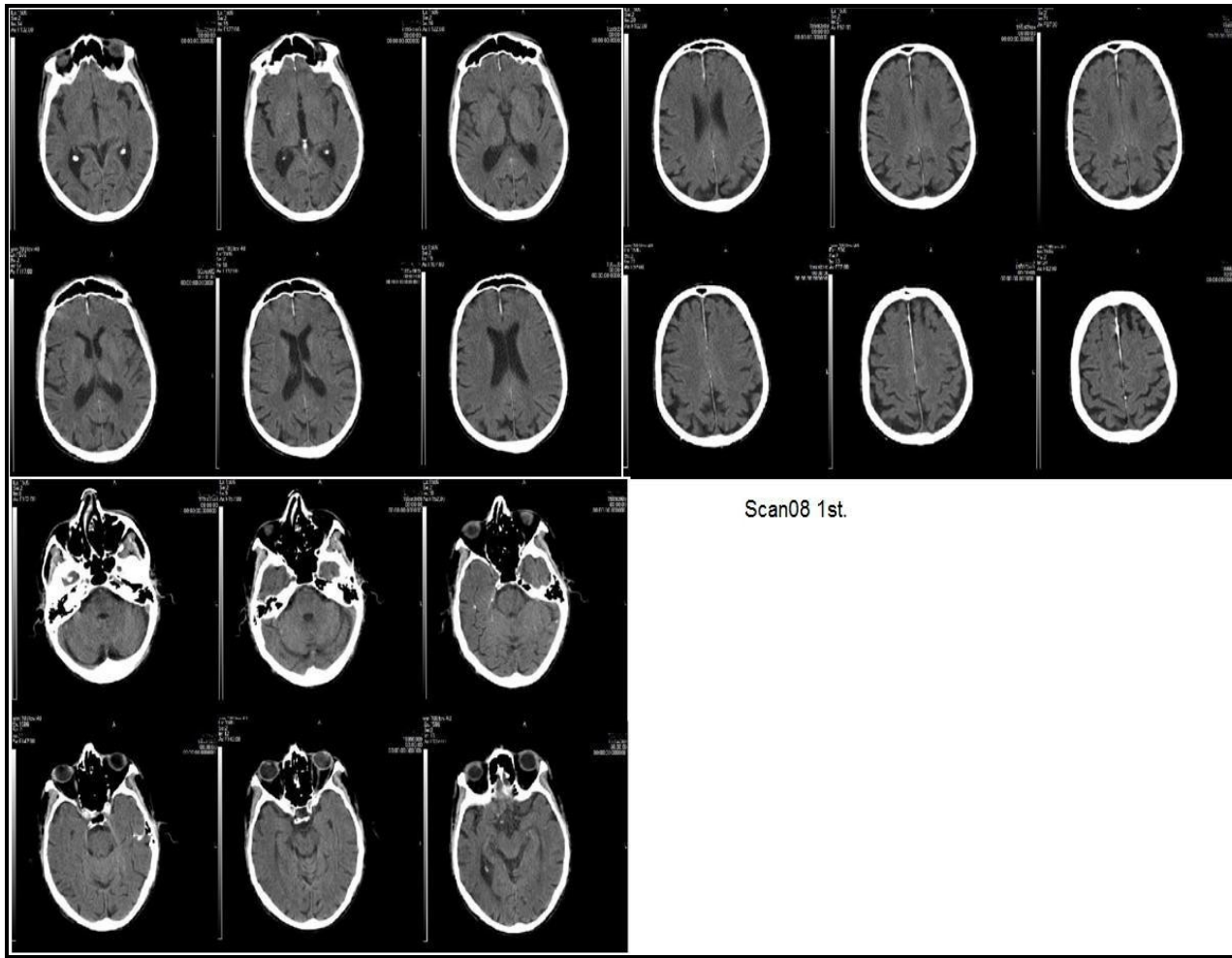




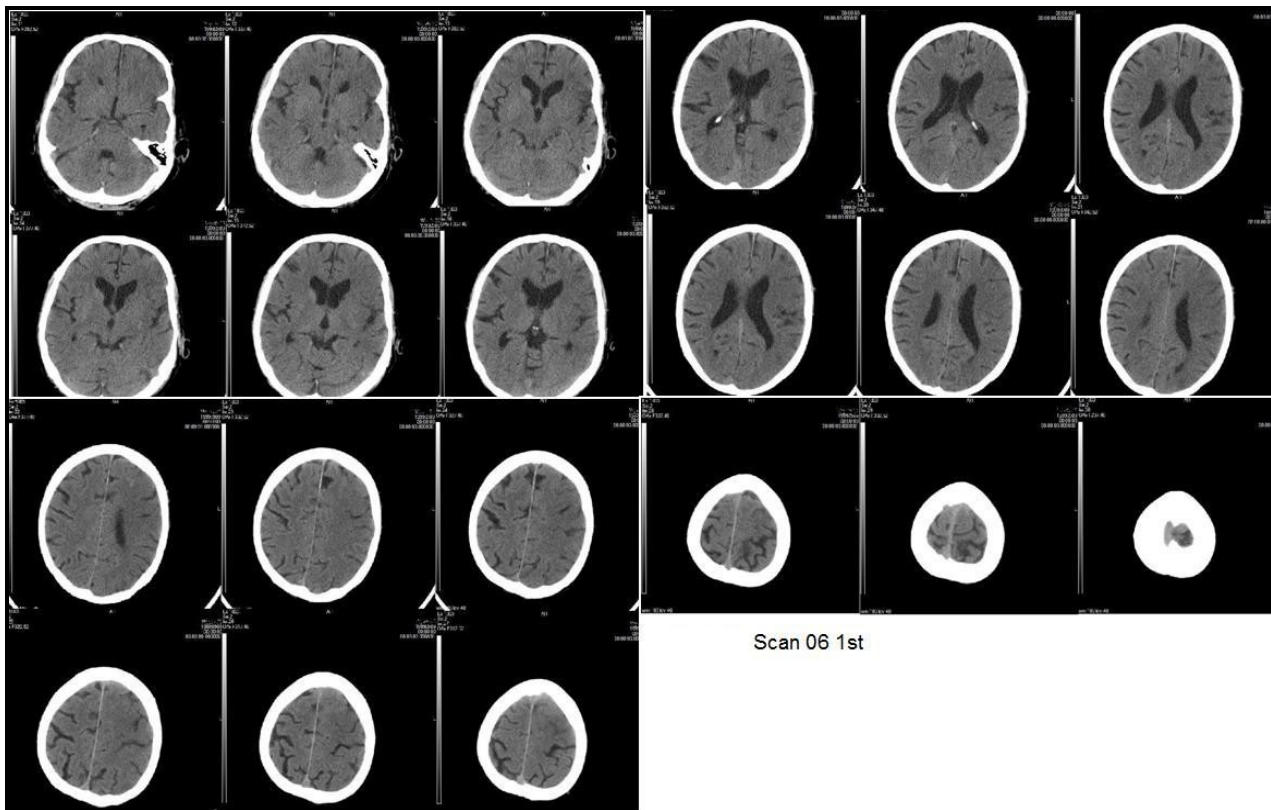






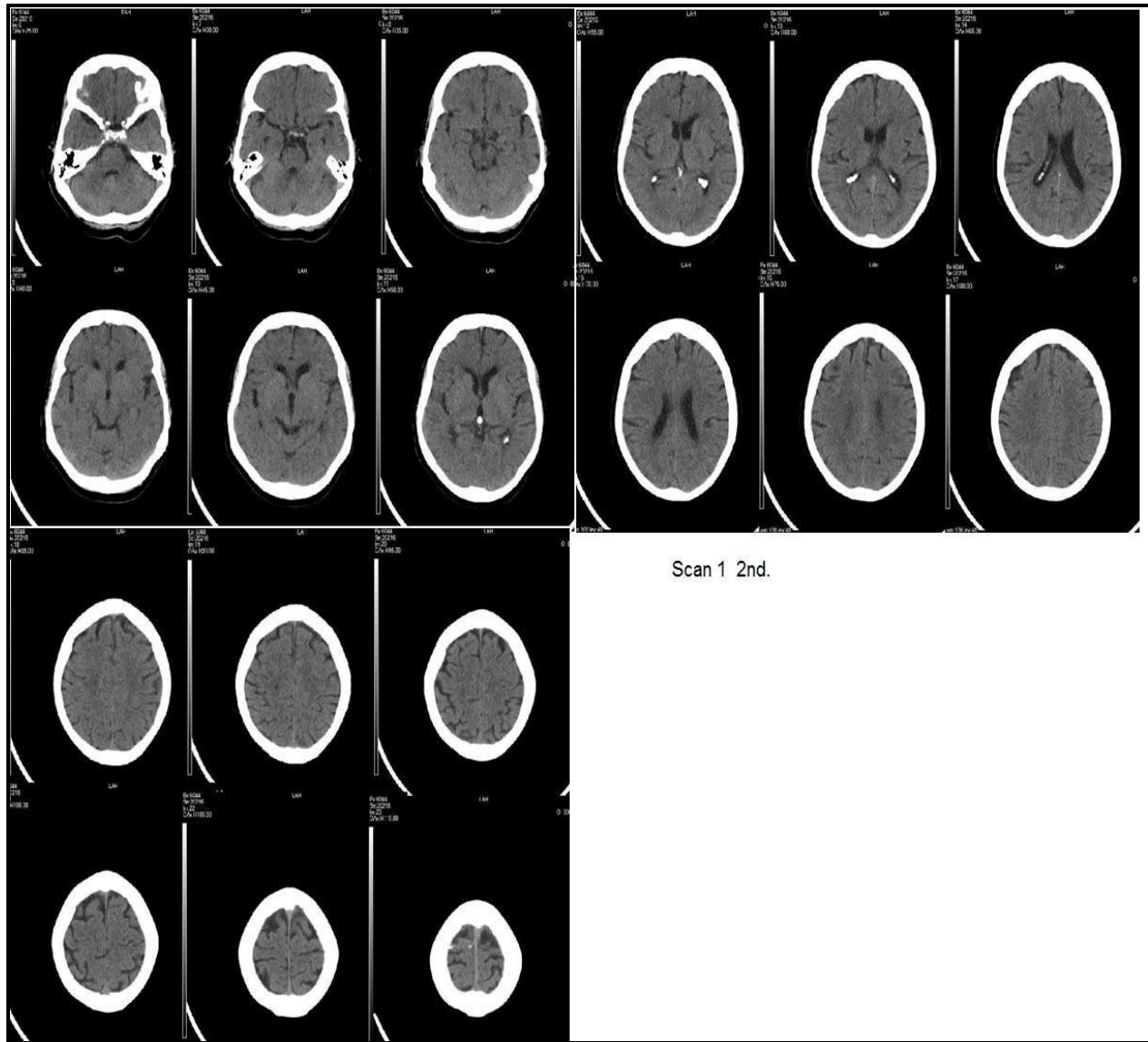


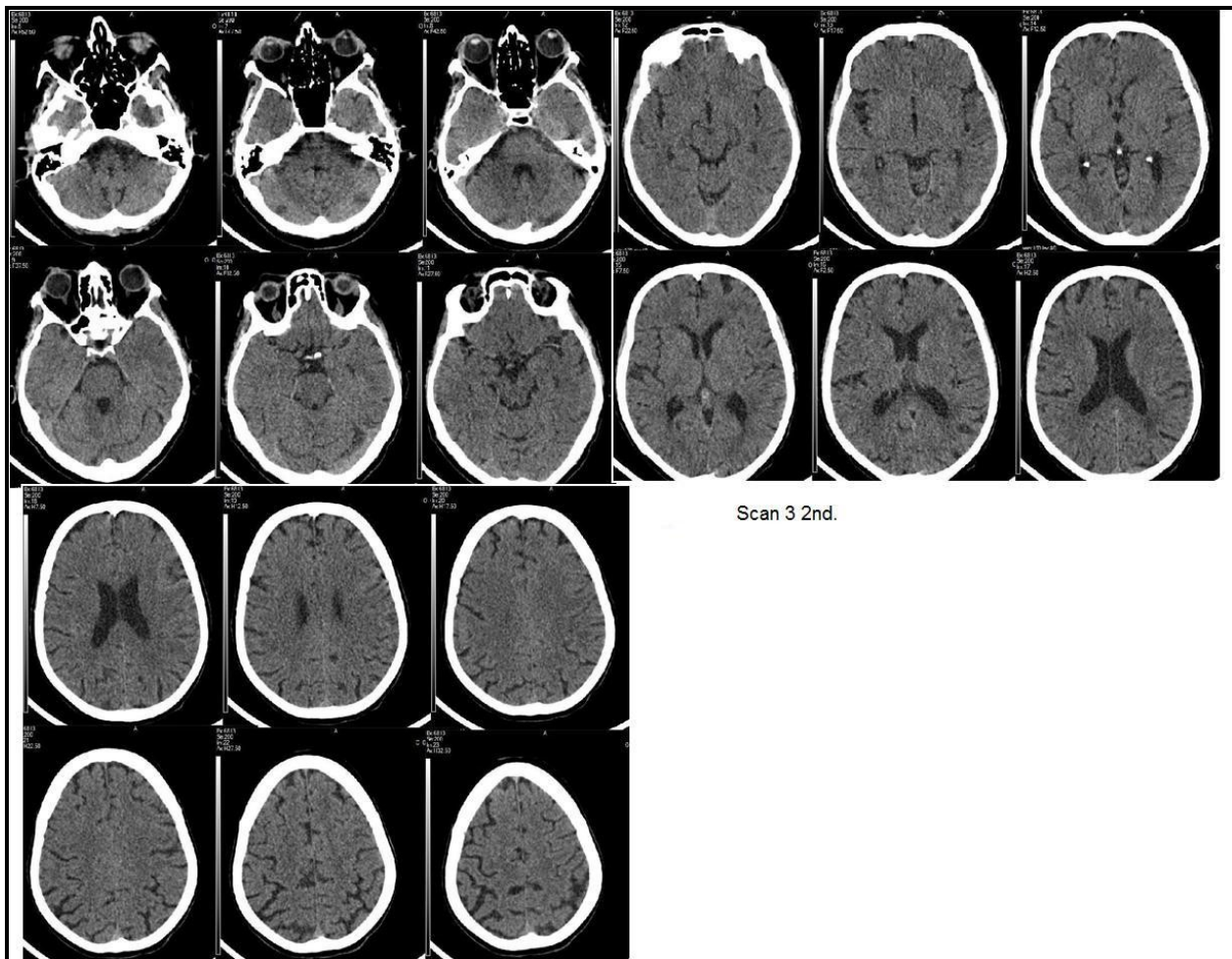
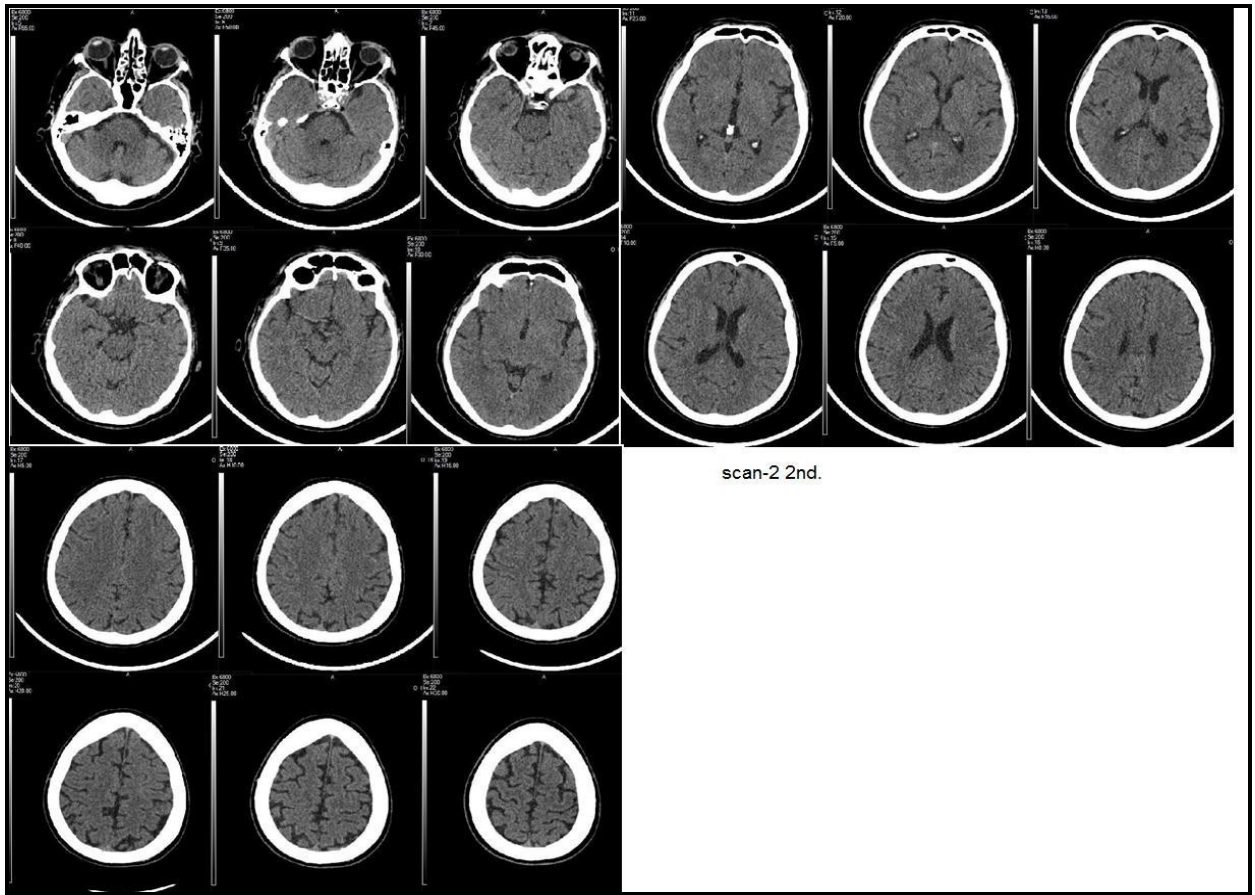
Scan08 1st.

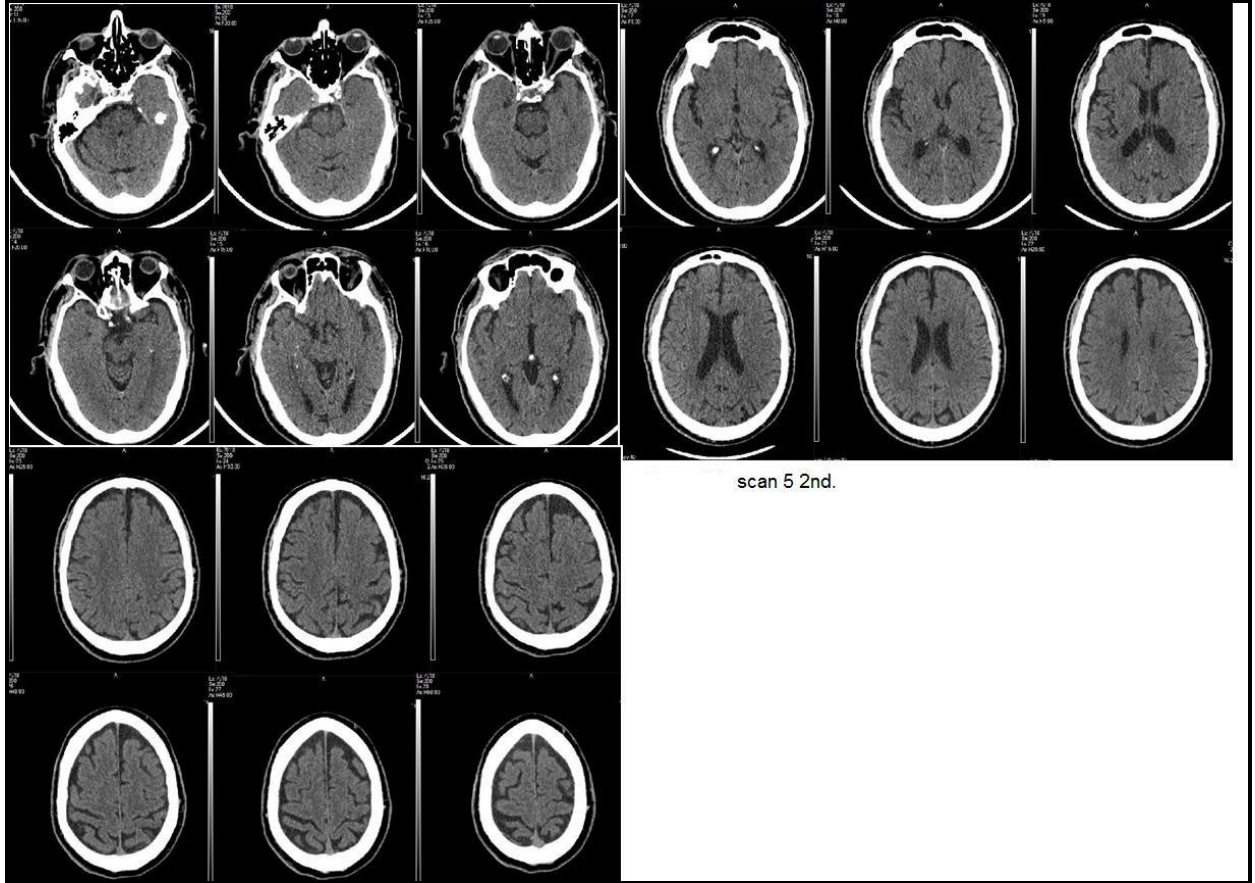
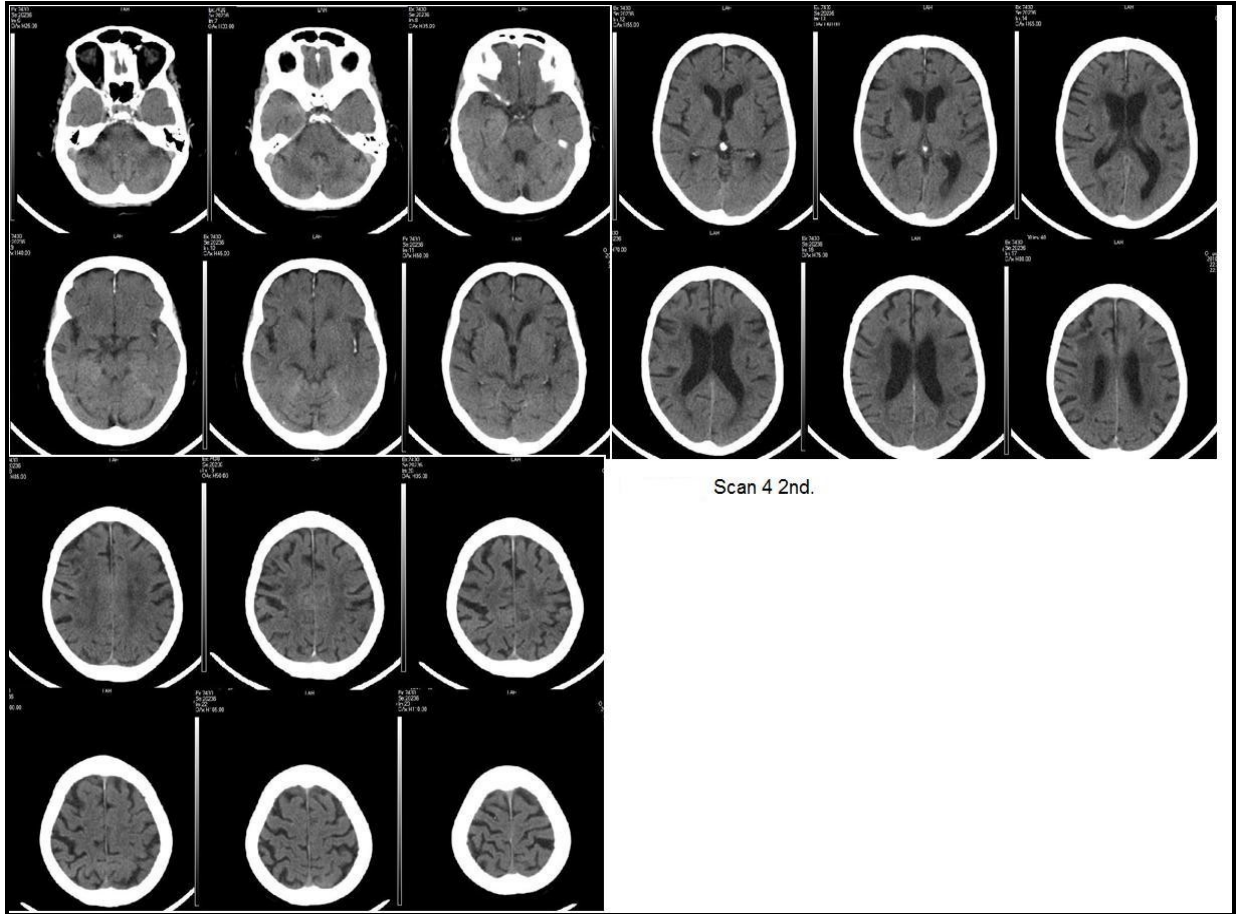


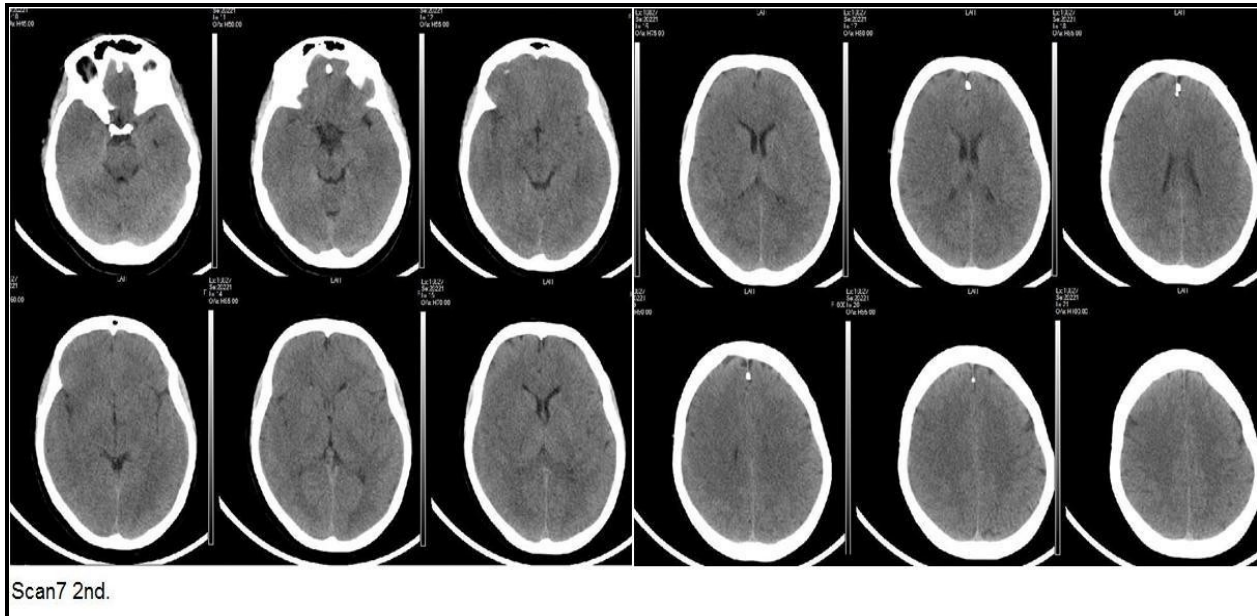
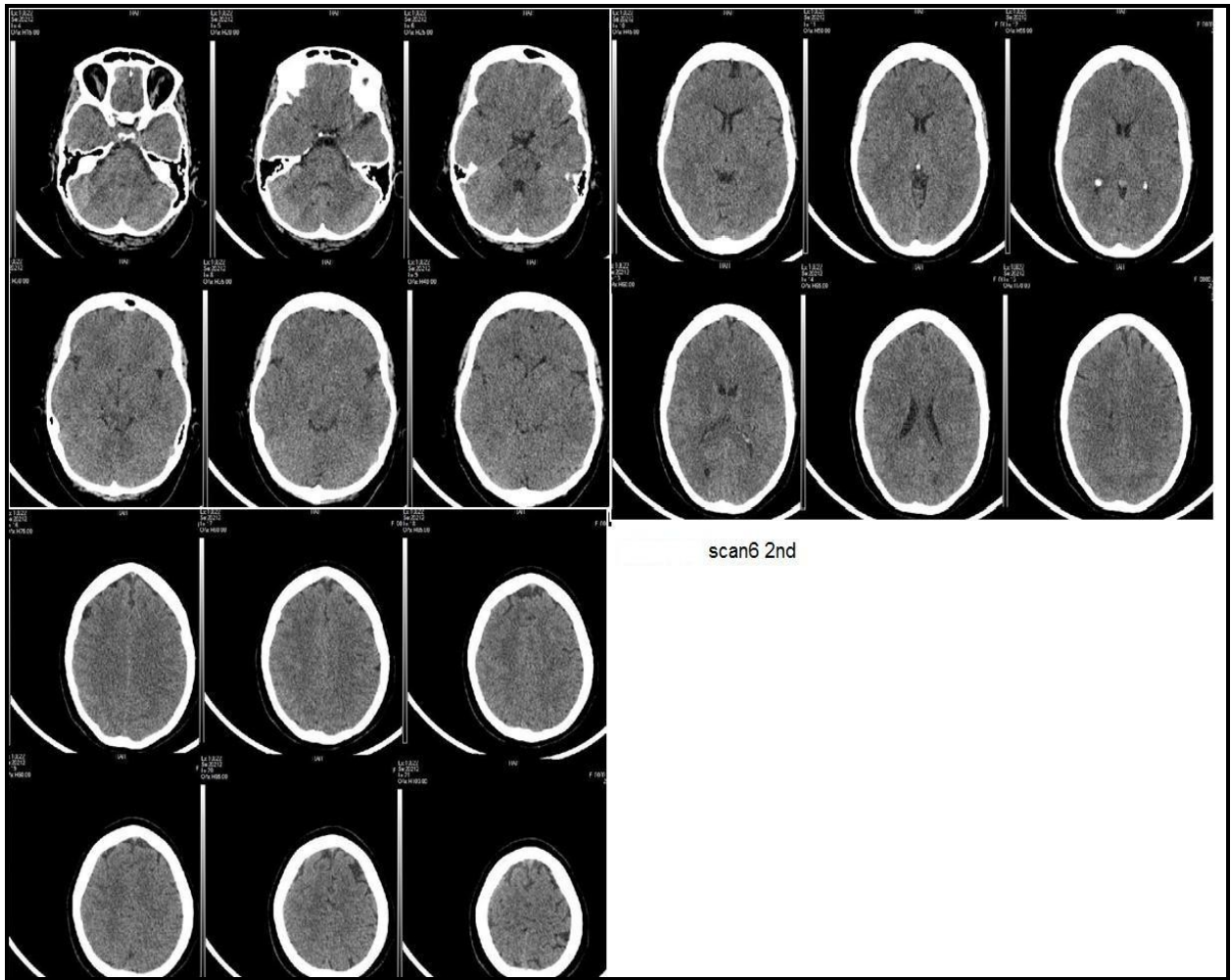
Scan 06 1st

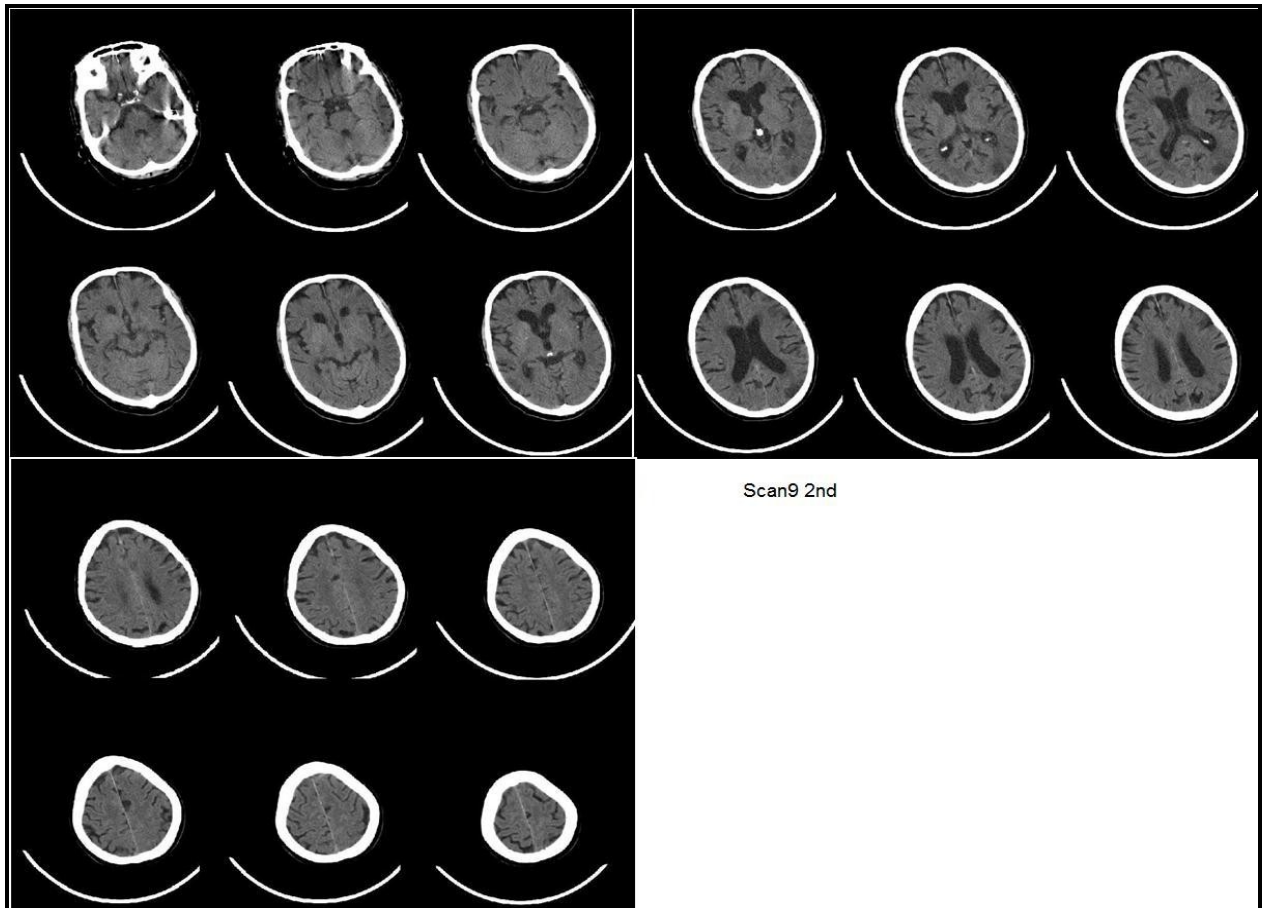
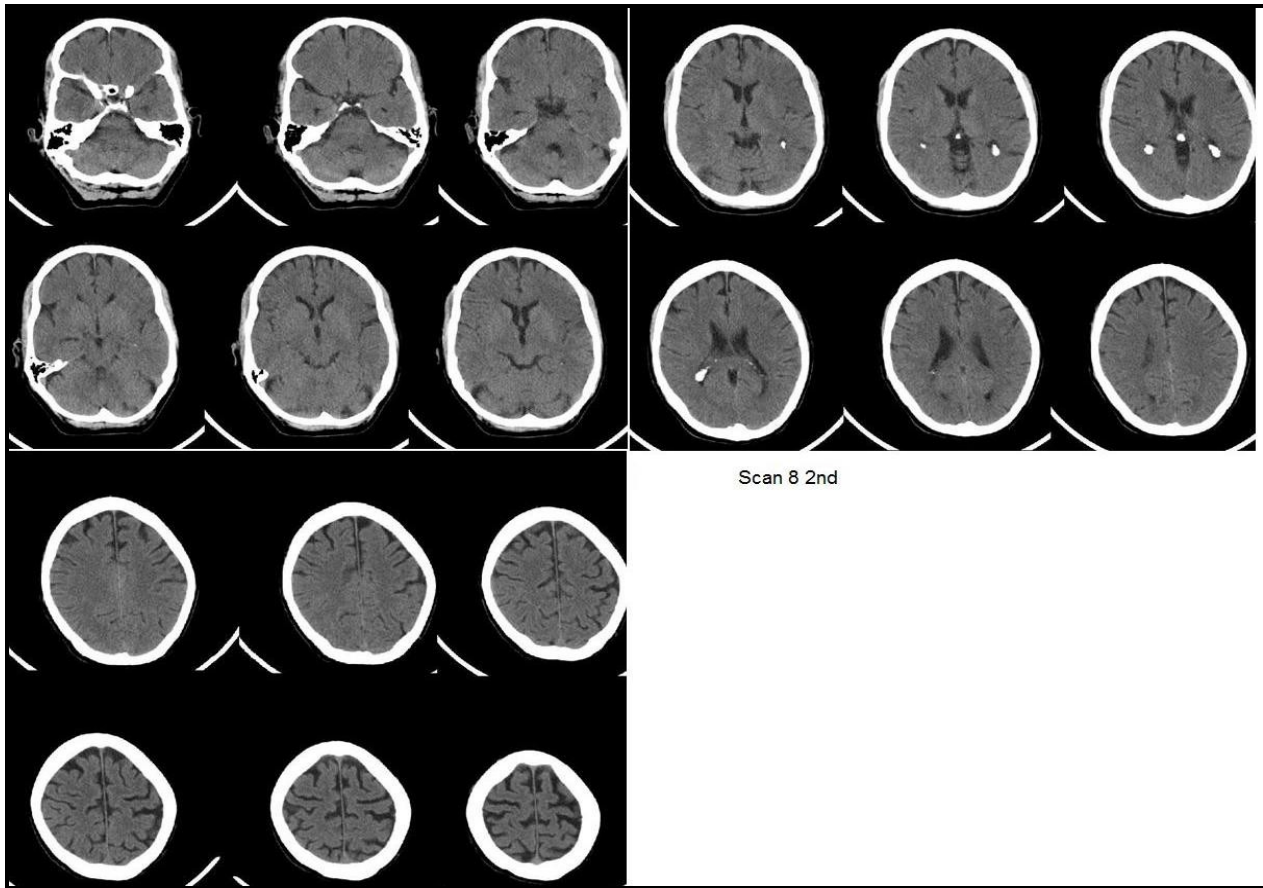
Figure (s) 6; Second Set Scans.

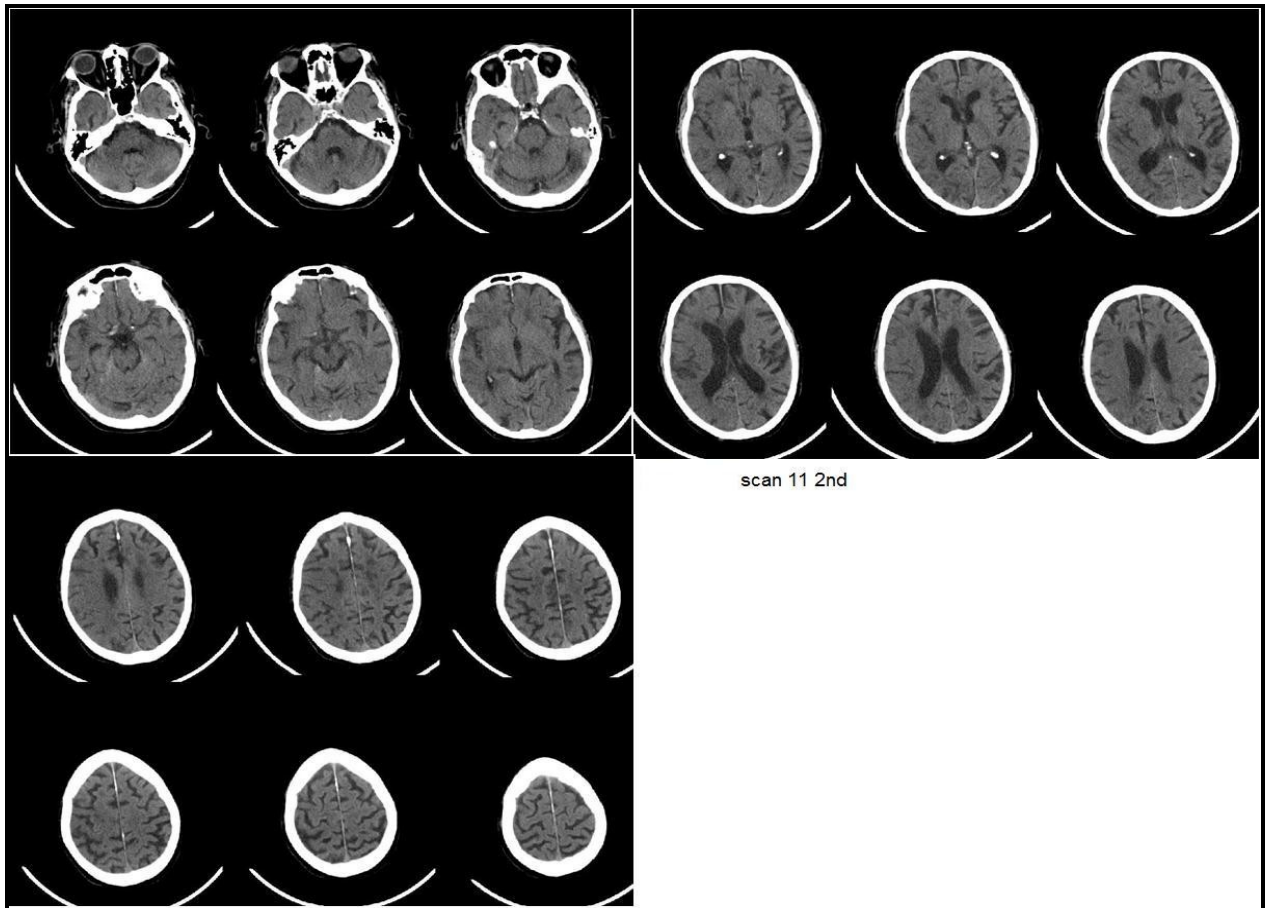
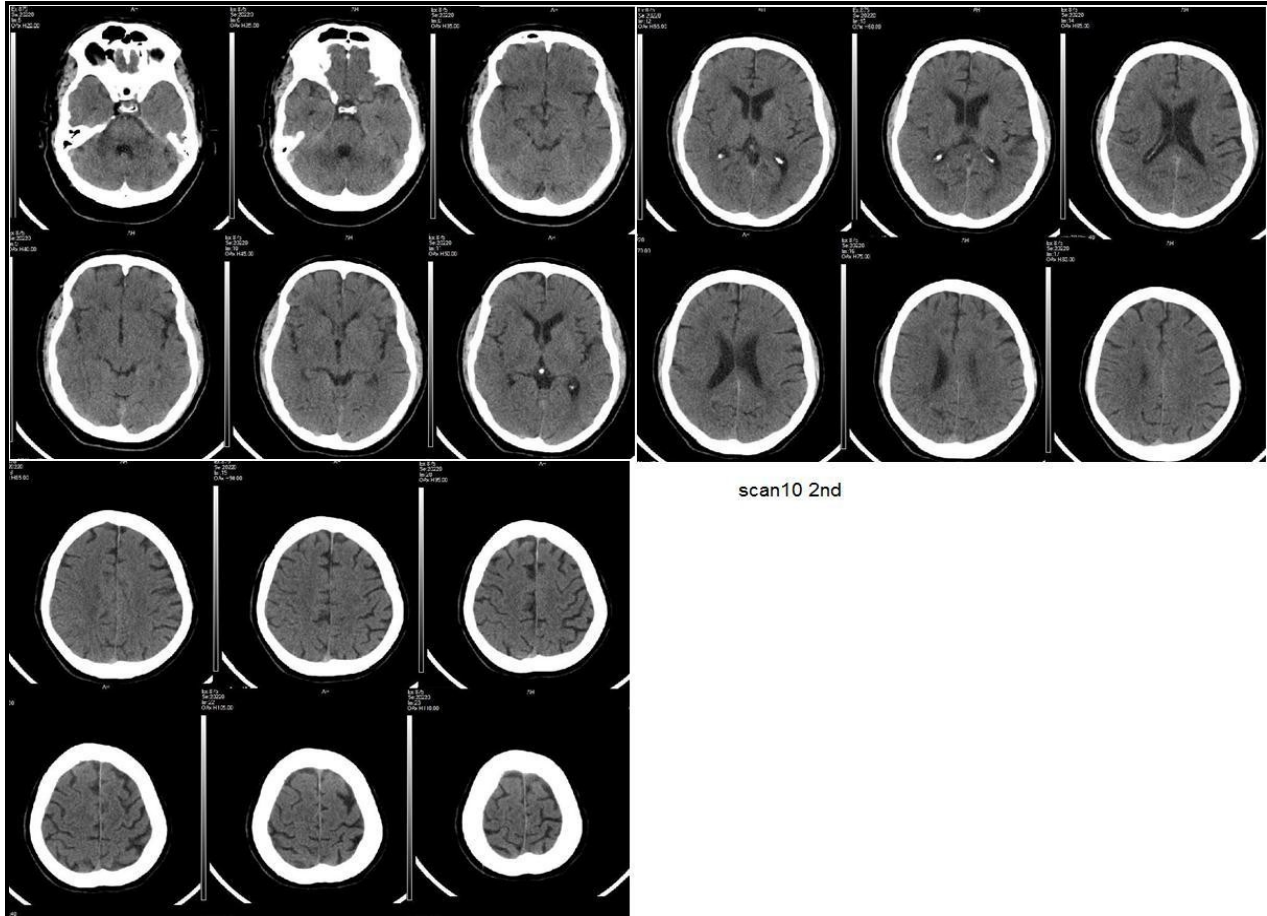


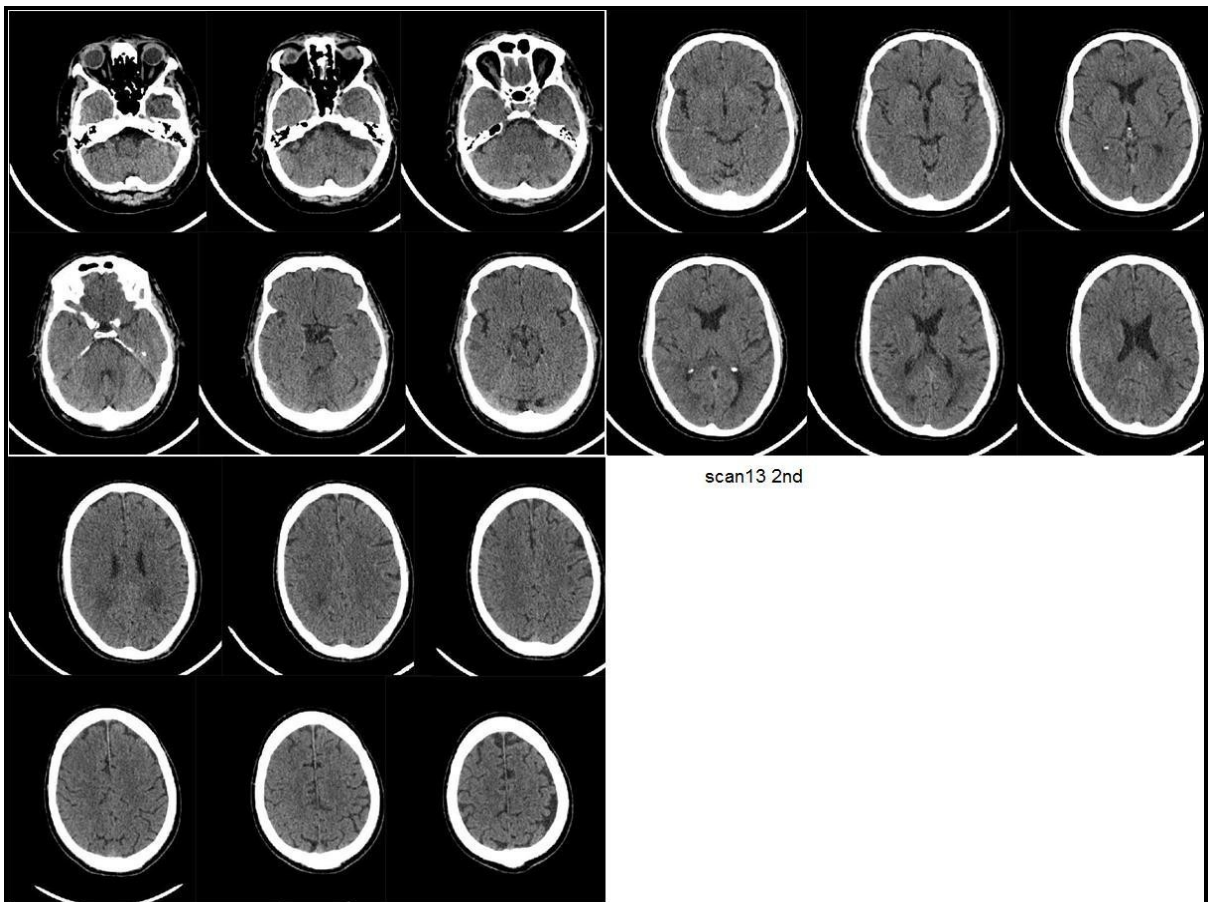
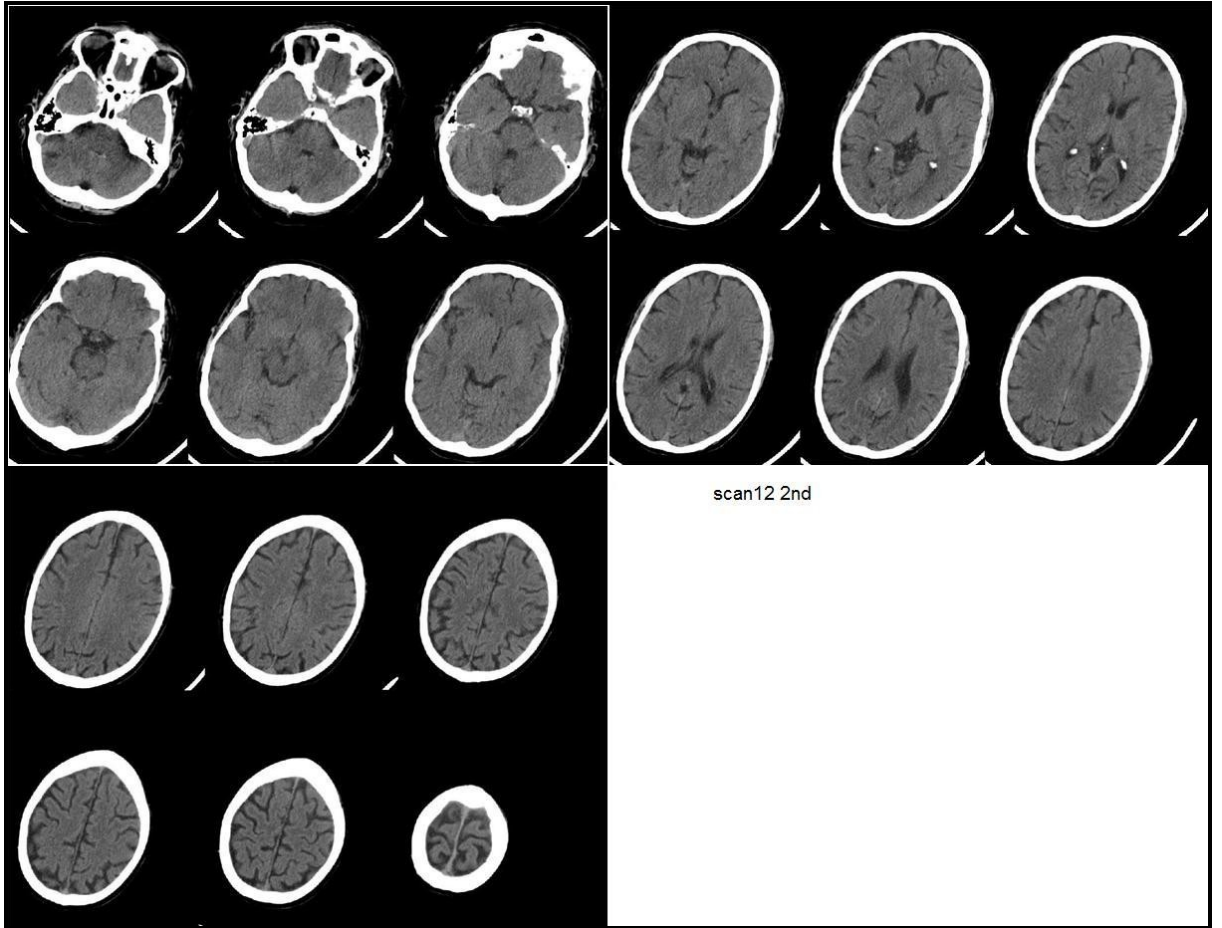


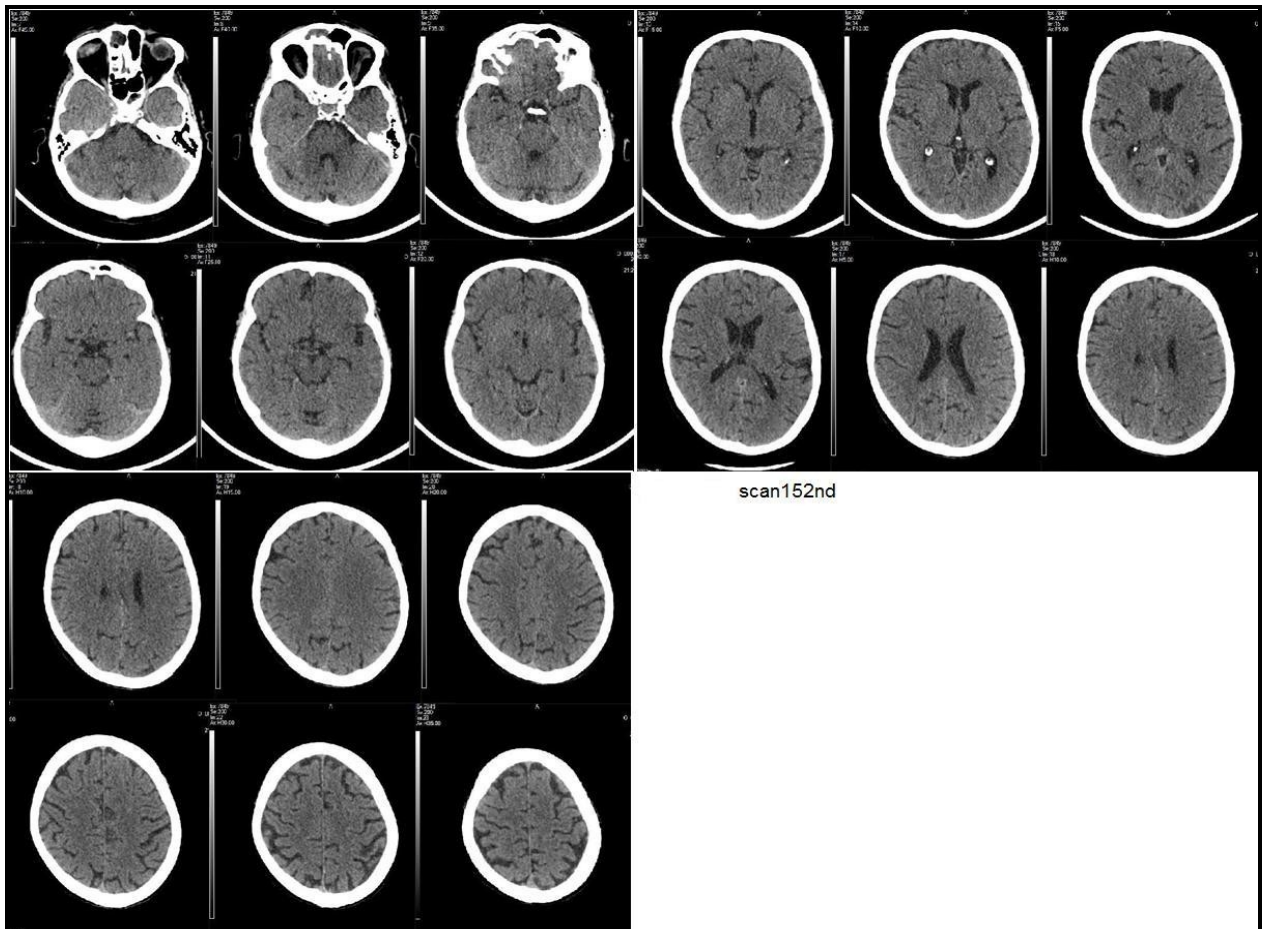
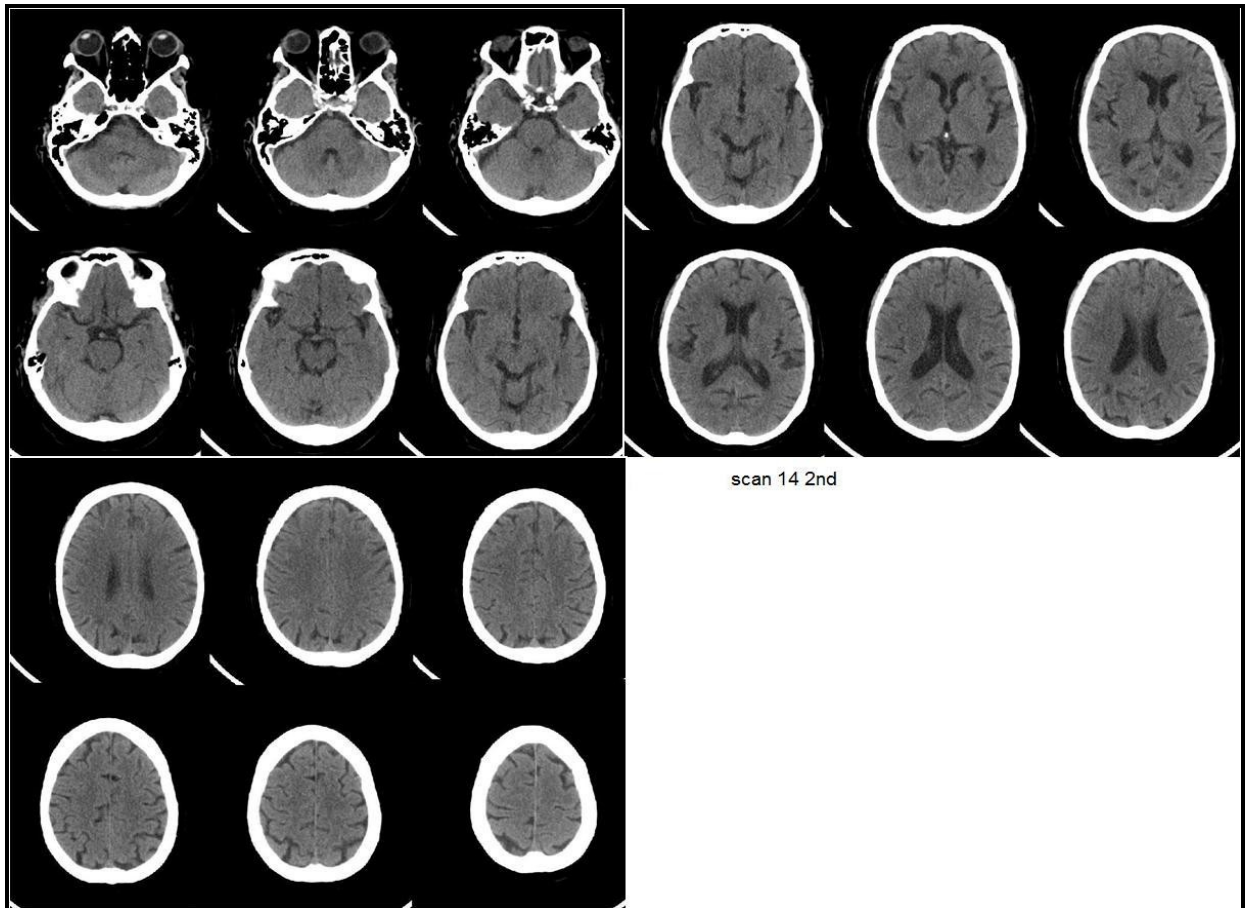


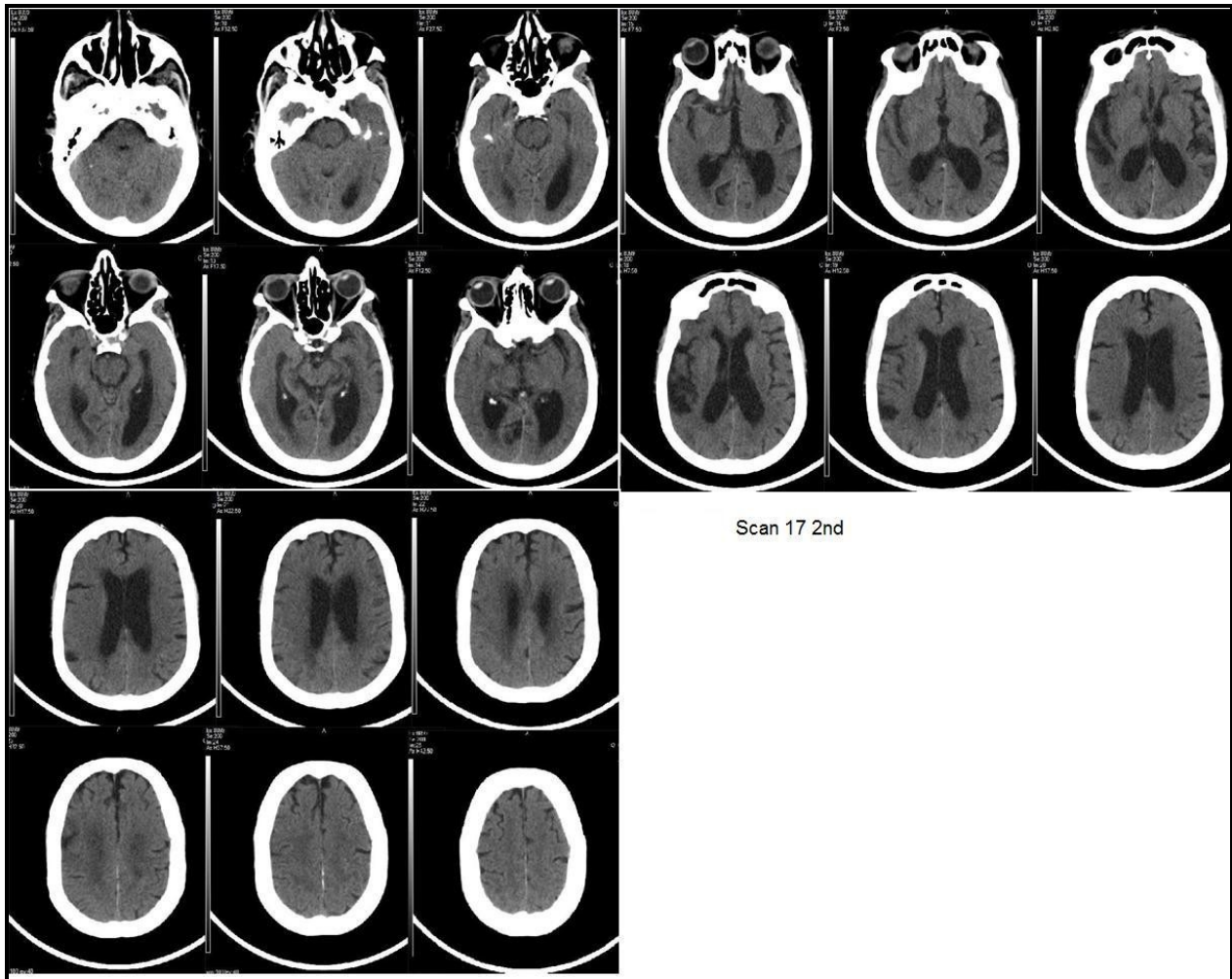
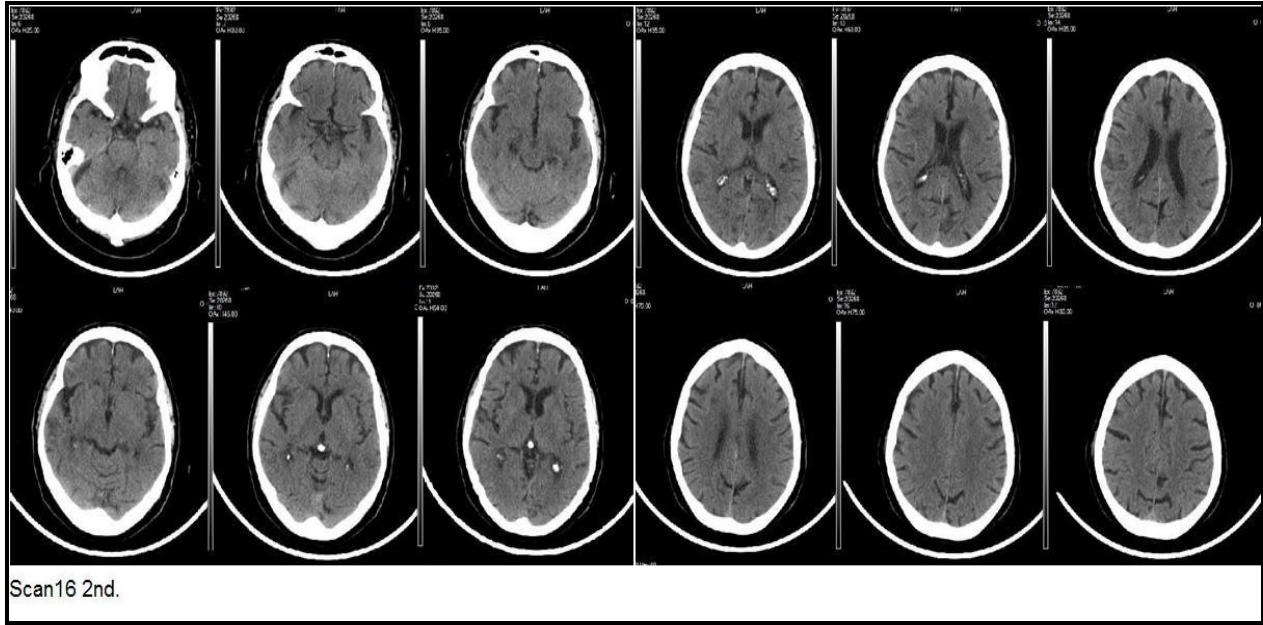


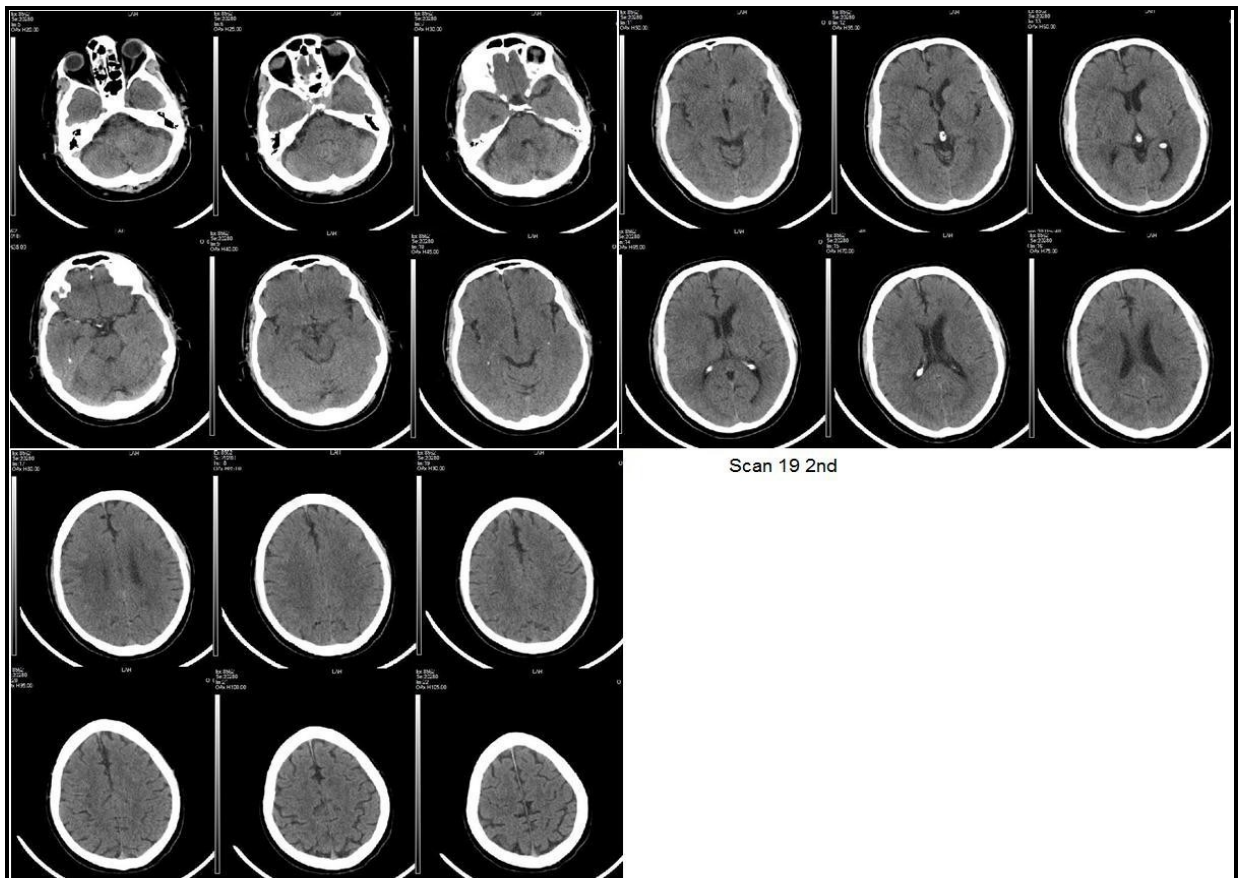
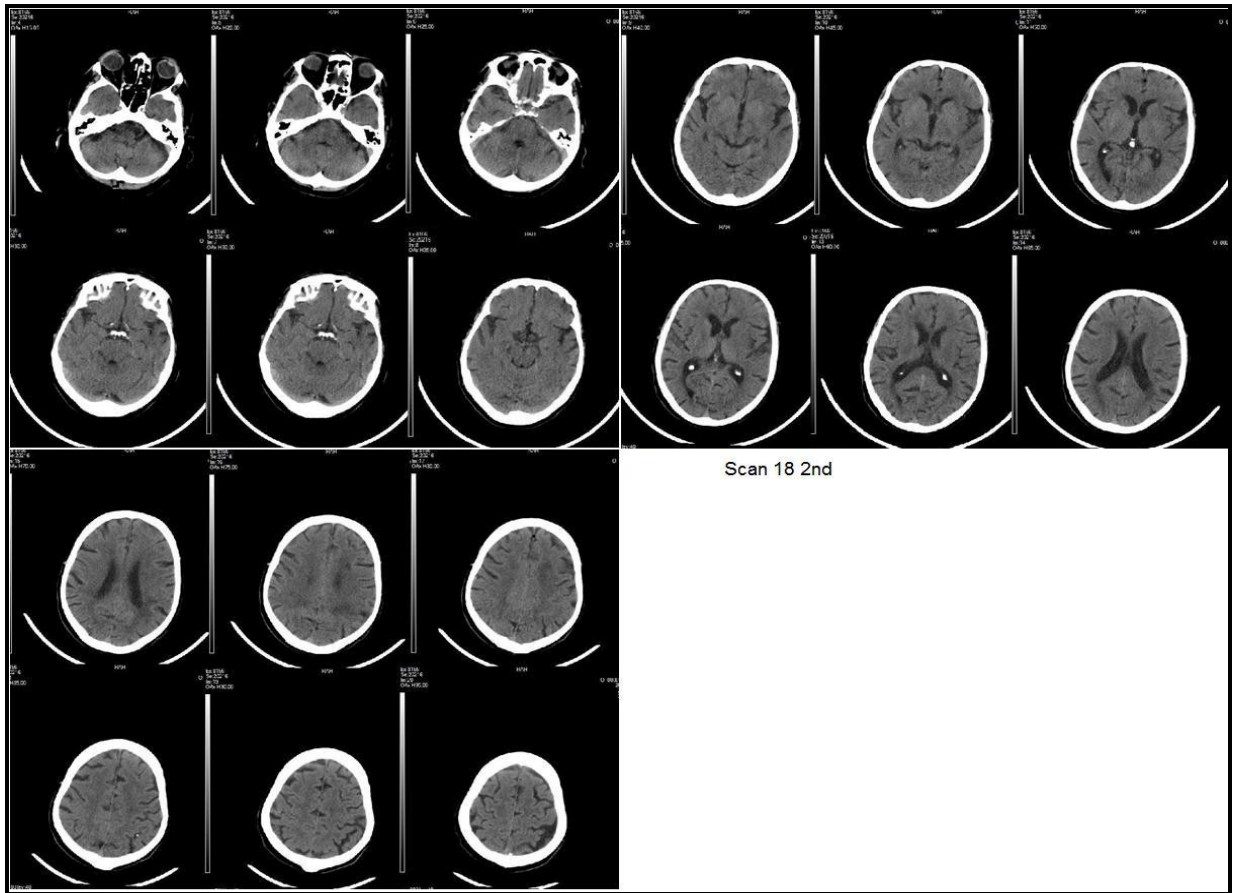


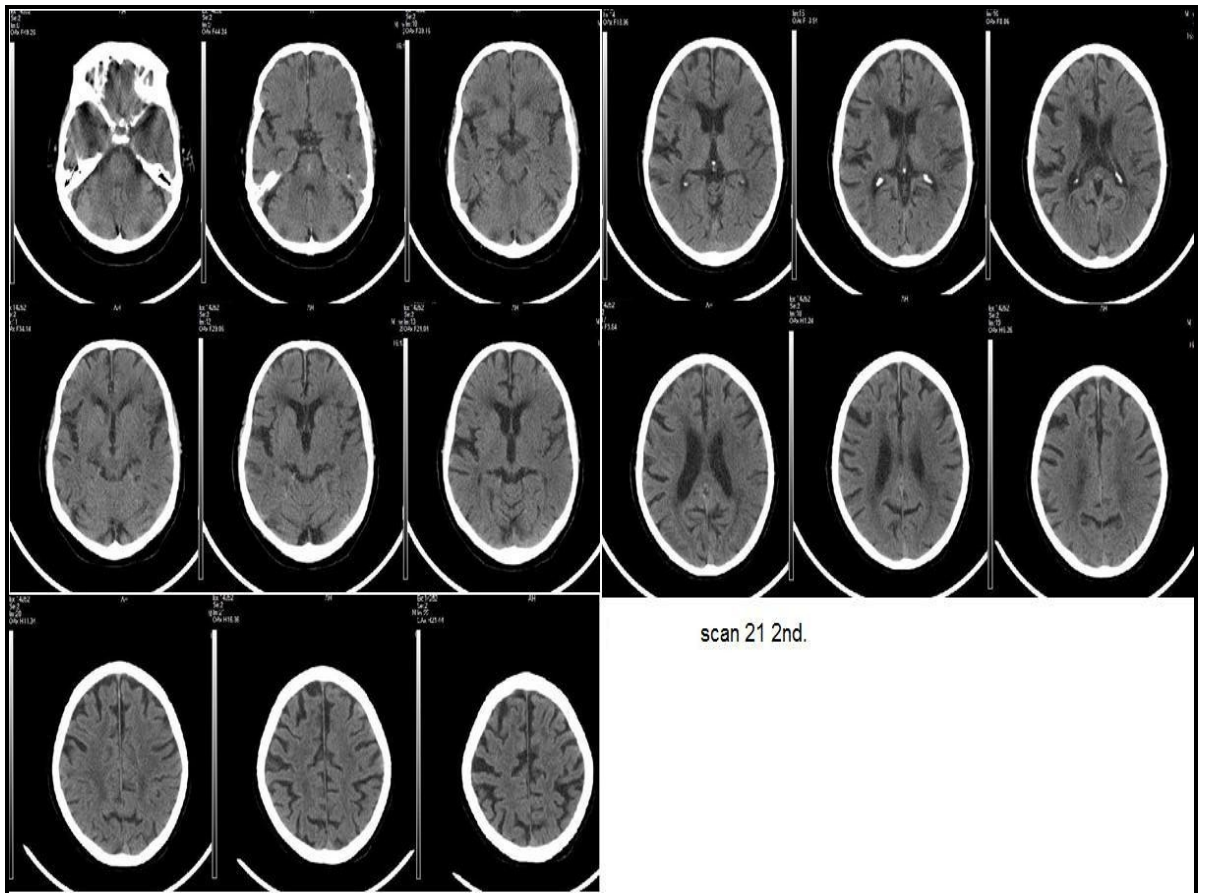
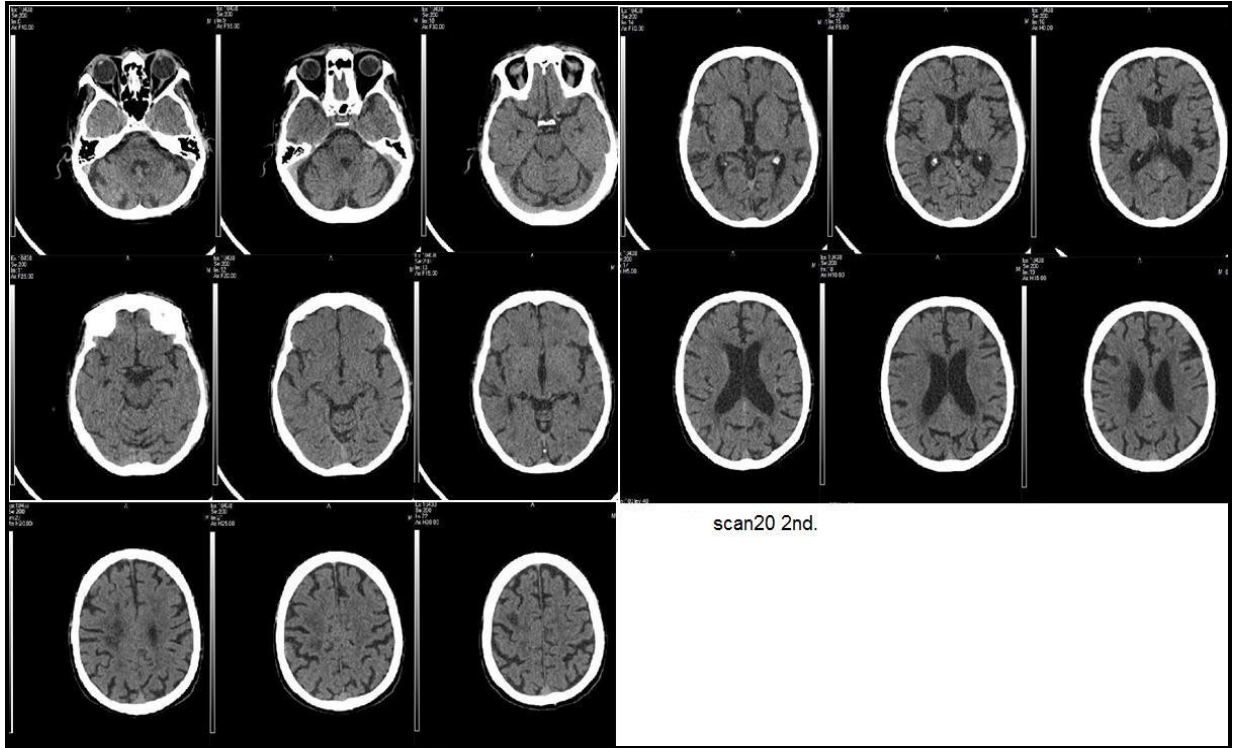


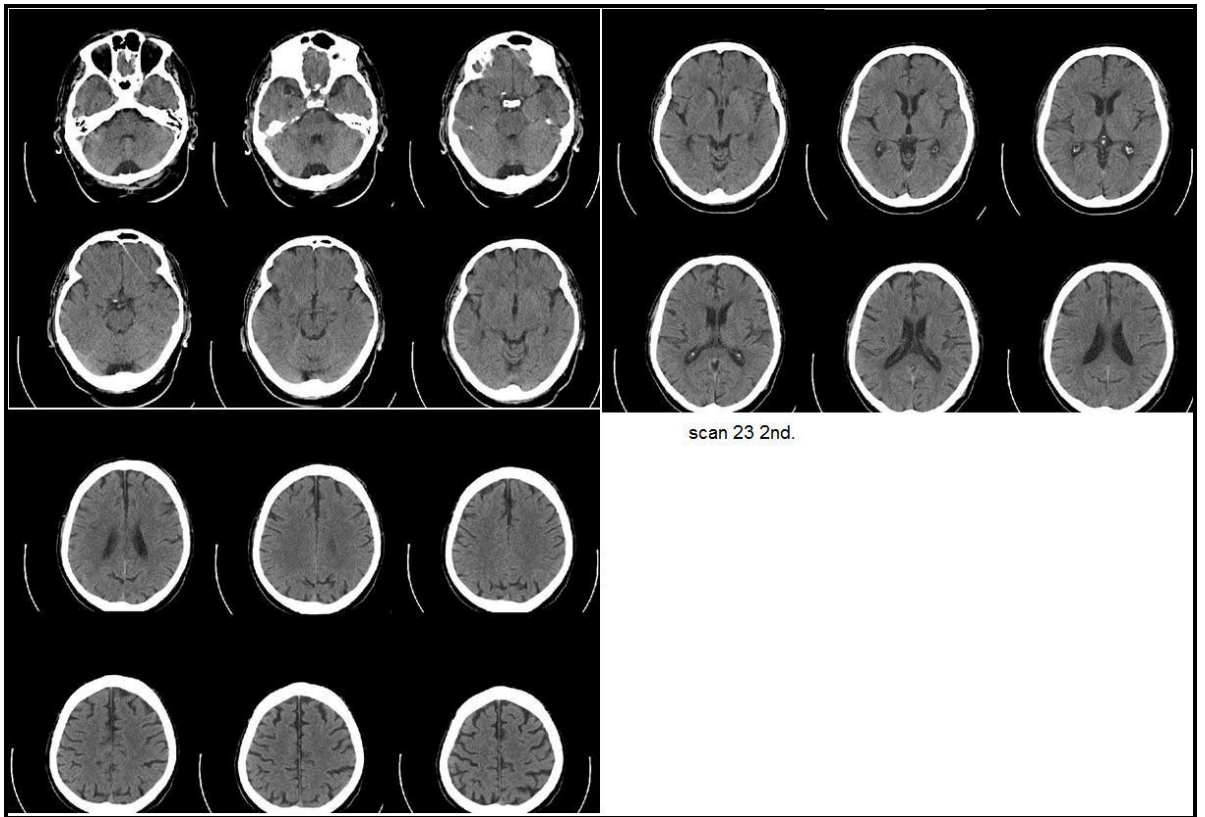
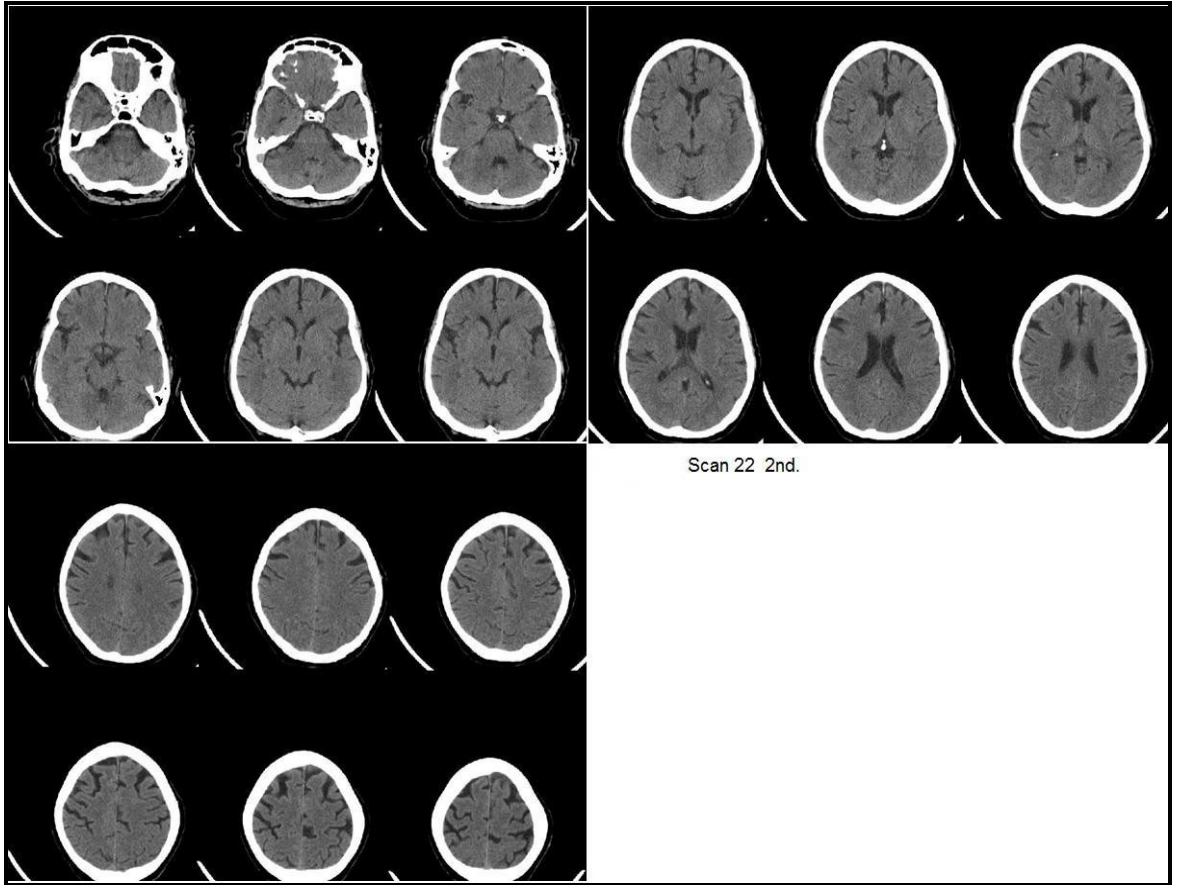


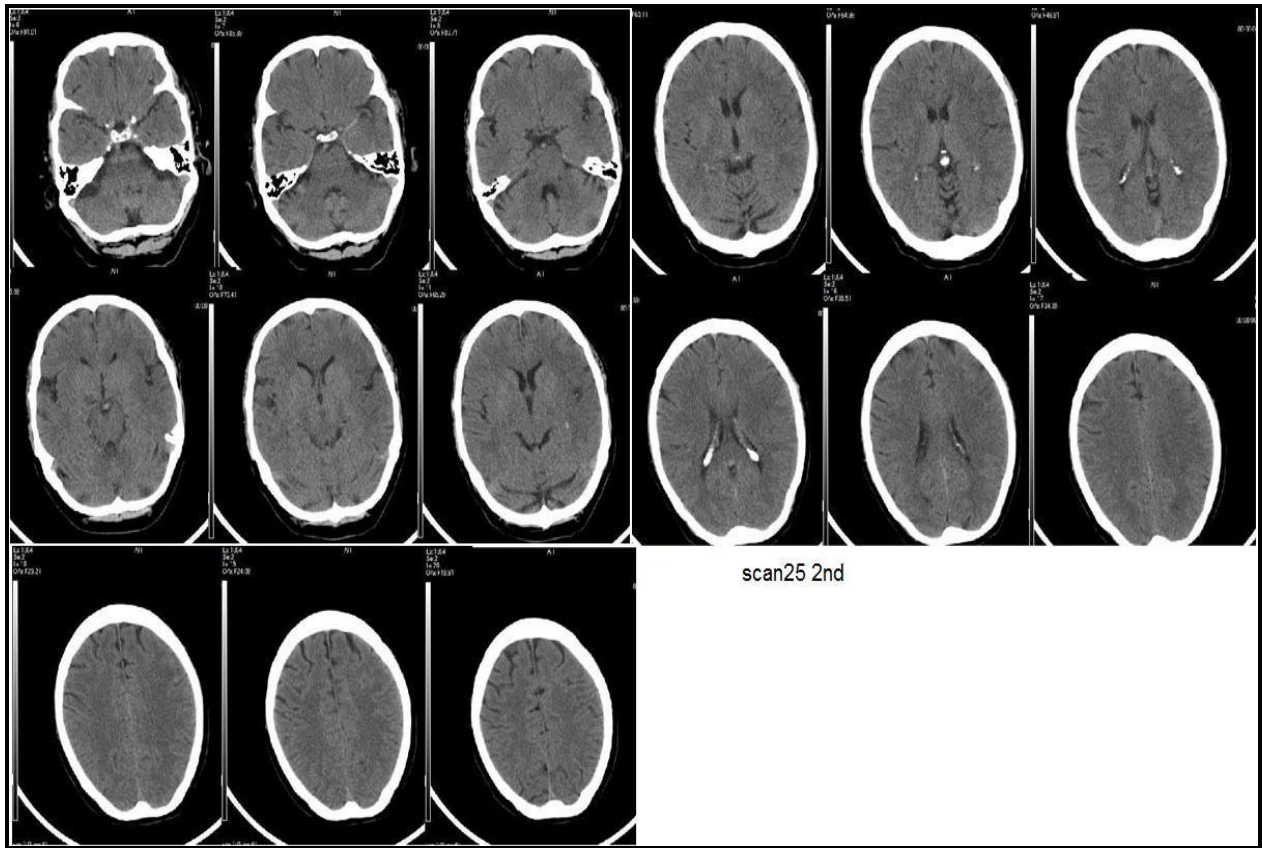
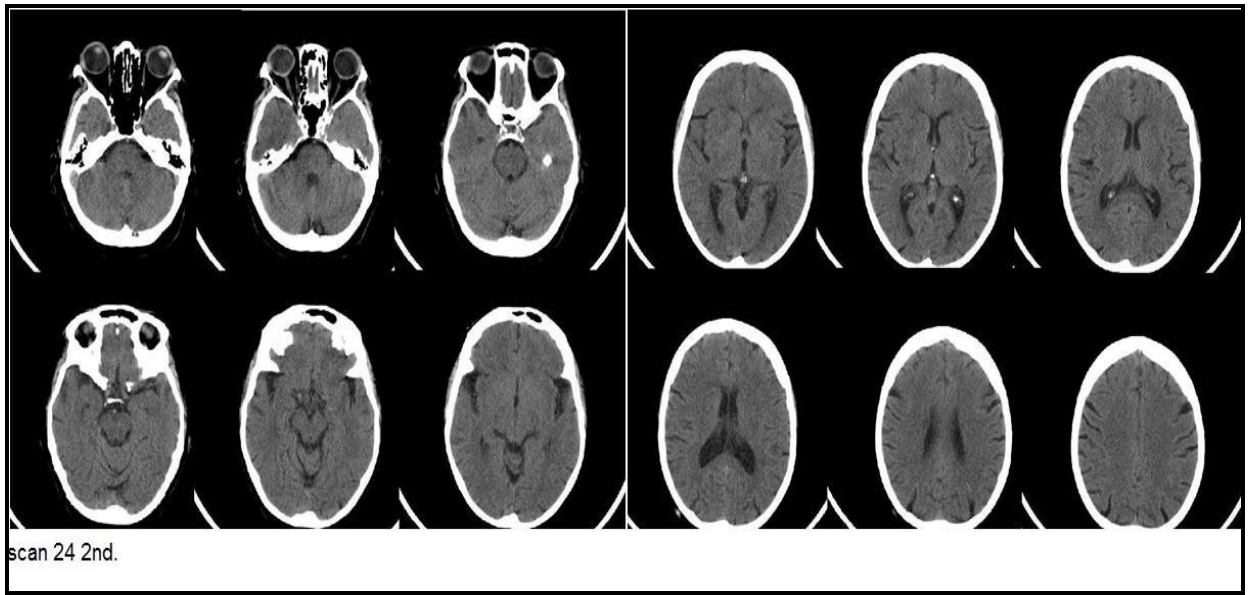


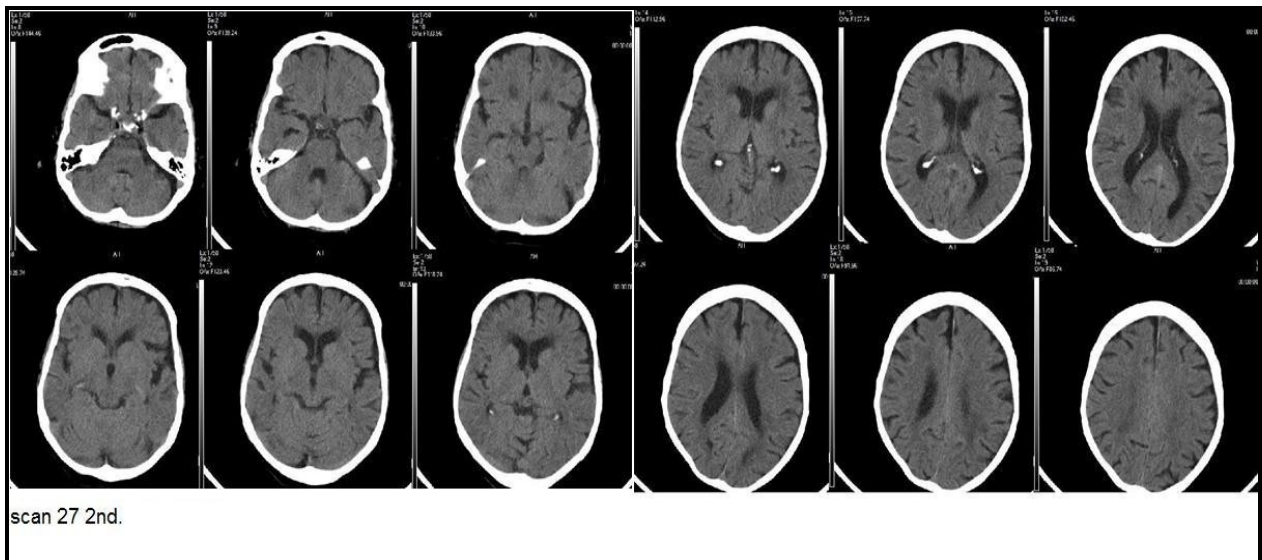
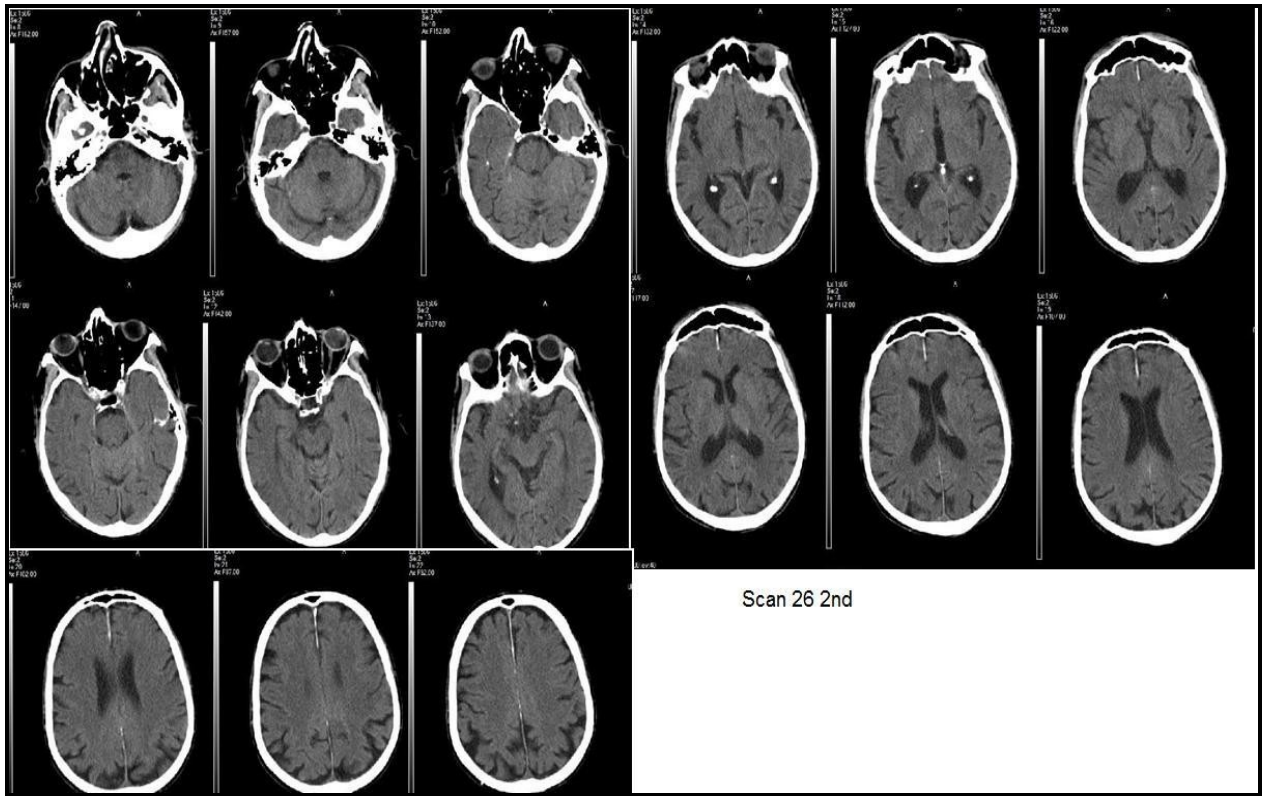


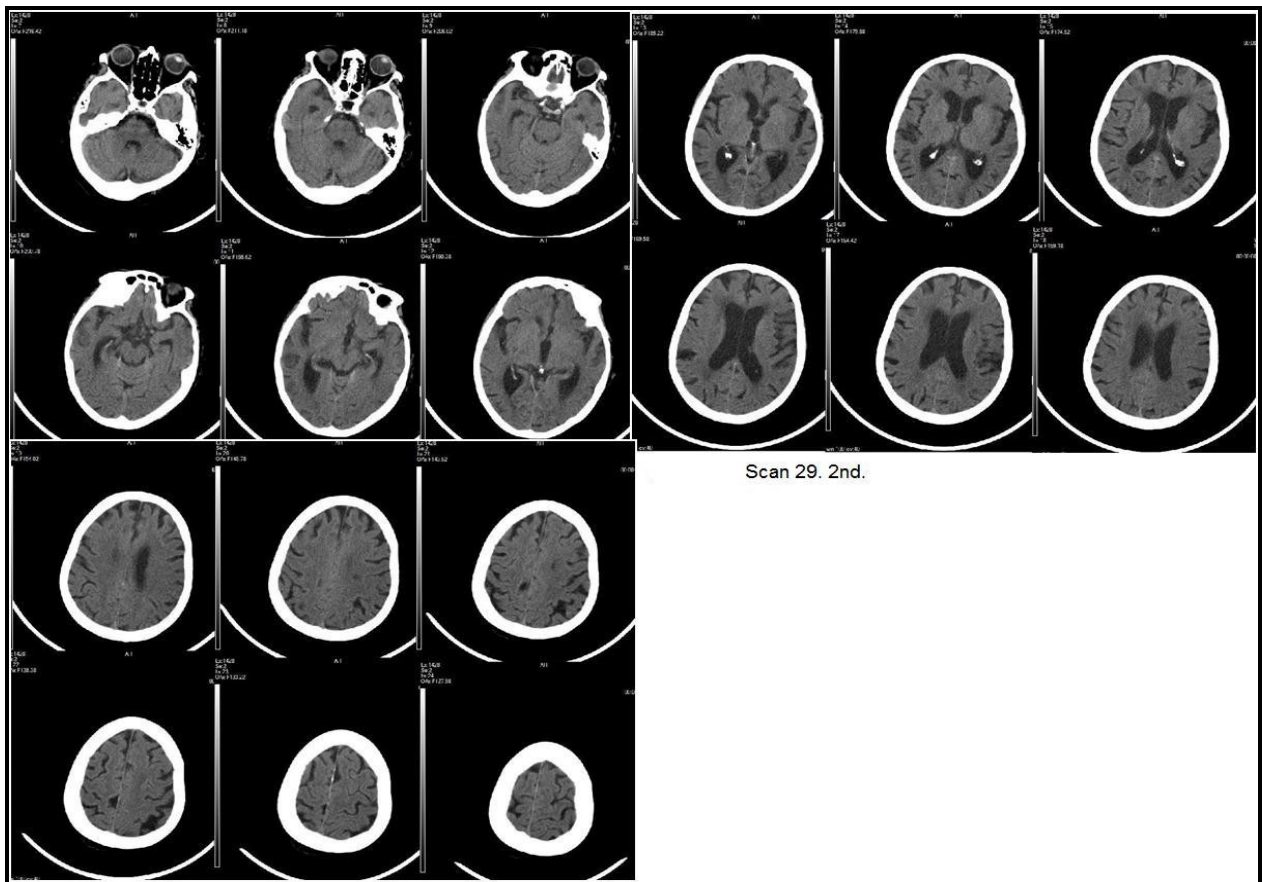
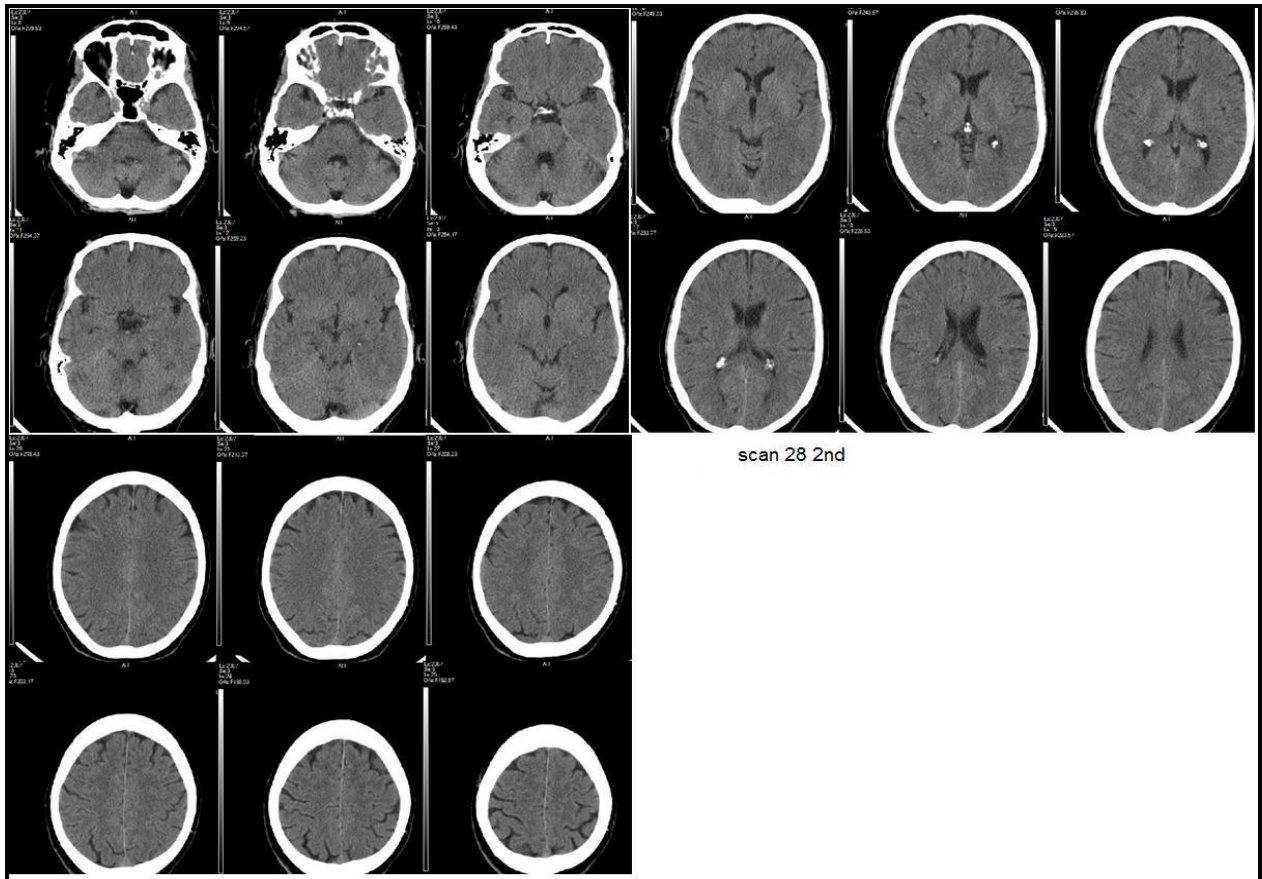


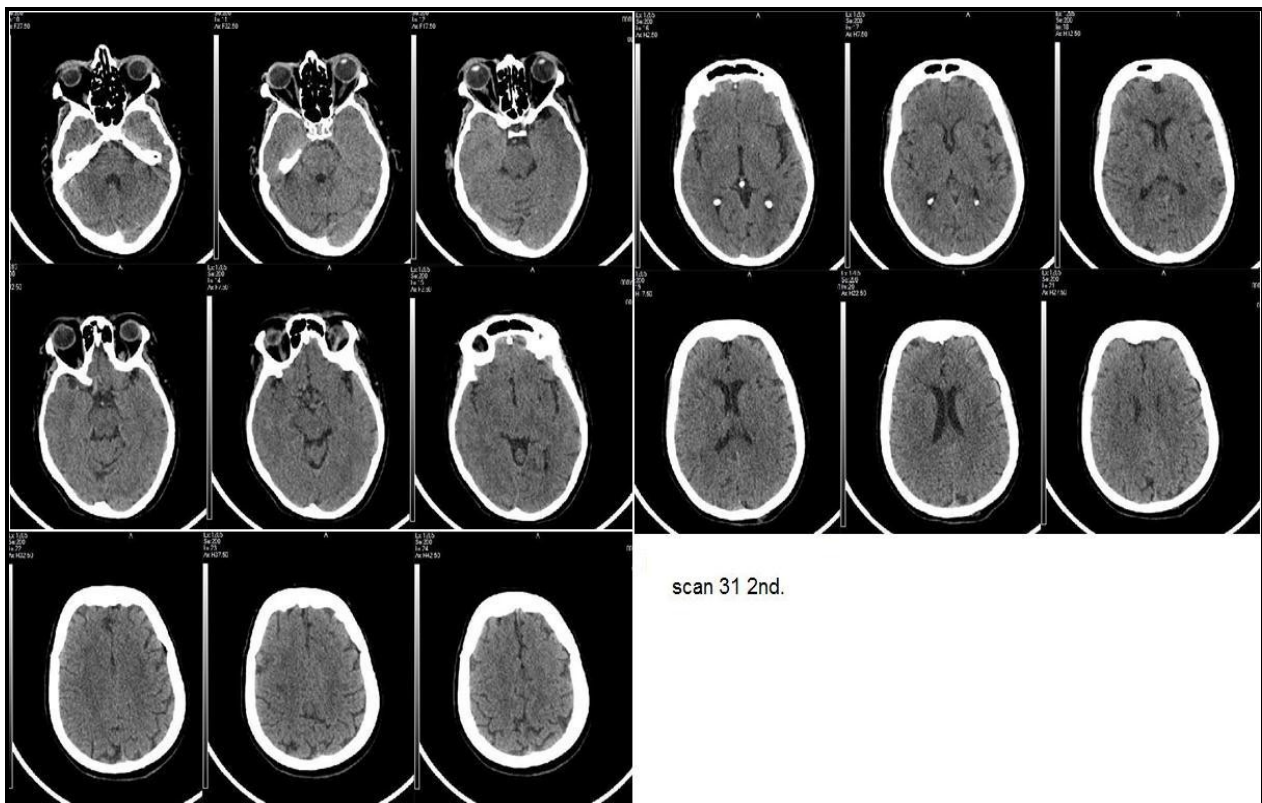
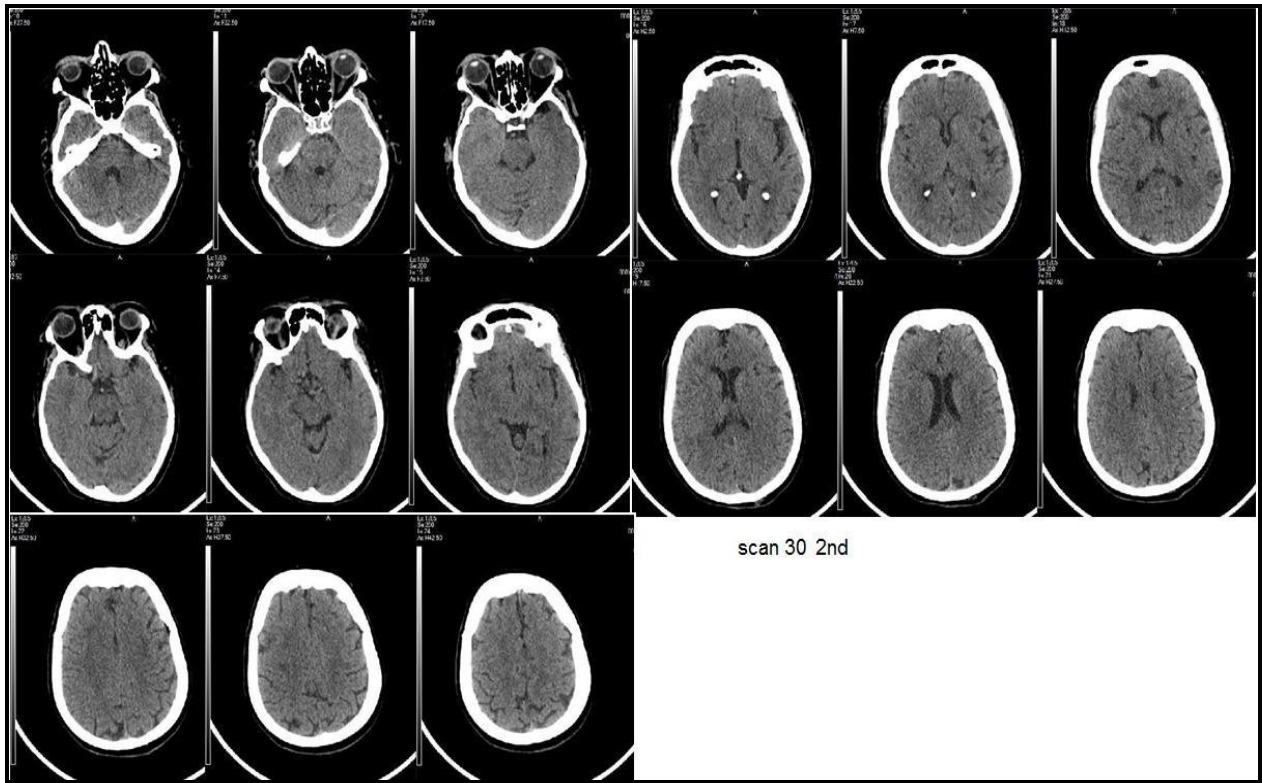


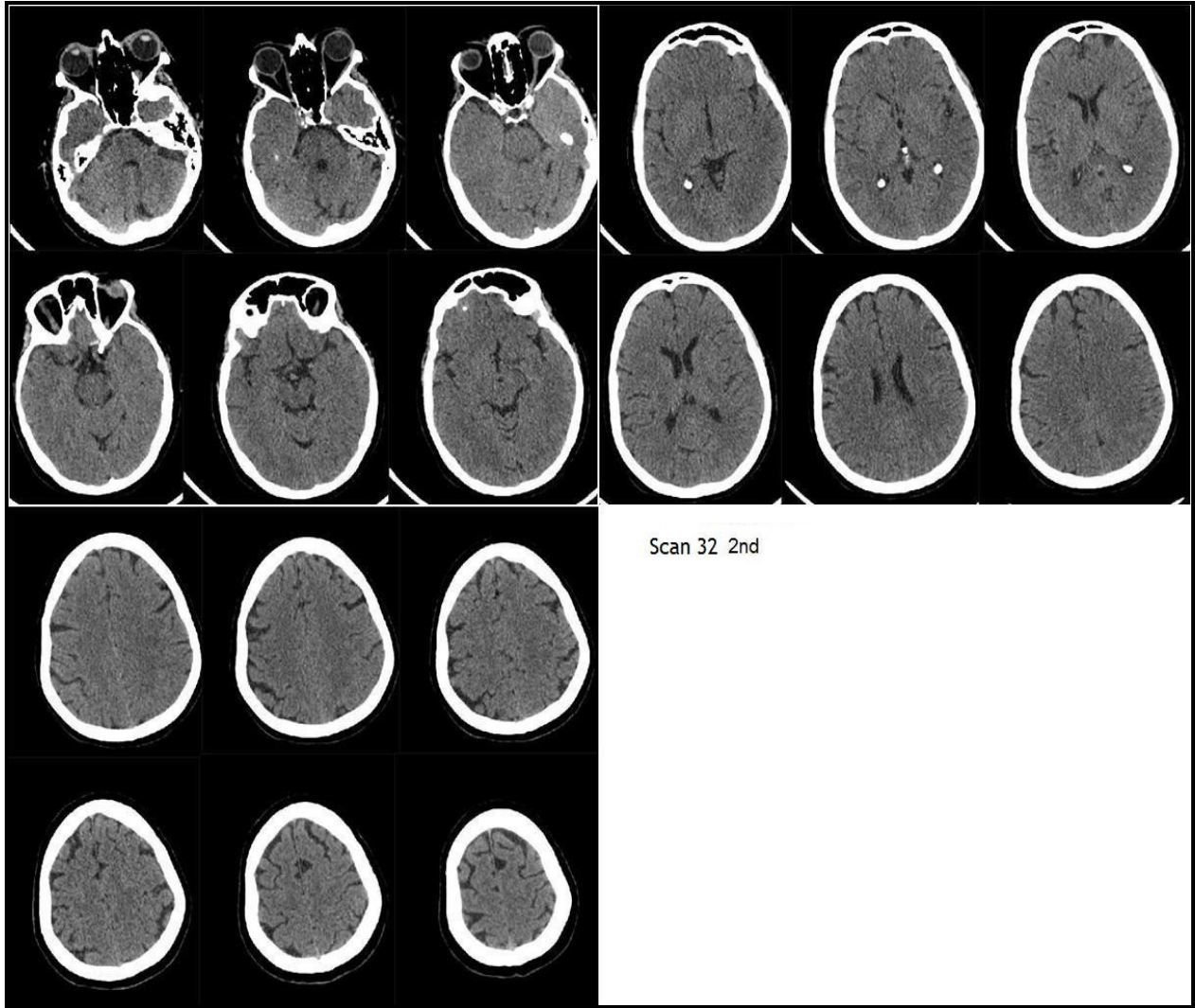












HYPODENSITY	CAUDATE	LENTIFORM	I.CAPSULE	INSULA	M1	M2	M3	M4	M5	M6
SCAN-1	0	0	0	1	0	0	0	0	2	0
SCAN-2	0	4	0	4	0	0	0	0	0	0
SCAN-3	0	1	1	3	0	2	0	1	2	0
SCAN-4	1	1	1	5	0	2	1	1	2	0
SCAN-5	1	4	1	2	1	2	1	0	0	0
SCAN-6	1	2	0	9	7	5	0	3	1	0
SCAN-7	2	2	1	2	1	5	7	3	1	5
SCAN-8	0	7	3	6	1	5	3	3	5	5
SCAN-9	4	7	3	6	5	6	6	6	6	6
SCAN-10	1	4	0	1	0	1	0	0	0	1
SCAN-11	0	0	0	0	1	1	4	3	0	0
SCAN-12	2	4	2	3	0	1	0	1	1	0
SCAN-13	0	0	0	1	0	7	6	0	1	1
SCAN-14	1	4	0	4	0	0	0	0	0	0
SCAN-15	0	1	0	1	0	0	0	1	2	2
SCAN-16	1	1	2	2	1	0	3	4	6	2
SCAN-17	2	2	2	5	1	2	3	1	3	2
SCAN-18	0	1	2	2	1	1	1	0	1	0
SCAN-19	7	9	5	6	4	4	1	0	2	0
SCAN-20	1	1	1	1	0	0	0	0	0	0
SCAN-21	0	0	0	0	0	1	0	2	6	0
SCAN-22	4	8	2	9	8	9	5	0	1	0
SCAN-23	0	7	1	9	4	5	0	5	5	1
SCAN-24	0	1	1	0	0	0	1	0	0	0
SCAN-25	7	6	1	3	0	1	0	0	0	0
SCAN-26	2	2	1	1	0	0	0	0	0	0
SCAN-27	0	4	3	7	7	8	4	2	4	0
SCAN-28	0	1	0	3	2	1	1	1	2	1
SCAN-29	0	0	1	0	0	0	1	0	2	2
SCAN-30	0	0	0	0	0	1	3	0	0	2
SCAN-31	1	7	3	3	2	0	0	1	0	0
SCAN-32	1	4	1	8	2	6	3	3	4	3

Table 4: Table of readers' responses to hypodensity in scans of second set.

FOCAL SWELLING	CAUDATE	LENTIFORM	I.CAPSULE	INSULA	M1	M2	M3	M4	M5	M6
SCAN-1	0	1	0	1	0	1	1	0	2	0
SCAN-2	0	0	0	6	2	4	3	0	2	1
SCAN-3	0	1	0	4	2	7	2	4	6	3
SCAN-4	0	0	0	3	0	1	0	1	4	2
SCAN-5	0	0	0	2	1	6	1	0	1	0
SCAN-6	1	1	0	4	6	6	0	1	2	0
SCAN-7	0	1	0	2	1	7	8	3	3	7
SCAN-8	0	1	0	3	4	5	6	7	8	8
SCAN-9	0	2	2	4	3	7	7	5	7	7
SCAN-10	0	0	0	0	0	1	1	0	0	0
SCAN-11	0	0	0	0	1	3	2	5	9	8
SCAN-12	0	2	0	1	0	1	0	1	2	1
SCAN-13	1	0	0	0	1	4	6	0	6	8
SCAN-14	0	1	0	1	2	1	1	0	1	0
SCAN-15	0	0	0	2	1	2	0	3	4	4
SCAN-16	0	0	0	0	2	2	5	3	6	6
SCAN-17	0	0	0	0	0	2	3	0	0	1
SCAN-18	1	0	0	3	3	4	2	2	4	2
SCAN-19	2	2	2	1	1	4	0	1	2	2
SCAN-20	0	0	0	1	1	2	2	2	3	3
SCAN-21	0	0	0	1	1	1	0	2	4	2
SCAN-22	1	3	0	6	5	4	5	1	3	3
SCAN-23	0	0	0	1	3	4	2	2	2	4
SCAN-24	0	0	0	1	0	2	5	0	1	0
SCAN-25	0	0	0	1	0	1	1	0	1	0
SCAN-26	1	0	0	0	0	0	0	1	0	1
SCAN-27	0	1	0	5	5	6	4	7	9	5
SCAN-28	0	0	0	2	3	3	2	2	3	1
SCAN-29	0	0	0	0	0	0	1	1	0	0
SCAN-30	0	0	0	1	0	1	3	0	0	5
SCAN-31	0	0	0	6	6	9	8	7	7	6
SCAN-32	0	2	1	3	6	6	3	4	5	4

Table 5: Table of responses to isodense swelling in scans of second set

<i>TOTAL</i>	R-1	R-2	R-3	R-4	R-5	R-6	R-7	R-8	R-9	R-10	R-11
<i>SCAN-1</i>	9	9	9	10	10	7	9	10	9	10	10
<i>SCAN-2</i>	8	8	6	10	9	7	6	10	7	7	8
<i>SCAN-3</i>	5	10	10	5	8	3	6	8	8	9	5
<i>SCAN-4</i>	9	9	9	7	6	7	8	10	7	6	9
<i>SCAN-5</i>	6	10	10	7	8	8	10	9	6	5	9
<i>SCAN-6</i>	5	8	7	7	9	5	6	5	6	7	7
<i>SCAN-7</i>	5	9	6	7	4	5	8	5	8	2	6
<i>SCAN-8</i>	2	5	1	5	4	3	1	8	7	6	5
<i>SCAN-9</i>	3	7	1	0	4	1	2	6	1	2	8
<i>SCAN-10</i>	9	10	8	8	10	9	10	8	10	8	10
<i>SCAN-11</i>	5	8	7	9	7	6	7	7	6	8	7
<i>SCAN-12</i>	6	10	5	5	10	8	7	8	10	10	10
<i>SCAN-13</i>	7	8	6	6	6	7	6	8	6	8	8
<i>SCAN-14</i>	8	10	8	10	9	4	10	8	9	10	8
<i>SCAN-15</i>	7	10	5	7	9	5	10	10	9	7	10
<i>SCAN-16</i>	6	10	6	6	8	6	7	7	8	0	9
<i>SCAN-17</i>	5	9	8	1	8	8	8	9	8	8	9
<i>SCAN-18</i>	3	10	8	8	4	6	10	9	5	9	9
<i>SCAN-19</i>	6	8	2	3	8	4	7	7	6	3	8
<i>SCAN-20</i>	8	10	7	4	10	10	10	10	10	2	10
<i>SCAN-21</i>	10	8	5	8	9	6	10	9	9	9	10
<i>SCAN-22</i>	3	7	3	2	5	4	6	5	4	6	5
<i>SCAN-23</i>	5	10	4	5	8	3	3	7	6	3	7
<i>SCAN-24</i>	8	9	10	10	9	6	10	8	8	10	10
<i>SCAN-25</i>	7	9	6	7	9	7	10	8	6	8	9
<i>SCAN-26</i>	8	9	10	10	10	9	10	10	10	5	10
<i>SCAN-27</i>	3	7	3	5	6	4	4	6	3	4	2
<i>SCAN-28</i>	10	9	2	7	9	7	7	10	10	9	8
<i>SCAN-29</i>	10	9	9	7	10	9	10	9	10	10	9
<i>SCAN-30</i>	8	8	7	10	9	9	10	8	8	10	10
<i>SCAN-31</i>	4	7	2	10	2	3	3	6	2	0	8
<i>SCAN-32</i>	4	7	7	3	3	3	6	5	7	0	10

Table 6: Total ASPECTS scores for Second set' scans.

<i>HYPODENSITY</i>	R-1	R-2	R-3	R-4	R-5	R-6	R-7	R-8	R-9	R-10	R-11
<i>SCAN-1</i>	10	9	9	10	10	10	9	10	10	10	10
<i>SCAN-2</i>	9	10	8	10	10	10	10	10	8	9	9
<i>SCAN-3</i>	8	10	10	9	8	10	8	8	10	9	10
<i>SCAN-4</i>	10	9	9	7	10	9	10	7	7	7	9
<i>SCAN-5</i>	9	10	10	7	10	10	10	10	7	6	9
<i>SCAN-6</i>	7	10	7	7	9	5	8	5	6	9	9
<i>SCAN-7</i>	5	9	8	7	8	6	8	5	8	7	9
<i>SCAN-8</i>	8	6	3	5	9	7	1	8	7	10	8
<i>SCAN-9</i>	3	9	1	0	7	7	6	6	1	7	8
<i>SCAN-10</i>	9	10	8	8	10	9	10	8	10	10	10
<i>SCAN-11</i>	9	8	9	9	9	9	10	8	8	10	10
<i>SCAN-12</i>	8	10	6	5	10	9	9	8	10	10	10
<i>SCAN-13</i>	8	10	8	6	8	10	8	8	7	10	10
<i>SCAN-14</i>	8	10	8	10	9	10	10	8	9	10	8
<i>SCAN-15</i>	10	10	8	7	10	10	10	10	9	9	10
<i>SCAN-16</i>	6	10	6	6	9	7	10	10	9	6	9
<i>SCAN-17</i>	6	9	9	1	10	8	8	9	8	10	9
<i>SCAN-18</i>	7	10	8	8	10	10	10	10	9	10	10
<i>SCAN-19</i>	8	9	5	3	9	4	7	7	6	6	8
<i>SCAN-20</i>	10	10	10	10	10	10	10	10	10	6	10
<i>SCAN-21</i>	10	8	9	8	9	9	10	9	9	10	10
<i>SCAN-22</i>	5	9	6	2	5	7	7	5	4	7	7
<i>SCAN-23</i>	5	10	4	5	8	4	6	8	7	9	7
<i>SCAN-24</i>	10	9	10	10	10	10	10	9	8	10	10
<i>SCAN-25</i>	8	9	6	7	9	8	10	8	6	9	9
<i>SCAN-26</i>	8	10	10	10	10	10	10	10	10	6	10
<i>SCAN-27</i>	5	10	7	5	6	6	7	6	6	8	5
<i>SCAN-28</i>	10	9	4	7	9	10	9	10	10	10	10
<i>SCAN-29</i>	10	9	9	7	10	10	10	9	10	10	10
<i>SCAN-30</i>	10	10	7	10	10	10	10	9	8	10	10
<i>SCAN-31</i>	9	9	9	10	8	8	10	8	7	6	9
<i>SCAN-32</i>	7	10	7	3	4	9	9	6	7	6	8

Table 7; ASPECTS scores for hypodensity. Second set

<i>I.SWELLING</i>	R-1	R-2	R-3	R-4	R-5	R-6	R-7	R-8	R-9	R-10	R-11
<i>SCAN-1</i>	9	10	10	10	10	7	9	10	9	10	10
<i>SCAN-2</i>	9	8	7	10	9	7	6	10	9	8	9
<i>SCAN-3</i>	7	10	10	5	8	3	6	9	8	10	5
<i>SCAN-4</i>	9	10	10	10	6	8	9	10	9	10	10
<i>SCAN-5</i>	7	10	10	10	8	8	10	9	8	9	10
<i>SCAN-6</i>	7	8	10	10	9	9	10	6	8	8	8
<i>SCAN-7</i>	8	9	6	10	4	8	8	5	8	5	7
<i>SCAN-8</i>	4	9	4	7	4	6	3	9	9	4	7
<i>SCAN-9</i>	5	8	3	10	4	4	2	10	5	5	10
<i>SCAN-10</i>	10	10	10	10	10	10	10	10	10	8	10
<i>SCAN-11</i>	6	8	8	10	7	7	7	7	7	8	7
<i>SCAN-12</i>	8	10	9	10	8	8	7	10	10	10	10
<i>SCAN-13</i>	8	8	8	6	6	7	6	8	7	8	8
<i>SCAN-14</i>	10	10	10	10	9	5	10	10	10	10	10
<i>SCAN-15</i>	7	10	5	10	9	5	10	10	10	8	10
<i>SCAN-16</i>	7	10	6	10	8	9	7	7	8	4	10
<i>SCAN-17</i>	9	10	9	10	8	10	10	10	10	8	10
<i>SCAN-18</i>	6	10	10	10	4	6	10	9	6	9	9
<i>SCAN-19</i>	8	9	7	10	9	10	7	7	9	7	10
<i>SCAN-20</i>	8	10	10	7	4	10	10	10	10	6	10
<i>SCAN-21</i>	10	10	5	10	9	7	10	9	10	9	10
<i>SCAN-22</i>	8	8	4	10	6	6	8	5	7	9	8
<i>SCAN-23</i>	10	10	10	10	9	9	3	9	8	4	10
<i>SCAN-24</i>	8	10	10	10	9	6	10	9	9	10	10
<i>SCAN-25</i>	9	10	10	10	10	9	10	10	9	9	10
<i>SCAN-26</i>	10	9	10	10	10	9	10	10	10	9	10
<i>SCAN-27</i>	6	7	3	10	6	8	4	7	5	6	6
<i>SCAN-28</i>	10	10	4	10	9	7	7	10	10	9	8
<i>SCAN-29</i>	10	10	10	10	10	9	10	10	10	10	9
<i>SCAN-30</i>	8	8	10	10	9	9	10	8	8	10	10
<i>SCAN-31</i>	5	8	3	10	3	5	3	8	3	4	9
<i>SCAN-32</i>	7	7	10	10	3	4	7	5	9	4	10

Table 8; ASPECTS scores for isodense swelling. Second set

	CAU HYPO	LEN HYPO	ICAPP HYPO	INS HYPO	M1 HYPO	M2 HYPO	M3 HYPO	M4 HYPO	M5 HYPO	M6 HYPO
SCAN-1	1	0	0	0	1	0	1	2	2	2
SCAN-2	1	1	0	1	0	0	0	0	0	0
SCAN-3	0	0	0	0	0	0	0	0	0	0
SCAN-5	0	1	0	2	0	0	0	1	0	0
SCAN-6	2	2	0	2	2	1	0	2	2	0
SCAN-7	0	1	0	1	0	0	1	0	1	0
SCAN-8	0	0	0	1	0	0	0	0	0	0
SCAN-9	0	0	0	0	0	0	0	0	0	0
SCAN-10	0	1	0	1	0	1	0	0	0	0
SCAN-11	0	0	0	0	1	0	0	2	1	0
SCAN-12	0	0	0	0	0	0	0	0	1	0
SCAN-13	1	2	0	3	3	2	1	2	2	1
SCAN-14	0	2	0	2	1	1	0	0	0	0
SCAN-15	0	0	0	0	1	0	1	2	2	2
SCAN-17	1	3	1	3	2	1	1	2	1	0
SCAN-18	0	1	0	0	0	0	0	0	1	0
SCAN-19	0	1	0	0	0	0	0	0	0	0
SCAN-20	1	3	0	2	1	0	0	1	0	1
SCAN-21	1	2	1	3	2	1	2	1	1	1
SCAN-22	0	0	0	0	0	0	0	0	0	0
SCAN-23	2	2	1	2	0	1	1	0	2	1
SCAN-24	0	1	1	0	0	0	0	0	0	0
SCAN-25	0	2	0	0	0	0	0	0	0	0
SCAN-26	0	0	0	0	0	0	0	0	0	0
SCAN-28	0	3	1	0	0	0	0	0	0	0
SCAN-29	0	0	0	0	0	0	1	0	2	0
SCAN-30	0	0	0	0	0	0	0	0	0	0
SCAN-31	1	2	0	1	0	0	0	0	1	0
SCAN-32	1	2	0	1	0	1	0	1	2	1
SCAN-33	0	0	0	0	0	0	0	0	0	0
SCAN-34	3	3	0	2	1	0	0	0	1	1
SCAN-35	0	0	0	0	0	0	0	0	0	0
SCAN-36	0	1	0	0	0	0	0	0	0	0
SCAN-37	0	0	0	0	0	0	0	0	0	0
SCAN-39	0	1	1	1	1	0	0	1	0	0
SCAN-40	1	2	1	2	2	2	2	2	1	0

Table 9; table of readers' responses to hypodensity of scans of first set

SCAN NUMBER	CAU SW	LEN SW	ICAP SW	INS SW	M1 SW	M2 SW	M3 SW	M4 SW	M5 SW	M6 SW
SCAN-1	0	0	0	0	0	0	0	2	2	2
SCAN-2	0	2	0	0	0	0	1	0	0	0
SCAN-3	0	0	0	0	0	0	0	0	0	0
SCAN-5	0	2	0	1	2	2	2	0	0	0
SCAN-6	0	0	0	0	0	0	0	2	2	1
SCAN-7	0	0	0	1	1	1	0	0	1	0
SCAN-8	0	0	0	0	0	0	0	0	0	0
SCAN-9	0	0	0	0	0	0	0	0	0	0
SCAN-10	0	0	0	0	1	0	0	0	0	0
SCAN-11	0	1	1	0	0	0	0	0	0	0
SCAN-12	0	0	0	0	0	0	0	0	0	0
SCAN-13	0	0	0	0	1	1	0	2	2	2
SCAN-14	1	0	0	0	2	2	1	1	0	1
SCAN-15	0	0	0	0	0	0	0	1	2	2
SCAN-17	1	1	1	1	1	1	1	3	3	2
SCAN-18	0	0	0	0	0	0	0	0	0	0
SCAN-19	0	0	0	0	0	0	0	0	2	1
SCAN-20	1	0	0	1	1	2	3	2	2	1
SCAN-21	0	0	0	0	2	2	1	1	2	2
SCAN-22	0	1	1	0	0	0	0	0	0	0
SCAN-23	1	1	1	1	0	1	1	0	0	0
SCAN-24	0	0	0	0	0	0	0	0	0	0
SCAN-25	0	0	0	1	0	1	1	0	1	1
SCAN-26	0	0	0	0	0	0	0	0	0	0
SCAN-28	1	0	0	0	1	1	0	0	0	0
SCAN-29	0	0	0	0	0	0	0	0	0	0
SCAN-30	0	0	0	0	0	0	1	0	0	0
SCAN-31	1	0	0	2	2	3	2	1	2	2
SCAN-32	0	0	1	2	2	2	0	2	2	2
SCAN-33	0	1	1	1	0	0	0	0	0	0
SCAN-34	0	0	0	0	0	0	0	0	0	0
SCAN-35	0	0	0	0	2	1	0	1	0	0
SCAN-36	0	1	0	1	1	1	1	2	2	0
SCAN-37	0	0	0	0	0	0	0	0	1	0
SCAN-39	1	1	0	1	2	1	0	0	1	1
SCAN-40	0	0	0	3	2	2	0	0	1	1

Table 10; table of readers' responses to isodense swelling of scans of first set

BOTH CHANGES	R-1	R-2	R-3	R-4	R-5	R-6	R-7	R-8	R-9
SCAN-1	8	7	5	6	10	6	6	7	10
SCAN-2	8	10	9	7	8	6	10	9	10
SCAN-3	10	10	10	10	10	10	10	10	10
SCAN-5	8	7	5	6	10	4	9	10	10
SCAN-6	3	8	2	0	6	4	2	2	9
SCAN-7	8	10	6	9	10	7	9	10	10
SCAN-8	8	9	10	7	10	10	10	10	10
SCAN-9	10	10	10	7	9	10	10	9	10
SCAN-10	7	10	8	9	10	8	10	9	10
SCAN-11	10	6	8	10	9	10	9	9	10
SCAN-12	9	10	9	10	8	10	10	10	10
SCAN-13	0	6	1	0	5	3	1	3	9
SCAN-14	2	7	3	7	7	5	9	6	10
SCAN-15	8	8	5	6	5	7	6	7	10
SCAN-17	0	3	0	9	10	5	10	6	10
SCAN-18	10	10	9	7	10	9	10	10	10
SCAN-19	9	10	8	10	5	8	10	10	8
SCAN-20	5	4	2	3	4	3	8	4	10
SCAN-21	7	7	2	3	10	1	2	8	10
SCAN-22	10	10	8	8	10	10	10	9	10
SCAN-23	6	5	2	8	7	7	6	4	10
SCAN-24	10	9	10	10	10	10	9	10	10
SCAN-25	8	10	4	9	8	9	10	8	10
SCAN-26	8	10	10	10	10	10	10	10	10
SCAN-28	7	8	8	5	8	7	9	10	10
SCAN-29	9	8	9	7	10	10	10	10	10
SCAN-30	9	10	9	10	10	10	10	10	10
SCAN-31	3	4	2	6	8	5	7	3	10
SCAN-32	4	6	2	2	10	3	2	8	10
SCAN-33	10	7	10	8	7	10	10	10	10
SCAN-34	5	5	7	8	2	7	7	7	10
SCAN-35	10	10	8	10	10	9	10	10	10
SCAN-36	9	10	4	8	7	7	10	5	9
SCAN-37	8	9	10	9	10	10	10	10	10
SCAN-39	0	8	6	8	9	5	9	8	7
SCAN-40	2	7	2	2	10	1	2	9	10

Table 11; ASPECTS scores for both changes. first set

ISODENSE SWELLING	R-1	R-2	R-3	R-4	R-5	R-6	R-7	R-8	R-9
SCAN-1	8	7	10	10	10	7	10	7	10
SCAN-2	8	9	9	10	10	9	10	10	10
SCAN-3	10	10	10	10	10	10	10	10	10
SCAN-5	8	8	5	10	10	7	10	10	10
SCAN-6	4	10	7	10	10	7	10	4	10
SCAN-7	8	10	7	10	10	9	10	10	10
SCAN-8	8	10	10	7	10	10	10	10	10
SCAN-9	10	10	10	8	10	10	10	10	10
SCAN-10	7	10	9	10	10	10	10	10	10
SCAN-11	10	8	10	10	10	10	9	10	10
SCAN-12	10	10	10	10	8	10	10	10	10
SCAN-13	0	10	7	10	10	5	10	5	10
SCAN-14	8	10	5	8	9	7	10	8	10
SCAN-15	8	8	10	10	6	7	10	7	10
SCAN-17	0	7	0	10	10	8	10	8	10
SCAN-18	10	10	10	8	10	10	10	10	10
SCAN-19	9	10	8	10	7	9	10	8	10
SCAN-20	5	8	3	10	9	6	10	4	10
SCAN-21	7	8	8	10	10	4	10	10	10
SCAN-22	10	10	8	10	10	10	10	10	10
SCAN-23	10	10	5	10	10	10	7	7	10
SCAN-24	10	10	10	10	10	10	9	10	10
SCAN-25	8	10	6	10	10	10	10	8	10
SCAN-26	8	10	10	10	10	10	10	10	10
SCAN-28	8	10	9	10	9	8	10	10	10
SCAN-29	9	10	10	10	10	10	10	10	10
SCAN-30	9	10	9	10	10	10	10	10	10
SCAN-31	7	4	3	10	8	8	10	5	10
SCAN-32	4	7	3	10	10	6	10	10	10
SCAN-33	10	7	10	10	10	10	10	10	10
SCAN-34	10	10	10	10	10	10	7	10	10
SCAN-35	10	10	8	10	10	8	10	10	10
SCAN-36	9	9	4	10	8	8	10	7	10
SCAN-37	8	9	10	10	10	10	10	10	10
SCAN-39	4	9	6	10	10	7	10	9	7
SCAN-40	2	8	8	10	10	8	10	10	10

Table 12; ASPECTS scores for isodense swelling. First set

HYPODENSITY	R-1	R-2	R-3	R-4	R-5	R-6	R-7	R-8	R-9
SCAN-1	9	10	6	6	10	6	6	9	10
SCAN-2	10	10	10	7	8	7	7	9	10
SCAN-3	10	10	10	10	10	10	10	10	10
SCAN-5	10	9	10	6	10	7	9	10	10
SCAN-6	6	8	5	0	7	4	2	2	9
SCAN-7	8	10	9	9	10	7	9	9	10
SCAN-8	10	9	10	7	10	10	10	10	10
SCAN-9	10	10	10	8	8	10	10	9	10
SCAN-10	9	10	9	9	10	8	10	9	10
SCAN-11	10	8	8	10	9	10	9	9	10
SCAN-12	10	10	9	10	8	10	10	10	10
SCAN-13	9	6	4	0	5	3	1	3	9
SCAN-14	8	7	9	7	7	8	9	8	10
SCAN-15	9	10	5	6	5	7	6	9	10
SCAN-17	9	6	4	9	10	5	10	8	10
SCAN-18	10	10	9	7	10	9	10	10	10
SCAN-19	10	10	10	10	8	9	10	10	10
SCAN-20	8	6	9	3	4	6	8	6	10
SCAN-21	10	9	4	3	10	1	2	8	10
SCAN-22	10	10	10	8	10	10	10	9	10
SCAN-23	6	5	6	8	7	7	6	7	10
SCAN-24	10	9	10	10	10	10	9	10	10
SCAN-25	10	10	9	9	8	9	10	10	10
SCAN-26	10	10	10	10	10	10	10	10	10
SCAN-28	7	8	9	6	8	9	9	9	10
SCAN-29	9	8	9	7	10	10	10	10	10
SCAN-30	10	10	10	10	10	10	10	10	10
SCAN-31	6	10	9	6	8	6	7	6	10
SCAN-32	10	9	9	2	10	3	2	8	10
SCAN-33	10	10	10	8	7	10	10	10	10
SCAN-34	5	5	7	8	2	7	7	7	10
SCAN-35	10	10	10	10	10	10	10	10	10
SCAN-36	10	10	10	8	9	9	10	8	9
SCAN-37	10	10	10	9	10	10	10	10	10
SCAN-39	6	9	10	8	9	6	9	9	10
SCAN-40	8	9	4	2	10	2	2	9	10

Table 13; ASPECTS scores for hypodensity. First set.

CBV ML\100G			MTT SEC			CBF ML\100G\SEC		
ISODENSE SWELLING	HYPOATT ENUATED	NORMAL	ISODENSE SWELLING	HYPOATT ENUATED	NORMAL	ISODENSE SWELLING	HYPOATT ENUATED	NORMAL
10.0787	1.3952	21.3818	5.52483	4.96873	2.676942	35.281	14.0337	25.974
10.3974	2.204	21.5996	6.33092	5.089803	2.720831	10.3974	4.1029	36.8785
10.84	2.47	21.778	6.731104	5.285573	2.720831	25.7133	12.4043	27.4187
11.5818	2.64	21.82	6.790278	5.285573	2.960313	26.5391	4.3642	27.2257
12.0177	2.886	21.8777	6.827653	5.925401	3.80616	14.3522	5.7064	21.8777
13.1	3.3188	22	6.84627	6.432465	4.169544	13.5213	2.886	32.7091
13.1523	3.4451	22.6	7.210319	6.459025	4.240913	18.34	4.0405	33.8719
13.19	3.8	23.2675	7.289161	6.629215	4.388145	17.7762	12.5324	29.3648
13.2671	4.0405	23.46	7.338825	6.686583	4.423879	15.6833	8.8026	26.896
13.4672	4.1029	23.543	7.37	7.164658	4.775658	12.0177	12.2352	21.3255
13.5213	4.1058	23.5748	7.521145	7.703123	4.857464	17.548	4.9638	24.661
13.82	4.166	23.582	7.79706	7.775641	4.96849	13.1523	4.1058	26.027
13.9	4.2604	23.84	7.80836	8.697246	4.996959	14.3157	36.194	31.0087
14.3157	4.3642	23.88	7.846077	8.949469	5.079731	19.9173	7.3055	13.7869
14.3522	4.4801	24.5824	7.933903	9.164581	5.115944	20.2681	9.7488	19.3519
14.4	4.5281	24.62	8.029411	9.22	5.131476	13.4672	7.65	21.3818
14.6056	4.804	24.661	8.261903	9.414064	5.157775	19.656	10.8023	49.3971
15	4.9638	25.1	8.751452	9.432243	5.278867	16.7603	3.3188	40.9325
15.612	4.9794	25.2617	8.96131	9.537468	5.288792	13.2671	12.1419	37.1262
15.6833	5.039	25.6644	9.056336	9.682783	5.294019	13.19	10.19	83.4675
16.191	5.2	25.8	9.390996	10.118181	5.427859	13.82	8.75	16.3568
16.1998	5.6	25.807	9.419049	10.13	5.43239	22.6	5.039	15.9132
16.7603	5.7064	25.974	9.647521	10.218151	5.462219	18.55	3.8	26.8622
16.788	5.7398	26.027	9.682783	10.228017	5.476491	20.3	2.64	12.7901
17.548	6.1205	26.12	9.720539	10.291421	5.485181	13.9	5.6	13.07
17.7762	6.143	26.1823	9.779921	10.318207	5.503384	30.97	5.2	15.2956
18.34	6.1569	26.2	9.85	10.345099	5.504539	18.344	17.4	19.6184
18.344	7.3055	26.26	9.991686	10.394518	5.527813	13.1	4.804	28.0735
18.55	7.65	26.64	10.00919	10.6	5.550259	16.788	4.166	15.3641
18.711	8.5382	26.8622	10.077245	10.881049	5.550831	10.0787	12.8725	17.3258
19.656	8.75	26.896	10.08857	10.89241	5.568498	15	8.5382	13.224
19.839	8.8026	27.2257	10.119399	10.991598	5.640055	14.4	9.482	20.3036
19.9173	9.1926	27.4187	10.155788	11.164637	5.701114	18.711	2.47	34.5326
20.2681	9.482	27.771	10.291421	11.197328	5.712409	23.1	3.4451	32.63
20.3	9.7488	28.0735	10.316151	11.204567	5.712409	11.5818	5.7398	23.46
21.0169	10.19	28.5	10.338224	11.307744	5.750449	34.1856	4.9794	18.8108
21.4394	10.3163	29.3648	10.364828	11.41869	5.780079	23.5837	4.4801	17.8481
22.6	10.76	30.16	10.889998	11.455635	5.80349	10.84	12.2891	20.83
22.7	10.8023	31.0087	11.177371	11.579246	5.821829	14.6056	4.5281	19.683
23.1	12.1419	32.03	11.41869	12.096177	5.833223	28.1922	6.1569	35.5415
23.215	12.2352	32.6237	11.459434	12.178389	5.836774	16.1998	12.2952	32.8193
23.5837	12.2891	32.63	11.552592	12.449391	5.928176	19.839	10.3163	20.289
25.293	12.2952	32.7091	12.104215	12.655656	5.977395	16.191	10.76	35.158
25.7133	12.4043	32.78	12.24752	12.733707	5.978883	21.0169	15.3431	21.5996
26.5391	12.5324	32.8193	12.641343	13.017704	5.988234	21.4394	6.143	23.88
28.1922	12.8725	33.8719	13.172432	13.373694	5.99	41.7056	4.2604	21.82
30.97	13.368	34.5326	13.258983	13.386538	6.035621	31.5593	2.204	26.64
31.5593	13.5393	35.158	13.575391	13.632531	6.044509	23.215	13.5393	24.5824
34.1856	14.0337	35.317	13.802231	13.757729	6.0563	25.293	9.1926	18.92
35.281	15.3431	35.346	14.167705	14.245719	6.05635	22.7	1.3952	15.81
41.7056	17.4	35.5415	14.198427	14.693551	6.06	15.612	6.1205	32.6237
	36.194	35.5851	14.291383	15.853109	6.082532		13.368	26.26
		36.8785	16.95	19.41	6.087055			23.543
		36.979			6.141673			32.03
		37.1262			6.244808			12.208
		40.8111			6.260478			35.317
		40.9325			6.296417			16.167
		41.485			6.296682			21.0207
		49.3971			6.301333			10.06
		83.4675			6.3033			23.582

Table 14; Perfusion parameters for each NCCT appearance.

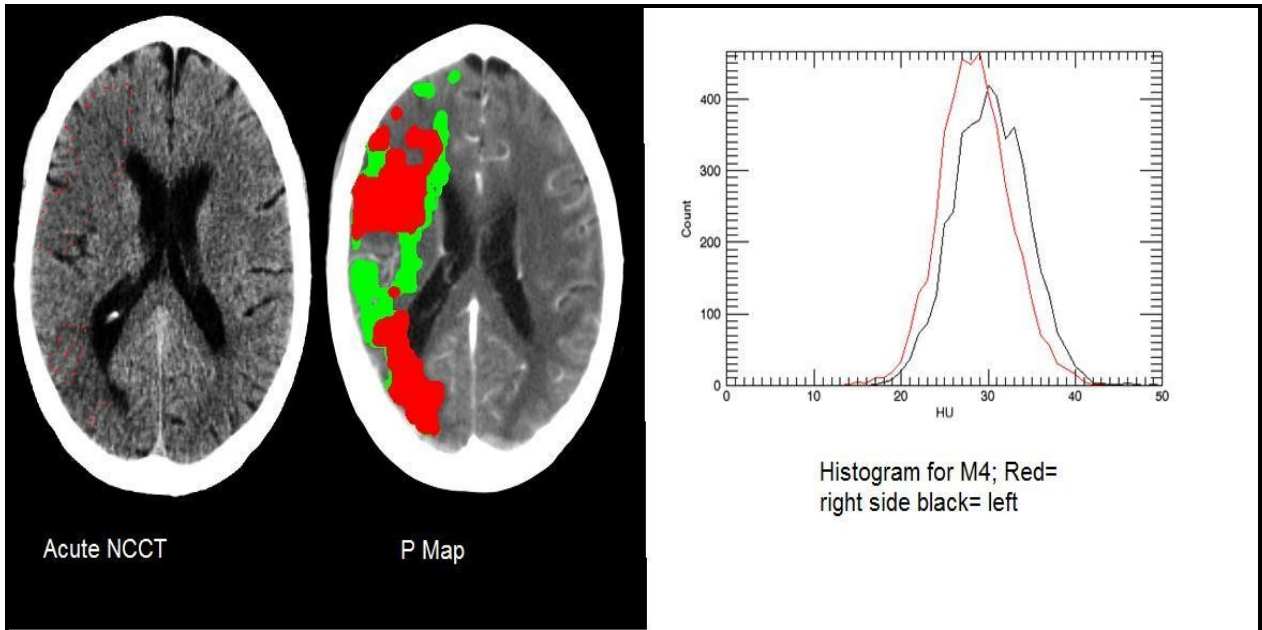


Figure 7: Scans analysis for consensus. Red dots; hypodensity. Green dots; isodense swelling.

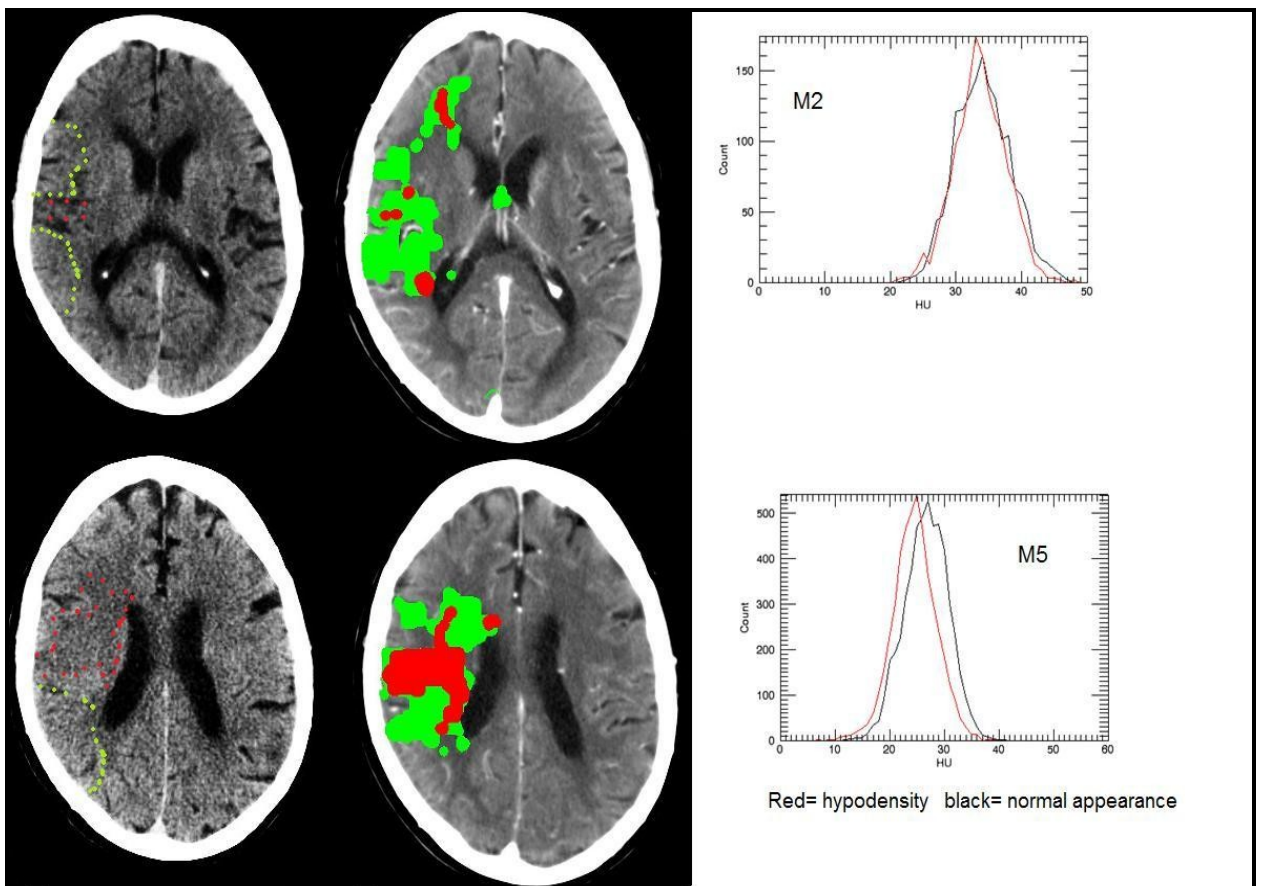


Figure 8: Scans of consensus. Red dots; hypodensity. green dots; isodense swelling.

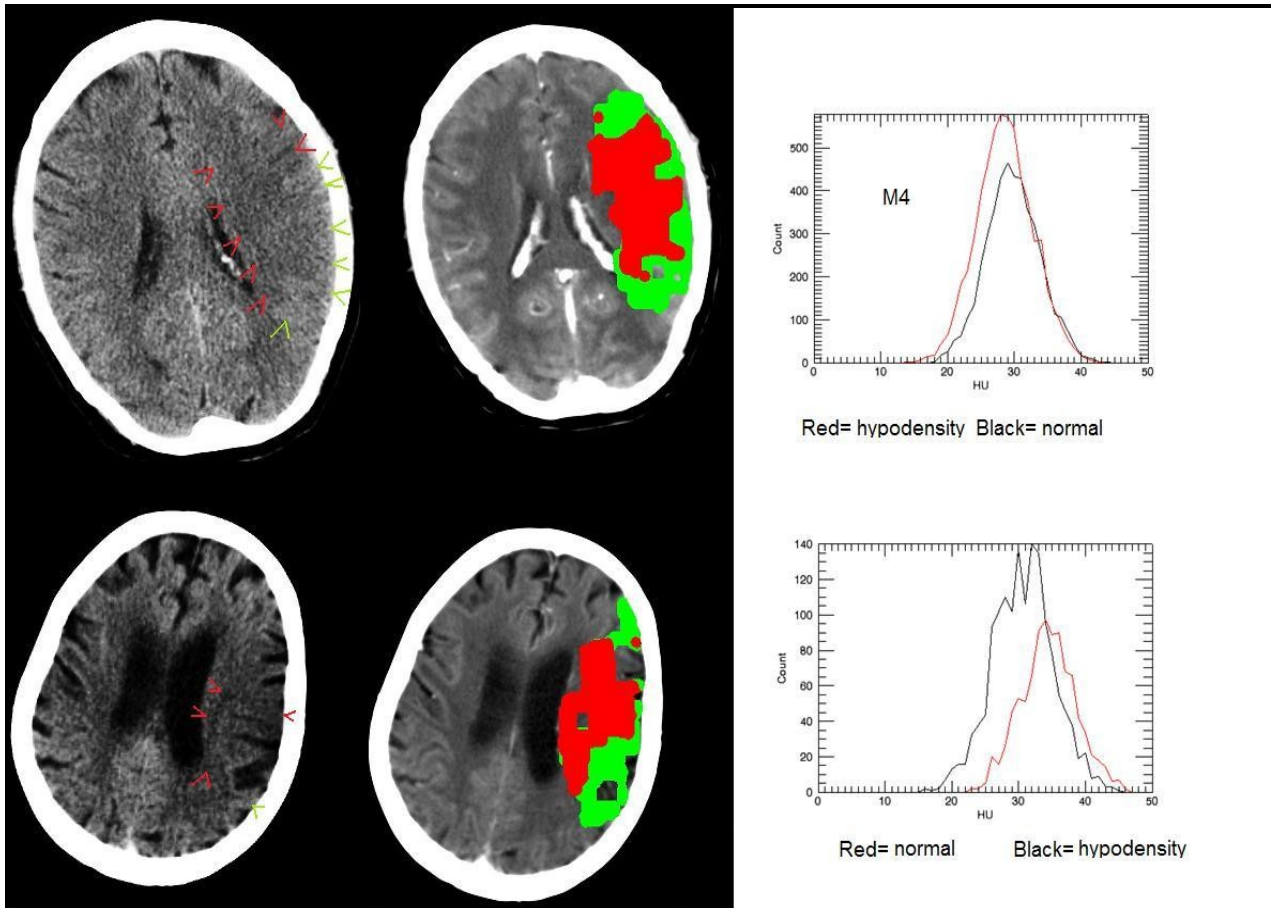


Figure 9: Consensus analysis. Red arrow heads; hypodensity. Green arrows head; Isodense swelling.

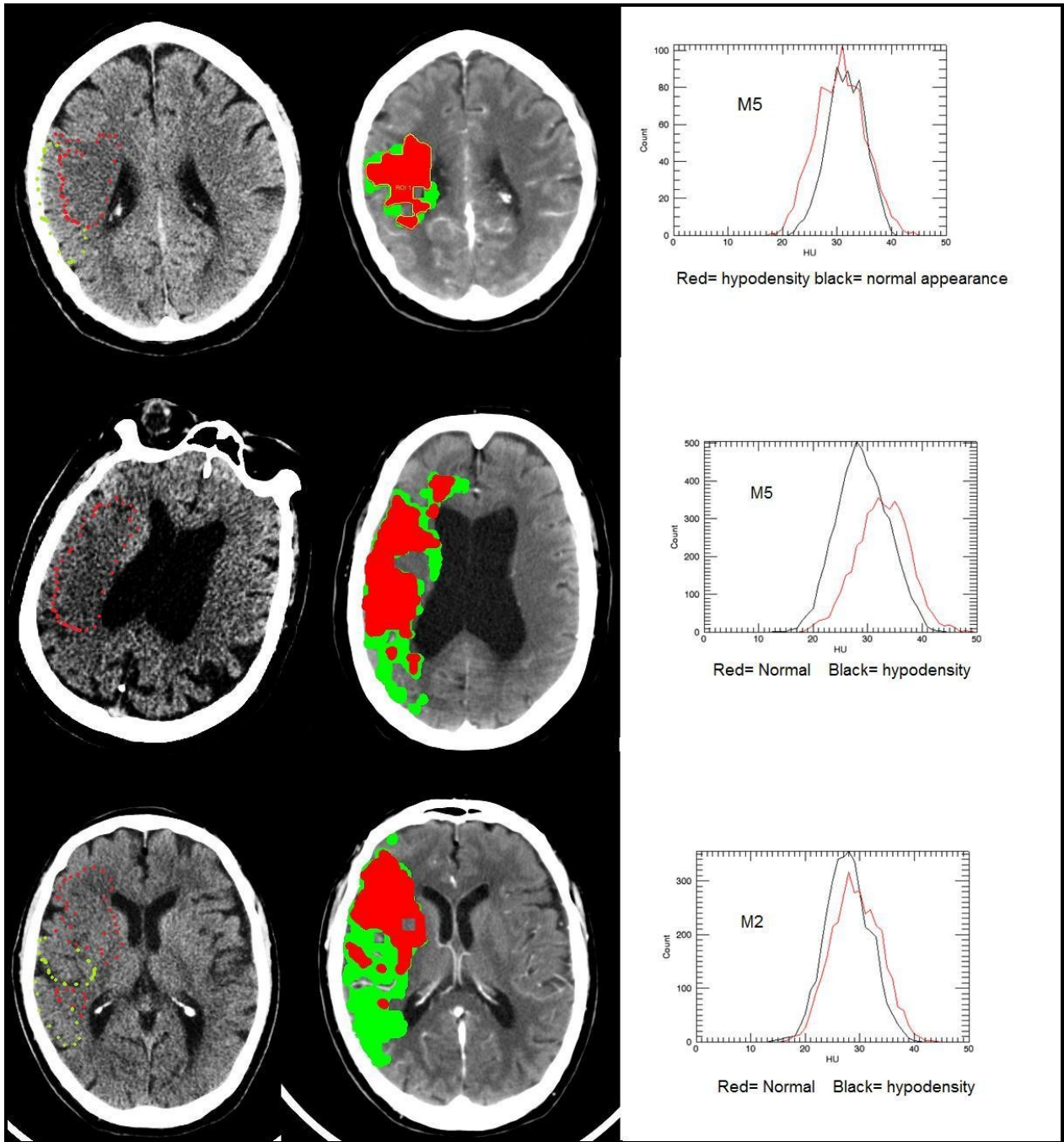


Figure 10: Consensus analysis; red dots; hypodensity. green dots; isodense swelling.

Pairwise kappa tables

Blinded set agreements (without clinical data)			Non-blinded set agreements (with clinical data)		
Total ASPECTS	Hypodensity	Isodense swelling	Total ASPECTS	Hypodensity	Isodense swelling
-0.001	-0.069	-0.103	-0.042	-0.04	-0.277
0.043	-0.043	-0.102	-0.04	0.01	-0.222
0.052	0.044	-0.091	-0.038	0.01	-0.171
0.058	0.046	-0.088	-0.009	0.03	-0.159
0.067	0.073	-0.086	0.008	0.032	-0.153
0.102	0.09	-0.077	0.03	0.033	-0.129
0.136	0.098	-0.07	0.041	0.038	-0.118
0.146	0.109	-0.064	0.055	0.042	-0.115
0.151	0.146	-0.062	0.065	0.049	-0.107
0.219	0.176	-0.061	0.087	0.061	-0.101
0.231	0.197	-0.045	0.096	0.103	-0.089
0.239	0.261	-0.014	0.154	0.13	-0.087
0.259	0.268	0	0.193	0.177	-0.077
0.261	0.288	0	0.368	0.195	-0.077
0.415	0.351	0	0.403	0.211	-0.072
0.456	0.364	0	0.404	0.272	-0.071
0.477	0.383	0	0.426	0.281	-0.01
0.509	0.402	0	0.429	0.288	-0.009
0.52	0.413	0	0.48	0.38	-0.008
0.528	0.444	0	0.516	0.432	-0.007
0.56	0.448	0.033	0.517	0.438	0.032
0.573	0.45	0.033	0.527	0.459	0.051
0.579	0.478	0.102	0.549	0.466	0.063
0.613	0.515	0.274	0.562	0.466	0.069
0.641	0.571	0.308	0.58	0.479	0.07
0.643	0.606	0.313	0.582	0.512	0.084
0.644	0.615	0.333	0.606	0.564	0.175
0.685	0.623	0.357	0.622	0.6	0.183
0.722	0.63	0.43	0.632	0.613	0.256
0.735	0.636	0.451	0.645	0.703	0.257
0.756	0.686	0.483	0.673	0.739	0.334
0.771	0.693	0.483	0.697	0.751	0.402
0.783	0.725	0.611	0.709	0.762	0.402
0.783	0.736	0.625	0.741	0.769	0.453
0.825	0.786	0.669	0.755	0.795	0.478
0.869	0.879	0.75	0.776	0.849	0.609

Table 15: Pairwise kappa for each ASPECTS category when scans are blinded and non-blinded.

Full clinical data			Minimum clinical data		
Total	Hypodensity	Isodense swelling	Total	Hypodensity	Isodense swelling
-0.055	0.017	-0.25	-0.273	-0.253	-0.41
-0.046	0.048	-0.177	-0.084	-0.119	-0.336
-0.025	0.06	-0.143	-0.054	-0.06	-0.317
-0.025	0.08	-0.131	-0.041	-0.059	-0.222
-0.008	0.1	-0.116	-0.007	-0.057	-0.17
0	0.154	-0.115	0.005	-0.034	-0.153
0.023	0.157	-0.084	0.009	-0.024	-0.138
0.151	0.166	-0.084	0.012	-0.02	-0.138
0.19	0.175	0	0.058	-0.008	-0.138
0.217	0.188	0	0.062	0.009	-0.135
0.222	0.241	0	0.094	0.043	-0.13
0.254	0.243	0	0.095	0.053	-0.128
0.348	0.265	0	0.135	0.096	-0.124
0.447	0.291	0	0.146	0.105	-0.115
0.495	0.308	0	0.162	0.207	-0.109
0.565	0.324	0	0.203	0.237	-0.105
0.565	0.339	0	0.217	0.292	-0.088
0.569	0.38	0	0.279	0.297	-0.078
0.604	0.419	0	0.313	0.301	-0.022
0.613	0.421	0	0.359	0.313	0.071
0.633	0.448	0	0.441	0.387	0.072
0.658	0.454	0	0.442	0.388	0.098
0.658	0.525	0.006	0.503	0.396	0.108
0.67	0.55	0.046	0.511	0.418	0.134
0.671	0.556	0.051	0.514	0.491	0.138
0.672	0.579	0.186	0.547	0.519	0.183
0.682	0.652	0.197	0.561	0.62	0.195
0.686	0.718	0.231	0.571	0.63	0.251
0.692	0.727	0.273	0.621	0.667	0.295
0.701	0.729	0.325	0.647	0.722	0.314
0.715	0.73	0.328	0.682	0.722	0.315
0.732	0.771	0.427	0.685	0.776	0.327
0.754	0.776	0.548	0.751	0.781	0.546
0.776	0.783	0.63	0.755	0.857	0.568
0.789	0.789	0.667	0.76	0.879	0.65
0.806	0.882	1	0.762	0.883	0.696

Table 16: Pairwise kappa for each set of scans in relation to amount of clinical data across the three categories of ASPECTS.

Thick slices scans (5mm)			Thin slices scans (0.9mm)		
Total	Hypodensity	Isodense swelling	Total	Hypodensity	Isodense swelling
0.053	0.067	-0.249	-0.144	-0.085	-0.168
0.07	0.088	-0.161	-0.11	-0.062	-0.145
0.071	0.089	-0.159	-0.084	-0.05	-0.136
0.074	0.109	-0.148	-0.077	-0.044	-0.11
0.09	0.114	-0.13	-0.041	-0.028	-0.106
0.093	0.13	-0.125	-0.02	-0.028	-0.088
0.201	0.184	-0.115	0	-0.024	-0.086
0.208	0.222	-0.11	0.022	-0.013	-0.08
0.354	0.266	-0.109	0.049	-0.004	-0.069
0.393	0.288	-0.101	0.057	0	-0.068
0.409	0.313	-0.096	0.088	0.027	-0.068
0.422	0.368	-0.068	0.119	0.084	-0.052
0.43	0.369	-0.036	0.167	0.149	-0.048
0.437	0.377	-0.033	0.192	0.208	-0.047
0.458	0.391	-0.017	0.197	0.266	-0.045
0.499	0.395	-0.017	0.3	0.275	-0.022
0.53	0.409	-0.016	0.412	0.277	-0.018
0.561	0.453	-0.003	0.412	0.312	0.015
0.626	0.499	0	0.423	0.363	0.016
0.63	0.543	0	0.432	0.377	0.079
0.655	0.565	0	0.444	0.394	0.089
0.661	0.566	0	0.466	0.4	0.095
0.663	0.585	0	0.468	0.411	0.099
0.673	0.591	0	0.474	0.444	0.113
0.677	0.62	0	0.538	0.45	0.114
0.68	0.636	0	0.545	0.46	0.116
0.682	0.638	0.126	0.565	0.476	0.246
0.687	0.683	0.138	0.614	0.512	0.287
0.694	0.705	0.168	0.641	0.555	0.348
0.73	0.728	0.203	0.673	0.59	0.365
0.734	0.741	0.249	0.698	0.613	0.432
0.746	0.758	0.517	0.703	0.616	0.436
0.76	0.78	0.636	0.719	0.684	0.506
0.77	0.862	0.644	0.763	0.764	0.508
0.832	0.862	0.665	0.764	0.798	0.535
0.846	0.866	0.723	0.793	0.814	0.566

Table 17: Pairwise kappa for scans with thick slices and scans with thin slices across the three categories of ASPECTS.

Scan's set	Total ASPECTS				Hypodensity				Isodense swelling			
Parameter	APK	CI*	SD**	variance	APK	CI*	SD**	variance	APK	CI*	SD**	variance
Blinded	0.45	0.35-0.54	0.27	0.074	0.39	0.31-0.48	0.26	0.066	0.14	0.06-0.23	0.26	0.068
Non-blinded	0.38	0.29-0.48	0.27	0.077	0.35	0.26-0.45	0.28	0.079	0.051	-0.02-0.12	0.22	0.047
t-test P value	0.965 0.34				0.53 0.62				0.089 1.72			
Full C\D	0.46	0.35-0.45	0.29	0.086	0.42	0.33-0.51	0.25	0.066	0.11	0.02-0.19	0.26	0.071
Minimum C\D	0.32	0.22-0.42	0.29	0.088	0.32	0.21-0.43	0.33	0.11	0.05	-0.05-0.14	0.27	0.77
t-test P value	1.97 0.05				1.42 0.16				548.5* 0.26			
Thick slices	0.50	0.42-0.58	0.24	0.062	0.46	0.38-0.55	0.24	0.061	0.066	-0.02-0.15	0.25	0.065
Thin slices	0.34	0.24-0.44	0.29	0.088	0.31	0.21-0.39	0.27	0.075	0.1	0.02-0.17	0.22	0.049
t-test P value	2.51 0.01				2.64 0.01				-0.60 0.55			

Table 18: Comparison of average pairwise kappa (APK) of each group of variables across the three ASPECTS' categories. [significance level is at $P < 0.05$]. [C\D clinical data, SD; standard deviation, CI; confidence interval]

Total ASPECTS		Hypodensity		Isodense swelling	
Trained	Untrained	Trained	Untrained	Trained	Untrained
0.418	0.072	0.5	0.031	0.301	0.06
0.446	0.587	0.273	0.588	0.473	0.356
0.669	0.505	0.613	0.33	0.649	-0.115
0.471	0.729	0.591	0.273	0.32	0.566
0.603	0.225	0.519	0.472	0.477	-0.045
0.656	0.559	0.633	0.213	0.419	-0.06
0.649	0.731	0.523	0.305	0.629	0.544
0.5	0.557	0.584	0.565	0.141	0.262
0.422	-0.029	0.494	0.042	0.402	0.008
0.213	0.601	-0.053	0.577	0.289	0.252
0.406	0.438	0.035	0.316	0.335	-0.119
0.117	0.537	-0.134	0.269	0.218	0.363
0.339	0.383	0.098	0.538	0.449	0.147
0.381	0.395	0.064	0.222	0.518	-0.188
0.419	0.504	0.273	0.45	0.277	0.304
0.18	0.02	0.106	0.051	0.109	0.026
0.405	0.617	-0.002	0.555	0.254	0.457
0.111	0.564	0.055	0.723	-0.027	-0.015
0.259	0.796	0.11	0.701	0.208	0.435
0.284	0.194	0.28	0.269	0.231	0.048
0.386	0.602	-0.012	0.495	0.454	-0.053
0.448	0.01	0.505	0.046	0.407	-0.053
0.261	0.5	0.305	0.503	0.2	-0.084
0.625	0.754	0.538	0.752	0.593	-0.108
0.534	0.78	0.5	0.782	0.287	-0.083
0.377	0.208	0.259	0.228	0.371	-0.075
0.414	0.109	0.593	0.052	-0.035	-0.058
0.209	0.539	0.266	0.541	0.47	0.259
0.386	0.248	0.13	0.278	0.029	-0.134
0.301	0.188	0.553	0.154	0.012	0.106
0.265	0.048	0.391	0.033	-0.056	0.054
0.419	0.521	0.428	0.534	0.135	0.479
0.337	0.716	0.411	0.866	0.12	-0.135
0.285	0.022	0.313	0.059	0.128	-0.05
0.391	0.538	0.634	0.611	0.174	0.005
0.471	0.064	0.352	0.133	0.589	-0.004
0.71		0.493		0.492	
0.531		0.634		0.321	
0.597		0.428		0.465	
0.522		0.372		0.395	
0.34		0.565		0.188	
0.379		0.294		0.051	
0.559		0.561		0.296	
0.395		0.619		0.064	
0.594		0.622		0.343	
0.565		0.581		0.27	
0.428		0.038		0.65	
0.622		0.461		0.533	
0.452		0.479		0.144	
0.499		0.464		0.366	
0.329		0.224		0.354	
0.513		0.658		0.408	
0.438		0.472		0.346	
0.399		0.317		0.376	
0.143		0.286		0.066	

Table 19: Pairwise kappa for each category of ASPECTS for trained and untrained groups of readers.

Untrained Readers	READE R-1	READER- 2	READER- 3	READER- 4	READER- 5	READER- 6	READER- 7	READER- 8	READER- 9
Pairwise kappa	0.072	-0.029	0.02	0.01	0.109	0.048	0.022	0.064	0.064
	0.587	0.601	0.617	0.5	0.539	0.521	0.538	0.538	0.022
	0.505	0.438	0.564	0.754	0.248	0.716	0.716	0.521	0.048
	0.729	0.537	0.796	0.78	0.188	0.188	0.248	0.539	0.109
	0.225	0.383	0.194	0.208	0.208	0.78	0.754	0.5	0.01
	0.559	0.395	0.602	0.602	0.194	0.796	0.564	0.617	0.02
	0.731	0.504	0.504	0.395	0.383	0.537	0.438	0.601	-0.029
0.557	0.557	0.731	0.559	0.225	0.729	0.505	0.587	0.072	
APK	0.49	0.42	0.50	0.47	0.26	0.53	0.47	0.49	0.039

Table 20: Pairwise kappa of each untrained reader on total ASPECTS with overall average [APK].

Trained Readers	Reader1	Reader2	Reader3	Reader4	Reader5	Reader6	Reader7	Reader8	Reader9	Reader 10	Reader 11
Pairwise kappa	0.418	0.406	0.284	0.209	0.391	0.34	0.565	0.499	0.438	0.143	0.143
	0.446	0.117	0.386	0.386	0.471	0.379	0.428	0.329	0.399	0.399	0.438
	0.669	0.339	0.448	0.301	0.71	0.559	0.622	0.513	0.513	0.329	0.499
	0.471	0.381	0.261	0.265	0.531	0.395	0.452	0.452	0.622	0.428	0.565
	0.603	0.419	0.625	0.419	0.597	0.594	0.594	0.395	0.559	0.379	0.34
	0.656	0.18	0.534	0.337	0.522	0.522	0.597	0.531	0.71	0.471	0.391
	0.649	0.405	0.377	0.285	0.285	0.337	0.419	0.265	0.301	0.386	0.209
	0.5	0.111	0.414	0.414	0.377	0.534	0.625	0.261	0.448	0.386	0.284
0.422	0.259	0.422	0.5	0.405	0.18	0.419	0.381	0.339	0.117	0.406	
APK	0.213	0.213	0.422	0.5	0.649	0.656	0.603	0.471	0.669	0.446	0.418
APK	0.50	0.28	0.42	0.37	0.49	0.45	0.53	0.41	0.50	0.35	0.37

Table 21: Pairwise kappa of each trained reader on total ASPECTS with overall average [APK].

Untrained	READER- 1	READER- 2	READER- 3	READER- 4	READER- 5	READER- 6	READER- 7	READER- 8	READER- 9
Pairwise Kappa	0.031	0.042	0.051	0.046	0.052	0.033	0.059	0.133	0.133
	0.588	0.577	0.555	0.503	0.541	0.534	0.611	0.611	0.059
	0.33	0.316	0.723	0.752	0.278	0.866	0.866	0.534	0.033
	0.273	0.269	0.701	0.782	0.154	0.154	0.278	0.541	0.052
	0.472	0.538	0.269	0.228	0.228	0.782	0.752	0.503	0.046
	0.213	0.222	0.495	0.495	0.269	0.701	0.723	0.555	0.051
	0.305	0.45	0.45	0.222	0.538	0.269	0.316	0.577	0.042
0.565	0.565	0.305	0.213	0.472	0.273	0.33	0.588	0.031	
APK	0.35	0.37	0.44	0.41	0.32	0.45	0.49	0.50	0.055

Table 22: Pairwise kappa of each untrained reader on hypodensity with overall average.

Trained	READER-1	READER-2	READER-3	READER-4	READER-5	READER-6	READER-7	READER-8	READER-9	READER-10	READER-11
Pairwise Kappa	0.5	0.035	0.28	0.266	0.634	0.565	0.581	0.464	0.472	0.286	0.286
	0.273	-0.134	-0.012	0.13	0.352	0.294	0.038	0.224	0.317	0.317	0.472
	0.613	0.098	0.505	0.553	0.493	0.561	0.461	0.658	0.658	0.224	0.464
	0.591	0.064	0.305	0.391	0.634	0.619	0.479	0.479	0.461	0.038	0.581
	0.519	0.273	0.538	0.428	0.428	0.622	0.622	0.619	0.561	0.294	0.565
	0.633	0.106	0.5	0.411	0.372	0.372	0.428	0.634	0.493	0.352	0.634
	0.523	-0.002	0.259	0.313	0.313	0.411	0.428	0.391	0.553	0.13	0.266
	0.584	0.055	0.593	0.593	0.259	0.5	0.538	0.305	0.505	-0.012	0.28
	0.494	0.11	0.11	0.055	-0.002	0.106	0.273	0.064	0.098	-0.134	0.035
-0.053	-0.053	0.494	0.584	0.523	0.633	0.519	0.591	0.613	0.273	0.5	
APK	0.47	0.05	0.36	0.37	0.40	0.46	0.44	0.44	0.47	0.17	0.41

Table 23: Pairwise kappa of trained readers on hypodensity with overall average.

Untrained	READER-1	READER-2	READER-3	READER-4	READER-5	READER-6	READER-7	READER-8	READER-9
Pairwise Kappa	0.06	0.008	0.026	-0.053	-0.058	0.054	-0.05	-0.004	-0.004
	0.356	0.252	0.457	-0.084	0.259	0.479	0.005	0.005	-0.05
	-0.115	-0.119	-0.015	-0.108	-0.134	-0.135	-0.135	0.479	0.054
	0.566	0.363	0.435	-0.083	0.106	0.106	-0.134	0.259	-0.058
	-0.045	0.147	0.048	-0.075	-0.075	-0.083	-0.108	-0.084	-0.053
	-0.06	-0.188	-0.053	-0.053	0.048	0.435	-0.015	0.457	0.026
	0.544	0.304	0.304	-0.188	0.147	0.363	-0.119	0.252	0.008
0.262	0.262	0.544	-0.06	-0.045	0.566	-0.115	0.356	0.06	
APK	0.20	0.13	0.22	-0.088	0.031	0.22	-0.08	0.22	-0.002

Table 24: Pairwise kappa untrained readers on isodense swelling with overall average.

Trained	READER-1	READER-2	READER-3	READER-4	READER-5	READER-6	READER-7	READER-8	READER-9	READER-10	READER-11
Pairwise Kappa	0.301	0.335	0.231	0.47	0.174	0.188	0.27	0.366	0.346	0.066	0.066
	0.473	0.218	0.454	0.029	0.589	0.051	0.65	0.354	0.376	0.376	0.346
	0.649	0.449	0.407	0.012	0.492	0.296	0.533	0.408	0.408	0.354	0.366
	0.32	0.518	0.2	-0.056	0.321	0.064	0.144	0.144	0.533	0.65	0.27
	0.477	0.277	0.593	0.135	0.465	0.343	0.343	0.064	0.296	0.051	0.188
	0.419	0.109	0.287	0.12	0.395	0.395	0.465	0.321	0.492	0.589	0.174
	0.629	0.254	0.371	0.128	0.128	0.12	0.135	-0.056	0.012	0.029	0.47
	0.141	-0.027	-0.035	-0.035	0.371	0.287	0.593	0.2	0.407	0.454	0.231
	0.402	0.208	0.208	-0.027	0.254	0.109	0.277	0.518	0.449	0.218	0.335
	0.289	0.289	0.402	0.141	0.629	0.419	0.477	0.32	0.649	0.473	0.301
APK	0.41	0.26	0.31	0.091	0.38	0.23	0.39	0.26	0.40	0.33	0.27

Table 25: Pairwise kappa of trained readers on isodense swelling with overall average(APK).

Untrained	Reader-1	Reader-2	Reader-3	Reader-6	Reader-8
Pairwise kappa	0.587	0.601	0.617	0.521	0.521
	0.729	0.537	0.796	0.796	0.617
	0.731	0.504	0.504	0.537	0.601
	0.557	0.557	0.731	0.729	0.587
APK	0.651	0.54975	0.662	0.64575	0.5815

Table 26: Pairwise kappa of untrained readers after exclusion of outliers on total ASPECTS with overall average.

Trained	Reader-1	Reader-3	Reader-5	Reader-7	Reader-9
Pairwise kappa	0.669	0.448	0.71	0.622	0.622
	0.603	0.625	0.597	0.594	0.559
	0.656	0.377	0.522	0.597	0.71
	0.649	0.422	0.649	0.603	0.669
APK	0.64425	0.468	0.6195	0.604	0.64

Table 27: Pairwise kappa of trained readers after exclusion of outliers on total ASPECTS with overall average.

Untrained	Reader-1	Reader-2	Reader-3	Reader-6	Reader-8
Pairwise kappa	0.588	0.577	0.555	0.534	0.534
	0.273	0.269	0.701	0.701	0.555
	0.305	0.45	0.45	0.269	0.577
	0.565	0.565	0.305	0.273	0.588
APK	0.43275	0.46525	0.50275	0.44425	0.5635

Table 28: Pairwise kappa of untrained readers after exclusion of outliers on hypodensity with overall average.

Trained	Reader-1	Reader-3	Reader-5	Reader-7	Reader-9
Pairwise kappa	0.613	0.505	0.493	0.461	0.461
	0.519	0.538	0.428	0.428	0.493
	0.523	0.259	0.259	0.538	0.505
	0.494	0.494	0.523	0.519	0.613
APK	0.53725	0.449	0.42575	0.4865	0.518

Table 29: Pairwise kappa of trained readers after exclusion of outliers on hypodensity with overall average.

Untrained	Reader-1	Reader-2	Reader-3	Reader-6	Reader-8
Pairwise kappa	0.356	0.252	0.457	0.479	0.479
	0.566	0.363	0.435	0.435	0.457
	0.544	0.304	0.304	0.363	0.252
	0.262	0.262	0.544	0.566	0.356
APK	0.432	0.29525	0.435	0.46075	0.386

Table 30: Pairwise kappa of untrained readers after exclusion of outliers on isodense swelling with overall average.

Trained	Reader-1	Reader-3	Reader-5	Reader-7	Reader-9
Pairwise kappa	0.649	0.407	0.492	0.533	0.533
	0.477	0.593	0.465	0.465	0.492
	0.629	0.371	0.371	0.593	0.407
	0.402	0.402	0.629	0.477	0.649
APK	0.53925	0.44325	0.48925	0.517	0.52025

Table 31: Pairwise kappa of trained readers after exclusion of outliers on isodense swelling with overall average.

Total ASPECTS		Hypodensity		Isodense swelling	
Pre-training	Post-training	Pre-training	Post-training	Pre-training	Post-training
0.395	0.111	0.213	-0.053	-0.188	-0.035
0.504	0.18	0.222	0.055	-0.083	-0.027
0.537	0.213	0.269	0.106	-0.06	0.109
0.557	0.259	0.273	0.11	-0.053	0.12
0.559	0.337	0.305	0.411	0.262	0.141
0.602	0.414	0.45	0.494	0.304	0.208
0.729	0.422	0.495	0.5	0.363	0.287
0.731	0.5	0.565	0.584	0.435	0.289
0.78	0.534	0.701	0.593	0.544	0.402
0.796	0.656	0.782	0.633	0.566	0.419

Table 32: Pairwise kappa of same readers before and after training for each ASPECTS category.

READER-A1	READER-A2	READER-B1	READER-B2	READER-C1	READER-C2	READER-D1	READER-D2	READER-E1	READER-E2
0.729	0.656	0.557	0.18	0.731	0.534	0.559	0.337	0.559	0.337
0.78	0.5	0.395	0.111	0.602	0.414	0.602	0.414	0.731	0.534
0.796	0.422	0.504	0.259	0.504	0.422	0.395	0.111	0.557	0.18
0.537	0.213	0.537	0.213	0.796	0.422	0.78	0.5	0.729	0.656
0.273	0.633	0.565	0.106	0.305	0.5	0.213	0.411	0.213	0.411
0.782	0.584	0.222	0.055	0.495	0.593	0.495	0.593	0.305	0.5
0.701	0.494	0.45	0.11	0.45	0.11	0.222	0.055	0.565	0.106
0.269	-0.053	0.269	-0.053	0.701	0.494	0.782	0.584	0.273	0.633
0.566	0.419	0.262	0.109	0.544	0.287	-0.06	0.12	-0.06	0.12
-0.083	0.141	-0.188	-0.027	-0.053	-0.035	-0.053	-0.035	0.544	0.287
0.435	0.402	0.304	0.208	0.304	0.208	-0.188	-0.027	0.262	0.109
0.363	0.289	0.363	0.289	0.435	0.402	-0.083	0.141	0.566	0.419

Table 33: Pairwise kappa of each reader before and after training for each ASPECTS category. (1) pre training (2) post training.

Total ASPECTS		Hypodensity		Isodense swelling	
Neuroradiologists	Stroke neurologists	Neuroradiologists	Stroke neurologists	Neuroradiologists	Stroke neurologists
0.143	0.669	0.266	0.613	0.47	0.649
0.391	0.471	0.13	0.591	0.029	0.32
0.471	0.603	0.313	0.519	0.128	0.477
0.209	0.656	0.634	0.633	0.174	0.419
0.386	0.422	0.352	0.494	0.589	0.402
0.285	0.213	0.286	-0.053	0.066	0.289
	0.513		0.658		0.533
	0.339		0.098		0.144
	0.381		0.064		0.407
	0.419		0.273		0.2
	0.18		0.106		0.593
	0.259		0.11		0.287
	0.622		0.461		0.296
	0.452		0.479		0.064
	0.448		0.505		0.343
	0.261		0.305		0.449
	0.625		0.538		0.518
	0.534		0.5		0.277
	0.559		0.561		0.109
	0.395		0.619		0.208
	0.594		0.613		0.408

Table 34: Pairwise kappa in each ASPECTS category for neuroradiologists and stroke physicians.

Stroke neurologists					
Total ASPECTS		Hypodensity		Isodense swelling	
Trained	Untrained	Trained	Untrained	Trained	Untrained
0.587, 0.601, 0.617	0.669, 0.339, 0.448	0.588, 0.577, 0.555	0.613, 0.098, 0.505	0.356, 0.252 0.566, 0.363	0.649, 0.2, 0.277 0.32, 0.593,
0.729, 0.537, 0.796	0.471, 0.381, 0.261	0.273, 0.269, 0.701	0.591, 0.064, 0.305	-0.045, 0.147 0.544, 0.304	0.109 0.477, 0.287,
0.225, 0.383, 0.194	0.603, 0.419, 0.625	0.472, 0.538, 0.269	0.519, 0.273, 0.538	0.262, 0.479 0.457, 0.259	0.208 0.419, 0.296,
0.731, 0.504, 0.557, 0.539, 0.521, 0.188,	0.656, 0.18, 0.534 0.422, 0.259, 0.559 0.213, 0.622, 0.395 0.513, 0.452, 0.594	0.305, 0.45, 0.565, 0.541, 0.534, 0.154,	0.633, 0.106, 0.5 0.494, 0.11, 0.561 -0.053, 0.461, 0.619 0.658, 0.479, 0.622	0.435, 0.106 0.048,	0.408 0.402, 0.064, 0.289, 0.343, 0.533, 0.449, 0.144, 0.518, 0.407, ,

Table 35: Pairwise kappa of stroke neurologists for each ASPECTS category before and after training.

Parameter	Neuroradiologists*			Stroke neurologists**		
	Trained	Untrained	P Value	Trained	Untrained	P value
Total ASPECTS	11.67	21	0.13	0.46	0.51	>0.05
Hypodensity	11.50	20	0.13	0.41	0.45	>0.05
Isodense swelling	8.33	0	0.13	0.35	0.30	>0.05

Table 36: Comparison of average pairwise kappa between different specialities before and after training.

Experts					
Total ASPECTS		Hypodensity		Isodense swelling	
Trained	Untrained	Trained	Untrained	Trained	Untrained
0.649, 0.285 0.5, 0.405 0.422, 0.111 0.213, 0.259 , 0.377 , 0.414	0.438, 0.564 0.537, 0.796 0.395, 0.602 0.504, 0.754 0.716, 0.78	0.523, 0.584, 0.494, -0.053 ,0.313, -0.002 0.055,0.11 ,0.259 ,0.593	0.316, 0.723 0.269, 0.701 0.222, 0.495 0.45, 0.752 0.866, 0.782	0.629, 0.254 0.141, -0.027 0.402, 0.208 0.289, 0.371 0.128, -0.035	-0.119, -0.015, 0.363, 0.435, -0.188, -0.053, 0.304, -0.108, -0.135, -0.083, , ,

Table 37: Pairwise kappa of trained and untrained expert readers for each ASPECTS category.

Trainees					
Total ASPECTS		Hypodensity		Isodense swelling	
Trained	Untrained	Trained	Untrained	Trained	Untrained
0.34, 0.565, 0.499	0.064, 0.539 0.109, 0.587	0.565, 0.581, 0.464	0.541, 0.133 0.588, 0.052	0.188, 0.27, 0.366	0.259, -0.004 0.356, -0.058
0.379, 0.428, 0.329	0.072, 0.225	0.294, 0.038, 0.224	0.472, 0.031	0.051, 0.65, 0.354	-0.045, 0.06
0.559, 0.622, 0.513		0.561, 0.461, 0.658		0.296, 0.533, 0.408	
0.395, 0.452, 0.594, 0.438, 0.143, 0.399,		0.619, 0.479, 0.622, 0.472, 0.286, 0.317,		0.064, 0.144, 0.343, 0.346, 0.066, 0.376,	

Table 38: Pairwise kappa of trained and untrained trainee readers for each ASPECTS category.

Reference List

- (1) Moustafa RR, Baron JC. Pathophysiology of ischaemic stroke: insights from imaging, and implications for therapy and drug discovery. *Br J Pharmacol* 2008 Mar;153 Suppl 1:S44-S54.
- (2) Donnan GA, Fisher M, Macleod M, Davis SM. Stroke. *The Lancet* 2008 May 10;371(9624):1612-23.
- (3) Feigin VL, Lawes CM, Bennett DA, Anderson CS. Stroke epidemiology: a review of population-based studies of incidence, prevalence, and case-fatality in the late 20th century. *The Lancet Neurology* 2003 Jan;2(1):43-53.
- (4) Falk E. Pathogenesis of Atherosclerosis. *J Am Coll Cardiol* 2006 Apr 18;47(8_Suppl_C):C7-12.
- (5) Brainin M, Heiss WD. *Textbook of Stroke Medicine*. Cambridge University Press; 2009.
- (6) Sacco RL, Benjamin EJ, Broderick JP, Dyken M, Easton JD, Feinberg WM, et al. Risk Factors. *Stroke* 1997 Jul 1;28(7):1507-17.
- (7) Strandgaard S, Paulson OB. Pathophysiology of Stroke. *Journal of Cardiovascular Pharmacology* 1990;15.
- (8) R.Ross JGalH. Response to injury and atherogenesis. *Am J Pathol* 1977;86 (3):675-84.
- (9) Alistair Lammie G. Pathology of small vessel stroke. *British Medical Bulletin* 2000 Jan 1;56(2):296-306.
- (10) Lammie GA, Brannan F, Slattery J, Warlow C. Nonhypertensive Cerebral Small-Vessel Disease : An Autopsy Study. *Stroke* 1997 Nov 1;28(11):2222-9.
- (11) Dirnagl U, Iadecola C, Moskowitz MA. Pathobiology of ischaemic stroke: an integrated view. *Trends in Neurosciences* 1999 Sep 1;22(9):391-7.
- (12) Wood JH. *Cerebral Blood Flow. Physiologic and Clinical Aspects*. 107 ed. 1987.
- (13) Zülch KJ & Hossmann V. Patterns of cerebral infarctions . In: Vinken PJ BGKHTJe, editor. *Handbook of Clinical Neurology: Vascular Disease* .Amsterdam: Elsevier Science ; 1988. p. 175
198.
- (14) LASSEN NA, CHRISTENSEN MS. PHYSIOLOGY OF CEREBRAL BLOOD FLOW. *British Journal of Anaesthesia* 1976 Aug 1;48(8):719-34.
- (15) Paciaroni M, Caso V, Agnelli G. The Concept of Ischemic Penumbra in Acute Stroke and Therapeutic Opportunities. *European Neurology* 2009;61(6):321-30.

- (16) Astrup J, Siesjo BK, Symon L. Thresholds in cerebral ischemia - the ischemic penumbra. *Stroke; a journal of cerebral circulation* 1981;12(6):723-5.
- (17) Fisher M, Ginsberg M. Current Concepts of the Ischemic Penumbra. *Stroke* 2004 Nov 1;35(11 suppl 1):2657-8.
- (18) Ramos-Cabrer P, Campos F, Sobrino T, Castillo J. Targeting the Ischemic Penumbra. *Stroke* 2011 Jan 1;42(1 suppl 1):S7-S11.
- (19) Hossmann KA. Viability thresholds and the penumbra of focal ischemia. *Ann Neurol* 1994;36(4):557-65.
- (20) Ginsberg MD PW. The ischemic penumbra, injury thresholds and therapeutic time window for acute stroke. *Ann Neurol* 1994;36:553-554:553-4.
- (21) Hakim AM. The cerebral ischemic penumbra. *The Canadian journal of neurological sciences Le journal canadien des sciences neurologiques* 1987;14:557-9.
- (22) Baron JC, von KR, del Zoppo GJ. Treatment of acute ischemic stroke. Challenging the concept of a rigid and universal time window. *Stroke* 1995 Dec;26(12):2219-21.
- (23) Markus HS. Cerebral perfusion and stroke. *J Neurol Neurosurg Psychiatry* 2004 Mar;75(3):353-61.
- (24) Powers WJ. Cerebral hemodynamics in ischemic cerebrovascular disease. *Ann Neurol* 1991;29(3):231-40.
- (25) Pulsinelli W. Pathophysiology of acute ischaemic stroke. *Lancet* 1992 Feb;339(8792):533-6.
- (26) Raichle ME. The pathophysiology of brain ischemia. *Ann Neurol* 1983;13(1):2-10.
- (27) Smith WS. Pathophysiology of Focal Cerebral Ischemia: a Therapeutic Perspective. *Journal of vascular and interventional radiology : JVIR* 15[1], S3-S12. 1-1-2004.
- Ref Type: Abstract
- (28) Gary A. Ischemic brain edema. *Progress in Cardiovascular Diseases* 1999 Nov;42(3):209-16.
- (29) Kahle KT, Simard JM, Staley KJ, Nahed BV, Jones PS, Sun D. Molecular Mechanisms of Ischemic Cerebral Edema: Role of Electroneutral Ion Transport. *Physiology* 2009 Aug 1;24(4):257-65.
- (30) Simard JM, Kent TA, Chen M, Tarasov KV, Gerzanich V. Brain oedema in focal ischaemia: molecular pathophysiology and theoretical implications. *The Lancet Neurology* 2007 Mar;6(3):258-68.
- (31) Matsumoto K, Lo EH, Pierce AR, Wei H, Garrido L, Kowall NW. Role of vasogenic edema and tissue cavitation in ischemic evolution on diffusion-weighted

imaging: comparison with multiparameter MR and immunohistochemistry. *American Journal of Neuroradiology* 1995 May 1;16(5):1107-15.

(32) Liang D, Bhatta S, Gerzanich V, Simard JM. Cytotoxic edema: mechanisms of pathological cell swelling. *Neurosurgical Focus* 2007 May 1;22(5):1-9.

(33) Klatzo I. Pathophysiological aspects of brain edema. *Acta Neuropathologica* 1987 Sep 1;72(3):236-9.

(34) Fisher M. Characterizing the Target of Acute Stroke Therapy. *Stroke* 1997 Apr 1;28(4):866-72.

(35) Heiss WD, Thiel A, Grond M, Graf R. Which Targets Are Relevant for Therapy of Acute Ischemic Stroke? *Stroke* 1999 Jul 1;30(7):1486-9.

(36) Albers GW APEJSRTP. Antithrombotic and thrombolytic therapy for ischemic stroke. American College of Chest Physicians evidence-based clinical practice guidelines (8th edition). National Guideline Clearinghouse,NGC 2008 Available from: URL: <http://www.guideline.gov>

(37) Gladstone DJ, Black SE. Update on intravenous tissue plasminogen activator for acute stroke: from clinical trials to clinical practice. *Canadian Medical Association Journal* 2001 Aug 7;165(3):311-7.

(38) Chiu D, Krieger D, Villar-Cordova C, Kasner SE, Morgenstern LB, Bratina PL, et al. Intravenous Tissue Plasminogen Activator for Acute Ischemic Stroke : Feasibility, Safety, and Efficacy in the First Year of Clinical Practice. *Stroke* 1998 Jan 1;29(1):18-22.

(39) Wardlaw JM, Sandercock PA, Berge E. Thrombolytic therapy with recombinant tissue plasminogen activator for acute ischemic stroke: where do we go from here? A cumulative meta-analysis. *Stroke* 2003 Jun;34(6):1437-42.

(40) Albers GW, Bates VE, Clark WM, Bell R, Verro P, Hamilton SA. Intravenous Tissue-Type Plasminogen Activator for Treatment of Acute Stroke. *JAMA: The Journal of the American Medical Association* 2000 Mar 1;283(9):1145-50.

(41) Wardlaw JM, Warlow CP, Counsell C. Systematic review of evidence on thrombolytic therapy for acute ischaemic stroke. *Lancet* 1997 Aug 30;350(9078):607-14.

(42) The National Institute of Neurological Disorders and Stroke NINDAS. Tissue Plasminogen Activator for Acute Ischemic Stroke. *N Engl J Med* 1995 Dec 14;333(24):1581-8.

(43) Hacke W, Kaste M, Fieschi C, Toni D, Lesaffre E, von KR, et al. Intravenous thrombolysis with recombinant tissue plasminogen activator for acute hemispheric stroke. The European Cooperative Acute Stroke Study (ECASS). *JAMA* 1995 Oct 4;274(13):1017-25.

(44) Hacke W, Kaste M, Fieschi C, von KR, Davalos A, Meier D, et al. Randomised double-blind placebo-controlled trial of thrombolytic therapy with intravenous

alteplase in acute ischaemic stroke (ECASS II). Second European-Australasian Acute Stroke Study Investigators. *Lancet* 1998 Oct 17;352(9136):1245-51.

(45) Clark WM, Wissman S, Albers GW, Jhamandas JH, Madden KP, Hamilton S, et al. Recombinant Tissue-Type Plasminogen Activator (Alteplase) for Ischemic Stroke 3 to 5 Hours After Symptom Onset. *JAMA: The Journal of the American Medical Association* 1999 Dec 1;282(21):2019-26.

(46) Albers GW, Clark WM, Madden KP, Hamilton SA. ATLANTIS Trial. *Stroke* 2002 Feb 1;33(2):493-6.

(47) Wahlgren N, Ahmed N, Davalos A, Ford GA, Grond M, Hacke W, et al. Thrombolysis with alteplase for acute ischaemic stroke in the Safe Implementation of Thrombolysis in Stroke-Monitoring Study (SITS-MOST): an observational study. *The Lancet* 2005;369(9558):275-82.

(48) Hacke W, Kaste M, Bluhmki E, Brozman M, Davalos A, Guidetti D, et al. Thrombolysis with alteplase 3 to 4.5 hours after acute ischemic stroke. *N Engl J Med* 2008 Sep 25;359(13):1317-29.

(49) Lansberg MG, Bluhmki E, Thijs VN. Efficacy and Safety of Tissue Plasminogen Activator 3 to 4.5 Hours After Acute Ischemic Stroke. *Stroke* 2009 Jul 1;40(7):2438-41.

(50) Wahlgren N, Ahmed N, Davalos A, Hacke W, Millan M+, Muir K, et al. Thrombolysis with alteplase 3-4.5 h after acute ischaemic stroke (SITS-ISTR): an observational study. *The Lancet* 2008 Oct 11;372(9646):1303-9.

(51) The benefits and harms of intravenous thrombolysis with recombinant tissue plasminogen activator within 6 h of acute ischaemic stroke (the third international stroke trial [IST-3]): a randomised controlled trial. *The Lancet* 2008;379(9834):2352-63.

(52) Davis SM, Donnan GA, Parsons MW, Levi C, Butcher KS, Peeters A, et al. Effects of alteplase beyond 3 h after stroke in the Echoplanar Imaging Thrombolytic Evaluation Trial (EPITHET): a placebo-controlled randomised trial. *Lancet Neurol* 2008 Apr;7(4):299-309.

(53) Graham GD. Tissue Plasminogen Activator for Acute Ischemic Stroke in Clinical Practice. *Stroke* 2003 Dec 1;34(12):2847-50.

(54) O'Connor RE, McGraw P, Edelson L. Thrombolytic Therapy for Acute Ischemic Stroke: Why the Majority of Patients Remain Ineligible for Treatment. *Annals of emergency medicine* 33[1], 9-14. 1-1-1999.

Ref Type: Abstract

(55) Carter-Jones CR. Stroke thrombolysis: Barriers to implementation. *International emergency nursing* 19[1], 53-57. 1-1-2011.

Ref Type: Abstract

- (56) Albers GW, Thijs VN, Wechsler L, Kemp S, Schlaug G, Skalabrin E, et al. Magnetic resonance imaging profiles predict clinical response to early reperfusion: The diffusion and perfusion imaging evaluation for understanding stroke evolution (DEFUSE) study. *Ann Neurol* 2006;60(5):508-17.
- (57) Zaheer Z, Robinson T, Mistri AK. Thrombolysis in acute ischaemic stroke: an update. *Therapeutic Advances in Chronic Disease* 2011 Mar 1;2(2):119-31.
- (58) Furlan AJ, Eyding D, Albers GW, Al-Rawi Y, Lees KR, Rowley HA, et al. Dose Escalation of Desmoteplase for Acute Ischemic Stroke (DEDAS): evidence of safety and efficacy 3 to 9 hours after stroke onset. *Stroke* 2006 May;37(5):1227-31.
- (59) Hacke W, Furlan AJ, Al-Rawi Y, Davalos A, Fiebich JB, Gruber F, et al. Intravenous desmoteplase in patients with acute ischaemic stroke selected by MRI perfusion-diffusion weighted imaging or perfusion CT (DIAS-2): a prospective, randomised, double-blind, placebo-controlled study. *Lancet Neurol* 2009 Feb;8(2):141-50.
- (60) Almandoz JED, Pomerantz SR, Gonz+ílez RG, Lev MH. Imaging of Acute Ischemic Stroke: Unenhanced Computed Tomography
Acute Ischemic Stroke. In: Gonz+ílez RG, Hirsch JA, Lev MH, Schaefer PW, Schwamm LH, editors. Springer Berlin Heidelberg; 2011. p. 43-56.
- (61) Moustafa R, Baron JC. Clinical review: Imaging in ischaemic stroke - implications for acute management. *Critical Care* 2007;11(5):227.
- (62) Lovblad KO, Baird A. Actual diagnostic approach to the acute stroke patient
308. *European Radiology* 2006 Jun 1;16(6):1253-69.
- (63) Guadagno JV. IMAGING IN STROKE. *Brain* 2004 Feb 1;127(2):452-4.
- (64) Kidwell C, Villablanca J, Saver J. Advances in neuroimaging of acute stroke. *Current Atherosclerosis Reports* 2000 Mar 1;2(2):126-35.
- (65) Muir KW, Buchan A, von Kummer R, Rother J, Baron JC. Imaging of acute stroke. *Lancet Neurol* 2006;5:755-68.
- (66) Irimia P, Asenbaum S, Brainin M, Chabriat H, Mart+?nez-Vila E, Niederkorn K, et al. Use of Imaging in Cerebrovascular Disease
420. *European Handbook of Neurological Management*. Wiley-Blackwell; 2010. p. 19-34.
- (67) Adams HP, del Zoppo G, Alberts MJ, Bhatt DL, Brass L, Furlan A, et al. Guidelines for the early management of adults with ischemic stroke: a guideline from the American Heart Association/American Stroke Association Stroke Council, Clinical Cardiology Council, Cardiovascular Radiology and Intervention Council, and the Atherosclerotic Peripheral Vascular Disease and Quality of Care Outcomes in Research Interdisciplinary Working Groups: the American Academy of Neurology affirms the value of this guideline as an educational tool for neurologists. *Stroke* 2007;38:1655-711.

- (68) Hand PJ, Wardlaw JM. CT for Acute Ischaemic Stroke. *Practical Neurology* 2001 Dec 1;1(2):82-92.
- (69) Hopyan J, Ciarallo A, Dowlatshahi D, Howard P, John V, Yeung R, et al. Certainty of Stroke Diagnosis: Incremental Benefit with CT Perfusion over Noncontrast CT and CT Angiography¹
425. *Radiology* 2010 Apr 1;255(1):142-53.
- (70) Bonaffini N, Altieri M, Rocco A, Di Piero V. FUNCTIONAL NEUROIMAGING IN ACUTE STROKE
424. *Clin Exp Hypertens* 2002 Jan 1;24(7-8):647-57.
- (71) Barber PA, Demchuk AM, Zhang J, Buchan AM. Validity and reliability of a quantitative computed tomography score in predicting outcome of hyperacute stroke before thrombolytic therapy
426. *The Lancet* 2000 May 13;355(9216):1670-4.
- (72) Muir KW, Santosh C. Imaging of acute stroke and transient ischaemic attack
427. *Journal of Neurology Neurosurgery and Psychiatry* 2005;76:19-28.
- (73) Dzialowski I, Weber J, Doerfler A, Forsting M, von KR. Brain tissue water uptake after middle cerebral artery occlusion assessed with CT. *J Neuroimaging* 2004 Jan;14(1):42-8.
- (74) von Kummer R, Bourquain H, Bastianello S, Bozzao L, Manelfe C, Meier D, et al. Early prediction of irreversible brain damage after ischemic stroke at CT. *Radiology* 2001;219:95-100.
- (75) Muir KW, Baird-Gunning J, Walker L, Baird T, Coutts SB, McCormick M. Can the ischemic penumbra be identified on noncontrast CT of acute stroke?
431. *Stroke* 2007;38:2485-90.
- (76) Brazzelli M, Sandercock PA, Chappell FM, Celani MG, Righetti E, Arestis N, et al. Magnetic resonance imaging versus computed tomography for detection of acute vascular lesions in patients presenting with stroke symptoms. *Cochrane Database Syst Rev* 2009;(4):CD007424.
- (77) Jañger HR. Diagnosis of stroke with advanced CT and MR imaging. *British Medical Bulletin* 2000 Jan 1;56(2):318-33.
- (78) Wardlaw JM, Lewis SC, Humphrey P, Young G, Collie D, Warlow CP. How does the degree of carotid stenosis affect the accuracy and interobserver variability of magnetic resonance angiography? *J Neurol Neurosurg Psychiatry* 2001 Aug;71(2):155-60.
- (79) Broderick J, Connolly S, Feldmann E, Hanley D, Kase C, Krieger D, et al. Guidelines for the Management of Spontaneous Intracerebral Hemorrhage in Adults. *Stroke* 2007 Jun 1;38(6):2001-23.

- (80) Jehangir Khan AuR. Comparison of clinical diagnosis with computed tomography in ascertaining type of stroke. *Journal of Ayub Medical College Abbottabad JAMC* 2011;17(3):65-7.
- (81) Mohr JP, Caplan LR, Melski JW, Goldstein RJ, Duncan GW, Kistler JP, et al. The Harvard Cooperative Stroke Registry. *Neurology* 1978 Aug 1;28(8):754.
- (82) Motto C, Aritzu E, Boccardi E, De Grandi C, Piana A, Candelise L. Reliability of Hemorrhagic Transformation Diagnosis in Acute Ischemic Stroke. *Stroke* 1997 Feb 1;28(2):302-6.
- (83) Franke CL, Ramos LM, Van Gijn J. Development of multifocal haemorrhage in a cerebral infarct during computed tomography. *Journal of Neurology, Neurosurgery & Psychiatry* 1990 Jun 1;53(6):531-2.
- (84) Alastair Buchan. Aspects of Stroke Imaging. *Can J Neurol Sci* 2011;28:99-100.
- (85) de Lucas EM, S+ínchez E, Guti+@rrez An, Mandly AsG, Ruiz E, FI+|rez AF, et al. CT Protocol for Acute Stroke: Tips and Tricks for General Radiologists1. *Radiographics* 2008 Oct;28(6):1673-87.
- (86) Latchaw RE, Alberts MJ, Lev MH, Connors JJ, Harbaugh RE, Higashida RT, et al. Recommendations for Imaging of Acute Ischemic Stroke. *Stroke* 2009 Nov 1;40(11):3646-78.
- (87) Wardlaw JM KSSJLSSPDMeal. What is the best imaging strategy for acute stroke? *Health Technology Assessment* 2004;8(1):21-57.
- (88) Chalela JA, Gomes J. Magnetic resonance imaging in the evaluation of intracranial hemorrhage. *Expert Rev Neurotherapeutics* 2004 Mar 1;4(2):267-73.
- (89) Fiebach JB, Schellinger PD, Gass A, Kucinski T, Siebler M, Villringer A, et al. Stroke Magnetic Resonance Imaging Is Accurate in Hyperacute Intracerebral Hemorrhage. *Stroke* 2004 Feb 1;35(2):502-6.
- (90) Jitendra L Ashtekar MM, Chief Editor: L Gill Naul M. *Intracranial Hemorrhage Evaluation with MRI*. Medscape Reference 2011.
- (91) John A.Marx MF. MRI May Be Superior to CT for Evaluation of Stroke. *Journal Watch Emergency Medicine* 2011.
- (92) Kidwell CS, Chalela JA, Saver JL, Starkman S, Hill MD, Demchuk AM, et al. Comparison of MRI and CT for Detection of Acute Intracerebral Hemorrhage. *JAMA: The Journal of the American Medical Association* 2004 Oct 20;292(15):1823-30.
- (93) Schellinger PD, Jansen O, Fiebach JB, Hacke W, Sartor K. A Standardized MRI Stroke Protocol : Comparison with CT in Hyperacute Intracerebral Hemorrhage. *Stroke* 1999 Apr 1;30(4):765-8.

- (94) von Kummer R, Holle R, Gizyska U, Hofmann E, Jansen O, Petersen D, et al. Interobserver agreement in assessing early CT signs of middle cerebral artery infarction. *American Journal of Neuroradiology* 1996 Oct 1;17(9):1743-8.
- (95) von Kummer R+. MRI: The New Gold Standard for Detecting Brain Hemorrhage? *Stroke* 2002 Jul 1;33(7):1748-9.
- (96) Kane I, Whiteley WN, Sandercock PAG, Wardlaw JM. Availability of CT and MR for Assessing Patients with Acute Stroke. *Cerebrovascular Diseases* 2008;25(4):375-7.
- (97) Martin DS. *Essentials of Neuroimaging*. 2nd ed. *Radiology* 1996 Oct 1;201(1):92.
- (98) Royal College of Physicians of London. Stroke; towards better management. Summary and recommendations. *JR Coil Phys Lond* 2011;(24):15-7.
- (99) Sandercock P MAWC. Value of computed tomography in patients with stroke: Oxfordshire community stroke project. *BMJ* 2011;290:193-7.
- (100) Wardlaw JM, Seymour J, Cairns J, Keir S, Lewis S, Sandercock P. Immediate Computed Tomography Scanning of Acute Stroke Is Cost-Effective and Improves Quality of Life. *Stroke* 2004 Nov 1;35(11):2477-83.
- (101) Wardlaw JM, von KR, Farrall AJ, Chappell FM, Hill M, Perry D. A large web-based observer reliability study of early ischaemic signs on computed tomography. The Acute Cerebral CT Evaluation of Stroke Study (ACCESS). *PLoS One* 2010;5(12):e15757.
- (102) Parsons MW, Pepper EM, Bateman GA, Wang Y, Levi CR. Identification of the penumbra and infarct core on hyperacute noncontrast and perfusion CT. *Neurology* 2007 Mar 6;68(10):730-6.
- (103) Sarikaya B, Provenzale J. Frequency of various brain parenchymal findings of early cerebral ischemia on unenhanced CT scans. *Emergency Radiology* 2010 Sep 1;17(5):381-90.
- (104) Truwit CL, Barkovich AJ, Gean-Marton A, Hibri N, Norman D. Loss of the insular ribbon: another early CT sign of acute middle cerebral artery infarction. *Radiology* 1990 Sep 1;176(3):801-6.
- (105) Koga M, Saku Y, Toyoda K, Takaba H, Ibayashi S, Iida M. Reappraisal of early CT signs to predict the arterial occlusion site in acute embolic stroke. *Journal of Neurology, Neurosurgery & Psychiatry* 2003 May 1;74(5):649-53.
- (106) Wardlaw JM, Mielke O. Early signs of brain infarction at CT: observer reliability and outcome after thrombolytic treatment--systematic review. *Radiology* 2005 May;235(2):444-53.

- (107) Butcher KS, Lee SB, Parsons MW, Allport L, Fink J, Tress B, et al. Differential Prognosis of Isolated Cortical Swelling and Hypoattenuation on CT in Acute Stroke. *Stroke* 2007 Mar 1;38(3):941-7.
- (108) Scott JN, Buchan AM, Sevick RJ. Correlation of Neurologic Dysfunction with CT Findings in Early Acute Stroke. *The Canadian Journal of Neurological Sciences* 1999 Nov 1;26(3):182-9.
- (109) Tomura N, Uemura K, Inugami A, Fujita H, Higano S, Shishido F. Early CT finding in cerebral infarction: obscuration of the lentiform nucleus. *Radiology* 1988 Aug 1;168(2):463-7.
- (110) Saenz RC. The Disappearing Basal Ganglia Sign. *Radiology* 2005 Jan 1;234(1):242-3.
- (111) Moulin T, Cattin F, Crepin-Leblond T, Tatu L, Chavot D, Piotin M, et al. Early CT signs in acute middle cerebral artery infarction. *Neurology* 1996 Aug 1;47(2):366-75.
- (112) Nakano S, Iseda T, Yoneyama T, Wakisaka S. Early CT signs in patients with acute middle cerebral artery occlusion: incidence of contrast staining and haemorrhagic transformations after intra-arterial reperfusion therapy. *Clinical Radiology* 2006 Feb;61(2):156-62.
- (113) Demchuk AM, Hill MD, Barber PA, Silver B, Patel SC, Levine SR, et al. Importance of Early Ischemic Computed Tomography Changes Using ASPECTS in NINDS rtPA Stroke Study. *Stroke* 2005 Oct 1;36(10):2110-5.
- (114) Beauchamp NJ, Barker PB, Wang PY, vanZijl PCM. Imaging of Acute Cerebral Ischemia. *Radiology* 1999 Aug 1;212(2):307-24.
- (115) Barber PA, Darby DG, Desmond PM, Gerraty RP, Yang Q, Li T, et al. Identification of Major Ischemic Change : Diffusion-Weighted Imaging Versus Computed Tomography. *Stroke* 1999 Oct 1;30(10):2059-65.
- (116) R J Cooper and D L Schriger. How accurate is a CT scan in identifying acute strokes? *West J Med* 1999;171(5-6):356-7.
- (117) Saur D, Kucinski T, Grzyska U, Eckert B, Eggers C, Niesen W, et al. Sensitivity and Interrater Agreement of CT and Diffusion-Weighted MR Imaging in Hyperacute Stroke. *American Journal of Neuroradiology* 2003 May 1;24(5):878-85.
- (118) Grond M, von KR, Sobesky J, Schmulling S, Rudolf J, Terstegge K, et al. Early x-ray hypoattenuation of brain parenchyma indicates extended critical hypoperfusion in acute stroke. *Stroke* 2000 Jan;31(1):133-9.
- (119) von KR, Allen KL, Holle R, Bozzao L, Bastianello S, Manelfe C, et al. Acute stroke: usefulness of early CT findings before thrombolytic therapy. *Radiology* 1997 Nov;205(2):327-33.

- (120) Na DG, Kim EY, Ryoo JW, Lee KH, Roh HG, Kim SS, et al. CT Sign of Brain Swelling without Concomitant Parenchymal Hypoattenuation: Comparison with Diffusion- and Perfusion-weighted MR Imaging¹. *Radiology* 2005 Jun 1;235(3):992-48.
- (121) Wardlaw JM, Farrall AJ, Perry D, von KR, Mielke O, Moulin T, et al. Factors influencing the detection of early CT signs of cerebral ischemia: an internet-based, international multiobserver study. *Stroke* 2007 Apr;38(4):1250-6.
- (122) Grotta JC, Chiu D, Lu M, Patel S, Levine SR, Tilley BC, et al. Agreement and Variability in the Interpretation of Early CT Changes in Stroke Patients Qualifying for Intravenous rtPA Therapy
299. *Stroke* 1999 Aug 1;30(8):1528-33.
- (123) Barber PA, Demchuk AM, Hudon ME, Pexman JHW, Hill MD, Buchan AM. Hyperdense Sylvian Fissure MCA "Dot" Sign : A CT Marker of Acute Ischemia. *Stroke* 2001 Jan 1;32(1):84-8.
- (124) Dzialowski I, Hill MD, Coutts SB, Demchuk AM, Kent DM, Wunderlich O, et al. Extent of early ischemic changes on computed tomography (CT) before thrombolysis: prognostic value of the Alberta Stroke Program Early CT Score in ECASS II. *Stroke* 2006 Apr;37(4):973-8.
- (125) von KR. Early major ischemic changes on computed tomography should preclude use of tissue plasminogen activator. *Stroke* 2003 Mar;34(3):820-1.
- (126) Hirano T, Yonehara T, Inatomi Y, Hashimoto Y, Uchino M. Presence of Early Ischemic Changes on Computed Tomography Depends on Severity and the Duration of Hypoperfusion. *Stroke* 2005 Dec 1;36(12):2601-8.
- (127) Silver B, Demaerschalk B, Merino JG, Wong E, Tamayo A, O'Callaghan C, et al. Improved Outcomes in Stroke Thrombolysis with Pre-specified Imaging Criteria
319. *The Canadian Journal of Neurological Sciences* 2001 May 1;28(2):113-9.
- (128) Silver B, Tamayo A, Wong EH, Demaerschalk B, Merino JG, Hachinski V. A reliable new method to estimate >1/3 middle cerebral artery infarction on early computed tomography scan
312. *Abstracts of the International Stroke Conference* 2001 Jan 1;32(1):325-a.
- (129) Kalafut MA, Schriger DL, Saver JL, Starkman S. Detection of Early CT Signs of >1/3 Middle Cerebral Artery Infarctions : Interrater Reliability and Sensitivity of CT Interpretation by Physicians Involved in Acute Stroke Care. *Stroke* 2000 Jul 1;31(7):1667-71.
- (130) Mak HKF, Yau KKW, Khong PL, Ching ASC, Cheng PW, Au-Yeung PKM, et al. Hypodensity of >1/3 Middle Cerebral Artery Territory Versus Alberta Stroke Programme Early CT Score (ASPECTS)
303. *Stroke* 2003 May 1;34(5):1194-6.

- (131) Coutts SB, Demchuk AM, Barber PA, Hu WY, Simon JE, Buchan AM, et al. Interobserver Variation of ASPECTS in Real Time. *Stroke* 2004 May 1;35(5):e103-e105.
- (132) Pexman JHW, Barber PA, Hill MD, Sevick RJ, Demchuk AM, Hudon ME, et al. Use of the Alberta Stroke Program Early CT Score (ASPECTS) for Assessing CT Scans in Patients with Acute Stroke
302. *American Journal of Neuroradiology* 2001 Sep 1;22(8):1534-42.
- (133) Phan TG, Donnan GA, Koga M, Mitchell LA, Molan M, Fitt G, et al. The ASPECTS template is weighted in favor of the striatocapsular region
324. *NeuroImage* 2006 Jun;31(2):477-81.
- (134) Hill MD, Rowley HA, Adler F, Eliasziw M, Furlan A, Higashida RT, et al. Selection of Acute Ischemic Stroke Patients for Intra-Arterial Thrombolysis With Pro-Urokinase by Using ASPECTS
301. *Stroke* 2003 Aug 1;34(8):1925-31.
- (135) Hirano T, Sasaki M, Tomura N, Ito Y, Kobayashi S. Low Alberta Stroke Program Early Computed Tomography Score Within 3 Hours of Onset Predicts Subsequent Symptomatic Intracranial Hemorrhage in Patients Treated with 0.6 mg/kg Alteplase. *Journal of Stroke and Cerebrovascular Diseases* 2011;(0).
- (136) Demaerschalk BM, Silver B, Wong E, Merino JG, Tamayo A, Hachinski V. ASPECT Scoring to Estimate >1/3 Middle Cerebral Artery Territory Infarction. *The Canadian Journal of Neurological Sciences* 2005 Jul 1;33(2):200-4.
- (137) Lyden P. Early Major Ischemic Changes on Computed Tomography Should Not Preclude Use of Tissue Plasminogen Activator. *Stroke* 2003 Mar 1;34(3):821-2.
- (138) Miller DJ, Simpson JR, Silver B. Safety of Thrombolysis in Acute Ischemic Stroke: A Review of Complications, Risk Factors, and Newer Technologies. *The Neurohospitalist* 2011 Jul 1;1(3):138-47.
- (139) Roberts HC, Dillon WP, Furlan AJ, Wechsler LR, Rowley HA, Fischbein NJ, et al. Computed Tomographic Findings in Patients Undergoing Intra-arterial Thrombolysis for Acute Ischemic Stroke due to Middle Cerebral Artery Occlusion. *Stroke* 2002 Jun 1;33(6):1557-65.
- (140) Bryan RN, Levy LM, Whitlow WD, Killian JM, Preziosi TJ, Rosario JA. Diagnosis of acute cerebral infarction: comparison of CT and MR imaging. *American Journal of Neuroradiology* 1991 Jul 1;12(4):611-20.
- (141) Fiebich J, Jansen O, Schellinger P, Knauth M, Hartmann M, Heiland S, et al. Comparison of CT with diffusion-weighted MRI in patients with hyperacute stroke. *Neuroradiology* 2001 Aug;43(8):628-32.
- (142) Jaillard A, Hommel M, Baird AE, Linfante I, Llinas RH, Caplan LR, et al. Significance of Early CT Signs in Acute Stroke. *Cerebrovascular Diseases* 2002;13(1):47-56.

(143) Lansberg MG, Albers GW, Beaulieu C, Marks MP. Comparison of diffusion-weighted MRI and CT in acute stroke. *Neurology* 2000 Apr 25;54(8):1557-61.

(144) Marks MP, Holmgren EB, Fox AJ, Patel S, von Kummer R, Froehlich J. Evaluation of Early Computed Tomographic Findings in Acute Ischemic Stroke. *Stroke* 1999 Feb 1;30(2):389-92.

(145) Mullins ME, Lev MH, Schellingerhout D, Koroshetz WJ, Gonzalez RG. Influence of Availability of Clinical History on Detection of Early Stroke Using Unenhanced CT and Diffusion-Weighted MR Imaging. *American Journal of Roentgenology* 2002 Jul 1;179(1):223-8.

(146) Mullins ME, Schaefer PW, Sorensen AG, Halpern EF, Ay H, He J, et al. CT and Conventional and Diffusion-weighted MR Imaging in Acute Stroke: Study in 691 Patients at Presentation to the Emergency Department¹. *Radiology* 2002 Aug 1;224(2):353-60.

(147) Aronovich BD, Reider-Groswasser II, Segev Y, Bornstein NM. Early CT changes and outcome of ischemic stroke. *European Journal of Neurology* 2004;11(1):63-5.

(148) Patel SC, Levine SR, Tilley BC, Grotta JC, Lu M, Frankel M, et al. Lack of Clinical Significance of Early Ischemic Changes on Computed Tomography in Acute Stroke. *JAMA: The Journal of the American Medical Association* 2001 Dec 12;286(22):2830-8.

(149) Lev MH, Farkas J, Gemmete JJ, Hossain ST, Hunter GJ, Koroshetz WJ, et al. Acute Stroke: Improved Nonenhanced CT Detection-Benefits of Soft-Copy Interpretation by Using Variable Window Width and Center Level Settings¹. *Radiology* 1999 Oct 1;213(1):150-5.

(150) Wardlaw JM, Dorman PJ, Lewis SC, Sandercock PA. Can stroke physicians and neuroradiologists identify signs of early cerebral infarction on CT? *J Neurol Neurosurg Psychiatry* 1999 Nov;67(5):651-3.

(151) Fiebich JB, Schellinger PD, Jansen O, Meyer M, Wilde P, Bender J, et al. CT and Diffusion-Weighted MR Imaging in Randomized Order. *Stroke* 2002 Sep 1;33(9):2206-10.

(152) von KR. Effect of training in reading CT scans on patient selection for ECASS II. *Neurology* 1998 Sep;51(3 Suppl 3):S50-S52.

(153) Ogura A, Hayakawa K, Miyati T, Maeda F. Improvement on detectability of early ischemic changes for acute stroke using nonenhanced computed tomography: Effect of matrix size. *European journal of radiology* 76[2], 162-166. 1-11-2010.

Ref Type: Abstract

(154) Tanaka C, Ueguchi T, Shimosegawa E, Sasaki N, Johkoh T, Nakamura H, et al. Effect of CT Acquisition Parameters in the Detection of Subtle Hypoattenuation in

Acute Cerebral Infarction: A Phantom Study. *American Journal of Neuroradiology* 2006 Jan;27(1):40-5.

(155) Francesca Ng, Yogish Joshi, Jozef Jarosz. Acute stroke imaging: Are thin slices useful? *RAD Magazine* 2011;37(434):19-20.

(156) Scharf J, Brockmann MA, Daffertshofer M, Diepers M, Neumaier-Probst E, Weiss C, et al. Improvement of sensitivity and interrater reliability to detect acute stroke by dynamic perfusion computed tomography and computed tomography angiography. *J Comput Assist Tomogr* 2006;30(1):105-10.

(157) A Gholkar MDDbAM. Early computed-tomography abnormalities in acute stroke. *The Lancet* 1988 Feb 28;351(9103):679.

(158) Leary MC, Kidwell CS, Villablanca JP, Starkman S, Jahan R, Duckwiler GR, et al. Validation of Computed Tomographic Middle Cerebral Artery "dot" Sign. *Stroke* 2003 Nov 1;34(11):2636-40.

(159) Krings T, Noelchen D, Mull M, Willmes K, Meister IG, Reinacher P, et al. The Hyperdense Posterior Cerebral Artery Sign. *Stroke* 2006 Feb 1;37(2):399-403.

(160) Ozdemir O, Leung A, Bussi+@re M, Hachinski V, Pelz D. Hyperdense Internal Carotid Artery Sign. *Stroke* 2008 Jul 1;39(7):2011-6.

(161) Kharitonova T, Ahmed N, Thoren M, Wardlaw JM, von KR, Glahn J, et al. Hyperdense middle cerebral artery sign on admission CT scan--prognostic significance for ischaemic stroke patients treated with intravenous thrombolysis in the safe implementation of thrombolysis in Stroke International Stroke Thrombolysis Register. *Cerebrovasc Dis* 2009;27(1):51-9.

(162) von KR, Meyding-Lamade U, Forsting M, Rosin L, Rieke K, Hacke W, et al. Sensitivity and prognostic value of early CT in occlusion of the middle cerebral artery trunk. *AJNR Am J Neuroradiol* 1994 Jan;15(1):9-15.

(163) Kim EY, Lee SK, Kim DJ, Suh SH, Kim J, Heo JH, et al. Detection of Thrombus in Acute Ischemic Stroke. *Stroke* 2005 Dec 1;36(12):2745-7.

(164) Riedel CH, Jensen U, Rohr A, Tietke M, Alfke K, Ulmer S, et al. Assessment of Thrombus in Acute Middle Cerebral Artery Occlusion Using Thin-Slice Nonenhanced Computed Tomography Reconstructions. *Stroke* 2010 Aug 1;41(8):1659-64.

(165) Manelfe C, Larrue V, von KR, Bozzao L, Ringleb P, Bastianello S, et al. Association of hyperdense middle cerebral artery sign with clinical outcome in patients treated with tissue plasminogen activator. *Stroke* 1999 Apr;30(4):769-72.

(166) Berge E, Nakstad PH, Sandset PM. Large middle cerebral artery infarctions and the hyperdense middle cerebral artery sign in patients with atrial fibrillation. *Acta Radiol* 2001 May;42(3):261-8.

(167) Kharitonova T, Thoren M, Ahmed N, Wardlaw JM, von KR, Thomassen L, et al. Disappearing hyperdense middle cerebral artery sign in ischaemic stroke patients treated with intravenous thrombolysis: clinical course and prognostic significance. *J Neurol Neurosurg Psychiatry* 2009 Mar;80(3):273-8.

(168) Konstas AA, Goldmakher GV, Lee TY, Lev MH. Theoretic Basis and Technical Implementations of CT Perfusion in Acute Ischemic Stroke, Part 2: Technical Implementations. *American Journal of Neuroradiology* 2009 May;30(5):885-92.

(169) Latchaw RE, Yonas H, Hunter GJ, Yuh WTC, Ueda T, Sorensen AG, et al. Guidelines and Recommendations for Perfusion Imaging in Cerebral Ischemia. *Stroke* 2003 Apr 1;34(4):1084-104.

(170) Meier P, Zierler KL. On the Theory of the Indicator-Dilution Method for Measurement of Blood Flow and Volume. *Journal of Applied Physiology* 1954 Jun 1;6(12):731-44.

(171) Tomandl BF, Klotz E, Handschu R, Stemper B, Reinhardt F, Huk WJ, et al. Comprehensive Imaging of Ischemic Stroke with Multisection CT1. *Radiographics* 2003 May 1;23(3):565-92.

(172) Konig M. Brain perfusion CT in acute stroke: current status. *European journal of radiology* 45, S11-S22. 1-3-2003.

Ref Type: Abstract

(173) Konstas AA, Lev MH. CT Perfusion Imaging of Acute Stroke: The Need for Arrival Time, Delay Insensitive, and Standardized Postprocessing Algorithms?1. *Radiology* 2010 Jan 1;254(1):22-5.

(174) Gillard JH, Minhas PS, Hayball MP, Bearcroft PW, Antoun NM, Freer CE, et al. Assessment of quantitative computed tomographic cerebral perfusion imaging with H2(15)O positron emission tomography. *Neurol Res* 2000 Jul;22(5):457-64.

(175) Kudo K, Terae S, Katoh C, Oka M, Shiga T, Tamaki N, et al. Quantitative Cerebral Blood Flow Measurement with Dynamic Perfusion CT Using the Vascular-Pixel Elimination Method: Comparison with H215O Positron Emission Tomography. *American Journal of Neuroradiology* 2003 Mar 1;24(3):419-26.

(176) Rother J, Jonetz-Mentzel L, Fiala A, Reichenbach JR, Herzau M, Kaiser WA, et al. Hemodynamic Assessment of Acute Stroke Using Dynamic Single-Slice Computed Tomographic Perfusion Imaging. *Arch Neurol* 2000 Aug 1;57(8):1161-6.

(177) Schramm P, Schellinger PD, Fiebich JB, Heiland S, Jansen O, Knauth M, et al. Comparison of CT and CT Angiography Source Images With Diffusion-Weighted Imaging in Patients With Acute Stroke Within 6 Hours After Onset. *Stroke* 2002 Oct 1;33(10):2426-32.

(178) Wintermark M, Reichhart M, Thiran JP, Maeder P, Chalaron M, Schnyder P, et al. Prognostic accuracy of cerebral blood flow measurement by perfusion computed

tomography, at the time of emergency room admission, in acute stroke patients. *Ann Neurol* 2002;51(4):417-32.

(179) Hoeffner EG, Case I, Jain R, Gujar SK, Shah GV, Deveikis JP, et al. Cerebral Perfusion CT: Technique and Clinical Applications¹. *Radiology* 2004 Jun 1;231(3):632-44.

(180) Shetty SK, Lev MH. CT Perfusion in Acute Stroke. *Neuroimaging Clinics of North America* 15[3], 481-501. 1-8-2005.

Ref Type: Abstract

(181) Wintermark M, Flanders AE, Velthuis B, Meuli R, van Leeuwen M, Goldsher D, et al. Perfusion-CT Assessment of Infarct Core and Penumbra. *Stroke* 2006 Apr 1;37(4):979-85.

(182) Bisdas S, Therapidis P, Kerl JM, Papadopoulos N, Burck I, Herzog C, et al. Value of cerebral perfusion computed tomography in the management of intensive care unit patients with suspected ischaemic cerebral pathology after cardiac surgery. *Eur J Cardiothorac Surg* 2007 Sep;32(3):521-6.

(183) Muir KW, Halbert HM, Baird TA, McCormick M, Teasdale E. Visual evaluation of perfusion computed tomography in acute stroke accurately estimates infarct volume and tissue viability. *Journal of Neurology, Neurosurgery & Psychiatry* 2006 Mar 1;77(3):334-9.

(184) Nabavi DG, LeBlanc LM, Baxter B, Lee DH, Fox AJ, Lownie SP, et al. Monitoring cerebral perfusion after subarachnoid hemorrhage using CT. *Neuroradiology* 2001 Jan 12;43(1):7-16.

(185) Pham M, Johnson A, Bartsch AJ, Lindner C, M++llges W, Roosen K, et al. CT perfusion predicts secondary cerebral infarction after aneurysmal subarachnoid hemorrhage. *Neurology* 2007 Aug 21;69(8):762-5.

(186) Bisdas S, Donnerstag F, Ahl B, Bohrer I, Weissenborn K, Becker H. Comparison of Perfusion Computed Tomography With Diffusion-Weighted Magnetic Resonance Imaging in Hyperacute Ischemic Stroke. *J Comput Assist Tomogr* 2004;28(6).

(187) Wintermark M, Reichhart M, Cuisenaire O, Maeder P, Thiran JP, Schnyder P, et al. Comparison of Admission Perfusion Computed Tomography and Qualitative Diffusion- and Perfusion-Weighted Magnetic Resonance Imaging in Acute Stroke Patients. *Stroke* 2002 Aug 1;33(8):2025-31.

(188) Na DG, Ryoo JW, Lee KH, Moon CH, Yi CA, Kim EY, et al. Multiphasic Perfusion Computed Tomography in Hyperacute Ischemic Stroke: Comparison with Diffusion and Perfusion Magnetic Resonance Imaging. *J Comput Assist Tomogr* 2003;27(2).

(189) Eastwood JD, Lev MH, Wintermark M, Fitzek C, Barboriak DP, Delong DM, et al. Correlation of Early Dynamic CT Perfusion Imaging with Whole-Brain MR Diffusion

and Perfusion Imaging in Acute Hemispheric Stroke. *American Journal of Neuroradiology* 2003 Oct 1;24(9):1869-75.

(190) Schaefer PW, Roccatagliata L, Ledezma C, Hoh B, Schwamm LH, Koroshetz W, et al. First-Pass Quantitative CT Perfusion Identifies Thresholds for Salvageable Penumbra in Acute Stroke Patients Treated with Intra-arterial Therapy. *American Journal of Neuroradiology* 2006 Jan;27(1):20-5.

(191) Gasparotti R, Grassi M, Mardighian D, Frigerio M, Pavia M, Liserre R, et al. Perfusion CT in Patients with Acute Ischemic Stroke Treated with Intra-Arterial Thrombolysis: Predictive Value of Infarct Core Size on Clinical Outcome. *American Journal of Neuroradiology* 2009 Apr;30(4):722-7.

(192) Hacke W, Albers G, Al-Rawi Y, Bogousslavsky J, Davalos A, Eliasziw M, et al. The Desmoteplase in Acute Ischemic Stroke Trial (DIAS): a phase II MRI-based 9-hour window acute stroke thrombolysis trial with intravenous desmoteplase. *Stroke* 2005 Jan;36(1):66-73.

(193) Murphy BD, Fox AJ, Lee DH, Sahlas DJ, Black SE, Hogan MJ, et al. Identification of Penumbra and Infarct in Acute Ischemic Stroke Using Computed Tomography Perfusion-Derived Blood Flow and Blood Volume Measurements. *Stroke* 2006 Jul 1;37(7):1771-7.

(194) Nabavi DG, Kloska SP, Nam EM, Freund M, Gaus CG, Klotz E, et al. MOSAIC: Multimodal Stroke Assessment Using Computed Tomography. *Stroke* 2002 Dec 1;33(12):2819-26.

(195) Lin K, Rapalino O, Law M, Babb JS, Siller KA, Pramanik BK. Accuracy of the Alberta Stroke Program Early CT Score during the First 3 Hours of Middle Cerebral Artery Stroke: Comparison of Noncontrast CT, CT Angiography Source Images, and CT Perfusion. *American Journal of Neuroradiology* 2008 May;29(5):931-6.

(196) Fiorella D, Heiserman J, Prenger E, Partovi S. Assessment of the Reproducibility of Postprocessing Dynamic CT Perfusion Data. *American Journal of Neuroradiology* 2004 Jan 1;25(1):97-107.

(197) Kloska SP, Nabavi DG, Gaus C, Nam EM, Klotz E, Ringelstein EB, et al. Acute Stroke Assessment with CT: Do We Need Multimodal Evaluation?1. *Radiology* 2004 Oct 1;233(1):79-86.

(198) del Zoppo GJ, Poeck K, Pessin MS, Wolpert SM, Furlan AJ, Ferbert A, et al. Recombinant tissue plasminogen activator in acute thrombotic and embolic stroke. *Ann Neurol* 1992;32(1):78-86.

(199) Katz DA, Marks MP, Napel SA, Bracci PM, Roberts SL. Circle of Willis: evaluation with spiral CT angiography, MR angiography, and conventional angiography. *Radiology* 1995 May 1;195(2):445-9.

- (200) Wildermuth S, Knauth M, Brandt T, Winter R, Sartor K, Hacke W. Role of CT Angiography in Patient Selection for Thrombolytic Therapy in Acute Hemispheric Stroke. *Stroke* 1998 May 1;29(5):935-8.
- (201) Berg MH, Manninen HI, Räsänen HT, Vanninen RL, Jaakkola PA. CT angiography in the assessment of carotid artery atherosclerosis: A comparative analysis with MR angiography with reference to contrast angiography and intravascular ultrasound. *Acta Radiologica* 2002 Mar 1;43(2):116-24.
- (202) Lev MH, Romero JM, Goodman DNF, Bagga R, Kim HYK, Clerk NA, et al. Total Occlusion versus Hairline Residual Lumen of the Internal Carotid Arteries: Accuracy of Single Section Helical CT Angiography. *American Journal of Neuroradiology* 2003 Jun 1;24(6):1123-9.
- (203) Walker LJ, Ismail A, McMeekin W, Lambert D, Mendelow AD, Birchall D. Computed Tomography Angiography for the Evaluation of Carotid Atherosclerotic Plaque. *Stroke* 2002 Apr 1;33(4):977-81.
- (204) Camargo ECS, Furie KL, Singhal AB, Roccatagliata L, Cunnane ME, Halpern EF, et al. Acute Brain Infarct: Detection and Delineation with CT Angiographic Source Images versus Nonenhanced CT Scans. *Radiology* 2007 Aug;244(2):541-8.
- (205) Hirai T, Korogi Y, Ono K, Nagano M, Maruoka K, Uemura S, et al. Prospective Evaluation of Suspected Stenoocclusive Disease of the Intracranial Artery: Combined MR Angiography and CT Angiography Compared with Digital Subtraction Angiography. *American Journal of Neuroradiology* 2002 Jan 1;23(1):93-101.
- (206) Lev MH, Farkas J, Rodriguez VR, Schwamm LH, Hunter GJ, Putman CM, et al. CT Angiography in the Rapid Triage of Patients with Hyperacute Stroke to Intraarterial Thrombolysis: Accuracy in the Detection of Large Vessel Thrombus. *J Comput Assist Tomogr* 2001;25(4).
- (207) Bash S, Villablanca JP, Jahan R, Duckwiler G, Tillis M, Kidwell C, et al. Intracranial Vascular Stenosis and Occlusive Disease: Evaluation with CT Angiography, MR Angiography, and Digital Subtraction Angiography. *American Journal of Neuroradiology* 2005 May 1;26(5):1012-21.
- (208) Wintermark M, Albers GW, Alexandrov AV, Alger JR, Bammer R, Baron JC, et al. Acute Stroke Imaging Research Roadmap. *Stroke* 2008 May 1;39(5):1621-8.
- (209) Sims JR, Rordorf G, Smith EE, Koroshetz WJ, Lev MH, Buonanno F, et al. Arterial Occlusion Revealed by CT Angiography Predicts NIH Stroke Score and Acute Outcomes after IV tPA Treatment. *American Journal of Neuroradiology* 2005 Feb 1;26(2):246-51.
- (210) Gonzalez RG, Lev MH, Goldmacher GV, Smith WS, Payabvash S, Harris GJ, et al. Improved Outcome Prediction Using CT Angiography in Addition to Standard

Ischemic Stroke Assessment: Results from the STOPStroke Study. PLoS ONE 2012 Jan 20;7(1):e30352.

(211) Mohr JP, Biller J, Hilal SK, Yuh WTC, Tatemichi TK, Hedges S, et al. Magnetic Resonance Versus Computed Tomographic Imaging in Acute Stroke. Stroke 1995 May 1;26(5):807-12.

(212) Boulanger JM, Coutts SB, Eliasziw M, Gagnon AJ, Simon JE, Subramaniam S, et al. Cerebral Microhemorrhages Predict New Disabling or Fatal Strokes in Patients With Acute Ischemic Stroke or Transient Ischemic Attack. Stroke 2006 Mar 1;37(3):911-4.

(213) Schaefer PW, Grant PE, Gonzalez RG. Diffusion-weighted MR Imaging of the Brain¹. Radiology 2000 Nov 1;217(2):331-45.

(214) Gonzalez RG, Schaefer PW, Buonanno FS, Schwamm LH, Budzik RF, Rordorf G, et al. Diffusion-weighted MR Imaging: Diagnostic Accuracy in Patients Imaged within 6 Hours of Stroke Symptom Onset. Radiology 1999 Jan 1;210(1):155-62.

(215) Warach S WPERR. Identification and characterization of the ischemic penumbra of acute human stroke using echo planar diffusion and perfusion imaging. In: Proceedings of the 12th Annual Meeting of the Society of Magnetic Resonance in Medicine. Berkeley, Ca; 1993;263.

(216) Lovblad KO, Baird AE, Schlaug G, Benfield A, Siewert B, Voetsch B, et al. Ischemic lesion volumes in acute stroke by diffusion-weighted magnetic resonance imaging correlate with clinical outcome. Ann Neurol 1997;42(2):164-70.

(217) Sobesky J, Weber OZ, Lehnhardt FG, Hesselmann V, Neveling M, Jacobs A, et al. Does the Mismatch Match the Penumbra? Stroke 2005 May 1;36(5):980-5.

(218) Wu O, Koroshetz WJ, Østergaard L, Buonanno FS, Copen WA, Gonzalez RG, et al. Predicting Tissue Outcome in Acute Human Cerebral Ischemia Using Combined Diffusion- and Perfusion-Weighted MR Imaging. Stroke 2001 Apr 1;32(4):933-42.

(219) Luby M, Ku KD, Latour LL, Merino JG, Hsia AW, Lynch JK, et al. Visual perfusion-diffusion mismatch is equivalent to quantitative mismatch. Stroke 2011 Apr;42(4):1010-4.

(220) White PM, Wardlaw JM, Easton V. Can Noninvasive Imaging Accurately Depict Intracranial Aneurysms? A Systematic Review¹. Radiology 2000 Nov 1;217(2):361-70.

(221) Zimmerman RD. Stroke Wars: Episode IV CT Strikes Back. American Journal of Neuroradiology 2004 Sep 1;25(8):1304-9.

(222) Hughes RL, Yonas H, Gur D, Latchaw R. Cerebral blood flow determination within the first 8 hours of cerebral infarction using stable xenon-enhanced computed tomography. Stroke 1989 Jun 1;20(6):754-60.

(223) Firlik AD, Kaufmann AM, Wechsler LR, Firlik KS, Fukui MB, Yonas H. Quantitative Cerebral Blood Flow Determinations in Acute Ischemic Stroke : Relationship to Computed Tomography and Angiography. *Stroke* 1997 Nov 1;28(11):2208-13.

(224) MedCalc - User-friendly statistical software Version 12.2.1 [computer program]. 2012.

(225) Allan Chang. StatTools. 2012.

Ref Type: Online Source

(226) Randolph JJ2. *Online Kappa Calculator*. 2012.

Ref Type: Online Source

(227) Faculty of Medicine UoCC. Understanding Alberta Stroke Program Early CT Score(ASPECTS). 2012.

Ref Type: Online Source

Recommendations by examiners for correction of this thesis;

- 1- Spelling and sentences composition corrections.
- 2- Addition of IST-III study to thrombolytic therapy section.
- 3- More information on how choosing the appropriate literature for literature review.
- 4- Explanation of absence of assessment of effect of other factors on agreement as old strokes and also absence of standard.
- 5- The broad assessment of agreement needs to be mentioned in conclusions.